FINITE ELEMENT METHOD IN THE CONTEXT OF ARCH DAMS – A CRITICAL STUDY

A THESIS SUBMITTED TO THE UNIVERSITY OF CALICUT
IN FULFILMENT OF THE REQUIREMENT FOR THE
AWARD OF THE DEGREE OF

DOCTOR OF PHILOSOPHY

in

ENGINEERING

of

UNIVERSITY OF CALICUT

by

SUSAN ABRAHAM

Department of Chemical Engineering
Government Engineering College Thrissur
Thrissur 680 009, Kerala

December 2007

ACKNOWLEDGEMENT

Not by might nor by power, but by His Spirit. The spirit of YHWH makes everything beautiful…

I am overwhelmed with gladness as I express my heart-felt, sincere thanks to ***Dr. K. V. Narayanan*** and ***Dr. K. Prabhakaran Nair*** who are more than guides to me for upholding me with their valuable time, talents and abilities in developing this research to the present stage. I place on record my sincere thanks for their consistent guidance and timely encouragements without which it would have been impossible for me to reach this level of achievement in the work.

I thank ***Dr. Mohammed Ameen*** who is my M. Tech Project guide for opening up my eyes to this topic and sustaining my heart with wisdom and encouragement. I also thank ***Dr. T. P. Somasundaran***, ***Dr. T. M. Madhavan Pillai***; Professors of the Department of Civil Engineering, *National Institute of Technology Calicut*, for their valuable advices, timely suggestions and guidance.

I sincerely acknowledge the valuable advices, sharing of experiences and help extended throughout the programme by ***Mr. R. Sathyadas, Mr. B. S. Radhakrishnan*** and ***Mr. R. S. Balachandran*** Chief Engineers of *Kerala State Electricity Board*. I place on record my sincere thanks to ***Mr. B. Raveendran,*** former Deputy Chief Engineer of *Kerala State Electricity Board,* for his timely help in the research in the comparison of the actual performance of Idukki arch dam with theoretical results.

This research was made an ever enjoyable sail with the constant, loving help and enabling by my husband ***Dr. Abraham George*** and the loving presence of our two wonderful daughters ***Ann*** and ***Evelyn***. But most of all, I thank the ***LORD ALMIGHTY*** who poured out HIS abundant grace and enabling on me in accomplishing this task that seemed too far… indeed beyond my reach.

Susan Abraham

ABSTRACT

The second half of the twentieth century witnessed construction of a variety of dams based on the materials of construction as well as the mode of behaviour to suit the site conditions, geology, geography and hydrology of the site. The design of dams further underwent many developments by way of incorporating improvements, new techniques of construction and led to the rational design of dams. Consideration of the tri-dimensional arch action to hold water load in a narrow gorge brought the idea of arch dam. Conventional methods adopted for the analysis of arch dams were *trial load* and *model analysis* methods. Later, accurate methods; by eliminating many assumptions made in the traditional methods, were necessitated for ensuring safety and economy which led to numerical methods such as *finite difference*, *finite element* and *boundary element* methods for the analysis of arch dams.

Elasto static analysis of arch dam structure using finite element method is taken as the key point of study in this research. The shape of an arch dam has of paramount importance in its ultimate behaviour, which eventually settles all other design criteria. Hence, the arch dam geometry is to be modeled very accurately which can be arrived effectively using higher order interpolation polynomials which is one of the main concerns of this research. The preprocessing stage of *finite element analysis* of arch dam requires preparation of data such as nodal coordinates and nodal connectivity of the continuum to be analyzed, which require considerable effort if all data are to be handled manually, especially in the case of finer discretisations. ***Hence development of an automatic mesh generation program in order to model the geometry and***

boundary conditions of an arch dam giving element connectivity and nodal coordinate data for the continuum to be analyzed is essential which can be arrived based on a simple three dimensional mapping technique is attempted in this research as the primary objective. The geometry is approximated using shape functions for higher order hexahedral elements which gives higher order polynomials in all the three directions arrived by Langrange family of elements.

Various loads vectors to be considered for the analysis of an arch dam; how effectively can be incorporated in the pseudo static finite element method, is the next concern of this research. Of these, the hydrostatic load plays the most important role which in most cases of available literature is taken as distributed surface traction applied at nodes with the help of coefficients to evaluate the normal effect. Definitely this involves certain degree of approximation which affects the accuracy of results. For an arch dam of complex geometry the water pressure at each point acts in a direction normal to the surface; surface being curved in both directions, the magnitude as well as direction of water pressure varies from point to point; element to element, depending on the height of water column. Thus, the hydrostatic pressure will have components in all the three directions. ***This can be effectively solved taking into consideration, the direction cosines of the pressure at each point and by numerical integration in the finite elements itself for which a program that resolves the pressure to all the three directions at a particular point is proposed to be arrived at, which is another objective of this research.*** The program makes the computer simulation possible in the design stage itself with various levels of reservoir water and load combinations giving in advance the dam monitoring results; *instrumentation values,* which can be made use of for verification with actual physical performance.

The other load vectors which decide the safety are the self weight of the dam, inertial as well as hydrodynamic effects due to seismic activity, silt and earth pressure, uplift and external concentrated loads.

In the analysis usually self weight is assumed to act at the centre of gravity; which is very difficult to arrive at, in the case of an arch dam of complex geometry. In finite element method this distributed loads can be assumed as lumped masses at the nodes of each element that also have certain degree of approximation. ***In fact, this self weight is a body force due to gravity and if arrived by numerical integration throughout the volume of each element, gives dependable results in finite element method. Similarly, the seismic effects on the body of the dam are inertial forces due to gravity depending on the ground peak acceleration in the horizontal as well as vertical directions. This can also be incorporated as body forces by numerical integration method in the pseudo static approach which is attempted in this work.***

In addition to the hydrostatic reservoir pressures, hydrodynamic pressures also are generated due to successive lateral movements of the upstream face of the dam against reservoir water occurring under earthquake. This pressure is found to be the same as that would occur if a body of water confined between a certain parabola and the face of the dam were forced to move with the dam while the rest of the reservoir remained inactive. Following the added mass concept and the code provisions for pseudo static analysis, this hydrodynamic effect; approximated as distributed pressure on the upstream face, is incorporated in this research by way of direction cosines and numerical integration. However, there are limitations in this approach since the seismic

forces are evaluated as if the structure is rigid whereas, actually it is flexible and the accelerations resulting from its dynamic response may be greater than that which when acts on a rigid structure. Hence, a dynamic response analysis is more reliable which is beyond the scope of this work.

The silt and earth deposited at the upstream face of the dam after impounding of reservoir exerts pressure on the surface. This is only for a particular height of the dam which is incorporated in the program as effective pressure due to submerged unit weight at the corresponding elements by numerical integration. The external loads, if any, which contribute to the self weight of the dam can be effectively applied directly as nodal loads. Uplift pressure occurs as internal pressure in the pores, cracks and seams in the dam and foundation and can be arrived at, by numerical integration method. In the case of a concrete dam, the chemical properties of concrete changes with aging; the modulus of elasticity increases considerably, giving deflection and stress values at a particular point with same loading condition varying with age. This can also be studied easily with the help of computer simulation.

Incorporating the above aspects, Analysis Software in Finite element method for the dam structure (Rock Mechanics not attempting) using various isoparametric elements like tri-linear and tri-quadratic will be developed. The accuracy of the results in fine, coarse descretisation of different type elements are intended. As most of the recent FEM software includes shell elements and tri-linear elements for continuum descretisation, three dimensional hexahedral elements are aimed here so as to accommodate thick arch dams also. ***Development of the software having efficient pre and post processing capabilities is proposed with the advanced object oriented***

programming technique; visual C^{++}, a simultaneous finite-element plotting program in Matlab corresponding to the C^{++} program arrived with various options of plotting; the original shape, deflected shape, sectional plan etc. Established works of similar nature and case studies are intended for verification and comparison of results along with parametric studies. This software can be used effectively for the elasto static analysis of any three dimensional solid continuum which as well can be extended for structures like retaining walls, dams; *both straight and curved*, and weirs.

Contents

List of Figures

List of Tables

Notations

LATIN SYMBOLS

x, y, z	Cartesian, Global axes
x_i, y_i, z_i	Global coordinates at node i of the element
$\{u^e\}$	Element nodal displacement vector
$\{\delta u^e\}$	Element nodal virtual displacement vector
u_i, v_i, w_i	Element nodal displacement degrees of freedom at node i
$[N]$	Interpolation or shape function matrix
$[B]$	Strain-displacement matrix
$[D]$	Constitutive matrix
E	Young's modulus
T	Temperature
V	Volume
V_e	Element volume
S	Surface
S_e	Element surface area
$\{r^e\}$	Element load vector
$[k^e]$	Element stiffness matrix
$\{b\}$	Element body force vector
$\{p\}$	Element surface force vector
[K]	Global stiffness matrix
$\{U\}$	Global displacement vector

n_{eq}	Number of equations
n	Number of nodes per element
$[J]$	Jacobian matrix
$\{R\}$	Global load vector
$\{R_f\}$	Applied loads
$\{R_r\}$	Support reaction
$\{U_f\}$	Free degrees of freedom
Z	Section modulus
$N_{\xi_i}, N_{\eta_j}, N_{\zeta_k}$	Shape functions of point (i, j, k) in ξ, η, ζ directions
L, T, H	Length, thickness and Height directions of a cube
nL, nT, nH	Divisions in Length, Thickness and Height
dA	Element face area
i, j, k	Unit vectors along x, y, z directions
e_1, e_2, e_3	Vectors along ξ, η, ζ directions
e'_1, e'_2, e'_3	Vectors along ξ', η', ζ' directions
$l \ m \ n$	Direction cosines
ρ_L	Fluid density
q	Intensity of pressure normal to any surface
z_{ref}	Fluid surface datum
N_i^s	Surface shape function for the node i.
p_e	Hydrodynamic pressure
C_s	Coefficient varies with shape and depth
w	Unit weight of water
h	Depth of reservoir in m

C_m	Maximum value of Cs
P_w	Maximum pressure intensity due to wave action
h_w	Height of wave

GREEK SYMBOLS

ξ, η, ζ	Local, Natural axes
ξ_i, η_i, ζ_i	Local coordinates at node i of the element
$\{\sigma\}$	Element stress vector
$\{\varepsilon\}$	Element strain vector
$\{\delta\varepsilon\}$	Virtual strain
μ	Poisson's ratio
α	Coefficient of thermal expansion
$\alpha_x, \alpha_y, \alpha_z$	Earth quake intensities in x, y, z directions
α_h	Design horizontal seismic coefficient

STRUCTURE OF THE THESIS

This dissertation is presented in seven chapters through which critical studies on various methods of analysis of arch dams, their limitations, relevance of approximation of geometry, and various load vectors in the case of an arch dam and how these are resolved effectively by finite element method are made.

First Chapter contains the studies on various types and methods of analysis of arch dams, a literature review of the researches done, limitations of the conventional methods, constraints of the available software for the analysis of thick multiple radius arch dams, reliability of three dimensional finite element method and the need of this research. According to the set objectives an appropriate methodology is also developed.

Second Chapter presents the steps and concepts in the finite element analysis of an elastostatic solid continuum. Concept of interpolation, strain-displacement and stress strain relations, finite element equations, assembly of element matrices, isoparametric formulation, coordinate transformation and Jacobian matrix, interpolation functions of 8, 20 and 27 noded hexahedral elements are included in this Chapter.

In the ***Third Chapter***, a basic general purpose finite element program for the three dimensional analysis of a solid continuum with hexahedral elements is developed using OOP taking into consideration the various input data like Geometry, Material Property, Displacement boundary conditions and Load. A pseudo code for the input to the finite element analysis program and various subroutines are presented. Knowing the

nodal displacements of an element, the strain at any point of the element is obtained by strain-displacement relations and the stresses by using the constitutive relations. The developed program is validated with standard numerical examples worked out for nodal loads, boundary conditions and comparing with structural mechanics solutions.

Chapter Four gives the development of an automatic mesh generator and making of it *problem specific*. The basic idea of mesh generation is to generate element connectivity and nodal coordinate data and modeling the irregular geometry for the continuum to be analyzed with *three dimensional mapping technique using higher order polynomials*. For varying degree of approximation, Lagrange family of elements is used and the results validated by plotting with *Matlab*.

In C***hapter Five****,* various loads considered, except temperature effects, in the analysis of an arch dam and how it can be effectively applied with finite element method is discussed in detail along with validation. The various loads acting on the structure are applied as Global and Element load vectors**.** The body and surface load vectors are incorporated at element level itself for accuracy including seismic effects and arrived by numerical integration. Hydrostatic and dynamic pressure have components in all the three directions which are effectively solved taking in to consideration, the direction cosines of the pressure at each point and by numerical integration in the finite elements itself.

Sixth Chapter includes the application of the program to a conventional USBR arch dam designed as per guidelines for various load vectors and discretisation. The results of deflections, hoop and vertical stresses are plotted and verified with the

available results. Convergence with various discretisation and influence of material properties like unit weight, modulus of elasticity in deflection and stresses developed are studied and results tabulated. A parametric study with respect to varying reservoir water level is also made and results arrived, tabulated, plotted and presented. In addition, a case study; *Idukki arch dam in Kerala which is a double curvature parabolic arch dam of 160 m height,* is modelled with varying degree in the respective direction and analyzed for various discretisations.

Seventh Chapter gives the summary and conclusion including scope for future work.

As an ***Annexure,*** Idukki Arch dam taken for case study and its geometry derived by 80 nodal points with varying degree of polynomial in the respective direction is analyzed, with the developed program for various discretisations and load combinations as required for arch dams and the results tabulated and plotted.

Chapter 01

1.0 INTRODUCTION

Dams are generally constructed for flood control and conservation. Various purposes for conservation are irrigation, power generation, navigation, domestic, recreational and industrial purposes. The selection of dam type depends on the purpose for which it is built, site topography, storage capacity, hydrology, availability of local construction materials etc.[1,2] Consideration of the tri-dimensional arch action to hold water load in a narrow gorge brought the idea of arch dam. Of all the dam types creating water storage facilities, arch dams curving across the breadth of the valley with one mighty vault are doubtlessly the most economic and elegant, exacting the needs of concrete and rock.[3,4] The conventional methods adopted for the analysis of all types of arch dams are *cylinder theory, method of independent arches, trial load and model analysis* which are found to be of limitations for multiple radius arch dams of height greater than 100 m.[5,6] Later, accurate methods are necessitated by eliminating many assumptions made in the traditional methods for ensuring safety and economy which led to numerical methods such as *finite difference, finite element* and *boundary element* for arch dams. Of these, finite element is the most effective method for handling a continuum like arch dam since, it gives a more realistic stress distribution and more flexibility with regard to geometry and boundary conditions than other methods.[6-9] Hence, a critical study on how the finite element method resolves the complexity in the case of an arch dam of varying geometry is presented in this thesis.

1.1 THE NEED

Earlier, finite element method with two dimensional analysis using plane stress and plane strain as well as shell theory that actually approximates three-dimensional problem by two-dimensional one were used. Though it gives good results for a thin arch dam, thick arch dam requires a rigorous three dimensional analysis.[9-12] Studies as well as software are seen developed so far using isoparametric brick elements; *8-21 nodes,* as well as shell elements; *16 nodes,* for modeling the geometry which will not accurately define the complex geometry of a thick arch dam of variable curvature especially the extrados curve.[12-20] Hence, there is an urgent need for considering the effect of variable curvature by approximating the geometry with higher order polynomials incorporating more nodal points at element level itself while modeling.

The available literature and software show that the hydrostatic pressure on the curved surface is seen approximated as *normal to the surface* by means of certain global coefficients to the horizontal pressure on vertical surface.[14-19] In fact, the magnitude as well as direction will be varying at each point, i.e. water pressure will be normal to the curved surface, *horizontal and vertical extrados,* with components in the three directions. In the finite element method, water pressure needs to be considered more accurately as actual distributed surface forces on each element by direction cosines and numerical integration.[20,21] Similarly the silt pressure, uplift and dynamic effect of the reservoir water also will have to be considered at element level itself.

In the available general purpose programs, the self-weight of each element is assumed to act at the centre of gravity and provided as lumped masses at the nodes

which is also approximate.[15-20] The load vector due to gravity, if taken as a body force by numerical integration throughout the volume of each element, can give more dependable results. The seismic inertial effects by way of equivalent static load components as horizontal and vertical peak ground acceleration then can also be incorporated in the body force like this.

Trial load analysis gives comparable results with 3D Finite element method only for the simple cylindrical shape and for variable curvature arch dams of greater height the trial load assumptions are dubious. Recent studies considering the various aspects of design, variable curvature arch dams are found to be more practical for valleys of heights exceeding 100m.[4,5,22,23] Hence, it is felt that there is a great need for rigorous three dimensional finite element analysis to study the actual performance of a practical arch dam structure by approximating the actual geometry with higher order polynomials considering the surface pressure components in all the three directions and body force components in the respective direction by developing a software using advanced programming technique equipped with effective pre-post processing facilities.[20-27]

1.2 TYPES OF ARCH DAMS

The definition for an arch dam by ICOLD includes all curved dams, where the base-thickness is less than 0.6 times the height.[2] Mainly arch dams are grouped into:

(i) Constant radius

(ii) Variable radius

(iii) Constant angle

(iv) Multiple arch

(v) Cupola (shell)

(vi) Arch gravity

(vii) Mixed type

1.3 METHODS OF ANALYSIS OF ARCH DAMS

This is decided by the shape optimization studies.[4] Main methods of design of arch dams according to Varshney are categorized into:

(i) *Preliminary methods*

a. Thin cylinder theory

b. Thick cylinder theory

c. Elastic theory

d. Active arch method

e. Cain's method

f. U.S.B.R. criteria

g. Institution of Engineers, London

h. R. S. Varshney's equations

(ii) *Elaborate methods*

a. Inclined arch method

b. Tolke method

(iii) *Trial load analysis*

USBR

(iii) *More elaborate methods*

a. Finite element method

b. Shell analysis method

c. Three-dimensional elastic solution

d. Finite difference method

e. Three-dimensional electric analogue

f. Dynamic relaxation of three-dimensional elastic solution

(v) *Experimental method*

Model studies

According to CBIP publication the methods of analysis commonly adopted are discussed below:[5]

(i) *Cylinder Theory*

The simplest and the earliest of the methods available for the design of an arch dam is the cylinder theory. In this theory, the stress in an arch dam is assumed to be the same as in a cylindrical ring of equal external radius. The arch thickness is calculated by the thin cylinder formula. The cylinder theory does not allow for the discontinuity of the arch at the abutment and is, therefore, highly approximate. The use of cylinder theory has been restricted to dams less than 30 m in height located in narrow valleys. A low value of permissible stress in concrete, usually about 60 per cent of the permissible stress, issued to allow for the highly approximate nature of the formula. The cylinder theory is only of historical importance now.

(ii) *Method of Independent Arches*

This method considers the dam to be made up of a series of arches with no interaction between them. It is assumed that all horizontal water loads are carried horizontally to the arch abutments by arch action and that only the dead load weights

plus the vertical water loads in the case of sloping upstream face are carried vertically to the foundation by cantilever action. If the canyon is relatively regular and narrow and the dam is of low height so that a symmetrical thin structure with large central angle can be adopted this method may give reasonably satisfactory results.

Practically the water load is transferred to the foundation and abutments, both by horizontal arch action and vertical cantilever action. The vertical cantilevers are restrained at the foundation and must bend under their share of water load until their deflected positions coincide with the deflected positions of horizontal arch elements. The theory that the entire water load is carried horizontally to the abutments is therefore, incorrect and the design that ignores vertical cantilever action can seldom be considered as wholly satisfactory.

(iii) ***Arch Cantilever (Trial Load) Method***

The most commonly accepted method of analysing arch dams assumes that the horizontal water load is divided between the arches and cantilevers so that the calculated arch and cantilever deflections are equal at all conjugate points in all parts of the structure. Because the required agreement of all deformations is obtained by estimating various load distributions and computing the resulting movements until the specified conditions are fulfilled, the procedure is logically called *trial-load method.* Trial load analyses may be classified into the following types depending on their relative accuracy and corresponding complexity.

a. Crown Cantilever Analysis

Crown-cantilever analysis consists of an adjustment of radial deflections at the crown cantilever with the corresponding deflections at the crowns of arches. This type

of analysis assumes a uniform distribution of radial load from the crowns of arches to their abutments and neglects the effects of tangential shear and twist. While the results obtained from this analysis are rather crude, it has the advantage of very short time to complete the analysis. If used with judgment, it is an effective tool for appraisal studies.

b. Radial Deflection Analysis

A radial deflection analysis is one in which radial deflection agreement is obtained at arch quarter points with several representative cantilevers by an adjustment of radial loads between these structural elements. With the use of this type of analysis, loads may be varied between the crowns and abutments of arches, thus producing a more realistic distribution of load in the dam. A radial deflection analysis may be used for a feasibility study.

c. Complete Trial Load Analysis

A complete trial-load analysis is carried out by properly dividing the radial, tangential and twists loads between the arch and cantilever elements until-agreement is reached for arch of the three axial and three rotational movements for each arch cantilever node point. The accuracy of this analysis is limited only by the exactness of the basic assumptions, the number of vertical and horizontal elements chosen, and the magnitude of the error permitted in the slope and deflection adjustments. In view of the comprehensive and involved nature of the complete trial-load analysis, it is desirable that preliminary studies of tentative dams are first carried out by simplified methods; *crown cantilever analysis and radial deflection analysis*, to obtain a dam; *proposed for complete trial load analysis*, which is most suitable for the given site and whose dimensions are as close to the final as practicable.

(iv) ***3D Finite Element Analysis***

The deformations and stresses in an arch dam can alternatively be determined by three-dimensional finite element analysis which provides a more accurate solution of the problem and is being increasingly used. The finite elements can be extended to include the foundation and appropriate moduli values can be used whether the foundation is homogeneous or not, which avoids the use of Vogt's approximate assumptions on contact area and distribution of loading. According to Zienkewicz, the trial load method gives comparable results with 3D finite element analysis only for the simple cylindrical shapes. In doubly curved dams of modern type, the trial load assumptions are dubious and recent comparisons show that, in fact, considerable differences exist between its results and those of full 3D treatment.

1.4 FINITE ELEMENT METHOD

Although the detailed analysis of an arch dam can be done by various methods as explained in Section 1.3, the most reliable and accurate method used is the finite element method. A theoretical prediction by using a mathematical model which contains a set of differential equations will be more reliable than a physical model; *experimental investigation,* because the small scale model may not always simulate all the features of the actual continua. For this purpose, it is appropriate to go for a mathematical description of the physical model; each ordinary as well as partial differential equations expresses a certain conservative principle. Here, for an arch dam, a three dimensional continua is to be analysed. Each variable inside the continua as well as its dependent variable must be in balance with various factors that influence the variable. Thus, for the quantitative description of physical phenomena an analyst go

for a system of partial and ordinary differential equations valid for a certain domain and impose on the system suitable boundary and initial conditions. Various forms of discretisations exist in which the infinite set of unknown functions is replaced by a finite number of unknown parameters.

Various numerical methods for continuum discretisations are finite difference, finite element and boundary element methods. Although finite element and finite difference methods discretise the continuum, both generate algebraic simultaneous equations to be solved for nodal degrees of freedom and of about the same accuracy. Finite element method is very much appropriate for the analysis of continua with irregular geometry and non homogeneous materials. Finite element method requires more computation time. This most accurate method, with most powerful modern computers, is used to analyse structural mechanics problems.

The merits of a computer aided finite element analysis of an arch dams are:

- The cost of a computer run will be far economical than a corresponding experimental investigation.
- Computational investigations will be of remarkable speed and designer can study the implications of different configurations faster and can choose the optimum design from among several possible designs.
- Computer solution gives detailed and complete information for all the relevant variables throughout the domain of interest.
- Realistic conditions can be simulated in the theoretical calculations and convergence achieved faster.

1.5 LITERATURE REVIEW

The researches done for the arch dam design, analysis, construction and functioning are summarized as under:

The search for the best shape for arch dams and the optimization of the shapes with relevant analysis methods taking in to account the effect of curvature and constraints of construction evolved various solutions like constant/variable angle, constant/variable curvature, single/double/multiple curvature arches, membrane shapes etc. These aspects have been very critically studied, papers consolidated and published.[4] A numerical model for membrane shape is seen developed to find the equilibrium position of a membrane shell under external loadings and boundary conditions. The automatic checking of the stresses were then done by the general finite element programs like ADAP, SAP etc or dependable methods of analysis like shell theory and complete adjustment methods. US Commission on Large Dams has concluded the next iteration of reporting on the numerical analysis of dams in June 1999, indicates that computer simulation of dams continues to be a topic of pressing national interest.[8]

In the shape optimization studies, the main methods adopted for finite element mesh formulation and refinement were movements of selected boundary nodes, boundary shapes and spline functions which eliminates higher order polynomials.[4] Since conventional methods were used for analysis, the most common trial load method in which the dam as an assemblage of arches and cantilevers, the finite element mesh was also developed along vertical and horizontal directions in resemblance with the arches and cantilevers.[26,27] Criteria for analysis and design of arch dams have been dealt with by many engineers and methods evolved as explained in 1.3.

Extensive researches are seen in the area of rock mechanics, since the characteristics of the foundation strata has of vital importance in the stability, using *boundary and block element* methods. Recently block theory has been widely used for the elastic visco plastic and stochastic analysis of discontinuous rock masses.[28-32] Arch dams were also analyzed by block elements and coupled trial load and block element method where the arch dam is considered as an arch cantilever system and foundation as block element system.[33] Stability analysis of dam abutments by 3D elasto plastic finite element method is seen in a case study with Hough gravity arch dam in China.[34] Sliding and stability analysis of dam foundation as well as slope stability analysis with *finite elements* was attempted for the stability of rock slopes for foundation and abutments.[35-39] Simulation and stability of cracks and fractures have been experimentally as well as with crack model studied, stability checked.[40-44] Fracture analysis of concrete with discrete crack model was done by the boundary element method seepage analysis of crack and cracking analysis with a three dimensional finite element model.[45] In many of the conferences it has came a matter of importance the numerical analysis of arch dams and the ultimate strength evaluation numerically.[4-9] Shell elements were widely used for the finite element analysis of thin curved dams and for which software have been developed.[14,46,47]

Boundary element method has been found very effective in reservoir descretisation and modeling for seismic analysis. Fluid domain may be more conveniently handled by the boundary element method and dam water foundation interaction effects.[48-51] Dynamic analysis of arch dam including hydro dynamic effect and seismic analysis with boundary element method are also attempted.[52,53] The finite element and boundary element methods are seen combined for the fluid

structure interaction studies in time domain.[54,55] Shaking table test for fragments of gravity and arch dams were also carried out.[56,57]. Dynamic response of arch dams in earthquake is experimentally and theoretically studied.[58-62] Researches are carried out for the seismic analysis which include dam water interaction and dam foundation interaction with instrumented structures case studies *California and Kobe* dam foundation rock interaction effects in frequency domain response functions.[63-66] Three dimensional analysis of spatially varying ground motions around a uniform canyon and impedance functions for foundation in a homogeneous half space.[67,68] The seismic response of a dam in frequency domain by boundary element, modal approach, (FE-HE)-BE model which allows for the rigorous representation of the dynamic interaction between the dam, foundation rock and water are studied.[69-74] Three dimensional fluid hyper element for dynamic analysis of concrete arch dams and impedance functions for three dimensional foundation supported on an infinitely long canyon of uniform cross-section in a homogeneous half-space are also studied.[75-77] Analysis of arch dam including seismic effect is attempted by continuum damage concrete model for gravity dam reservoir systems.[78-81] Distributed memory parallel element by element scheme based on *Jacobi* conditioned conjugate gradient for 3D finite element analysis is seen developed.[82]

Most investigators recently use *Finite Element Method,* a procedure by which a three dimensional continuum is approximated by an assemblage of discrete elements interconnected only at a finite number of nodal points having a finite number of unknowns, for the numerical simulation of the continuum. Detailed formulations of the FEM are given using isoparametric elements and three dimensional mapping techniques.[6,9,20,21,24] *Zienkiewicz* has developed an automatic mesh generator

scheme for plane and curved surfaces using isoparametric coordinates in which a complex region is divided into eight noded quadrilaterals which are viewed in the form of a rectangular pattern.[10] Saini in 1991, has attempted finite element static analysis for the *Kasari* dam. As two-dimensional analysis is an approximation in the transition zone of the dam where rapid changes occur in the thickness of the dam, in order to obtain a realistic picture of the stress distribution and the region of stress concentration, a three-dimensional finite element analysis was carried out using twenty noded elements. But this analysis is applicable for straight gravity dams only. Dynamic analysis was also done for the effect of seismic forces.

S. S Rao carried out a two-dimensional stress analysis for selected concrete dams by the finite element method and this was also intended for straight concrete gravity dams.[11] Bathe, Wilson, and Peterson in 1974 and *Ghanaat* in 1993 has developed two widely used software for finite element analysis of arch dams namely *SAP-IV* and *GDAP*.[14] *SAP-IV* is a general purpose finite element computer program for the static and dynamic analysis of linearly elastic structures and continua. This program has been designed for the analysis of large structural systems. Its element library for dam analysis includes eight node and variable number node, 3D solid elements.[16] The program can handle various static loads including hydrostatic pressures, temperature, gravity due to weight of the material, and concentrated loads applied at the nodal points. *However, the program lacks pre and post processing capabilities. Thus, finite element meshes of the dam and foundation must be constructed manually from the input nodal coordinates and element connectivities.*

GDAP has been specifically designed for the analysis of arch dams. It uses the basic program organization and numerical techniques of *SAP-IV* but has pre and post processing capabilities. It uses thick shell elements, which is represented by its mid surface nodes. *The 16 noded shell element in the GDAP and general 3D solid elements of 8 and 21 nodes are found used for modeling the geometry.* An appropriate finite element mesh for an arch dam can only be achieved by careful consideration of the dam geometry and the type of analysis for which the dam is modeled. For example, the finite element model of a double curvature thin shell structure differs from the model of a thick gravity arch section.[15] Other general purpose FEM programs such as *ABAQUS (1988), NISA (2001), STAD PRO 2005* etc., can also be used in the analysis of three dimensional continuums by shell or tri linear quadratic elements, but not specific to the point of thick curved elements. *One of the most important requirements in arch dam analysis is to develop accurate models, representative of the actual 3D behavior of the system.*

The necessary Geometric Data for constructing a finite element mesh of an arch dam is obtained from drawings containing information defining the geometry of the dam shape.[7,9,15] These include the plan view and section along the reference plane. In practice, arch dams are geometrically described as multi centered arches with their centers varied by elevation in addition to the arch opening angles and radii varying for each side with elevation. *Preparation of finite element mesh data from these geometric data is very time consuming especially for multi layer meshes because most general purpose finite element programs cannot directly handle these data which is another draw back.*

1.6 LIMITATIONS OF THE RESEARCH

A specialized arch dam analysis program is necessary which can automatically generate coordinates of all nodal points, element data, element distributed loads and the nodal boundary conditions from the available limited geometric data. Though studies have been done for the analysis of arch dams by various numerical methods, the main ambiguity is whether the model represents the three dimensional geometry effectively; which then accompanies with a model study. Moderately thick arch dams are modeled essentially similar to the thin arch dams, except that 3D solid elements should be used near the base and the abutment regions where the shell behavior assumption becomes invalid due to excessive thickness of the arch whereas gravity arch dams should be modeled by two or more layers of solid elements in the thickness direction depending on their section thickness. *It is very important to note that multilayer element meshes are essential to determine a detailed stress distribution across the thickness of a thick arch dam. A three dimensional automatic mesh generator is essential for the pre processing stage of such a multilayer descretisation.* A sketch showing half of an arch dam on Rock canyon is shown in Fig 1.1 and the plan and elevations in Fig 1.2 and 1.3 respectively.

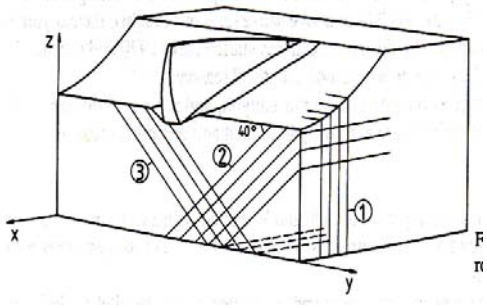

Fig 1.1: ***Arch dam on rock canyon***

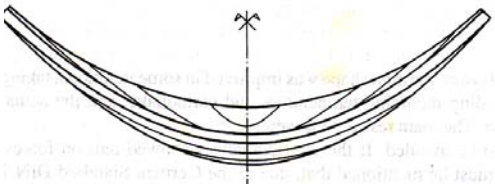

Fig 1.2: ***Plan view of the arch dam***

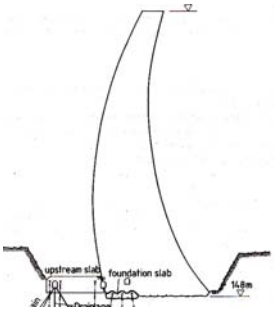

Fig 1.3: ***Sectional Elevation***

The arch dam descretisation are seen as an assemblage of horizontal arches and vertical cantilevers. The 16 node shell and general 3D solid elements of 8 and 21 nodes provided for modeling the geometry are not sufficient to accurately define the shape of a thick variable curvature arch dam. *This limitation in shape approximation as explained above is to be resolved by the help of higher order polynomial shape functions including more number of nodes at element level relevant to the curve in each direction to take care of the curvature effect.*[24,26,83,84] *The descretisation using tri quadratic brick element and vertical arch-cantilever system is shown in* Fig 1.4.

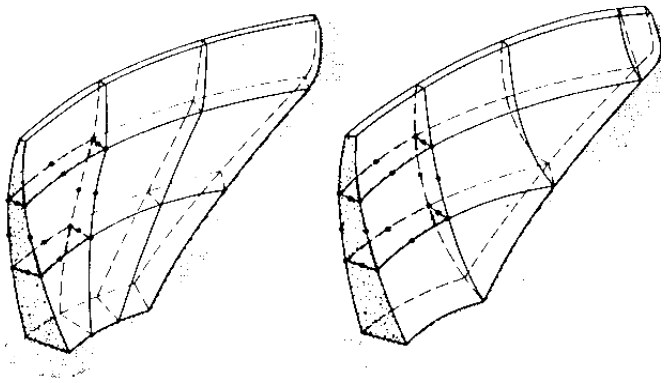

Fig 1.4: ***Half of an arch dam; Different descretisation***

In most of the studies and programs intended for concrete gravity dams as explained above, the hydrostatic pressure is considered to act normal to the surface and thus acts in the same direction for all the elements of that face. Even in the finite element method analysis studies for an arch dam, the load vectors assumed with certain coefficients for horizontal hydrostatic pressure. For an arch dam of complex geometry, the water pressure on each point acts in a direction normal to the surface; the surface being curved in both directions the magnitude as well as direction of water pressure varies from point to point; element to element depending on the height of water column. This normal hydrostatic pressure to the surface will have components in all the three directions which have to be dealt accurately in the finite element method rather using coefficients.[20] Similarly the pressure due to the accumulated silt is also to be considered. *This aspect is to be effectively solved taking in to consideration, the direction cosines of the pressure at each point and by numerical integration in the finite elements itself for which a program which resolves the pressure to all the three directions at a particular point is required.* Fig1.5 gives a schematic representation of the distribution of loads and radial deflection of cantilevers in the Trial load method.

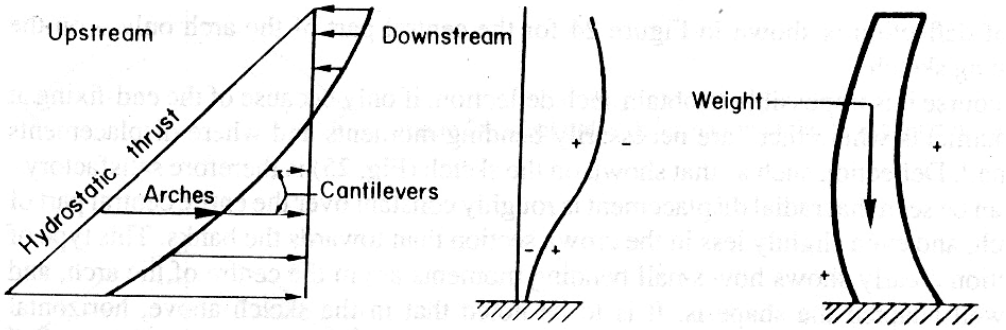

Fig 1.5: ***Distribution of Loads and radial deflection cantilevers;*** *Trial Load Method*

In addition, hydrodynamic pressure is also generated due to successive lateral movements of the upstream face of the dam against reservoir water occurring under earthquake. This pressure is found to be the same as that would occur if a body of water confined between a certain parabola and the face of the dam were forced to move with the dam while the rest of the reservoir remained inactive.[23,85,86] *Depending on the direction of peak ground acceleration, this hydro dynamic effect is to be incorporated as surface pressures at element level by numerical integration and direction cosines as well as inertial forces acting on the dam and water body.* Arch dams constructed in the narrowest gorges in the river contour for forming the reservoir causes chances of generation of water waves due to gravity as well as wind effects. These formed waves on impinging causes energy dissipation or reflected standing waves. This dynamic effect of water pressure incorporated in the finite element program by suitable methods will improve the efficiency.

The other possible load vectors due to change in chemical properties with aging, temperature effects, silt pressure, uplift, fluctuation of reservoir level, gravity and body forces, seismic effect etc which affects deflection and stress values will have to be

considered in the finite element program.[5,9,85,86] This will be required for obtaining a reliable computer simulation.

It is felt from the above limitations that, apart from the general purpose software, a problem specific software for the 3D analysis of an arch gravity dam structure using quadratic hexahedral elements, defining the geometry accurately with the help of advanced computer programming technique with verification by plotting capable of handling various load vectors and applicable to a variety of structural mechanics problems is essential to be developed.

Hence the scope of the present work is to find out suitable methods for resolving the above limitations using finite element method and the development of a finite element analysis software for the elastostatic analysis of an arch dam having efficient pre and post processing capabilities equipped with the above load vectors which is capable of handling a variety of structural mechanic problems using the advanced object oriented programming technique: *Visual* C^{++}, a simultaneous finite-element plotting program in *Matlab* corresponding to the *Visual* C^{++} program arrived with various options of plotting the original shape, deflected shape, sectional plan.[87] Established works of similar nature/case studies are intended for verification and comparison of results along with parametric studies.

1.7 OBJECTIVES

Objectives are formulated based on the above limitations as follows:

- To develop an accurate basic ***Finite Element Software*** having pre and post processing capabilities for three dimensional elasto static analysis of a solid continuum using linear and quadratic hexahedral elements capable of accommodating an arch dam geometry using the Object Oriented Programming Technique; *Visual* C^{++}.
- To develop a more reliable method for approximating an arch dam geometry of complexity; *variable curvature,* using three dimensional mapping with higher order polynomials of the required degree in the respective directions and to supplement with a problem specific ***Automatic Mesh Generator*** which gives two and three dimensional plots of the original and deflected profile directly in *Matlab*.
- To develop a method to handle the varying ***hydrostatic pressure*** for each reservoir levels acting on the curved boundary of an arch dam in magnitude and direction from element to element so as to improve the result of analysis and further verification of the actual instrumentation values. Similarly, ***silt pressure*** as well as ***hydrodynamic pressure*** due to reservoir water during earthquake, ***self weight*** as body force due to gravity at element level by numerical integration and ***inertial forces*** of dam due to horizontal and vertical earthquake accelerations.
- Validation of the Mesh Generator by plotting in *Matlab* and analysis software developed with linear quadratic elements and various load vectors by comparing the results with basic structural mechanics solutions and established similar works.
- To study the applicability of the developed program in the effect of curvature, different loading conditions, varying reservoir levels; *parametric study,* with coarse and fine discretisation and comparison of the results such as deflections at nodal points, element and nodal stresses with established works.

1.8 METHODOLOGY

A flow diagram to arrive the above objectives of the research is shown below. Finite element program is developed for a three dimensional solid continuum in *Visual* C^{++} and plots using *Matlab.*

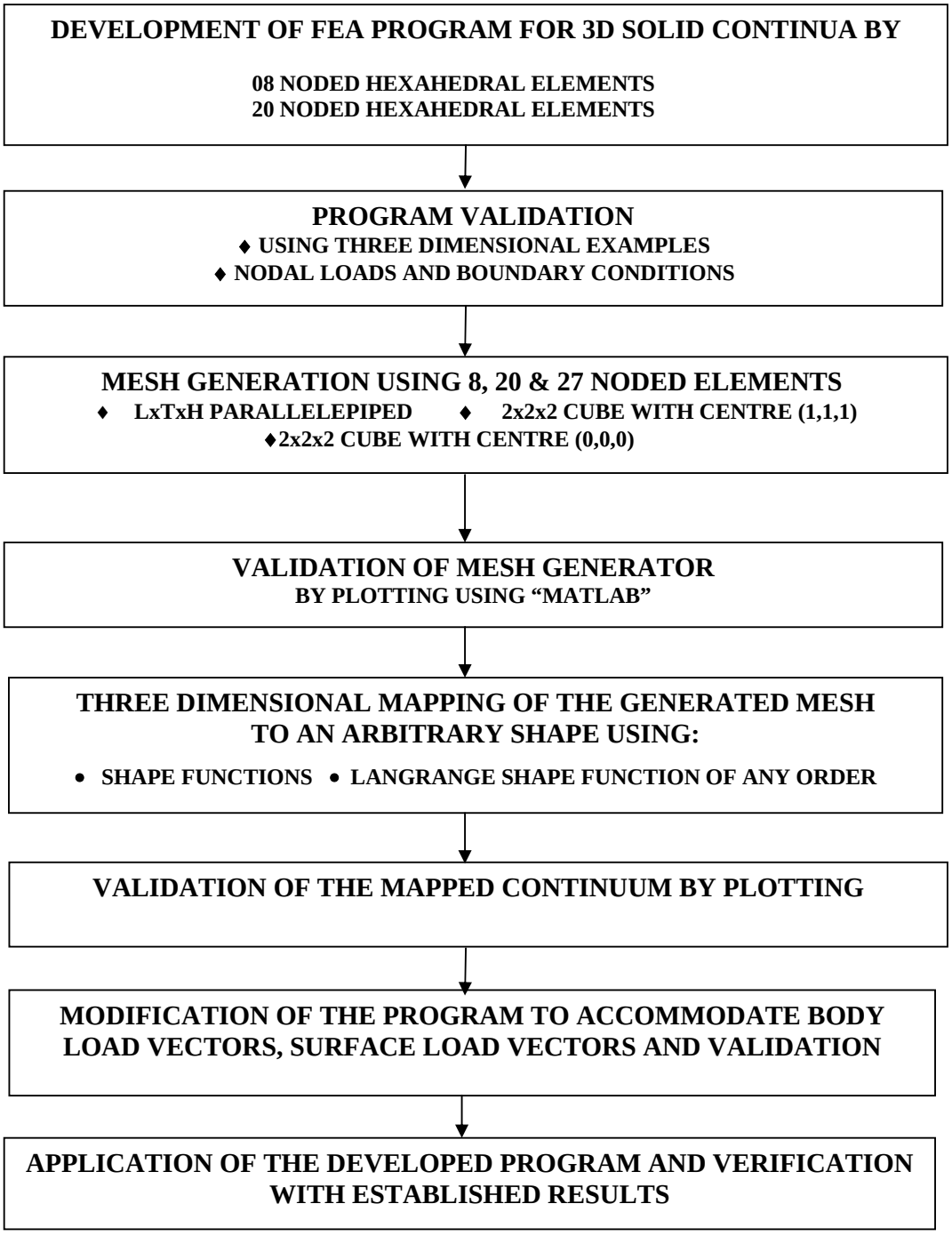

Chapter 02

2.0 CONCEPTS IN THE FINITE ELEMENTANALYSIS OF AN ELASTO STATIC SOLID CONTINUUM

Finite element method has been established as a powerful and versatile numerical procedure for analysing a variety of engineering problems. In the research, finite element method is used for the elastostatic analysis of a solid continuum like arch dams, which are modeled in a three dimensional domain. This method models a continuum as an assemblage of small elements of simple geometry that is easier to analyse than the actual structure. Thus, a complex solution is approximated by a model that consists of piece-wise continuous simple solutions.

2.1 STEPS OF FINITE ELEMENT ANALYSIS

Major steps involved in the finite element analysis of a structure are:

1. Discretisation of continuum into many sub regions called finite elements. Formulation of element properties, loads, deformations associated with degrees of freedom, boundary conditions.
2. Assemblage of elements to obtain finite element model of the structure.
3. Application of known loads in terms of nodal forces and moments.
4. Application of displacement boundary conditions.
5. Solution of simultaneous algebraic equations to determine nodal degrees of freedom, which are the basic unknowns of the problem.

6. Calculation of strains and stresses and output the results by an interpretation program.

The entire domain is discretised into a large number of sub regions of different sizes, shapes and orientations called finite elements. These finite elements are assumed to be connected to each other only at a finite number of points called 'nodes'. The field variables; *in the present case, displacements,* are approximated by piecewise continuous functions. Nodal values of the field variables are treated as the unknowns and are determined by making use of related variational principles. Once the nodal displacements are determined, the secondary variables such as stresses and strains are obtained by means of *strain-displacement* and *stress-strain* relations.

2.1.1 Concept of Interpolation

Interpolation means approximation of the value of a function between known values by operating on the known values with a formula different from the function itself. In the finite element context, the known values are the degrees of freedom to be found by solving algebraic equations.

The nodal displacements of each element are assumed by known means. The nodal displacement vector for the element is given by:

$$\{u^e\} = \left[u_1\ v_1\ w_1\ u_2\ v_2\ w_2 ... u_n\ v_n\ w_n\right]^T \tag{2.1}$$

where u_i, v_i, w_i are the nodal displacement degrees of freedom. Knowing the element displacement vector $\{u^e\}$, the interior displacement field within the element is obtained by interpolation.[21]

$$\begin{Bmatrix} u(x,y,z) \\ v(x,y,z) \\ w(x,y,z) \end{Bmatrix} = \sum N_i u_i = \begin{bmatrix} N_1 & 0 & 0 & N_2 & 0 & 0 & ... & N_n & 0 & 0 \\ 0 & N_1 & 0 & 0 & N_2 & 0 & ... & 0 & N_n & 0 \\ 0 & 0 & N_1 & 0 & 0 & N_2 & ... & 0 & 0 & N_n \end{bmatrix} \begin{Bmatrix} u_1 \\ v_1 \\ w_1 \\ . \\ . \\ . \\ u_n \\ v_n \\ w_n \end{Bmatrix} \quad (2.2)$$

$$\{u\} = N_1 u_1 + N_2 u_2 + ... + N_n u_n = [N]\ \{u^e\} \quad (2.3)$$

where [N] is called the interpolation or shape function matrix.

2.1.2 Strain Displacement Relation

Once the displacement vector at any point is known, the strain vector is obtained by making use of the strain displacement relations. For three-dimensional elastostatic problems these relations are given by:

$$\begin{Bmatrix} \varepsilon_x \\ \varepsilon_y \\ \varepsilon_z \\ \gamma_x \\ \gamma_y \\ \gamma_z \end{Bmatrix} = \begin{bmatrix} \frac{\partial}{\partial x} & 0 & 0 \\ 0 & \frac{\partial}{\partial y} & 0 \\ 0 & 0 & \frac{\partial}{\partial z} \\ \frac{\partial}{\partial y} & \frac{\partial}{\partial x} & 0 \\ 0 & \frac{\partial}{\partial z} & \frac{\partial}{\partial y} \\ \frac{\partial}{\partial z} & 0 & \frac{\partial}{\partial x} \end{bmatrix} \begin{Bmatrix} u \\ v \\ w \end{Bmatrix} \quad (2.4)$$

or

$$\{\varepsilon\} = [L]\{u\} \tag{2.5}$$
$$= [L][N]\{u^e\}$$
$$= [B]\{u^e\}$$

where [B], which relates the interior element strain field to the element nodal displacement vector, is very important in the finite element analysis. It is called the strain-displacement matrix.

2.1.3 Stress Strain Relation

The stress vector $\{\sigma\}$ and the strain vector $\{\varepsilon\}$ for a three dimensional homogeneous linearly elastic isotropic continuum is related to each other by the constitutive matrix [D].

$$\{\sigma\}_{(6\text{ x }1)} = [D]_{(6\text{ x }6)}\ \{\varepsilon\}_{(6\text{ x }1)} \tag{2.6}$$

The matrix [D] is given by:

$$[D] = \overline{E}\begin{bmatrix} (1-\mu) & \mu & \mu & 0 & 0 & 0 \\ & (1-\mu) & \mu & 0 & 0 & 0 \\ & & (1-\mu) & 0 & 0 & 0 \\ & & & \frac{1-2\mu}{2} & 0 & 0 \\ & \textit{symmetric} & & & \frac{1-2\mu}{2} & 0 \\ & & & & & \frac{1-2\mu}{2} \end{bmatrix} \tag{2.7}$$

where, $\overline{E} = \dfrac{E}{(1+\mu)(1-2\mu)}$

In the above E and μ are the Young's modulus and Poisson's ratio respectively. Thus, the stress field in the element can be found.

2.1.4 Finite Element Equations

Basic finite element equation can be arrived at by the principle of virtual work.[21] The virtual displacement field within the element by imposing a virtual displacement field can be written as:

$$\delta u = [N]\{\delta u^e\} \tag{2.8}$$

The virtual strain corresponding to the above element nodal virtual displacement vector $\{\delta u^e\}$ is given by:

$$\{\delta\varepsilon\} = [B]\{\delta u^e\} \tag{2.9}$$

By equating the internal virtual work done to the external virtual work,

$$\int_{V_e} \{\delta\varepsilon\}^T \{\sigma\} dV_e = \int_{V_e} \{\delta u\}^T \{b\} dV_e + \int_{S_e} \{\delta u\}^T \{p\} dS_e \tag{2.10}$$

where, V_e and S_e are the element volume and surface area respectively; $\{b\}$ is the body force vector and $\{p\}$ denotes the surface force acting over the periphery of the element. Making use of Eq. (2.7), (2.8) and (2.9) in Eq. (2.10) we get:

$$\{\delta u^e\}^T \int_{V_e} B^T DB dV_e \{u^e\} = \{\delta u^e\}^T \left[\int_{V_e} N^T \{b\} dV_e + \int_{S_e} N^T \{p\} dS_e \right] \tag{2.11}$$

Since $\{\delta u^e\}$ represents an arbitrary nodal virtual displacement vector, Eq. (2.11) can be written as:

$$[k^e]\{u^e\} = \{r^e\} \tag{2.12}$$

where
$$[k^e] = \int_{V_e} B^T DB dV_e \tag{2.13}$$

and
$$\{r^e\} = \int_{V_e} N^T \{b\} dV_e + \int_{S_e} N^T \{p\} dS_e \tag{2.14}$$

In the above, $[k^e]$ is called the *element stiffness matrix* and $\{r^e\}$ is called the *element load vector*.

2.1.5 Assembly of Element Matrices

Element stiffness matrices and load matrices are combined by a process known as the *assembly*, to arrive at the finite element equations of the entire structure. Thus

$$[K]\{U\} = \{R\} \tag{2.15}$$

where, $$[K] = \sum_{e=1}^{nElems} [k^e] \text{ and}$$

$$\{R\} = \sum_{e=1}^{nElems} \{r^e\} \tag{2.16}$$

Eq. (2.15) is a set of simultaneous linear algebraic equations. Once boundary conditions are prescribed, it can be solved to arrive at the global displacement vector $\{U\}$ from which the element nodal displacement vector $\{u^e\}$ can be extracted from which the displacement, strain and stress fields within the element can be found.

2.2 ISOPARAMETRIC FORMULATION

Isoparametric formulation is used to generate elements with irregular shapes and curved boundaries, which are needed in modelling arch dams.

2.2.1 Concept of Isoparametric Formulation

The same set of polynomial interpolation functions are used for defining the geometry and interpolating the displacement field in an isoparametric element. Thus the components of the displacement vector at any interior point are interpolated from the nodal values as;

$$u(\xi,\eta,\zeta) = \sum_{i=1}^{n} N_i u_i$$

$$v(\xi,\eta,\zeta) = \sum_{i=1}^{n} N_i v_i$$

$$w(\xi,\eta,\zeta) = \sum_{i=1}^{n} N_i w_i \tag{2.17}$$

where n is the number of nodes per element and N_i are the interpolation polynomials. The isoparametric mapping is given by

$$x(\xi,\eta,\zeta) = \sum_{i=1}^{n} N_i x_i$$

$$y(\xi,\eta,\zeta) = \sum_{i=1}^{n} N_i y_i$$

$$z(\xi,\eta,\zeta) = \sum_{i=1}^{n} N_i z_i \tag{2.18}$$

where, x_i, y_i, z_i are the global coordinates of the nodal points of the element.

2.2.2 Coordinate Transformation and Concept of Jacobian Matrix

Derivatives of the displacement field with respect to *x, y, z* coordinates are needed in order to determine the strain components. These are not readily available as the displacement field is known in terms of the local coordinates ξ, η, ζ and not in terms of the global coordinates *x, y, z* as given by Eq. (2.17). Required derivatives are obtained by means of the following transformation which follows from the chain rule of partial differentiation.

$$\begin{Bmatrix} \frac{\partial}{\partial \xi} \\ \frac{\partial}{\partial \eta} \\ \frac{\partial}{\partial \zeta} \end{Bmatrix} = \begin{bmatrix} \frac{\partial x}{\partial \xi} & \frac{\partial y}{\partial \xi} & \frac{\partial z}{\partial \xi} \\ \frac{\partial x}{\partial \eta} & \frac{\partial y}{\partial \eta} & \frac{\partial z}{\partial \eta} \\ \frac{\partial x}{\partial \zeta} & \frac{\partial y}{\partial \zeta} & \frac{\partial z}{\partial \zeta} \end{bmatrix} \begin{Bmatrix} \frac{\partial}{\partial x} \\ \frac{\partial}{\partial y} \\ \frac{\partial}{\partial z} \end{Bmatrix} = [J] \begin{Bmatrix} \frac{\partial}{\partial x} \\ \frac{\partial}{\partial y} \\ \frac{\partial}{\partial z} \end{Bmatrix} \tag{2.19}$$

In the above [*J*] is called the Jacobian matrix. It is obtained by making use of

Eq. (2.18). Thus $J = \begin{bmatrix} \sum N_{i,\xi} x_i & \sum N_{i,\xi} y_i & \sum N_{i,\xi} z_i \\ \sum N_{i,\eta} x_i & \sum N_{i,\eta} y_i & \sum N_{i,\eta} z_i \\ \sum N_{i,\zeta} x_i & \sum N_{i,\zeta} y_i & \sum N_{i,\zeta} z_i \end{bmatrix}$

$$= \begin{bmatrix} N_{1,\xi} & N_{2,\xi} & \dots & N_{n,\xi} \\ N_{1,\eta} & N_{2,\eta} & \dots & N_{n,\eta} \\ N_{1,\zeta} & N_{2,\zeta} & \dots & N_{n,\zeta} \end{bmatrix} \begin{bmatrix} x_1 & y_1 & z_1 \\ x_2 & y_2 & z_2 \\ \vdots & \vdots & \vdots \\ x_n & y_n & z_n \end{bmatrix} \tag{2.20}$$

2.2.3 Interpolation Functions

Standard eight, twenty, twenty seven noded and higher order hexahedral elements are proposed for modeling the three-dimensional elastic continuum. The interpolation functions used for the eight-noded elements are the *Lagrangian* tri-linear interpolation polynomials.[20,24,84] These are given by

$$N_i = \frac{1}{8}(1+\xi\xi_i)(1+\eta\eta_i)(1+\zeta\zeta_i) \qquad i = 1, 2, 3\dots 8 \tag{2.21}$$

where, ξ_i, η_i, ζ_i are the local coordinates at node *i*. The twenty-noded element belongs to the serendipity family and the interpolation polynomials are given by:

Corner nodes:

$$N_i = \frac{1}{8}(1+\xi\xi_i)(1+\eta\eta_i)(1+\zeta\zeta_i)(\xi\xi_i + \eta\eta_i + \zeta\zeta_i - 2) \qquad i = 1 \text{ to } 8$$

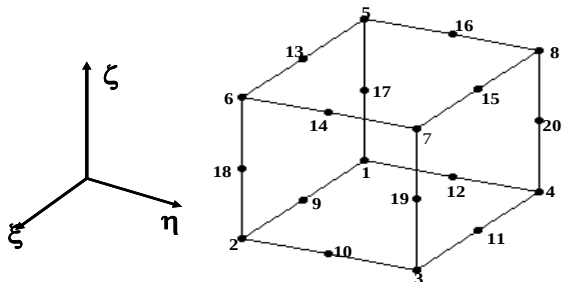

Fig 2.1: ***Local axes 20 noded element***

Mid side nodes in ξ direction

$$N_i = \frac{1}{4}(1-\xi^2)(1+\eta\eta_i)(1+\zeta\zeta_i) \quad i = 9, 11, 13, 15$$

Mid side nodes in η direction

$$N_i = \frac{1}{4}(1-\eta^2)(1+\xi\xi_i)(1+\zeta\zeta_i) \quad i = 10, 12, 14, 16$$

Mid side nodes in ζ direction

$$N_i = \frac{1}{4}(1-\zeta^2)(1+\xi\xi_i)(1+\eta\eta_i) \quad i = 17, 18, 19, 20 \qquad (2.22)$$

The twenty seven noded elements belong to the Lagrangian tri-quadratic family and the interpolation polynomials are arrived.[24,25]

Corner Nodes

$$N_i = \frac{1}{8}(1+\xi\xi_i)(1+\eta\eta_1)(1+\zeta\zeta_i)(\xi\xi_i+\eta\eta_i+\zeta\zeta_i-2)(\xi\xi_i\eta\eta_i\zeta\zeta_i)$$

Mid side nodes in ξ direction

$$N_i = \frac{1}{4}(1-\xi^2)(1+\eta\eta_i)(1+\zeta\zeta_i)\,\eta\eta_i\ \zeta\zeta_i$$

Mid side nodes in η direction

$$N_i = \frac{1}{4}(1-\eta^2)(1+\xi\xi_i)(1+\zeta\zeta i)\xi\xi_i\ \zeta\zeta_i$$

Mid side nodes in ζ direction

$$N_i = \frac{1}{4}(1-\zeta^2)(1+\xi\xi_i)(1+\eta\eta_i)\,\xi\xi_i\;\eta\eta_i$$

Mid face nodes in ξ direction

$$Ni = \frac{1}{2}(1-\zeta^2)(1-\eta^2)(1+\xi\xi)\xi\xi_i$$

Mid face nodes in η direction

$$N_i = \frac{1}{2}(1-\zeta^2)(1-\xi^2)(1+\eta\eta_i)\,\eta\eta_i$$

Mid face nodes in ζ direction

$$N_i = \frac{1}{2}(1-\xi^2)(1-\eta^2)(1+\zeta\zeta_i)\;\zeta\zeta_i$$

Mid body node

$$N_i = (1-\xi^2)(1-\eta^2)(1-\zeta^2)$$

where i = 1, 2, 3, … ,27 (2.23)

2.2.4 Element Stiffness Matrix

Strains are obtained from displacements as

$$\{\varepsilon\} = [L]\,\{u\} \quad (2.24)$$

where, $\{u\} = [N]\,\{u^e\}$

Substituting in Eq.2.24 $\{\varepsilon\} = [L]\,[N]\,\{u^e\}$ (2.25)

$$\{\varepsilon\} = [B]\,\{u^e\}$$

Thus, $[B] = [L]\,[N]$ (2.26)

[*B*] is called strain-displacement transformation matrix.

$$\text{where } [L] = \begin{bmatrix} \frac{\partial}{\partial x} & 0 & 0 \\ 0 & \frac{\partial}{\partial y} & 0 \\ 0 & 0 & \frac{\partial}{\partial z} \\ \frac{\partial}{\partial y} & \frac{\partial}{\partial x} & 0 \\ 0 & \frac{\partial}{\partial z} & \frac{\partial}{\partial y} \\ \frac{\partial}{\partial z} & 0 & \frac{\partial}{\partial x} \end{bmatrix} \tag{2.27}$$

$$\text{and } [N] = \begin{bmatrix} N_1 & 0 & 0 & N_2 & 0 & 0 & \cdots & N_n & 0 & 0 \\ 0 & N_1 & 0 & 0 & N_2 & 0 & \cdots & 0 & N_n & 0 \\ 0 & 0 & N_1 & 0 & 0 & N_2 & \cdots & 0 & 0 & N_n \end{bmatrix} \tag{2.28}$$

$[N]$ expressed in terms of ξ, η, ζ coordinates can be changed to x, y, z coordinates by invoking chain rule for $\frac{\partial}{\partial x}, \frac{\partial}{\partial y}, \frac{\partial}{\partial z}$. The element stiffness matrix $[k^e]$ from the principle of virtual work as arrived earlier is then:

$$[k^e] = \int_{V_e} B^T D B \, dV_e = \int_{-1}^{1}\int_{-1}^{1}\int_{-1}^{1} B^T D B \, dx\, dy\, dz = \int_{-1}^{1}\int_{-1}^{1}\int_{-1}^{1} B^T D B J \, d\xi\, d\eta\, d\zeta \tag{2.29}$$

The above integral is evaluated by using numerical integration method. The Gauss integration method is most widely used in finite element analysis, for evaluating the integral of a function.[21, 25]

$$\int_{-1}^{+1}\int_{-1}^{+1}\int_{-1}^{+1} \Phi(\xi\, \eta\, \zeta)\, d\xi\, d\eta\, d\zeta = \sum_i \sum_j \sum_k W_i W_j W_k \Phi(\xi_i\, \eta_j\, \zeta_k) \tag{2.30}$$

Using Gauss quadrature rule the above integral in Eq. (2.29) will become:

$$[k^e] = \sum_i \sum_j \sum_k W_i W_j W_k B^T D B(\xi, \eta, \zeta) J \tag{2.31}$$

Chapter 03

3.0 DEVELOPMENT OF ANALYSIS SOFTWARE IN C++

Finite element analysis involves three stages of activities namely:

Pre processing, that involves the preparation of data such as nodal coordinate connectivity, boundary conditions and loading and material properties.

Processing, that involves stiffness generation, stiffness modification, solution of equations resulting in the evaluation of nodal variables, other derived quantities such as stresses, strains etc.

Post processing, that deals with the presentation of results such as deformed configuration, stress and strain distributions etc.

In this chapter, main finite element analysis program is developed in *Visual C++*. Its accuracy is ascertained by solving simple examples and verifying the results obtained with worked out results, using basic strength of materials solution.[20,87] Once, basic program is validated, it can be applied to the required domain and problem evaluated.

3.1 DESCRIPTION OF THE FINITE ELEMENT PROGRAM

A basic, general purpose finite element program for the three dimensional analysis of a solid continuum is developed using *OOP* using the *FORTRAN* subroutine *QUAD4* for a four noded plane element.[24]

3.1.1 Functions used in the Program

Main program requires various input data for analysis, which are listed below:

Geometry data, which includes the number of nodes, number of elements, nodal coordinates and element connectivity.

Material property data, for each element which consists of the Modulus of elasticity, Poisson's ratio and the Unit weight of material.

Displacement boundary conditions data, that includes the list of nodes with partial or complete displacement restraints, and the list of restraint degrees of freedom at each such node.

Load data, that reads all types of loads applied to the structure such as concentrated nodal loads, distributed surface loads; *water pressure, silt pressure, and load due to road traffic,* and distributed body forces; *static loads due to self weight and ground acceleration.*

Mesh generator program provides all the above data and the output of the mesh generator can directly be fed in the input for the finite element analysis program. A pseudo code for the input to the finite element analysis program developed is modified for a solid continuum as given below.[87]

```
Input nNodes, nElems
For i = 1, nNodes
input k, x(k), y(k),  z(k)
```

Element connectivity data

Input the node number corresponding to the node numbers of the basic element in the same order for all the elements.

```
For i = 1, number of elements
```

```
Input k, node (1, k), node (2, k), node (n, k)
```

where, n is the number of nodes of the basic element chosen.

Displacement boundary conditions

Destination array is used to store the addresses to which the elements of the matrices $[k^e]$ and $\{r^e\}$ must be posted. This destination array is first initialized with zeros. The destination array is a rectangular matrix which has many columns as the number of nodes and as many rows as the number of degrees of freedom per node. The displacement boundary conditions are fed into this array as 1's and 0's.

Initialise destination array

```
For i = 1, number of nodes
      For j = 1, 2, 3
      Destn (i, j) = 0
```

The number of nodes with displacement boundary condition prescribed is then input. Corresponding to each of this node, the boundary condition should be input as follows:

```
For i = 1,nDisplRestraints
Input k, destn(1, k), destn(2, k), destn(3, k)
```

Input '1' for degrees of freedom which are restrained and '0' for degrees of freedom which are free.

The destination array is now scanned column wise and each column from top to bottom. Each '1' is converted into '0' and '0' is replaced by a counter. In this way the elements of the destination array represent the degree of freedom number. The last number in the destination array represents the number of equations, i.e., the total number of degrees of freedom of the finite element model.

For updating the destination array the following procedure is followed.

```
neq = 0;

for i = 1, nNodes
for j = 1, 3
if destn (i, j) = 0;
       neq = neq + 1;
       id(i, j) = neq;
else: id(i, j) = 0;
       destn(i, j) = 0;
endif
```

Assembling of element stiffness matrices

The *nod* array and the *destn* array are used to assemble the element stiffness matrices and the load vectors to get the global stiffness matrix and the global load vector respectively. Before assembly, these global arrays are initialized.

Concentrated nodal loads, if any acting in the degrees of freedom direction, it is fed directly into the global load vector as,

```
For i = 1, neq
R(i) = 0;
For j = 1, neq
K(i, j) = 0;
```

Input nNconc,

where, Nconc is the number of nodes at which concentrated loads are applied.

```
For i = 1, nNconc

input k, Fx, Fy, Fz;
dof1 = destn(k, 1)
dof2 = destn(k, 2)
dof3 = destn(k, 3)
R(dof1) = Fx
R(dof2) = Fy
R(dof3) = Fz
```

Assembly of global matrices

Invoke element subprogram to get element stiffness matrix and the load vector.

```
      For n = 1, nElems
      call elem stiffness;
      nod 1 = nod(1, n);
      nod 2 = nod(2, n);
      nod 3 = nod(3, n);
      …        …
      …        …
      nod i = nod(i, n);

      kk(1) = destn(1, nod 1)
      kk(2) = destn(2, nod 1)
      kk(3) = destn(3, nod 1)
      kk(4) = destn(1, nod 2)
      kk(5) = destn(2, nod 2)
      kk(6) = destn(3, nod 2)
      kk(7) = destn(1, nod 3)
      kk(8) = destn(2, nod 3)
      kk(9) = destn(3, nod 3)
      …           …       …
      …           …       …
      kk(3i - 2) = destn(1, nod i)
      kk(3i - 1) = destn(2, nod i)
      kk(3i) = destn(3, nod i)


For i = 1,  6
      if kk(i) > 0;
            krow = kk(i);
      R(krow) = R(krow) + r(i)
      endif

For j = 1,  6
      if kk(j) > 0;
      kcol = kk(j);
      K(krow, kcol) = K(krow, kcol) +ke(i, j)
```

3.1.2 Solution of Equations

We have, $$[K]\{U\} = \{R\} \qquad (3.1)$$

where $[K]$ – global stiffness matrix

$\{R\}$ – global load vector

These matrices are obtained by a process called “assembly” that can be mathematically represented as:

$$[K] = \sum_{e=1}^{nElems} [k^e]$$

$$\{R\} = \sum_{e=1}^{nElems} \{r^e\}$$

This summation implies a special type of matrix addition called 'assembly'.

Eq (3.1) can be partitioned as:

$$\begin{bmatrix} K_{ff} & K_{fr} \\ K_{rf} & K_{rr} \end{bmatrix} \begin{Bmatrix} U_f \\ U_r \end{Bmatrix} = \begin{Bmatrix} R_f \\ R_r \end{Bmatrix} \tag{3.2}$$

Showing the restrained and free (subscripts *r* and *f*) degrees of freedom. In general $\{U_r\} = 0$; the null vector equation becomes

$$[K_{ff}]\{U_f\} = \{R_f\} \tag{3.3}$$

Thus only K_{ff} part of the stiffness matrix; *the reduced stiffness matrix,* need be stored. $\{R_f\}$ are applied loads and $\{R_r\}$ are the support reaction. The support reactions are obtained after solving equations above for the unknown free degrees of freedom $\{U_f\}$. The element nodal displacements are extracted from $\{U\}$ and are used to calculate $\{r^e\}$ knowing $\{u^e\}$.

$$[k^e]\ \{u^e\} = \{r^e\}$$

Once the global stiffness matrix and the global load vector have been assembled we arrive at a system of linear algebraic equations as given by $[K_{ff}]\{U_f\} = \{R_f\}$ whose solution gives the unknown free degrees of freedom $\{U_f\}$ of the problem for which Gauss elimination method is adopted in the program and outlined in 3.3.

3.2 LINEAR AND QUADRATIC ELEMENTS

Depending on the profile of the surface; the degree of curve, the analysis can be carried out using linear quadratic hexahedral elements as explained in 2.2.3.

3.3 COMPUTATION OF DEFLECTION

The global stiffness matrix obtained will be symmetric and banded for structural mechanics problems. The *symmetry* and *bandedness* of the stiffness matrix can be utilized to save the computational time and memory requirement in the present work. The developed finite element program gives global displacements in the three dimensions as detailed above by *Gauss elimination method*.[21,84]

void gauss(void)

```
{
//Converting the FORTRAN statements from R D Cook et al (p595)
      int lim;
      int semiband;
      semiband = neq;
// Treat the case of one or more independent equations
      if (semiband <= 1)
      {
            for (i=1; i<=neq; ++i)
            global_disp[i]=global_load[i]/ global_stiffness[neq][1];
            return;
      }

// Forward reduction of stiffness matrix
      for (n=1; n<=neq-1; ++n)
      {
            lim = min(semiband, neq + 1 - n);
            for (l=2; l<=lim; ++l)
            {
                  dum=global_stiffness[n][l]/global_stiffness[n][1];
                  i = n + l - 1;
                  j = 0;
                  for (k=l; k<=lim; ++k)
                  {
                  j ++;
                  global_stiffness[i][j]-dum*global_stiffness[n][k];
                  }
                  global_stiffness[n][l] = dum;
            }
      }

// Forward reduction of load vector
      for (n=1; n<=neq-1; ++n)
      {
            lim = min(semiband, neq + 1 - n);
            for (l=2; l<=lim; ++l)
            {
                  i = n + l - 1;
            global_load[i]-= global_stiffness[n][l]*global_load[n];
            }
            global_load[n] = global_load[n]/global_stiffness[n][1];
```

```
      }
      global_load[neq] = global_load[neq]/global_stiffness[neq][1];

// Back substitution phase
      for (n=neq-1; n>=1; --n)
      {
            lim = min(semiband, neq + 1 - n);
            for (l=2; l<=lim; ++l)
            {
                  k = n + l - 1;
            global_load[n]-=global_stiffness[n][l] * global_load[k];
            }
      }
      for (i=1; i<=neq; ++i)
            global_disp[i] = global_load[i];
      return;
}
```

3.4 COMPUTATION OF STRESSES AND STRAINS

Once nodal displacements of an element are known, it is possible to obtain the displacements at any point on the element using interpolation. Then, strain at any point on the element can be obtained by making use of the strain-displacement relations, and the stresses by using constitutive relations. As the *strain-displacement* relation involves partial differentiation and as numerical differentiation always introduces additional errors, the strains; *hence the stresses too,* are evaluated with less accuracy. As a general observation, it is stated that stresses computed at the nodes are least accurate. On the other hand, in most of the finite element analyses, it is convenient and important to obtain the nodal values of the stresses. Stresses are evaluated with maximum accuracy at a few points on the element called optimal points also known as the *Barlow points,* which are located in the interior of the element. The stress values at the finite element nodes can be obtained by extrapolating from the values at the optimal sampling points after averaging the values obtained at each node from the neighboring elements. For Isoparametric elements these sampling points are located at the Gauss points of one

order less than that required for full integration of the element stiffness matrix. There exists a standard Gauss rule for each type of element. For example, for a plane four-noded quadrilateral element a 2x2 Gauss rule is sufficient, and for an 8 or 9-noded quadratic element, a 3x3 rule is needed. For these elements, the Barlow points are located at the Gauss points corresponding to 1x1 rules for the four-noded element and 2x2 rules for the 8 or 9-noded element. Stresses at Gauss points can be interpolated or extrapolated to other points in the element.[21,88] This concept is extended to three dimensional isoparametric elements and applied in this project. Since, on finer dicretisation the nodal values of stresses show higher values, the elemental stresses are found based on the average value of Gauss points for each element. The stresses at the centroid of the element found by inputting (0,0,0) for the local coordinates are compared with this. The analysis is done with 4x4x4 Gauss rule so that the stress values corresponding to 3x3x3 Gauss points are obtained for each element. Thus, the most optimal 27 stress and strain values for each element are averaged to get more reliable element stresses and strains.

```
      // Computation of element stresses at Gauss points
fout << " Sig_x    Sig_y   Sig_z   Sig_xy    Sig_yz  Sig_xz \n  " ;
      double pxi, pet, pze;
      double stress[7], strain[7];
      for ( n=1;  n<= no_of_elems; ++n)
      {
      for (int ii=1; ii<=20; ++ii)
                  {
                        xl[ii] = x[nod[ii][n]];
                        yl[ii] = y[nod[ii][n]];
                        zl[ii] = z[nod[ii][n]];
                  }
            for (i=1; i<=ngauss-1; ++i)
                        {
                              pxi = place[i][ngauss-1];
                              for (j=1; j<=ngauss-1; ++j)
                              {
                              pet = place[j][ngauss-1];
                   for (k=1; k<=ngauss-1; ++k)
                                    {
                                        pze = place[k][ngauss-1];
quad20_stress(n, pxi, pet, pze);  //pxi=pet=pze=0 gives stress at centroid
```

```
fout << "\n " << n << " (" << i << ", " << j << ", " << k << ")";
      for (int kk=1; kk<=6; ++kk)
                  fout << stress[kk] << "   ";
                              }
                        }
                  }
            }


// Compute strains at element guassian points
fout << "  Eps_x    Eps_y   Eps_z   Eps_xy  Eps_yz  Eps_xz\n";
            double pxi, pet, pze;
            for (n=1; n<=no_of_elems; ++n)
            {
                  for (int ii=1; ii<=20; ++ii)
                  {
                        xl[ii] = x[nod[ii][n]];
                        yl[ii] = y[nod[ii][n]];
                        zl[ii] = z[nod[ii][n]];
                  }
                  for (i=1; i<=ngauss - 1; ++i)

                  {
                        pxi = place[i][ngauss-1];
                        for (j=1; j<=ngauss - 1; ++j)
                        {
                              pet = place[j][ngauss-1];
                              for (k=1; k<=ngauss - 1; ++k)
                              {
                                    pze = place[k][ngauss-1];
                                    quad20_stress(n, pxi, pet, pze);
fout<< "\n  " << n << " (" << i << ", " << j << ", " << k << ")  ";
                                    for (int kk=1; kk<=6; ++kk)
                                    fout << strain[kk] << "   ";
                              }
                        }
                  }
            }
void quad20_stress (int elem, double pxi, double pet, double pze)
      {
        int i, j, k;
        double u[61],DB[7][61];

      //Get element displacement vector
                              int dof, dof1, node;
                              dof1 = 0;

      for (i=1; i<=20; ++i)
                              {
                                    node = nod[i][elem];
                                    for (j=1; j<=3; ++j)
                                    {
                                          dof1 ++;
                                          dof = id[j][node];
                              if (dof != 0)
                              u[dof1] = global_disp[dof];

            else
                  u[dof1] = 0;
                        }
                              }
```

```
// Get B matrix
      shape_fun (pxi, pet, pze);

// [D]*[B]
      for (i=1; i<=6; ++i)
      {
            for (j=1; j<=60; ++j)
            {
                  DB[i][j] = 0;
                  for (k=1; k<=6; ++k)
                        DB[i][j] += D[i][k] * B[k][j];
            }
      }
// Compute stress as DB * u and strains as B * u
      for (i=1; i<=6; ++i)
      {
            stress[i] = 0;
            strain[i] = 0;
            for (j=1; j<=60; ++j)
            {
                  stress[i] += DB[i][j] * u[j];
                  strain[i] +=  B[i][j] * u[j];
            }
}
```

3.5 PROGRAM VALIDATION

Standard numerical examples are worked out with the basic program developed as explained above for the three dimensional finite element analysis of continuum using 8-noded and 20-noded hexahedral elements. Output from the *Mesh generator program* is directly fed as the input to the *Main Analysis Program* for 'Nodal Input' data. This general purpose program for the analysis of 3D solid continuum is applied for the solved problems for nodal loads and boundary conditions.[20,87]

3.5.1 Nodal Load Vector

Straight Cantilever Beam Example 1

A straight cantilever beam of length 1000, thickness 1, depth 100, modulus of elasticity = 200000; *(all in consistent units)* and Poisson's ratio = 0.2 is analyzed for

various descretisation using the developed program of 20-noded elements for a vertical point load of 100 units at the free end.[87]

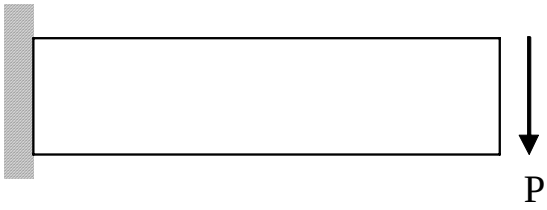

Fig 3.1: ***Cantilever beam; point load at free end***

The theoretical solution from strength of materials for the beam is:

Maximum deflection = 2.0, Maximum bending stress at the support; M/Z = 60. The solution arrived from the program is tabulated below in Table 3.1 and is found of very good conformity with the strength of materials solution. Deflected profiles are shown in Fig 3.2 and Fig 3.3.

Table 3.1: **Deflection at free end of a cantilever due to vertical point load**

Discretisation	Number of elements	Number of nodes	Deflection	Max Gauss point stress	Max Gauss point strain
1x1x1	**1**	**20**	**-1.5343**	**26.5066**	**0.000000**
4x1x1	4	56	-1.97449	44.807	0.0002207
10x1x4	40	353	-2.00584	57.849	0.0002699

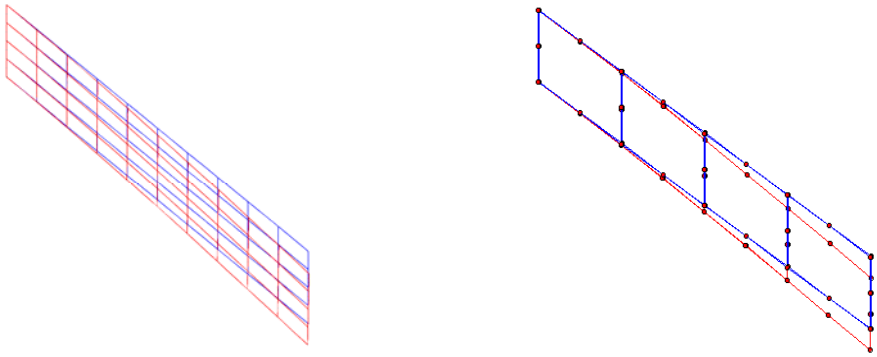

Fig 3.2: ***Deflected Profile of Cantilever 40 & 4 elements***

The program input and output for 1x1x1 discretisation is outlined below as an example.

if stream ("fem20.inp"); // *Output of Mesh Generator Program*

```
1          20         4        //  no_of_elems >> no_of_nodes >> ngauss;
200000   0.2        0        // E  >>   po  >>  gama;


// Nodal coordinates
1    0    0     0          2     0   0.5  0        3    0   1   0          4     0     0    50          5    0   1  50
6    0    0  100          7     0  0.5  100       8    0  1  100          9   500    0    0          10  500  1  0
11  500 0 100          12   500 1  100       13  1000  0    0        14  1000  0.5   0          15  1000  1  0
16  1000  0  50       17  1000  1  50       18  1000  0  100     19  1000  0.5  100       20  1000  1  100

// Nodal connectivity
1  3  1  13  15  8  6  18  20  2  9  14  10  7  11  19  12  5  4  16  17
8                    // Nodes at which displacements restricted
1          1 1 1     2          1 1 1     3          1 1 1     4          1 1 1
5          1 1 1     6          1 1 1     7          1 1 1     8           1 1 1
8          // Concentrated global loads at nodes
13         0          0          -20                14         0          0          -5
15         0          0          -20                16         0          0          -5
17         0          0          -5                 18         0          0          -20
19         0          0          -5                 20         0          0          -20
```

of stream fout ("fem20.out")

Three Dimensional Problems with 20 Noded Quadratic Brick Elements

Number of elements = 1

Number of nodes = 20

Number of gaussian points = 4

E = 200000 po = 0.2 gama solid = 0 Ebar = 277778

D is:

222222	55555.6	55555.6	0	0	0
55555.6	222222	55555.6	0	0	0
55555.6	55555.6	222222	0	0	0
0	0	0	83333.3	0	0
0	0	0	0	83333.3	0
0	0	0	0	0	83333.3

Nodal Coordinates

Node	X	Y	Z
1	0	0	0
2	0	0.5	0
3	0	1	0
4	0	0	50
5	0	1	50
6	0	0	100
7	0	0.5	100
8	0	1	100
9	500	0	0
10	500	1	0
11	500	0	100

12	500	1	100
13	1000	0	0
14	1000	0.5	0
15	1000	1	0
16	1000	0	50
17	1000	1	50
18	1000	0	100
19	1000	0.5	100
20	1000	1	100

Element Connectivity

1	2	3	4	5	6	7	8	9	10	11	12	13	14	15	16	17	18	19	20
3	1	13	15	8	6	18	20	2	9	14	10	7	11	19	12	5	4	16	17

Number of nodes at which displacement is prescribed = 8

1 1 1 1	2 1 1 1	3 1 1 1	4 1 1 1
5 1 1 1	6 1 1 1	7 1 1 1	8 1 1 1

ID Array

0 0 0 0 0 0 0 0	0	1	4	7	10	13	16	19	22	25	28	31	34
0 0 0 0 0 0 0 0	0	2	5	8	11	14	17	20	23	26	29	32	35
0 0 0 0 0 0 0 0	0	3	6	9	12	15	18	21	24	27	30	33	36

Number of degrees of freedom = 36

Semiband width = 36

No of Loaded Joints=8

13 0 0 -20	14 0 0 -5	15 0 0 -20	16 0 0 -5
17 0 0 -5	18 0 0 -20	19 0 0 -5	20 0 0 -20

Global Load Array

Node	load-X	load-Y	load-Z
1	0	0	0
2	0	0	0
3	0	0	0
4	0	0	0
5	0	0	0
6	0	0	0
7	0	0	0
8	0	0	0
9	0	0	0
10	0	0	0
11	0	0	0
12	0	0	0
13	0	0	-20
14	0	0	-5
15	0	0	-20
16	0	0	-5
17	0	0	-5
18	0	0	-20
19	0	0	-5
20	0	0	-20

Global Displacement Array

Node	disp-X	disp-Y	disp-Z
1	0	0	0
2	0	0	0
3	0	0	0

4	0	0	0
5	0	0	0
6	0	0	0
7	0	0	0
8	0	0	0
9	-0.077340231	-1.96767344e-005	-0.399360978
10	-0.077340229	1.84593572e-005	-0.399360978
11	0.077340229	1.84783826e-005	-0.399360978
12	0.077340231	-1.96577090e-005	-0.399360978
13	-0.147120923	-6.77299848e-006	-1.534326585
14	-0.147120928	-2.43562359e-006	-1.534326688
15	-0.147120918	1.90175089e-006	-1.534326586
16	-2.40348e-009	-2.39898812e-006	-1.533245892
17	2.39423e-009	-2.39898811e-006	-1.533245892
18	0.147120918	1.97777770e-006	-1.534326585
19	0.147120928	-2.35959678e-006	-1.534326688
20	0.147120923	-6.69697165e-006	-1.534326586

Stresses at Element Gauss Points

Element	Gauss-Points	Sig_x	Sig_y	Sig_z	Sig_xy	Sig_yz	Sig_xz
1	(1, 1, 1)	-20.74483708	-0.524467518	1.688209784	-0.001190341	0.00975507155	-2.7039137
1	(1, 1, 2)	3.609358e-007	-3.4168702e-008	-1.58379e-008	1.214081e-008	0.009755071	-2.649879028
1	(1, 1, 3)	20.7448378	0.5244674505	-1.688209816	0.0011903198	0.00975507	-2.703913707
1	(1, 2, 1)	-20.74483815	-0.524467664	1.68820961	-1.1630845e-008	2.54658516e-010	-2.70391268
1	(1, 2, 2)	-1.85703811e-009	-2.61681054e-011	-5.810891045e-009	1.21436927e-008	0	-2.649878005
1	(1, 2, 3)	20.74483815	0.524467660	-1.688209628	-9.4965509e-009	1.455191523e-011	-2.70391268
1	(1, 3, 1)	-20.74483781	-0.5244674497	1.688209802	0.00119031774	-0.00975507089	-2.703913533
1	(1, 3, 2)	-3.646502e-007	3.411567e-008	4.214072e-009	1.211678e-008	-0.009755070	-2.649878854
1	(1, 3, 3)	20.74483708	0.524467518	-1.688209794	-0.001190338902	-0.009755071063	-2.703913526
1	(2, 1, 1)	-22.7530768	1.163500713	-0.9695088917	0.0008991945472	-0.01140229407	1.075857606
1	(2, 1, 2)	3.8406597e-007	2.587210e-008	4.09301e-008	-9.373196e-009	-0.01140229467	1.129892279
1	(2, 1, 3)	22.75307757	-1.163500662	0.9695089735	-0.0008991787401	-0.01140229512	1.075857601
1	(2, 2, 1)	-22.75307789	1.163500511	-0.9695091083	7.82441794e-009	5.31144905e-010	1.075855946
1	(2, 2, 2)	-6.06889e-010	5.488620e-011	1.5332807e-009	-9.36765e-009	-8.731149e-011	1.129890622
1	(2, 2, 3)	22.75307789	-1.163500511	0.9695091114	7.985966937e-009	-5.5661075e-010	1.075855947
1	(2, 3, 1)	-22.75307758	1.163500661	-0.9695089725	-0.000899178914	0.01140229512	1.075857699
1	(2, 3, 2)	-3.852798e-007	-2.576219e-008	-3.786426e-008	-9.37711e-009	0.0114022945	1.129892377
1	(2, 3, 3)	22.75307681	-1.163500713	0.9695088968	0.0008991946938	0.01140229413	1.075857704
1	(3, 1, 1)	-26.50667475	-4.129964007	-5.372585813	0.002988726258	-0.00637928666	-2.703911209
1	(3, 1, 2)	4.055975e-007	8.55790e-008	9.003905e-008	-3.230056e-008	-0.00637928	-2.649876535
1	(3, 1, 3)	26.50667557	4.129964178	5.372585993	-0.002988676354	-0.006379287134	-2.703911212
1	(3, 2, 1)	-26.50667587	-4.12996427	-5.372586079	2.34279142e-008	2.08274286e-010	-2.703915548
1	(3, 2, 2)	-9.602843e-010	-2.025235e-010	1.198344e-009	-3.229144e-008	-3.8198e-011	-2.64988080
1	(3, 2, 3)	26.50667587	4.12996427	5.372586082	2.64953043e-008	-2.528395271e-010	-2.703915548
1	(3, 3, 1)	-26.50667558	-4.129964181	-5.372585993	-0.002988679421	0.006379287085	-2.70391119
1	(3, 3, 2)	-4.07518e-07	-8.598407e-08	-8.764181e-08	-3.2302e-08	0.0063792868	-2.6498765130
1	(3, 3, 3)	26.50667476	4.129964009	5.372585818	0.002988729327	0.006379286612	-2.703911186

Strains at Element Gauss Points

Element	Gauss-Points	Eps_x	Eps_y	Eps_z	Eps_xy	Eps_yz	Eps_xz
1	(1, 1, 1)	-0.000104887	1.643428e-005	2.97103535e-005	-1.428409e-008	1.170608e-007	-3.2446961e-005
1	(1, 1, 2)	1.8546853e-012	-5.15941e-013	-4.0595477e-013	1.456791e-013	1.170608e-007	-3.17985e-005
1	(1, 1, 3)	0.0001048879	-1.6434290e-005	-2.9710354e-005	1.4283838e-008	1.170608e-007	-3.244696e-005
1	(1, 2, 1)	-0.0001048879	1.6434290e-005	2.971035e-005	-1.3955049e-013	3.108624e-015	-3.2446956e-005
1	(1, 2, 2)	-3.447765782e-015	7.536337582e-015	-2.71703191e-014	1.457283814e-013	0	-3.179853606e-005
1	(1, 2, 3)	0.0001048873	-1.6434290e-005	-2.9710353e-005	-1.1396562e-013	1.1102230e-016	-3.244695e-005
1	(1, 3, 1)	-0.0001048879	1.6434290e-005	2.9710354e-005	1.4283812e-008	-1.1706085e-007	-3.244696e-005
1	(1, 3, 2)	-1.8615808e-012	5.310144e-013	3.5160687e-013	1.4542199e-013	-1.1706085e-007	-3.1798546e-005
1	(1, 3, 3)	0.0001048879	-1.64342897e-005	-2.9710353e-005	-1.4284066e-008	-1.1706085e-007	-3.24469e-005
1	(2, 1, 1)	-0.00011395937	2.9540089e-005	1.6742031e-005	1.079033e-008	-1.3682752e-007	1.291029e-005
1	(2, 1, 2)	1.853527e-012	-2.95635e-013	-2.05287614e-013	-1.1251167e-013	-1.3682753e-007	1.35587073e-005
1	(2, 1, 3)	0.000113959379	-2.954008e-005	-1.674203e-005	-1.079014e-008	-1.368275e-007	1.29102912e-005
1	(2, 2, 1)	-0.0001139593	2.954008e-005	1.674203e-005	9.3873452e-014	6.4392935e-015	1.291027136e-005
1	(2, 2, 2)	-4.6225869e-015	-6.513242e-016	8.217385e-015	-1.1240504e-013	-9.9920072e-016	1.3558687e-005
1	(2, 2, 3)	0.00011395938	-2.9540089e-005	-1.6742031e-005	9.583369e-014	-6.7168492e-015	1.2910271e-005
1	(2, 3, 1)	-0.00011395937	2.9540089e-005	1.6742032e-005	-1.0790146e-008	1.3682754e-007	1.291029e-005
1	(2, 3, 2)	-1.8627726e-012	2.943329e-013	2.217221e-013	-1.1254125e-013	1.3682753e-007	1.355870e-005
1	(2, 3, 3)	0.00011395937	-2.9540089e-005	-1.6742031e-005	1.0790336e-008	1.3682752e-007	1.2910292e-005
1	(3, 1, 1)	-0.000123030824	1.1229440e-005	3.7737097e-006	3.586471e-008	-7.6551439e-008	-3.2446934e-005
1	(3, 1, 2)	1.8523696e-012	-6.7741304e-014	-4.0981757e-014	-3.8761778e-013	-7.6551442e-008	-3.1798e-005
1	(3, 1, 3)	0.000123030827	-1.1229440e-005	-3.773709e-006	-3.586411e-008	-7.655144e-008	-3.244693e-005
1	(3, 2, 1)	-0.000123030829	1.122946e-005	3.7737097e-006	2.8113387e-013	2.4563684e-015	-3.24466e-005
1	(3, 2, 2)	-5.7973809e-015	-1.250860e-015	7.1559490e-015	-3.8749539e-013	-4.996003e-016	-3.179857e-005
1	(3, 2, 3)	0.0001230308	-1.122944e-005	-3.7737097e-006	3.1794260e-013	-3.0114799e-015	-3.2446986e-005
1	(3, 3, 1)	-0.0001230308	1.1229440e-005	3.7737097e-006	-3.5864153e-008	7.6551444e-008	-3.2446938e-005
1	(3, 3, 2)	-1.8639644e-012	6.5239575e-014	5.529241e-014	-3.8762453e-013	7.6551442e-008	-3.179851e-005
1	(3, 3, 3)	0.000123030824	-1.1229440e-005	-3.773709e-006	3.586475e-008	7.6551439e-008	-3.244693e-005

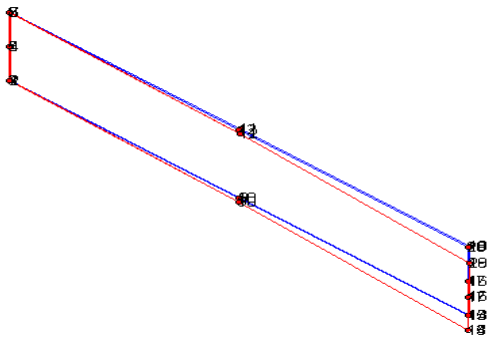

Fig 3.3: ***Deflected Profile of Cantilever 1 element***

Straight Cantilever Beam Example 2

A straight cantilever beam of length 200 cm, breadth 20 cm, depth 30 cm, modulus of elasticity = 2000 kN/cm^2 and Poisson's ratio = 0.0 is analysed for various descretisation using the developed program of 20 and 8-noded elements as given in Fig 3.4(a) and 3.4 (b).[20]

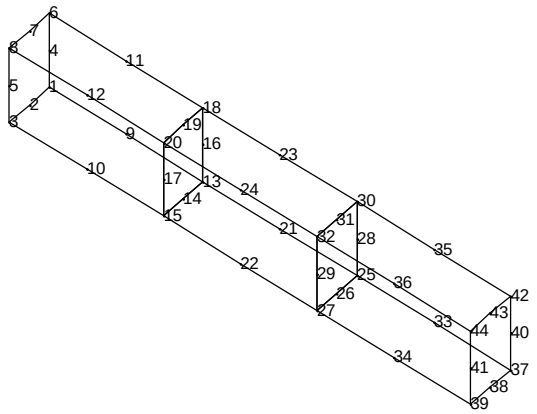

Fig 3.4: ***(a) Straight Cantilever 20 noded 3 elements***

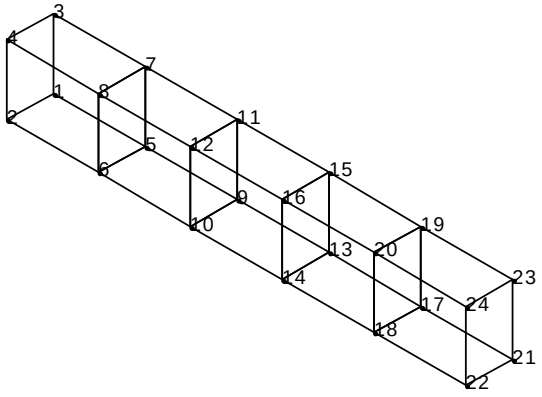

Fig 3.4: ***(b) Straight Cantilever 08 noded 5 elements***

Axial load of 10 kN at free end

An axial load of 10 kN is applied at the free end of a cantilever beam as shown in Fig 3.5 and analysis done for various descretisation using the developed program and the results compared with the theoretical deflection at free end given by $\frac{PL}{AE}$; Table 3.2.[20] Stresses are given in Table 3.3.

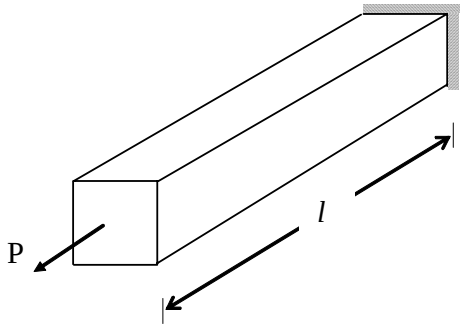

Fig 3.5: ***Cantilever beam; axial load at free end***

Table 3.2: **Deflection at free end of a cantilever due to axial load**

Hexahedral element chosen	**Number of elements**	**Number of nodes**	**Deflections at free end in cm**	
			Program	**Theory**
8 noded	5 10	24 44	0.00166667 0.00166667	0.00166667 ”
20 noded	2 5	32 68	0.00166667 0.00166667	” ”

Table 3.3: **Stresses at element Gauss points; 20 noded 5 elements**

Element	**Gauss point**	**Sig_x**	**Sig_y**	**Sig_z**	**Sig_xy**	**Sig_yz**	**Sig_xz**
1	(2, 2, 2)	0.01666	1.036e-14	1.76e-14	1.17e-17	-4.74e-18	-1.69e-17
2	(2, 2, 2)	0.01666	-4.943e-14	-9.21e-14	-6.72e-19	4.97e-18	-8.22e-18
3	(2, 2, 2)	0.01666	2.004e-13	3.72e-013	-5.64e-18	1.24e-17	-1.20e-17
4	(2, 2, 2)	0.01666	-6.602e-13	-1.44e-01	-4.66e-18	-2.49e-18	-1.56e-17
5	(2, 2, 2)	0.01666	3.443e-12	6.19e-12	2.34e-17	1.68e-17	1.49e-18

Stress at fixed end = 0.0166 kN/cm^2 (theory)

Point load of 10 kN at free end

A concentrated load of 10 kN is applied at the free end of a cantilever beam shown in Fig 3.6 in the vertical direction and analysis done for various descretisation using the developed program of 8 and 20 noded elements and the results tabulated in Table 3.4 and 3.5 are compared with the theoretical deflection and stress at free end given by $\frac{PL^3}{3EI}$. Deflected profile is given in Fig 3.7.

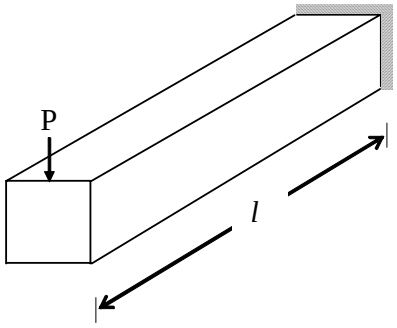

Fig 3.6: ***Cantilever beam; point load at free end***

Table 3.4: **Deflection at free end of cantilever due to point load of 10 kN at free end**

Hexahedral element chosen	**Number of elements**	**Number of nodes**	**Deflections at free end in cm**	
			Program	**Theory**
8 noded	5 10 20 25	24 44 84 104	-0.158627 -0.245152 -0.283800 -0.289340	-0.296297 ” ” ”
20 noded	2 5	32 68	-0.289921 -0.299275	” ”

Table 3.5: **Stresses at element gauss points with 20 noded 5 elements**

Element No.	Distance from free end	Sig kN/cm^2	Sig kN/cm^2	Sig kN/cm^2
1	180.0	0.598465	3.54059e-006	-6.498908e-006
2	140.0	0.474524	3.03625e-006	-2.493193e-005
3	100.0	0.350604	-2.17938e-005	0.000122288
4	60.0	0.226638	0.000122	-0.000482863
5	20.0	0.102690	-0.000610	0.001893046

Theoretical maximum stress = 0.6000 kN/cm^2

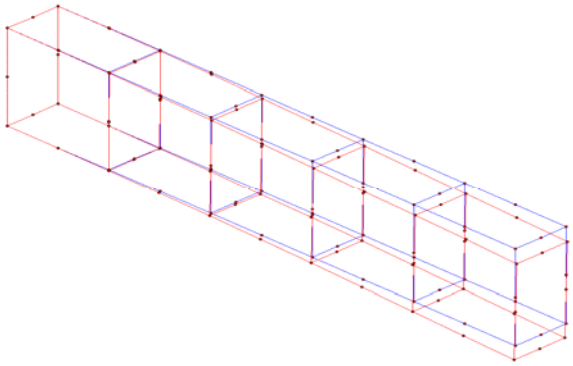

Fig 3.7: ***Deflected Profile of Cantilever beam 5 elements***

Curved Cantilever Beam Example 3

A concentrated load of 10 kN is applied at the free end of a curved cantilever beam Section 20 x 30 cm, radius 100 cm inside shown in Fig 3.8 towards the radial direction and analysis is done using the developed program of 20-noded elements and are compared with the deflection at the free end, as arrived.[21] The maximum deflection from the example is 0.25577 (with error 2.6%) whereas obtained from the program is tabulated below in Table 3.6 and found conforming. Deflected profile is shown in Fig 3.9.

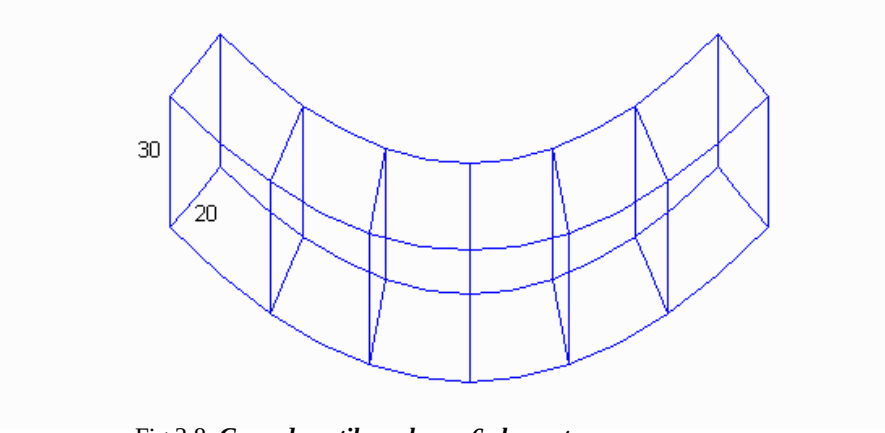

Fig 3.8: ***Curved cantilever beam 6 elements***

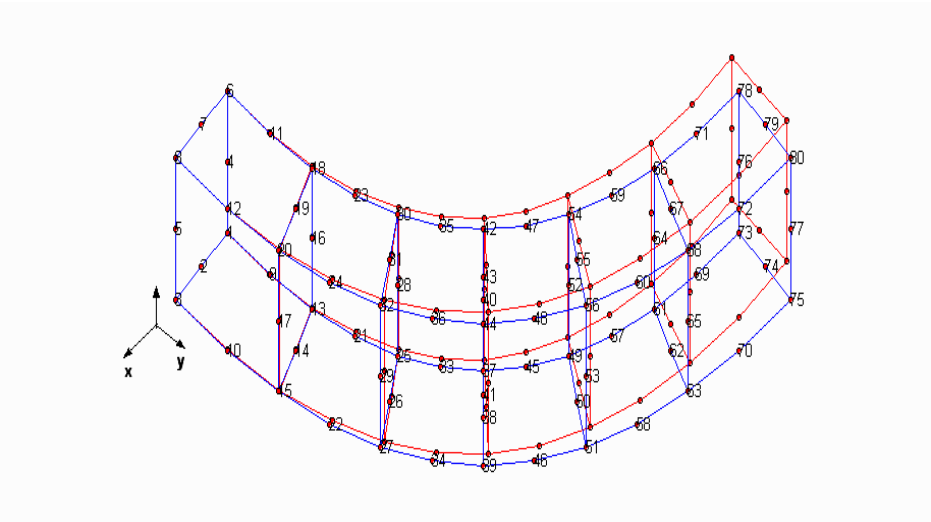

Fig 3.9: ***Deflected profile of curved cantilever beam***

Table 3.6: **Deflection at the free end of the curved cantilever**

Node	Disp-x	Disp-y	Disp-z
73	-0.0653267	-0.2347983	0.0001501
74	-0.0486148	-0.2515638	7.11e-05
75	-0.031837	-0.2684533	-2.86e-05
76	-0.0653232	-0.2345978	-2.72e-14
77	-0.0318144	-0.2682405	-2.28e-14
78	-0.0653267	-0.2347983	-0.0001501
79	-0.0486148	-0.2515638	-7.11e-05
80	-0.031837	-0.2684533	2.86e-05

Chapter 04

4.0 AUTOMATIC MESH GENERATOR

The preparation of data and post processing require considerable effort if all data are to be handled manually, especially for finer descretisation. The tedium of handling the data and the possibility of errors creeping in as the number of elements increase, make the problem complicated. Hence, finite element analyst should present a systematic development of preprocessing and post processing considerations, in order to make the finite element analysis an 'interesting and useful' computational tool using an efficient mesh generator. The basic function of mesh generation is to generate element connectivity and nodal coordinate data for the continuum to be analyzed. Here, a single complex three-dimensional finite element model requires a mesh generator for descretising the solid continuum into the chosen basic elements, ensuring *intra-element* and *inter-element* continuity and connectivity with the coordinates of each nodal point to be found. At the same time, this *Automatic Mesh Generator* should represent the geometry of the solid continuum, where, arch dam accurately can be arrived by Langrange shape functions of higher order.

4.1 BASIC MESH GENERATOR

Here the concept is primarily, to generate an automatic mesh on a cuboid of size (L, T, H) units, discretising into ($nL \times nT \times nH$) elements where, nL, nT, nH are

the number of elements in L, T and H dimensions in global X, Y, Z directions respectively. Then each element of the cuboid will be of size ($L/nL \times T/nT \times H/nH$) units and number of nodes in each direction will be (nL+1) (nT+1) (nH+1) respectively using eight-noded elements. If the elements selected are twenty-noded, then number of nodes will change as:

```
nNodes = node;
int nNodeLine1, nNodeLine2;
nNodeLine1 = 2*nT + 1;
nNodeLine2 = nT + 1;
int nNodeFace1, nNodeFace2;
nNodeFace1 = nNodeLine1*(nH + 1) + nNodeLine2*nH;
nNodeFace2 = nNodeLine2*(nH + 1);
nNodes = nNodeFace1*(nL + 1) + nNodeFace2*nL;
```

A program for arriving the nodal coordinates and nodal connectivity is attempted in Cartesian coordinate system using eight noded elements and developed for twenty noded elements also.

```
// Generate nodal coordinate data
      int node = 0;
      double xx, zz;
      for (k=1; k<=nL + 1; k++)
      {
            xx = L/(nL)*(k - 1);
            for (j=1; j<=nH + 1; j++)
            {
                  zz = H/(nH)*(j - 1);
                  for (i=1; i<=2*nT + 1; i++)
                  {
                        node ++;
                        x[node] = xx;
                        y[node] = T/(2*nT)*(i - 1);
                        z[node] = zz;
                  }
                  if (j == nH + 1)
                        continue;
                  zz += H/(2*nH);
                  for (i=1; i<=nT + 1; i++)
                  {
                        node ++;
                        x[node] = xx;
                        y[node] = T/nT*(i - 1);
                        z[node] = zz;
                  }
            }
            if (k == nL + 1)
                  continue;
            xx += L/(2*nL);
```

```
            for (j=1; j<=nH + 1; j++)
            {
                  zz = H/(nH)*(j - 1);
                  for (i=1; i<=nT + 1; i++)
                  {
                        node ++;
                        x[node] = xx;
                        y[node] = T/(nT)*(i - 1);
                        z[node] = zz;
                  }
            }
      }

// Generation of element connectivity data
// first element
      nod[1][1]  = 3;
      nod[2][1]  = 1;
      nod[3][1]  = nNodeFace1 + nNodeFace2 + 1;
      nod[4][1]  = nod[3][1] + 2;
      nod[6][1]  = nNodeLine1 + nNodeLine2 + 1;
      nod[5][1]  = nod[6][1] + 2;
      nod[7][1]  = nod[3][1] + nNodeLine1 + nNodeLine2;
      nod[8][1]  = nod[7][1] + 2;
      nod[9][1]  = 2;
      nod[10][1] = nNodeFace1 + 1;
      nod[11][1] = nod[3][1] + 1;
      nod[12][1] = nod[10][1] + 1;
      nod[13][1] = nod[6][1] + 1;
      nod[14][1] = nNodeFace1 + nNodeLine2 + 1;
      nod[15][1] = nod[7][1] + 1;
      nod[16][1] = nod[14][1] + 1;
      nod[18][1] = nNodeLine1 + 1;
      nod[17][1] = nod[18][1] + 1;
      nod[19][1] = nod[3][1] + nNodeLine1;
      nod[20][1] = nod[19][1] + 1;
```

This can be extended for a 27 noded element as shown below:

```
      nNodes = node;
      int nNodeLine, nNodeFace;
      nNodeLine = 2*nT + 1;
      nNodeFace = nNodeLine*(2*nH + 1) ;
      nNodes = nNodeFace*(2*nL+ 1) ;

// Generate element connectivity data
// first element
      nod[1][1]  = 3;
      nod[2][1]  = 1;
      nod[3][1]  = 2*nNodeFace +1;
      nod[4][1]  = nod[3][1] + 2;
      nod[6][1]  = 2* nNodeLine+1 ;
      nod[5][1]  = nod[6][1] + 2;
      nod[7][1]  = nod[3][1] + nNodeLine*2;
      nod[8][1]  = nod[7][1] + 2;
      nod[9][1]  = 2;
      nod[10][1] = nNodeFace + 1;
      nod[11][1] = nod[3][1] + 1;
      nod[12][1] = nod[10][1] + 2;
      nod[13][1] = nod[6][1] + 1;
```

```
nod[14][1] = nNodeFace + nNodeLine*2 + 1;
nod[15][1] = nod[7][1]  + 1;
nod[16][1] = nod[14][1] + 2;
nod[18][1] = nNodeLine + 1;
nod[17][1] = nod[18][1] + 2;
nod[19][1] = nod[3][1] + nNodeLine;
nod[20][1] = nod[19][1] + 2;
nod[21][1] = nod[18][1]+1;
nod[22][1] = nod[10][1]+  nNodeLine;
nod[23][1]  = nod[19][1] +1;
nod[25][1]  = nod[10][1] + 1;
nod[26][1]  = nod[14][1] + 1;
nod[27][1]  = nod[22][1] +1;
nod[24][1]  = nod[27][1] + 1;
```

For the purpose of three dimensional mapping, one basic element in the local coordinate system is selected as L = T = H = 2 units with centre of cube at (1, 1, 1) and modified with centre (0, 0, 0) so that the extreme nodal point will be (-1, -1, -1) and (+1, +1, +1) so as to make use of Gauss quadrature formula for element integral computation. Now, this basic element can be discretised to any number of divisions in each direction. This basic cubical element in the local coordinate system is to be mapped to the actual distorted continuum, which is done by isoparametric curvilinear mapping knowing the global coordinates of the corresponding global nodal points of the actual continuum. To avoid violent distortion of the mesh, degree of polynomial in each direction selected should match the curve in the respective direction. Therefore, to approximate complex geometry like that of the arch dam, *Langrange shape functions* of higher order hexahedral elements, even with varying degree in the three directions, can be used for mapping the continuum.[83,87]

4.1.1 Three Dimensional Mapping

The three-dimensional mesh with the required number of basic *n-noded* elements along the three directions is generated inside a cuboid of side 2 units and is

mapped into the actual three-dimensional structure. This cube in the local coordinate system is to be mapped to the actual distorted continuum, knowing the global coordinates of the corresponding nodal points in the actual continuum with that of the basic element as in Fig 4.1. If the basic element chosen is *an 'n' noded one*, then, knowing the corresponding global values of the *n points*, the global coordinates of other points can be arrived with the help of shape functions.

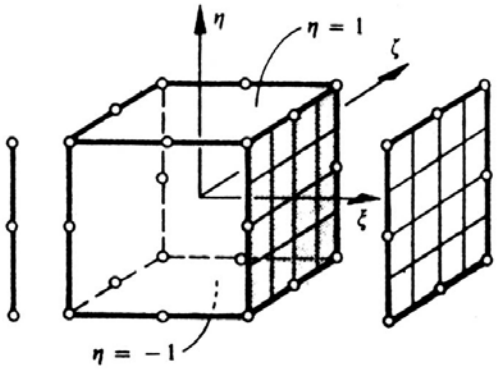

(a)

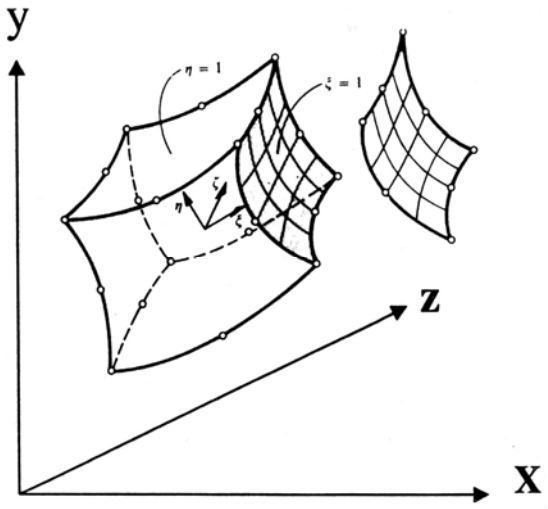

(b)

Fig 4.1: ***Three-dimensional mapping of hexahedral elements***:
(a) Local coordinates (b) Cartesian map

Any point in the local mesh generator is given by:

$$x = \sum_{i=1}^{n} N_i x_i,\ y = \sum_{i=1}^{n} N_i y_i,\ z = \sum_{i=1}^{n} N_i z_i \tag{4.1}$$

Thus, all the corresponding points of the continuum can be found out. The descretisation in the basic element can be mapped into the distorted continuum. Corresponding to each local coordinate, a single global cartesian coordinate will be obtained. Violent distortion may be avoided to guard against non-uniqueness for which the degree of polynomial selected should match the curve.

4.1.2 Langrange Shape Functions

The arch dam geometry has to be modeled primarily, since this research is intended for the analysis of arch dams. Being irregular and curved boundaries, the polynomial function selected for each direction should define the curve in the respective direction accurately. Lagrange family of elements is useful for varying degree of approximation. Shape functions for Lagrange family of elements can be found out by the simple product of the shape functions in each direction at a point. Thus, the shape function at the point (i, j, k) is given by:

$$N = N_{ijk} = N_{\xi_i} N_{\eta_j} N_{\zeta_k}$$

where,

$$N_{\xi_i} = \sum_{i=1}^{(\deg \xi + 1)} \frac{(\xi - \xi_j)}{(\xi_i - \xi_j)} \qquad i \neq j$$

$$N_{\eta_j} = \sum_{i=1}^{(\deg \eta + 1)} \frac{(\eta - \eta_j)}{(\eta_i - \eta_j)} \qquad i \neq j$$

$$N_{\zeta_k} = \sum_{i=1}^{(\deg \zeta + 1)} \frac{(\zeta - \zeta_j)}{(\zeta_i - \zeta_j)} \qquad i \neq j$$

N_{ξ_i}, N_{η_j}, N_{ζ_k} are the shape functions for the point (*i, j, k*) in ξ, η, ζ directions. The shape function components in each direction at a particular point can be found by the above relationship. The shape function at a point (ξ_i, η_j, ζ_k) will be the product of the component shape function as above.[24,25,84,89] A program for the shape functions of Lagrange family of elements is developed.

```
// nL, nT, nH divisions in the respective global X,Y,Z  directions

//degL, degT, degH are degree of interpolation in the respective
       direction

     fin >> degL >> degT >> degH;
     nPoints = ( degL + 1)*( degT + 1)*( degH + 1);

// Read global coordinates the key nodal points
     for (i=1; i<=nPoints; i++)
     {
           fin >> k;
           fin >>   Xg[k] >>Yg[k] >>Zg[k];
     }
     nElems = nL * nT * nH;


// Transform the coordinates and print
     for (i=1; i<=nNodes; i++)
     {
           double pxi, pet, pze;
           pxi = x[i] - 1;
           pet= y[i] - 1;
           pze = z[i] - 1;

shapeFunc(degL,degT,degH, pxi, pet, pze);

           xNew[i] = yNew[i] = zNew[i] = 0;
           for (j=1; j<=nPoints; j++)
           {
                 xNew[i] += N[j]*Xg[j];
                 yNew[i] += N[j]*Yg[j];
                 zNew[i] += N[j]*Zg[j];
           }
     }
```

In certain cases of complex geometry, the degree of curve in all the three directions may vary, which is accommodated using Langrange shape function as given below:

//Langrange shape function of required degree in any direction (function call)

```
void shapeFunc(int degL, int degT,int degH, double pxi, double pet,
double pze)

{
      ofstream fout("shape.out");
      double xxi[100],yyi[100],zzi[100],Nxii[100],Neti[100],
Nzet[100];
      int i, j, k;
      xxi[1] = yyi[1] = zzi[1] = -1;
    for (i=2; i<= degL + 1; i++)
      {
            xxi[i] = xxi[i-1] + 2.0/degL;
      }
    for (i=2; i<=degT + 1; i++)
      {
            yyi[i] = yyi[i-1] + 2.0/degT;
      }
    for (i=2; i<=degH + 1; i++)
      {
            zzi[i] = zzi[i-1] + 2.0/degH;
      }
for (i=1; i<=degL + 1; i++)
            {
            Nxii [i] = 1;
            for (j=1; j<=degL + 1; j++)
            {
                  if (j != i)
                  {
                  Nxii [i] *= (pxi - xxi[j])/(xxi[i] - xxi[j]);

                  }
            }
      }
for (i=1; i<=degT + 1; i++)
      {
            Neti [i] = 1;
            for (j=1; j<=degT + 1; j++)
            {
                  if (j != i)
                  {
                  Neti [i] *= (pet - yyi[j])/(yyi[i] - yyi[j]);

                  }
            }
for (i=1; i<=degH + 1; i++)
      {
            Nzet [i] = 1;
       for (j=1; j<=degH + 1; j++)
            {
                  if (j != i)
                  {
                  Nzet [i] *= (pze - zzi[j])/(zzi[i] - zzi[j]);

                  }
            }
      }
      int node = 0;
      for (i=1; i<=degH + 1; i++)
      {
```

```
            for (j=1; j<=degT + 1; j++)
            {
                  for (k=1; k<=degL + 1; k++)
                  {
                        node ++;
                        N[node] = Nxii[k] * Neti[j] * Nzet[i];
                  }
            }
      }
```

4.2 PLOTTING THE MESH

The mesh generated is plotted with *Matlab* for which an 8-noded element is first taken and then developed for 20 and 27 nodes.[87,90] The program outlined below is for a 20 noded brick element.

//plotting the mesh in Matlab

```
void plot(int plot_node, char file[10])
{
      ofstream fout(file);
      int i, j;
      double PI,  th1,  th2, xp[1000], yp[1000] ;

// Transform to isometric coordinates
      for (i=1; i<=nNodes; ++i)
      {
            xp[i] = xNew[i]*cos(th1) + yNew[i]*cos(th2);
            yp[i] = zNew[i] - (xNew[i]*sin(th1) + yNew[i]*sin(th2));
      }
      fout << "\nrotate3d;";
      for (i=1; i<=nElems; ++i)
      {
            for (j=1; j<=4; ++j)
            {
                  int m, n, p;
                  // plot bottom base
                  m = j;
                  n = j + 8;
                  if (j == 4)
                        p = 1;
                  else
                        p = j + 1;
fout << "\nx = [" << xp[nod[m][i]] << " " << xp[nod[n][i]] << "];";
fout << "\ny = [" << yp[nod[m][i]] << " " << yp[nod[n][i]] << "];";
fout << "\nplot(x,y,'" << color <<"','Linewidth',1.25)";
fout << "\nhold on";
fout << "\nx = [" << xp[nod[n][i]] << " " << xp[nod[p][i]] << "];";
fout << "\ny = [" << yp[nod[n][i]] << " " << yp[nod[p][i]] << "];";
fout << "\nplot(x,y,'" << color <<"','Linewidth',1.25)";
fout << "\nhold on";
//plot top base
```

```
                m = j + 4;
                n = j + 12;
                if (j == 4)
                      p = 5;
                else
                      p = j + 5;
fout << "\nx = [" << xp[nod[m][i]] << " " << xp[nod[n][i]] << "];";
fout << "\ny = [" << yp[nod[m][i]] << " " << yp[nod[n][i]] << "];";
fout << "\nplot(x,y,'" << color <<"','Linewidth',1.25)";
fout << "\nhold on";
fout << "\nx = [" << xp[nod[n][i]] << " " << xp[nod[p][i]] << "];";
fout << "\ny = [" << yp[nod[n][i]] << " " << yp[nod[p][i]] << "];";
fout << "\nplot(x,y,'" << color <<"','Linewidth',1.25)";
fout << "\nhold on";
// plot mid points
                m = j;
                n = j + 16;
                if (j == 4)
                      p = 8;
                else
                      p = j + 4;
fout << "\nx = [" << xp[nod[m][i]] << " " << xp[nod[n][i]] << "];";
fout << "\ny = [" << yp[nod[m][i]] << " " << yp[nod[n][i]] << "];";
fout << "\nplot(x,y,'" << color <<"','Linewidth', .5)";
fout << "\nhold on";
fout << "\nx = [" << xp[nod[n][i]] << " " << xp[nod[p][i]] << "];";
fout << "\ny = [" << yp[nod[n][i]] << " " << yp[nod[p][i]] << "];";
fout << "\nplot(x,y,'" << color <<"','Linewidth', .5)";
fout << "\nhold on";
            }
      }
      if(plot_node == 0)
            for (i=1; i<=nNodes; ++i)
            {
fout << "\nx = "<< xp[i] <<";\ny = "<< yp[i] <<";\ni = " << i <<";";

fout<<"\nplot(x,y,'o','MarkerFaceColor','r','MarkerEdgeColor','k','Mar
kerSize', 1.5)";

fout << "\nhold on";
            }
fout << "\naxis off"; }
}
```

4.2.1 Mesh Validation

The mesh generator developed is validated with simple examples.

a. Cube (1x1x1) unit

A cube of size (1x1x1) is discretised in to 8 elements using 8, 20 and 27- noded brick elements and is plotted with the above program in Fig 4.2.a-c. That is, on giving input as L = 2, T = 2, H = 2, nL = 2, nT = 2, nH = 2; a cube can be descretised

betweeen -1,-1,-1 and +1,+1,+1 with 20 noded brick element. Element connectivity and nodal coordinates are given in Table 4.1 and Table 4.2 respectively.

Output

No of elements = 8
No of nodes = 81

Table 4.1: **Element Connectivity of Cube 20 noded 8 elements**

1	03	01	31	33	11	09	39	41	02	22	32	23	10	25	40	26	07	06	36	37
2	05	03	33	35	13	11	41	43	04	23	34	24	12	26	42	27	8	07	37	38
3	11	09	39	41	19	17	47	49	10	25	40	26	18	28	48	29	15	14	44	45
4	13	11	41	43	21	19	49	51	12	26	42	27	20	29	50	30	16	15	45	46
5	33	31	61	63	41	39	69	71	32	52	62	53	40	55	70	56	37	36	66	67
6	35	33	63	65	43	41	71	73	34	53	64	54	42	56	72	57	38	37	67	68
7	41	39	69	71	49	47	77	79	40	55	70	56	48	58	78	59	45	44	74	75
8	43	41	71	73	51	49	79	81	42	56	72	57	50	59	80	60	46	45	75	76

Table 4.2: **Nodal Coordinates of Cube 20 noded 8 elements**

Node	X	Y	Z	Node	X	Y	Z
1	-1	-1	-1	42	0	0.5	0
2	-1	-0.5	-1	43	0	1	0
3	-1	0	-1	44	0	-1	0.5
4	-1	0.5	-1	45	0	0	0.5
5	-1	1	-1	46	0	1	0.5
6	-1	-1	-0.5	47	0	-1	1
7	-1	0	-0.5	48	0	-0.5	1
8	-1	1	-0.5	49	0	0	1
9	-1	-1	0	50	0	0.5	1
10	-1	-0.5	0	51	0	1	1
11	-1	0	0	52	0.5	-1	-1
12	-1	0.5	0	53	0.5	0	-1
13	-1	1	0	54	0.5	1	-1
14	-1	-1	0.5	55	0.5	-1	0
15	-1	0	0.5	56	0.5	0	0
16	-1	1	0.5	57	0.5	1	0
17	-1	-1	1	58	0.5	-1	1
18	-1	-0.5	1	59	0.5	0	1
19	-1	0	1	60	0.5	1	1
20	-1	0.5	1	61	1	-1	-1
21	-1	1	1	62	1	-0.5	-1
22	-0.5	-1	-1	63	1	0	-1
23	-0.5	0	-1	64	1	0.5	-1
24	-0.5	1	-1	65	1	1	-1
25	-0.5	-1	0	66	1	-1	-0.5
26	-0.5	0	0	67	1	0	-0.5
27	-0.5	1	0	68	1	1	-0.5
28	-0.5	-1	1	69	1	-1	0
29	-0.5	0	1	70	1	-0.5	0
30	-0.5	1	1	71	1	0	0
31	0	-1	-1	72	1	0.5	0

32	0	-0.5	-1	73	1	1	0
33	0	0	-1	74	1	-1	0.5
34	0	0.5	-1	75	1	0	0.5
35	0	1	-1	76	1	1	0.5
36	0	-1	-0.5	77	1	-1	1
37	0	0	-0.5	78	1	-0.5	1
38	0	1	-0.5	79	1	0	1
39	0	-1	0	80	1	0.5	1
40	0	-0.5	0	81	1	1	1
41	0	0	0				

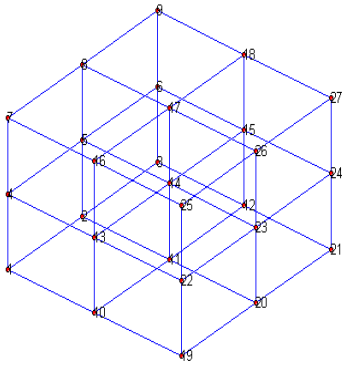

Fig 4.2: **a *Discretisation of Cube 8 noded element***

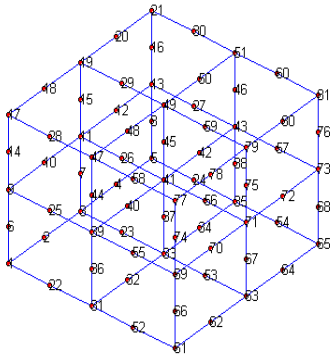

Fig 4.2: **b *Discretisation of Cube 20 noded element***

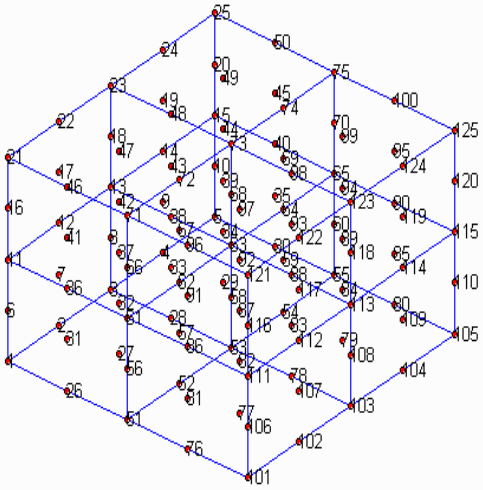

Fig 4.2: **c *Discretisation of Cube 27 noded brick element***

b. Cantilever Beam

Generated mesh of a cantilever beam with L=200cm, T=20cm, H=30cm, nL=5, nT=1, nH=1 is shown below in Fig 4.3 and element connectivity in Table 4.3.

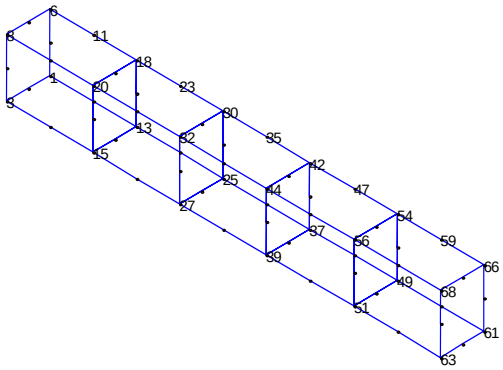

Fig 4.3: ***Cantilever beam generated mesh***

Table 4.3: ***Element Connectivity of cantilever 20 noded 5 elements***

1	03	01	13	15	08	06	18	20	02	09	14	10	07	11	19	12	05	04	16	17
2	15	13	25	27	20	18	30	32	14	21	26	22	19	23	31	24	17	16	28	29
3	27	25	37	39	32	30	42	44	26	33	38	34	31	35	43	36	29	28	40	41
4	39	37	49	51	44	42	54	56	38	45	50	46	43	47	55	48	41	40	52	53
5	51	49	61	63	56	54	66	68	50	57	62	58	55	59	67	60	53	52	64	65

c. Arbitrary arch

For verifying the generator developed using three dimensional mapping technique, an arbitrary arch whose global coordinates are known is used. The structure is mapped with Lagrange shape functions of degree 2 and descretisation done using 20 noded isoparametric elements. The obtained coordinates are found to be in accordance with the required descretisation; by observing the results. Secondly, to verify the connectivity, the mesh generator program, supplemented by a 'mesh plotting' program explained in 4.2 using *'Matlab', is used.* The obtained mesh when plotted is found conforming. Thus, the plot for the discretised continuum is also obtained. Automatic mesh generator gives the nodal coordinates of the discretised continuum, element connectivity as in Table 4.4 and plot of the discretised continuum Fig 4.4.

Input

Number of divisions in length direction = 3

Number of divisions in thickness direction = 1

Number of divisions in height direction = 2

Number of Gaussian points = 3

	Xg	Yg	Zg
1	-130	0	0
2	-120	-50	0
3	-138	-58	0
4	-150	0	0
5	-130	0	300
6	-93	-93	300
7	-107	-107	300
8	-150	0	300
9	-126	-24	0
10	-130	-53	0
11	-146	-28	0
12	-140	0	0
13	-120	-50	300
14	-100	-100	300
15	-138	-58	300
16	-140	0	300
17	-130	0	150
18	-108	-72	150
19	-123	-83	150
20	-150	0	150
21	-125	-38	150
22	-116	-77	150
23	-143	-43	150
24	-140	0	150
25	-137	-25	0
26	-129	-52	300
27	-135	-40	150

Out put

Number of elements = 6

Number of nodes = 70

Nodal data

Node	X	Y	Z
1	-150	0	0
2	-140	0	0
3	-130	0	0
4	-150	0	75
5	-130	0	75
6	-150	0	150
7	-140	0	150

8	-130	0	150
9	-150	0	225
10	-130	0	225
11	-150	0	300
12	-140	0	300
13	-130	0	300
14	-149.111	-9.11111	0
15	-128.889	-7.77778	0
50	-121.333	-68.4444	300
51	-112.889	-65.1111	300
52	-141.111	-47.7778	0
53	-122.222	-41.1111	0
54	-131.111	-70	150
55	-115	-61.1111	150
56	-119.444	-91.6667	300
57	-103.889	-79.4444	300
58	-138	-58	0
59	-130	-53	0
60	-120	-50	0
61	-130.625	-70.625	75
62	-114.375	-61.125	75
63	-123	-83	150
64	-116	-77	150
65	-108	-72	150
66	-115.125	-95.125	225
67	-100.875	-82.625	225
68	-107	-107	300
69	-100	-100	300
70	-93	-93	300

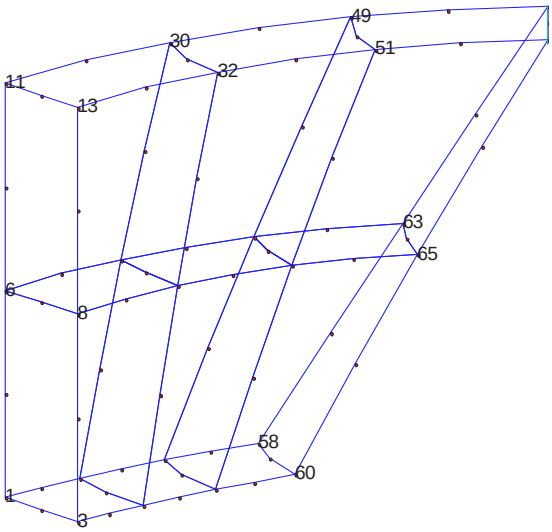

Fig 4.4: ***Arbitrary arch generated mesh***

Table 4.4: **Element Connectivity; Test arch**

1	03	01	20	22	08	06	25	27	02	14	21	15	07	16	26	17	05	04	23	24
2	08	06	25	27	13	11	30	32	07	16	26	17	12	18	31	19	10	09	28	29
3	22	20	39	41	27	25	44	46	21	33	40	34	26	35	45	36	24	23	42	43
4	27	25	44	46	32	30	49	51	26	35	45	36	31	37	50	38	29	28	47	48
5	41	39	58	60	46	44	63	65	40	52	59	53	45	54	64	55	43	42	61	62
6	46	44	63	65	51	49	68	70	45	54	64	55	50	56	69	57	48	47	66	67

d. USBR arch half

Since the finite element analysis program is also intended to be modified for an arch dam, the validation of the mesh generator is done for preliminary arbitrary design of an arch dam. Arch dam geometry is arrived according to the guidelines for preliminary design of arch dams as per USBR recommendation. Mesh is arrived with the following input and nodal coordinates as in Table 4.5. Output nodal coordinates are given in Table 4.6 and table 4.7 respectively. Mesh arrived with 6 elements is shown in Fig 4.5 and 70 elements, in Fig 4.6 respectively.

Input

Number of divisions in length direction = 3
Number of divisions in thickness direction = 1
Number of divisions in height direction = 2
Number of Gaussian points = 3
Degree of polynomial = 3

Table 4.5: **Nodal coordinates USBR arch half; Input**

	X	**Y**	**Z**
3	0	228.09	0
9	31.3327	210	0
7	48.6533	220	0
1	0	248.09	0

21	0	227.19	150
27	196.7523	113.595	150
25	203.2475	117.345	150
19	0	234.69	150
6	18.09	223.2428	0
8	39.99305	215	0
4	28.09	240.5633	0
2	0	238.09	0
24	113.595	196.7523	150
26	199.9999	115.47	150
22	117.345	203.2475	150
20	0	230.94	150
12	0	234.69	75
18	131.7657	158.865	75
16	148.2205	168.115	75
10	0	253.69	75
15	76.075	214.7387	75
17	139.993	163.365	75
13	85.575	230.7602	75
11	0	244.19	75
5	23.09	231.903	0
23	15.47	199.9999	150
14	80.825	222.533	75

Output

Number of elements= 6

Number of nodes = 105

Table 4.6: **Nodal coordinates USBR arch half; Output**

Node	X	Y	Z
1	0	248.09	0
2	0	238.09	0
3	0	228.09	0
4	0	253.965	37.5
5	0	243.559	37.5
6	0	233.152	37.5
7	0	253.69	75
8	0	244.19	75
9	0	234.69	75
10	0	247.265	112.5
11	0	239.984	112.5
12	0	232.702	112.5
13	0	234.69	150

14	0	230.94	150
15	0	227.19	150
16	10.1996	247.03	0
17	8.38411	237.218	0
18	6.56858	227.407	0
19	21.8033	251.698	37.5
20	19.9141	241.488	37.5
21	18.0248	231.438	37.5
22	31.0727	250.46	75
23	29.348	241.139	75
24	27.6232	232.031	75
25	38.0078	243.314	112.5
73	149.473	180.664	150
74	147.084	177.778	150
75	144.696	174.891	150
76	42.6352	228.303	0
77	35.0461	221.825	0
78	27.4571	215.347	0
79	91.1396	211.667	37.5
80	83.2422	204.926	37.5
81	75.3448	198.469	37.5
82	129.886	193.41	75
83	122.677	187.256	75
84	115.467	181.481	75
85	158.875	173.531	112.5
86	153.35	168.814	112.5
87	147.824	164.382	112.5
88	178.107	152.03	150
89	175.261	149.601	150
90	172.415	147.172	150
91	48.6533	220	0
92	39.993	215	0
93	31.3328	210	0
94	104.004	193.918	37.5
95	94.9922	188.715	37.5
96	85.9801	183.699	37.5
97	148.22	168.115	75
98	139.993	163.365	75
99	131.766	158.865	75
100	181.302	142.591	112.5
101	174.996	138.95	112.5
102	168.69	135.497	112.5
103	203.248	117.345	150
104	200	115.47	150
105	196.752	113.595	150

Table 4.7: **Element Connectivity USBR arch half; 6 elements**

1	3	1	31	33	9	7	37	39	2	16	32	18	8	22	38	24	6	34	4	36
2	9	7	37	39	15	13	43	45	8	22	38	24	14	28	44	30	12	40	10	42
3	33	31	61	63	39	37	67	69	32	46	62	48	38	52	68	54	36	64	34	66
4	39	37	67	69	45	43	73	75	38	52	68	54	44	58	74	60	42	70	40	72
5	63	61	91	93	69	67	97	99	62	76	92	78	68	82	98	84	66	94	64	96
6	69	67	97	99	75	73	103	105	68	82	98	84	74	88	104	90	72	100	70	102

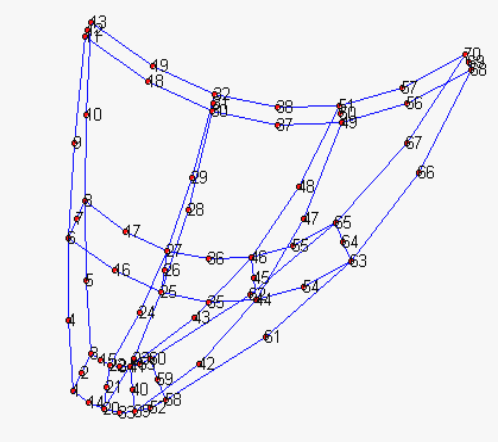

Fig 4.5: ***Node numbering pattern USBR half arch*** *6 elements*

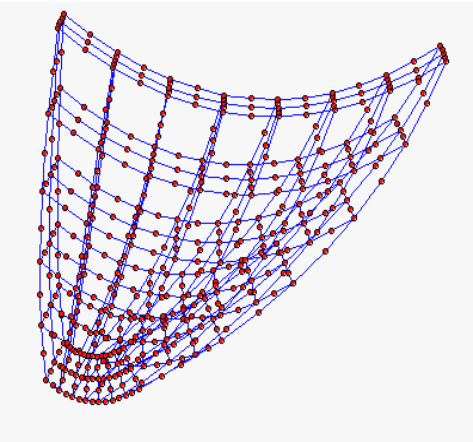

Fig 4.6: ***Descretisation 20 noded USBR half arch*** *70 elements*

The discretisation of the same geometry with 27 noded elements is shown below in Fig 4.7 & 4.8

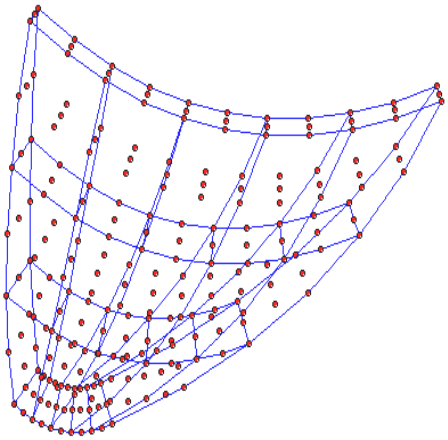

Fig 4.7: ***Descretisation 27 noded USBR half arch*** *15 elements*

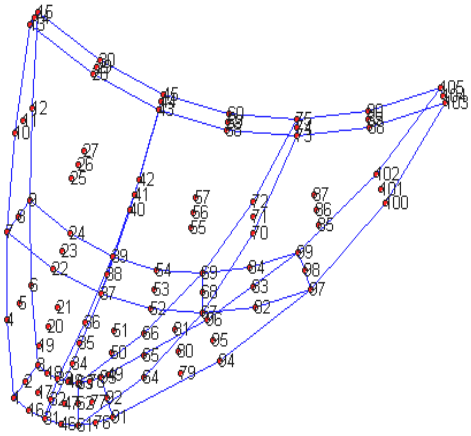

Fig 4.8: ***Node numbering pattern 27 noded USBR half arch.*** *6 elements*

e. USBR full arch

The same arch dam when modeled in full with varying degree of curve (2, 4, 2) inputting the corresponding 3x5x3 number of basic nodal coordinates gave the plot as in Fig 4.9 given below.

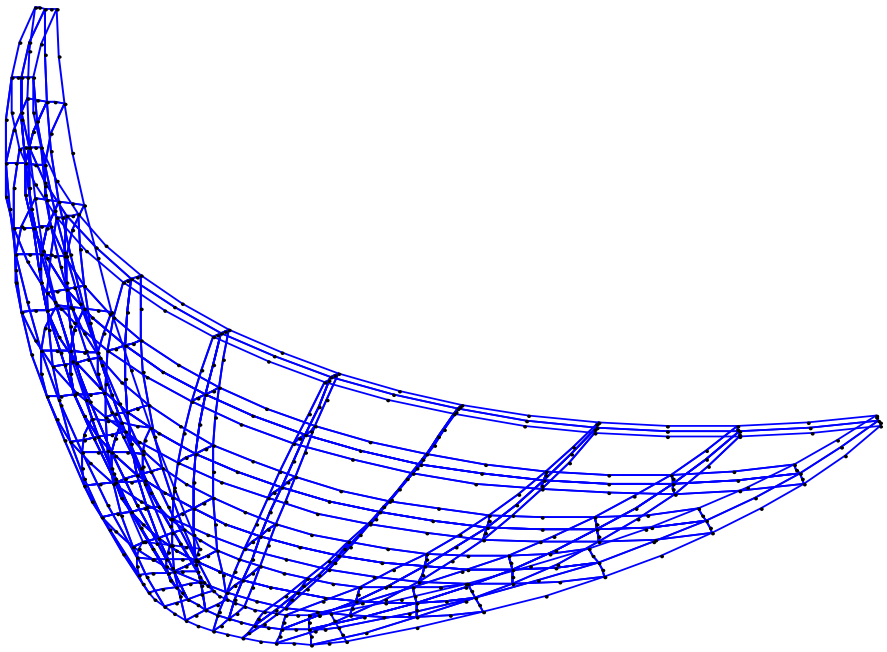

Fig 4.9: ***Generated mesh USBR arch full***

Input

Number of divisions in length direction = 8

Number of divisions in thickness direction = 2

Number of divisions in height direction = 5

Number of Gaussian points = 4

Degree of polynomial in height and thickness= 2

Degree of polynomial in length = 4

Nodal Coordinates

01	-48.6533	220.000	000
02	-39.9930	215.000	000
03	-31.3327	210.000	000
04	-28.0900	240.563	000
05	-23.0900	231.903	000
06	-18.0900	223.242	000
07	0.000000	248.090	000
08	0.000000	238.090	000
09	0.000000	228.090	000
10	28.09000	240.563	000
11	23.09000	231.903	000
12	18.09000	223.242	000

13	48.65330	220.000	000
14	39.99305	215.000	000
15	31.33279	210.000	000
16	-148.220	168.115	075
17	-139.993	163.365	075
18	-131.765	158.865	075
19	-85.5750	230.760	075
20	-80.8250	222.533	075
21	-76.0750	214.738	075
22	0.000000	253.690	075
23	0.000000	244.190	075
24	0.000000	234.690	075
25	85.57500	230.760	075
26	80.82500	222.533	075
27	76.07500	214.738	075
28	148.2205	168.115	075
29	139.9930	163.365	075
30	131.7657	158.865	075
31	-203.247	117.345	150
32	-199.999	115.470	150
33	-196.752	113.595	150
34	-117.345	203.247	150
35	-115.470	199.999	150
36	-113.595	196.752	150
37	0.000000	234.690	150
38	0.000000	230.940	150
39	0.000000	227.190	150
40	117.3450	203.247	150
41	115.4700	199.999	150
42	113.5950	196.752	150
43	203.2475	117.345	150
44	199.9999	115.470	150
45	196.7523	113.595	150

f. Sectional Plan at Various Levels

The mesh plotting program is capable of giving the sectional plan of the structure at various levels for which half of a symmetric USBR arch dam is given in Fig 4.10 and full in Fig 4.11. The plots can be conveniently be adjusted with suitable isometric angles as below.

Number of divisions in length direction = 6

Number of divisions in thickness direction = 2

Number of divisions in height direction = 6

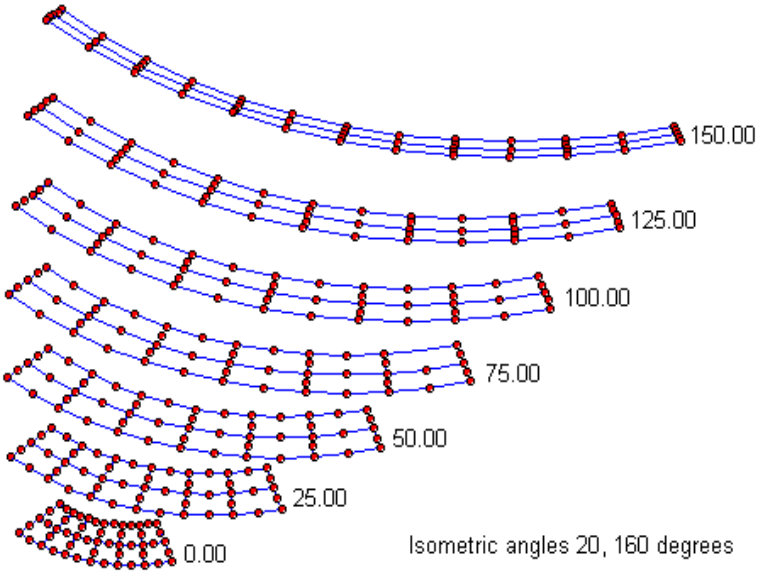

Fig 4.10:. ***Sectional plan at various elevations; half arch***

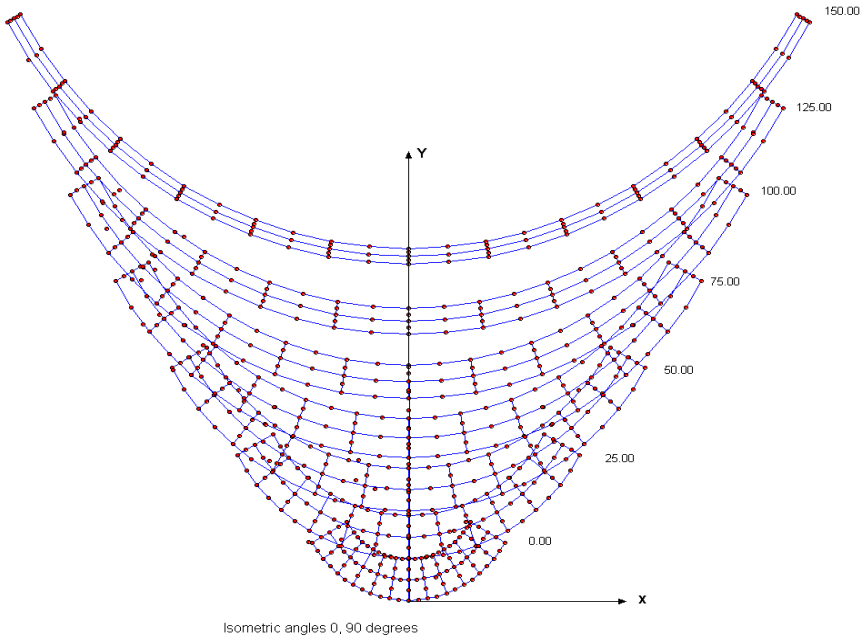

Fig 4.11: ***Sectional plan at various elevations; full arch***

Number of divisions in length direction = 12

Number of divisions in thickness direction = 2

Number of divisions in height direction = 6

f. Symmetry of the continuum

If the three dimensional continuum to be analysed is symmetric in geometry and loading with respect to any direction, this advantage can be made use of with the help of suitable boundary conditions so that the problem can be resolved within manageable proportions; similarly the use of repeatability. The geometry of a USBR arch dam can be plotted as in Fig 4.12.

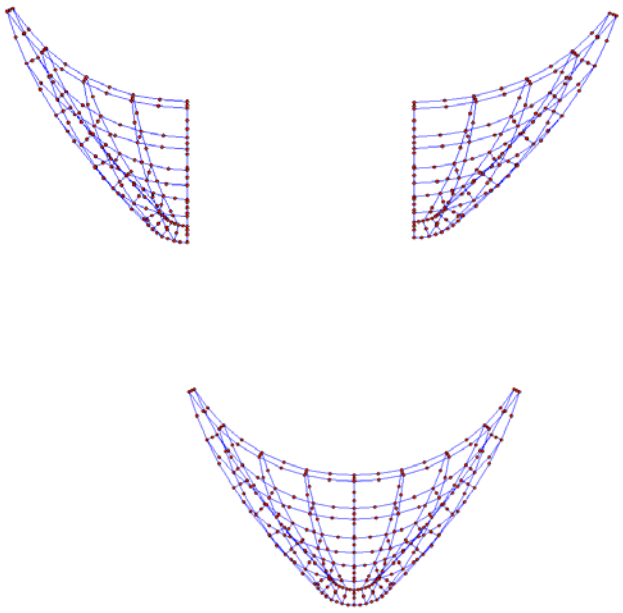

Fig 4.12: ***Symmetry of dam continuum***

f. Segments of continuum between elevations

The segments of dam between various elevations can be arrived at, with the help of the plotting program, as in Fig 4.13.

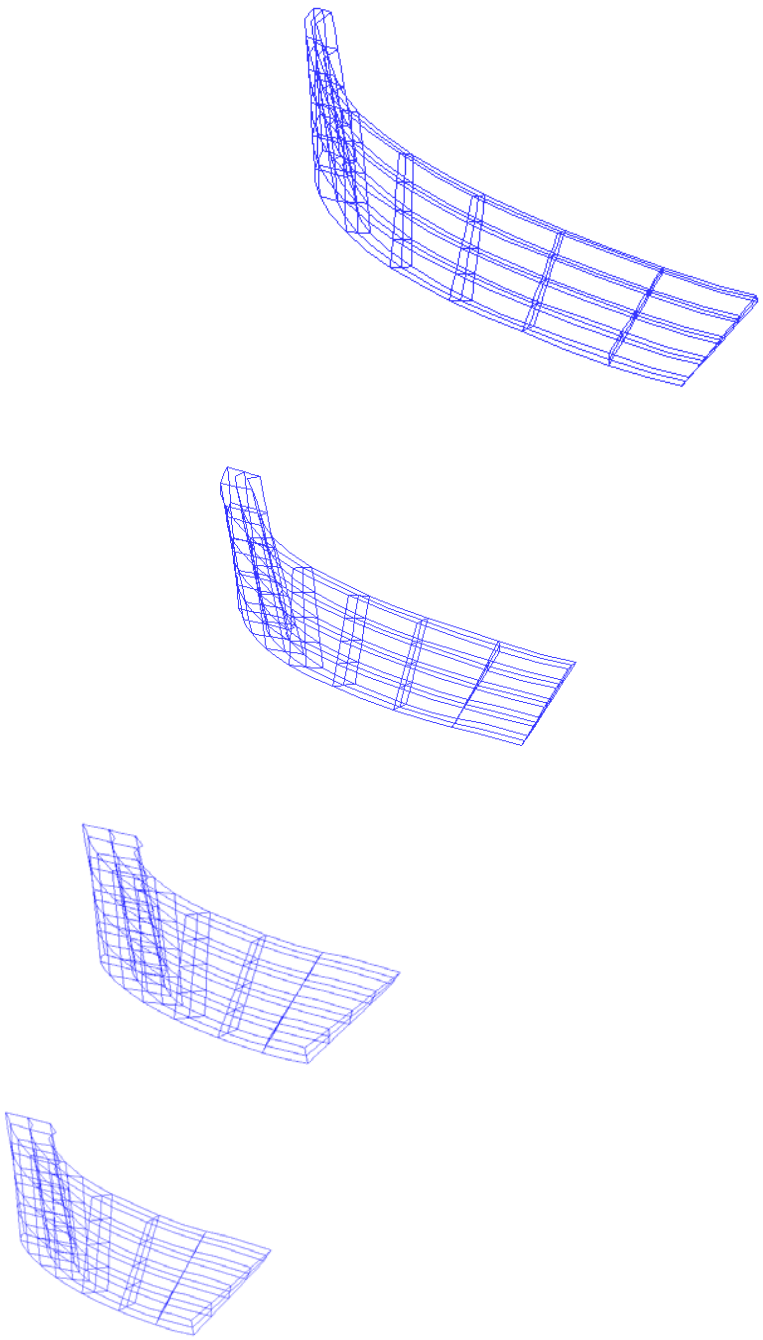

Fig 4.13: ***Segments of continuum between elevations***

g . Multi layer discretisation of the continuum

Moderately thick arch dams are modeled by two or more layers of solid elements in the thickness direction depending on their section thickness. Multilayer element meshes are essential to determine a detailed stress distribution across the thickness of a thick arch dam. This three dimensional automatic mesh generator developed is found very effective in the pre processing stage of such a multilayer descretisation as arrived in Fig 4.14.

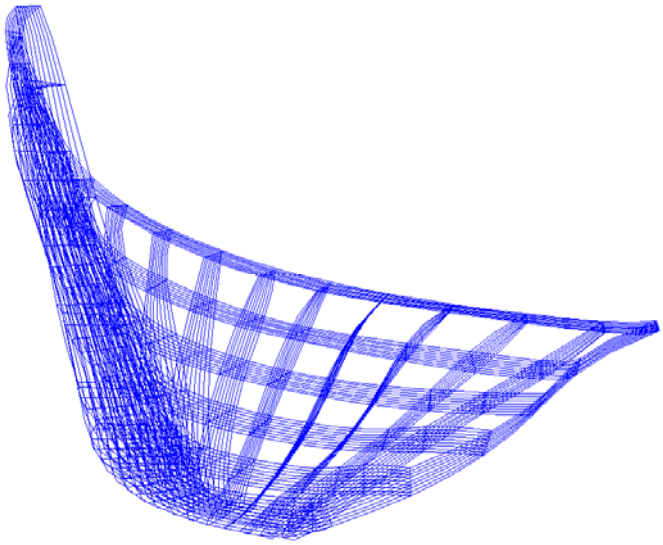

Fig 4.14: ***Multi layer discretisation of the continuum***

Chapter 06

6.0 APPLICATION OF THE PROGRAM

Once a dam is designed using preliminary guidelines; *site geographical conditions and service requirements,* it has to be analyzed in detail to avoid failure after construction and proper functioning.[22] An economic solution is one of the criteria to decide its geometry. Computer simulations give good results for all these including the impounding of a reservoir in stages can be studied in advance so that an optimal solution is arrived at. Since, finite element analysis program developed is to be applied for an arch dam; validation is to be done for an arch dam also for which a conventional arch dam and a case study is included in this chapter. Various loading conditions such as self weight alone during construction, and other 'combination of loads', 'irregular geometry' interpolated by a three-dimensional mapping using higher order elements and 'fluid pressure on curved irregular surface' arrived by numerical integration are now applied for the required continuum of an arch dam, various aspects studied and presented in this chapter.

6.1 CONVENTIONAL ARCH DAM

Since, the finite element analysis program generated is for arch dam, validation of the mesh generator is done for a preliminary conventional design of an arch dam.

Arch dam geometry is arrived according to the guidelines for the preliminary design of arch dams as per *USBR* recommendations given by *Boggs* and *Colerado*.

U.S.B.R guidelines for preliminary design

Preliminary layout of arch dams may be done as suggested by USBR; *United States Bureau of Reclamation.* This has been outlined in the following paragraphs. All original equations that are in *fps* units are converted into metric units; Fig 6.1.

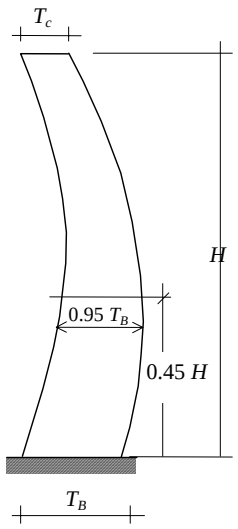

Fig. 6.1: ***Section of an arch dam***

Knowing the following:

(i) The structural height H (m)

(ii) Chord length L_1 (straight line distance in m at crest elevation between abutments assumed excavated to sound rock) and

(iii) Chord length L_2 (straight line distance in m at 0.15 H above base, between abutments assumed excavated to sound rock)

Crown cantilever can be described as below.

(a) Thickness at crest (m)

$$Tc = 0.01\ (H + 1.2L_1)$$

(b) Base thickness (m)

$$T_B = \sqrt[3]{0.001 HL_1.L_2\left(\frac{H}{122}\right)^{H/122}}$$

(c) Thickness at 0.45 H (m)

$$T_{0.45}H = 0.95\ T_B$$

(d) Crown cantilever projections at crest level

Maximum upstream projection, USP = 0.0

Maximum downstream projection, DSP = Tc

Crown cantilever projections at base

USP = $0.95\ T_B$

DSP = 0.0

Total concrete volume in cubic m is given by:

$$V = V_1 + V_2$$

V = estimated volume of dam in cubic metre

$$V_1 = 0.0001777\ H^2.\ L_2\left\{\frac{(H + 0.8L_1)^2}{L_1 - L_2}\right\}$$

$$V_2 = 0.0108\ H.L_1\ (H + 1.1\ L_1)$$

Upper end limits of the above equations are

$$30 \le H \le 370$$

$$30 \le L_1 \le 1825$$

$$4.5 \le L_2 \le 370$$

Above relations are developed by *USBR* after pooling the data for all types of canyons, irrespective of the respective canyon profile. Proportioning of cantilevers as suggested by USBR in *Design Supplement-2* on arch dams is given below.

Top thickness

There are two methods for fixing the top thickness:

a) In case a road is provided at the top of dam, often, specified width of roadways, walks, curbs and parapets require a greater thickness than what is necessary for satisfactory arch and cantilever stresses. In such cases, the required widths are provided.

b) When no arbitrary governing criteria are made, and data on similar structures are not available, the thickness of the top arch may be estimated from the results obtained by the following empirical formulae.

$$Tc = 0.012\ (H + L_1)$$

$$T_B = 0.03\ R_{axis}$$

R_{axis} = radius to axis of top arch.

Full radial abutments are advantageous for good bearing against rock. However, where excessive excavation would result from the use of full-radial abutments, and the rock has required strength and stability, there the abutments may be reduced to half radial.

6.1.1 Analysis of Arch Dam Symmetric half

An arch dam is designed with the above stated preliminary guidelines. The input of 27 points to the program gives the mapped continuum, which can be discretised to

any number of divisions in each direction. The plot of the mesh for the dam by assuming a symmetric geometry is shown in Fig 6.2.

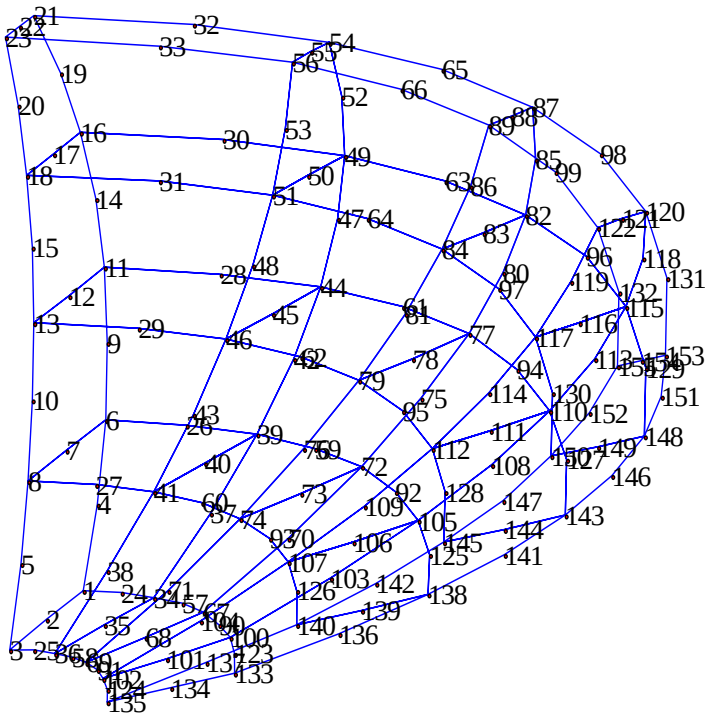

Fig 6.2: ***Generated mesh of USBR arch dam half***

Design Data

Bottom width of gorge; L_B = 80m

Top width of gorge; L_1 = 400m

Height of gorge; H = 120m

Top width of dam; T_C = 7.5m

The dam being symmetric only half of it is selected for analysis. The node numbering pattern, deformed shapes for loading condition, self weight and hydrostatic

pressure upto117.00 m using 9, 32 and 24 elements are given in Fig 6.3, Fig 6.4, Fig 6.5 and Fig 6.6 respectively.

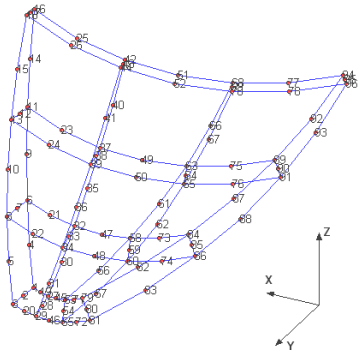

Fig 6.3: ***Symmetric Arch Dam.***
Node numbering pattern

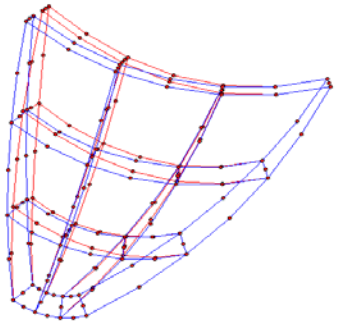

Fig 6.4: ***Symmetric Arch Dam.***
Deflected profile 9 elements

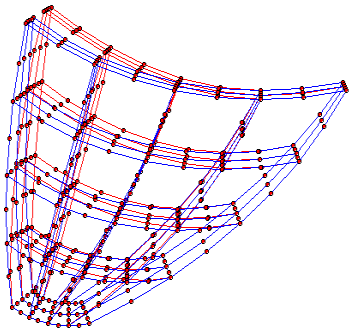

Fig 6.5: ***Symmetric Arch Dam.***
Deflected profile 32 elements

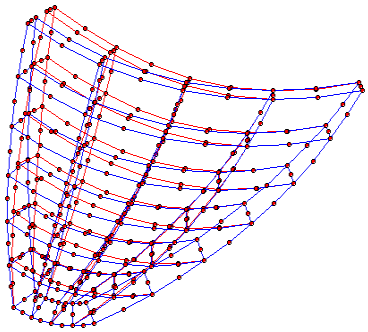

Fig 6.6: ***Symmetric Arch Dam***.
Deflected profile 24 elements

The deflection and stress under crown of the dam is plotted and verified with the standard USBR results.[20,24] The deflections and stresses due to self-weight and water pressure under crown for a symmetric arch dam with 24; 48 total, number of elements are tabulated in Table 6.1, 6.2, 6.3 and plotted in Fig 6.7, 6.8 and 6.9.

Number of elements = 24

Height of dam =120.0 m

Reservoir water level = 117.0m

Unit weight of dam material = 25 kN/m^3

Modulus of elasticity E = 2000 kN/cm^2

Table 6.1: **Deflection of down stream crown section**

Node	Displ X cm	Displ Y cm	Displ Z cm	H m
01	0	0	0	00.0
04	0	-0.340305	-0.290206	10.0
06	0	-0.891409	-0.401761	20.0
09	0	-1.482735	-0.439557	30.0
11	0	-2.100450	-0.436812	40.0
14	0	-2.704198	-0.408066	50.0
16	0	-3.277860	-0.387198	60.0
19	0	-3.812427	-0.377764	70.0
21	0	-4.310352	-0.380078	80.0
24	0	-4.766217	-0.393117	90.0
26	0	-5.187187	-0.418377	100.0
29	0	-5.581434	-0.459314	110.0
31	0	-5.977100	-0.516325	120.0

Radial deflection, hoop stress and vertical stress at the upstream crown section are plotted with dam height and the variation is respectively compared with the graphs given by Krishnamoorthy. All the results are found conforming.

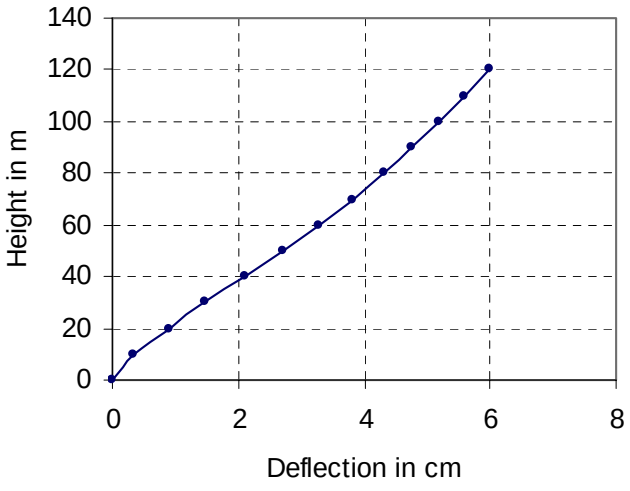

Fig 6.7: ***Radial deflection at crown Vs Height of dam***

The hoop stress, as in Table 6.2, at the extreme upstream crown section of water face varies from a maximum tensile stress of 22.28 kg/cm^2 at dam bottom, to a maximum compressive stress of 52.25 kg/cm^2 at 90 m elevation,. It decreases thereafter; hoop stress at extreme downstream crown section of air face, varies from compressive stress of 21.08 kg/cm^2 at dam bottom to a maximum compressive stress of 33.68 kg/cm^2 at dam top.

Table 6.2: **Hoop Stress at crown section**

Height in m	Stress downstream in kg/cm2	Stress upstream in kg/cm2
0	-21.0851	22.283
10	-16.3329	2.1844
20	-13.1962	-13.722
30	-13.2165	-26.136
40	-15.0134	-34.247
50	-17.3486	-40.165
60	-18.8142	-45.788
70	-21.8644	-49.259
80	-24.3089	-51.663
90	-26.8006	-52.252
100	-29.1408	-51.910
110	-31.5433	-49.724
120	-33.6847	-46.975

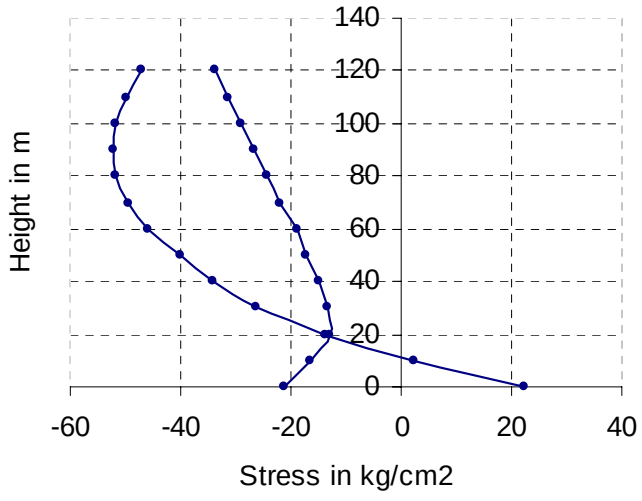

Fig 6.8: ***Hoop stress at crown Vs Height of dam***

The vertical stress as in Fig. 6.9 downstream crown section air face varies from a maximum compressive stress of 84.3 kg/cm2 at dam bottom to a maximum tensile stress of 18.9 kg/cm2 at an elevation 80 m and thereafter decreases to nearly zero at dam top; vertical stress at upstream crown section water face varies from a maximum tensile stress of 89.15 kg/cm2 at dam bottom to a maximum compressive stress of 23.7 kg/cm2 at an elevation 70 m and thereafter decreases to nearly zero at dam top.

Table 6.3: **Vertical Stress at crown section**

Height in m	**Stress upstream** in kg/cm^2	**Stress downstream** in kg/cm^2
0	89.154	-84.308
10	43.566	-56.515
20	15.116	-21.872
30	-4.288	-10.035
40	-12.235	2.614
50	-17.245	10.605
60	-22.327	16.521
70	-23.718	17.9014
80	-23.128	18.925
90	-20.017	15.731
100	-15.027	11.442
110	-11.424	5.514
120	-1.517	-0.877

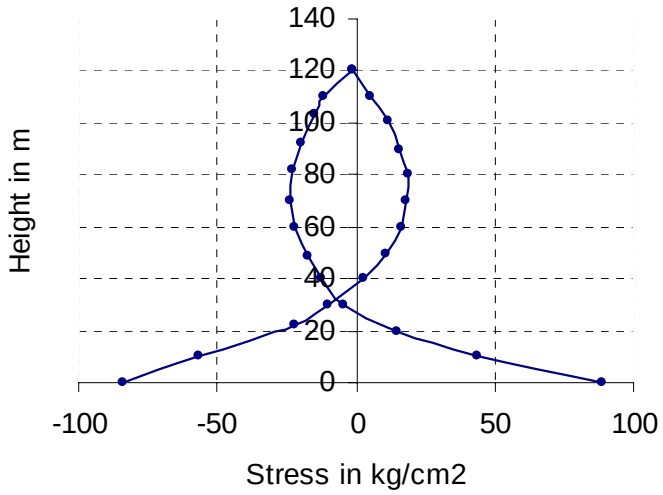

Fig 6.9: ***Vertical stress at crown Vs Height of dam***

Seismic and Hydrodynamic effect

In the same dam section, the effect of hydrodynamic pressure is included and analysed. Then the effect of horizontal earthquake acceleration in the dam body is combined and analysed. The deformed profile is plotted in Fig 6.10. The results tabulated in Table 6.4 and variation in radial deflection is shown in the graph Fig 6.11 comparing with the hydrostatic and dam body weight.

Table 6.4: **Deflection at crown section due to various loading**

	Hydrostatic and Hydrodynamic			**Hydrostatic, Hydrodynamic and Seismic(0.2g horizontal)**			
Node	**u**	**v cm**	**w cm**	**u**	**v cm**	**w cm**	**H m**
1	0	0	0	0	0	0	0.0
4	0	-0.4202	-0.3402	0	-0.4416	-0.3553	10.0
6	0	-1.1115	-0.4484	0	-1.1754	-0.4659	20.0
9	0	-1.8455	-0.4602	0	-1.9668	-0.4756	30.0
11	0	-2.5992	-0.4218	0	-2.7818	-0.4326	40.0
14	0	-3.3211	-0.3527	0	-3.5732	-0.3576	50.0
16	0	-3.9895	-0.2960	0	-4.3099	-0.2970	60.0
19	0	-4.5963	-0.2574	0	-4.9905	-0.2573	70.0
21	0	-5.1448	-0.2355	0	-5.6116	-0.2374	80.0
24	0	-5.6330	-0.2300	0	-6.1776	-0.2373	90.0
26	0	-6.0702	-0.2409	0	-6.6933	-0.2574	100.0
29	0	-6.4714	-0.2721	0	-7.1808	-0.3013	110.0
31	0	-6.8692	-0.3221	0	-7.6681	-0.3670	120.0

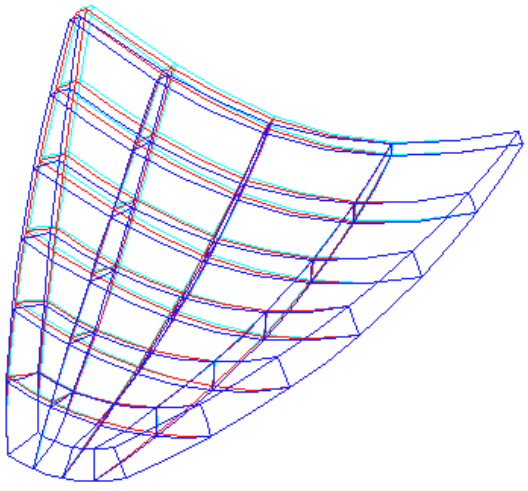

Fig 6.10: ***Deformed profiles due to various loading***

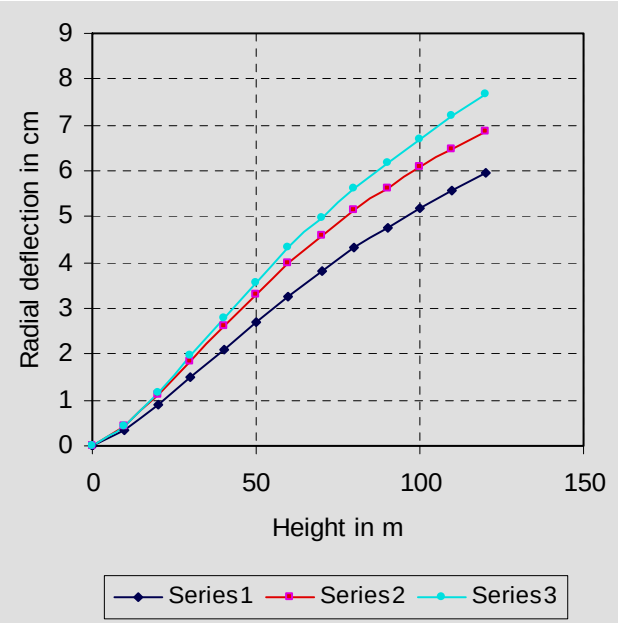

Series 1- Hydrostatic and Self weight
Series 2- Hydrostatic, Self weight and Hydrodynamic
Series 3- Hydrostatic, Self weight, Hydrodynamic and Seismic

Fig 6.11: ***Radial deflection due to various loading***

It is seen that due to the hydrodynamic effect and seismicity, the stresses are considerably increased which is compared in Table 6.5

Table 6.5: **Stresses due to various loading conditions**

	Series 1			Series 2			Series 3		
Elem	Sig x	Sig y	Sig z	Sig x	Sig y	Sig z	Sig x	Sig y	Sig z
1	-6.216	-6.097	-0.6375	-6.613	-7.013	-1.994	-6.235	-6.946	-0.127
2	-17.46	-7.161	-9.200	-21.388	-8.678	-6.729	-21.896	-8.934	-5.523
3	-25.8	-4.644	-9.452	-31.826	-5.499	-8.208	-33.31	-5.664	-7.481
4	-31.32	-3.387	-8.403	-38.108	-3.961	-7.919	-40.537	-4.092	-7.548
5	-34.1	-2.678	-6.006	-40.659	-3.094	-5.875	-44.006	-3.212	-5.734
6	-34.29	-1.886	-2.493	-39.987	-2.126	-2.491	-44.276	-2.226	-2.479
7	-7.678	-8.117	-10.42	-8.339	-9.369	-7.079	-8.199	-9.407	-5.738
8	-14.33	-11.837	-14.374	-17.462	-14.264	-13.64	-17.866	-14.846	-13.11
9	-18.76	-9.414	-13.433	-23.026	-11.121	-13.61	-24.099	-11.68	-13.43
10	-21.28	-7.280	-10.653	-25.844	-8.512	-11.04	-27.56	-9.026	-11.00
11	-22.13	-5.675	-6.774	-26.367	-6.586	-7.02	-28.672	-7.073	-7.024
12	-21.49	-4.600	-2.327	-24.943	-5.273	-2.365	-27.737	-5.795	-2.363
13	-7.071	-12.305	-14.402	-7.6126	-14.51	-12.842	-7.518	-14.828	-12.27
14	-10.4	-18.659	-17.125	-12.469	-23.001	-17.718	-12.78	-24.132	-17.73
15	-11.57	-15.242	-14.17	-14.019	-18.581	-14.702	-14.729	-19.798	-14.77
16	-11.51	-11.144	-10.299	-13.923	-13.423	-10.505	-14.974	-14.555	-10.54

17	-10.74	-7.969	-6.307	-12.927	-9.599	-6.290	-14.249	-10.641	-6.290
18	-9.945	-6.055	-2.209	-12.077	-7.468	-2.1374	-13.60	-8.495	-2.113
19	-5.642	-17.283	-14.136	-5.929	-20.337	-13.159	-6.107	-21.049	-13.07
20	-6.825	-22.636	-14.112	-7.587	-27.514	-13.255	-7.955	-29.024	-13.25
21	-6.257	-18.118	-11.536	-7.1637	-22.083	-10.739	-7.661	-23.8	-10.69
22	-5.24	-12.459	-8.838	-6.175	-15.212	-8.291	-6.760	-16.884	-8.222
23	-4.046	-7.550	-6.008	-4.991	-9.4517	-5.776	-5.638	-10.961	-5.714
24	-2.778	-3.59	-2.662	-3.780	-5.008	-2.672	-4.458	-6.288	-2.642

6.1.2 Analysis of Arch Dam in full

The same Arch dam is analyzed in full, to validate the program; to see whether the same values of deflection and stresses are obtained, at identical locations**.** The input of 45 points to the program gives the mapped continuum, which can be discretised to any number of divisions in each direction. The plot of the mesh for the dam by assuming a symmetric geometry is shown in Fig 6.12 and deformed profile in Fig 6.13.

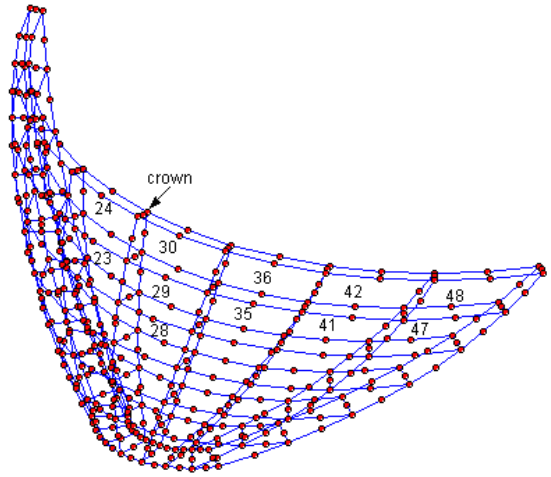

Fig 6.12: ***Mesh of full arch dam***

Number of elements = 48

Height of dam =120.0 m

Reservoir water Level = 117.0m

Unit weight of dam material = 25 kN/m^3

Modulus of elasticity E = 2000 kN/cm^2

Poisson's Ratio = 0.15

No of Gaussian points = 4

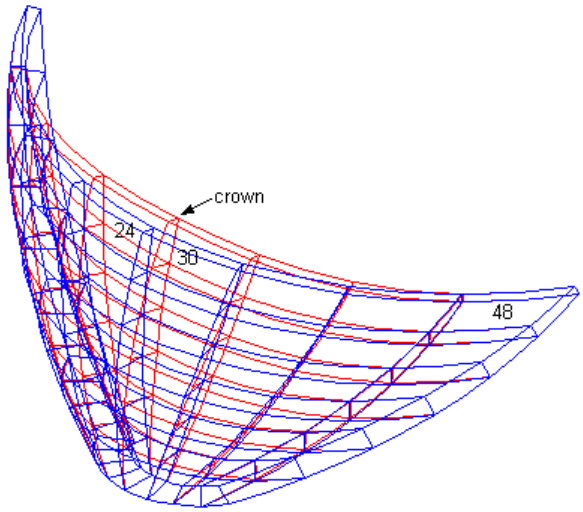

Fig 6.13: ***Deformed profile of the full arch dam***

Table 6.6: **Deflection of down stream crown section**

Node	Displ X cm	Displ Y cm	Displ Z cm	H m
189	0	0	0	00.0
192	0	-0.3437	-0.3065	10.0
194	0	-0.9125	-0.4210	20.0
197	0	-1.5288	-0.4572	30.0
199	0	-2.1706	-0.4551	40.0
202	0	-2.7933	-0.4276	50.0
204	0	-3.3816	-0.4089	60.0
207	0	-3.9260	-0.4028	70.0
209	0	-4.4281	-0.4093	80.0
212	0	-4.8828	-0.4269	90.0
214	0	-5.2962	-0.4564	100.0
217	0	-5.6776	-0.5013	110.0
219	0	-6.0535	-0.5607	120.0

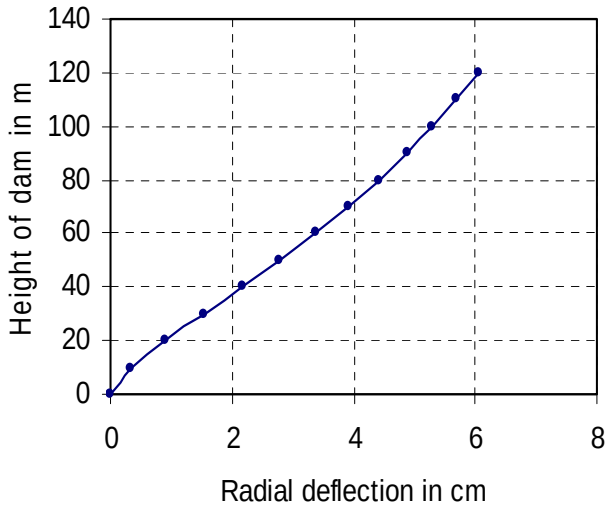

Fig 6.14: ***Radial deflection at down crown of the full arch dam***

Radial deflection at downstream crown section is tabulated, recorded in Table 6.6 and plotted in Fig 6.14. It is observed to conform very well to the values obtained in the case of half the arch. Similarly, the hoop stress at upstream water face and downstream air face are tabulated in Table 6.7 and plotted in Fig 6.15 and is seen that very well conforming to the values obtained for half the arch.

Table 6.7: **Hoop Stress at crown section**

Height in m	**Stress downstream in kg/cm2**	**Stress upstream in kg/cm2**
0	-21.5005	21.83447
10	-16.1344	2.249562
20	-13.1344	-13.6519
30	-13.1951	-25.9911
40	-15.1716	-33.909
50	-17.3735	-40.1468
60	-19.7059	-45.7411
70	-22.4936	-49.2995
80	-25.0306	-51.7552
90	-27.6503	-52.3489
100	-30.0816	-51.6463
110	-32.2792	-49.9863
120	-34.3459	-47.3353

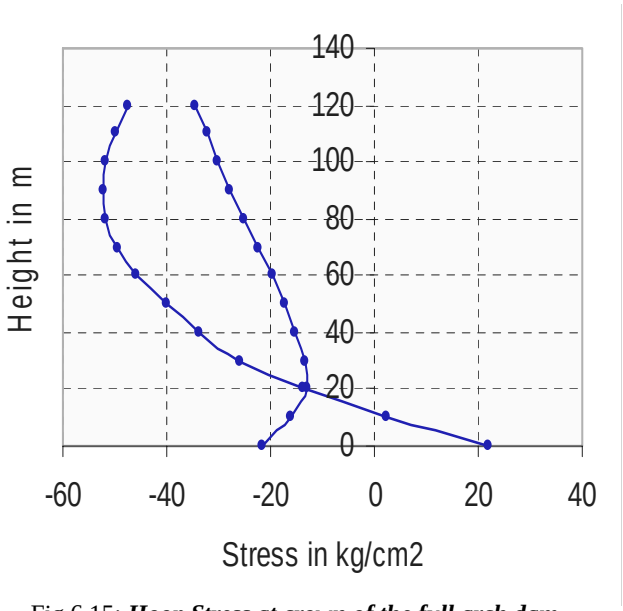

Fig 6.15: ***Hoop Stress at crown of the full arch dam***

The elemental stresses as obtained from the program at the centre of each element as average of 27 Gaussian points are tabulated below in Table 6.8 and found that for elements at identical locations, the values are the same.

Table 6.8: **Stresses at Element Centre as average of Gauss points**

Element	sig x	sig y	sig z	sig xy	sig yz	sig xz
1	-6.2138	-21.61	-22.224	-2.8282	-16.641	-2.5541
2	-6.6409	-24.269	-15.335	-3.7706	-14.716	-2.5061
3	-5.6773	-18.754	-11.539	-3.6845	-11.133	-1.5847
4	-4.5185	-12.899	-8.3	-3.2358	-7.5306	-1.2255
5	-3.1279	-7.9422	-5.268	-2.883	-4.4846	-0.9874
6	-1.8074	-3.9708	-1.7827	-2.2854	-1.6614	-0.4679
7	-6.5764	-13.717	-19.879	-1.1444	-11.885	-4.7299
8	-9.4308	-17.945	-14.137	-5.1383	-10.927	-5.8012
9	-11.258	-14.364	-13.438	-7.2125	-8.9137	-5.2792
10	-11.715	-10.835	-10.127	-7.6653	-5.9756	-4.4905
11	-11.258	-8.1732	-6.5906	-7.7666	-3.2789	-3.5311
12	-10.689	-6.7667	-2.5658	-7.8421	-1.1436	-1.8036
13	-5.9595	-9.3564	-14.533	-0.3747	-10.678	-4.3095
14	-12.936	-10.92	-11.409	-5.0178	-7.9133	-6.9099
15	-18.276	-8.0767	-12.81	-7.7788	-5.487	-7.3166
16	-21.413	-6.2355	-10.091	-8.3177	-3.0021	-6.1922
17	-22.686	-4.9095	-6.3765	-8.4022	-0.8653	-4.3277
18	-22.471	-4.1128	-2.2484	-8.6007	0.16465	-1.7966
19	-5.3683	-7.6882	-9.5248	-0.0504	-9.9308	-1.7261
20	-16.017	-6.5896	-6.5114	-2.0814	-5.2185	-3.3228
21	-24.556	-3.6294	-8.6157	-3.3895	-2.0279	-3.8198
22	-29.733	-2.5349	-7.4506	-3.6478	-0.1254	-3.3273
23	-32.091	-1.8355	-5.0525	-3.6138	1.0126	-2.2731
24	**-31.836**	**-0.9868**	**-1.7916**	**-3.628**	**0.80187**	**-0.7729**

25	-5.3683	-7.6882	-9.5248	0.05047	-9.9308	1.7261
26	-16.017	-6.5896	-6.5114	2.0814	-5.2185	3.3228
27	-24.556	-3.6294	-8.6157	3.3895	-2.0279	3.8198
28	-29.733	-2.5349	-7.4506	3.6478	-0.1254	3.3273
29	-32.091	-1.8355	-5.0525	3.6138	1.0126	2.2731
30	**-31.836**	**-0.9868**	**-1.7916**	**3.6286**	**0.80187**	**0.77295**
31	-5.9595	-9.3564	-14.533	0.37475	-10.678	4.3095
32	-12.936	-10.92	-11.409	5.0178	-7.9133	6.9099
33	-18.276	-8.0767	-12.81	7.7788	-5.487	7.3166
34	-21.413	-6.2355	-10.091	8.3177	-3.0021	6.1922
35	-22.686	-4.9095	-6.3765	8.4022	-0.8653	4.3277
36	-22.471	-4.1128	-2.2484	8.6007	0.16465	1.7966
37	-6.5764	-13.717	-19.879	1.1444	-11.885	4.7299
38	-9.4308	-17.945	-14.137	5.1383	-10.927	5.8012
39	-11.258	-14.364	-13.438	7.2125	-8.9137	5.2792
40	-11.715	-10.835	-10.127	7.6653	-5.9756	4.4905
41	-11.258	-8.1732	-6.5906	7.7666	-3.2789	3.5311
42	-10.689	-6.7667	-2.5658	7.8421	-1.1436	1.8036
43	-6.2138	-21.61	-22.224	2.8282	-16.641	2.5541
44	-6.6409	-24.269	-15.335	3.7706	-14.716	2.5061
45	-5.6773	-18.754	-11.539	3.6845	-11.133	1.5847
46	-4.5185	-12.899	-8.3	3.2358	-7.5306	1.2255
47	-3.1279	-7.9422	-5.268	2.883	-4.4846	0.98744
48	-1.8074	-3.9708	-1.7827	2.2854	-1.6614	0.46799

6.2 RESULTS AND DISCUSSIONS

Half of a symmetrical *USBR* arch dam is analyzed with the boundary condition due to symmetry assumed. The dam is assumed fixed at bottom and sides. At the crown section, the tangential deflection is assumed *zero.* The graph obtained conforms to the standard available as given by *Zienkewicz*, *Varshney* and *Krishnamoorthy* for *USBR* type arch dams.[2,20,24,26]

6.2.1 Convergence

a. Various descretisation

For convergence study, the dam is analysed for various discretisations and the variation of deflection is plotted in the same graph, Fig 6.16 for adjacent discretisation. The results are tabulated in Table 6.9.

Table 6.9: **Deflection of dam for various discretisations**

Sl. No	Number of elements	Number of nodes	Number of DOF	No. of displ prescribed	Deflection downstream crest of dam in cm							
					Height 30.0 m		Height 60.0 m		Height 90.0 m		Height 120.0 m	
					Radial	Vertical	Radial	Vertical	Radial	Vertical	Radial	Vertical
1.	1(1x1x1)	20	16	18	-	-	-1.5811	-0.4594	-	-	-2.5362	-0.0334
2	2(1x1x2)	32	32	28	-1.0246	-0.35536	-1.92211	-0.27788	-2.54900	-0.34526	-2.8866	-0.36679
3	4(2x1x2)	51	74	33	-1.1563	-0.39339	-2.60930	-0.4112	-3.6630	-0.42009	-4.4831	-0.4861
4	6(3x1x2)	70	116	38	-1.2263	-0.42187	-2.8551	-0.49644	-4.1944	-0.5500	-5.36312	-0.6927
5	16(4x1x4)	155	316	63	-1.3880	-0.4289	-3.0346	-0.4047	-4.3872	-0.4000	-5.4285	-0.4966
6	24(4x1x6)	221	474	83	-1.4146	-0.4287	-3.0899	-0.3798	-4.4320	-0.3765	-5.4744	-0.4776
7	36(6x1x6)	315	726	93	-1.4210	-0.4289	-3.1111	-0.3805	-4.4801	-0.3828	-5.5572	-0.4939
8	48(6x1x8)	409	968	113	-1.4389	-0.4368	-3.1331	-0.4368	-4.4923	-0.37027	-5.5593	-0.4851

The values are found converging on finer discretisation. Hence, graphs of higher discretisations are not visible.

Number of Gaussian points = 4

Modulus of elasticity, E = 2e+007 kN/m^2

Poisson's ratio = 0.2

Unit weight of dam material = 25 kN/m^3

Unit weight of water = 10 kN/m^3

Water level = 115m

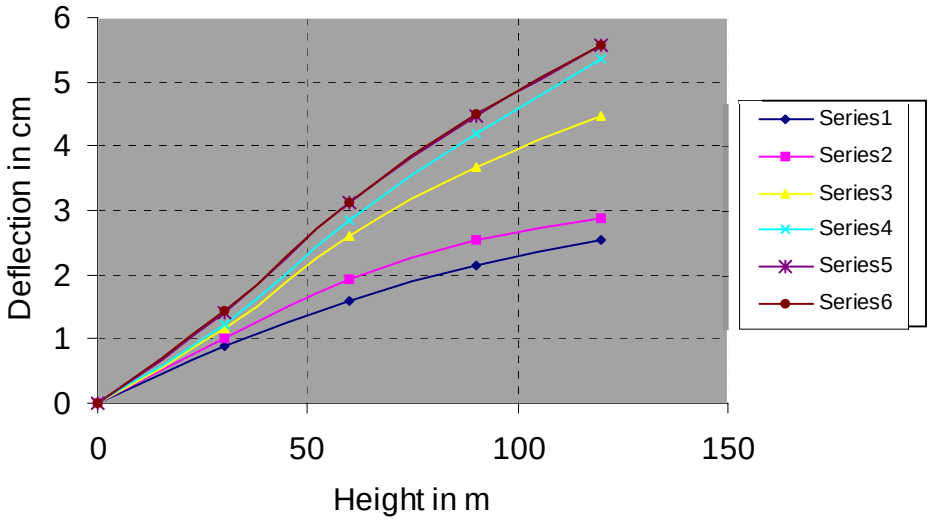

Fig 6.16: ***Radial deflection at crown due to various discretisations***

b. Material Properties

The selected dam is analysed for various materials by changing the unit weight to find the influence of material on deflection of dam Table 6.10. It is found that the variation in crown radial deflection due to unit weight is not direct but inverse after a particular level in Fig 6.17. Though there is not much variation in radial deflection, substantial variation in vertical deflection is found in Fig 6.18.

(i) ***Unit weight of dam material***

Number of elements = 36

Number of nodes = 315

Number of Gaussian points = 4

Modulus of elasticity, E = 2e+007 kN/m^2

Unit weight of liquid = 10 kN/m^3

Unit weight of dam material = 20 kN/m^3, 24 kN/m^3, 28 kN/m^3

Water level = 110m

Table 6.10: **Deflection due to change in material unit weight**

Node	Height of dam	Deflection at crown in c m					
		Dam unit weight 20 kN/m^3		Dam unit weight 24 kN/m^3		Dam unit weight 28 kN/m^3	
		Radial	Vertical	Radial	Vertical	Radial	Vertical
1	0	0	0	0	0	0	0
4	10.0	-0.311	-0.251	-0.303	-0.258	-0.296	-0.264
6	20.0	-0.805	-0.333	-0.773	-0.357	-0.741	-0.382
9	30.0	-1.323	-0.341	-1.266	-0.390	-1.210	-0.438
11	40.0	-1.841	-0.312	-1.765	-0.386	-1.689	-0.459
14	50.0	-2.326	-0.258	-2.238	-0.357	-2.150	-0.456
16	60.0	-2.758	-0.209	-2.669	-0.332	-2.579	-0.454
19	70.0	-3.130	-0.171	-3.050	-0.314	-2.970	-0.458
21	80.0	-3.443	-0.139	-3.383	-0.302	-3.323	-0.465
24	90.0	-3.694	-0.117	-3.663	-0.297	-3.632	-0.478
26	100.0	-3.888	-0.102	-3.897	-0.299	-3.905	-0.497
29	110.0	-4.043	-0.103	-4.097	-0.315	-4.151	-0.528
31	120.0	-4.187	-0.115	-4.292	-0.343	-4.397	-0.570

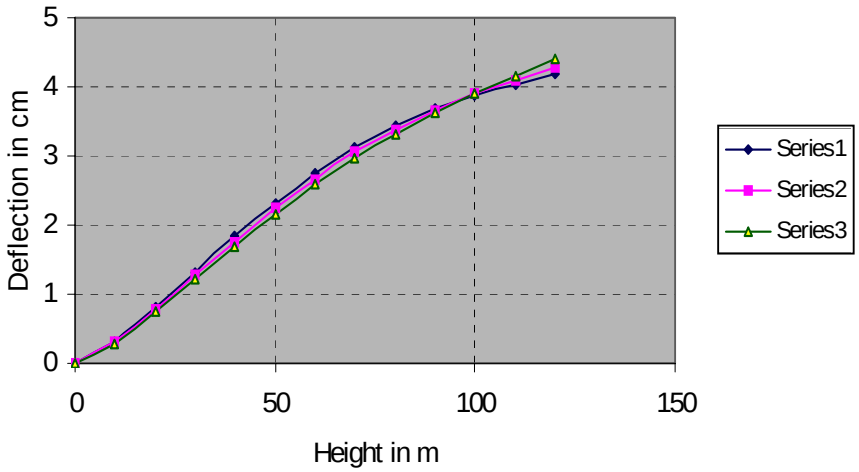

Fig 6.17: ***Radial deflection at crown due to variation in unit weight***

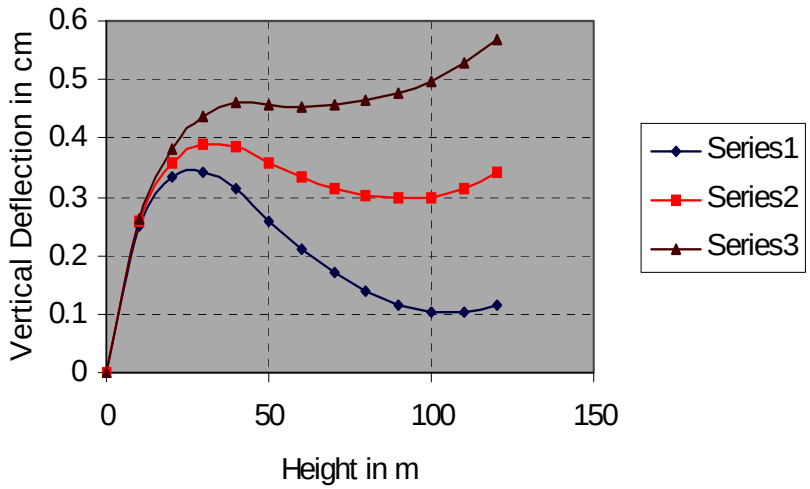

Fig 6.18: ***Vertical deflection at crown due to variation in unit weight***

(ii) ***Modulus of elasticity***

Also the modulus of elasticity is varied and the deflection compared Table 6.11. On increasing the modulus of elasticity radial as well as vertical deflection at crown section is found decreasing as given in Fig 6.19. This study is useful to select the ideal material for dam construction.

Number of elements = 36

Height of dam =120.0 m

Reservoir water level = 110.0m

Unit weight of dam material = 25 kN/m^3

Modulus of elasticity, E = 1500 kN/cm^2, 2000 kN/cm^2, 2500 kN/cm^2

Number of Gaussian points = 4

Table 6.11: **Variation in deflection due to modulus of elasticity**

Node	Height of dam	Deflection at crown in cm					
		E = 1500 kN/cm2		E = 2000 kN/cm2		E =2500 kN/cm2	
		Radial	Vertical	Radial	Vertical	Radial	Vertical
1	0	0	0	0	0	0	0
4	10.0	-0.402	-0.346	-0.301	-0.259	-0.241	-0.207
6	20.0	-1.020	-0.485	-0.765	-0.364	-0.612	-0.291
9	30.0	-1.670	-0.536	-1.252	-0.402	-1.002	-0.321
11	40.0	-2.328	-0.539	-1.746	-0.404	-1.397	-0.323
14	50.0	-2.955	-0.509	-2.216	-0.381	-1.773	-0.305
16	60.0	-3.529	-0.484	-2.646	-0.363	-2.117	-0.290
19	70.0	-4.040	-0.467	-3.030	-0.350	-2.424	-0.280
21	80.0	-4.490	-0.458	-3.368	-0.343	-2.694	-0.274
24	90.0	-4.874	-0.457	-3.655	-0.343	-2.924	-0.274
26	100.0	-5.199	-0.465	-3.899	-0.349	-3.119	-0.279
29	110.0	-5.481	-0.491	-4.110	-0.368	-3.288	-0.295
31	120.0	-5.758	-0.533	-4.318	-0.400	-3.455	-0.320

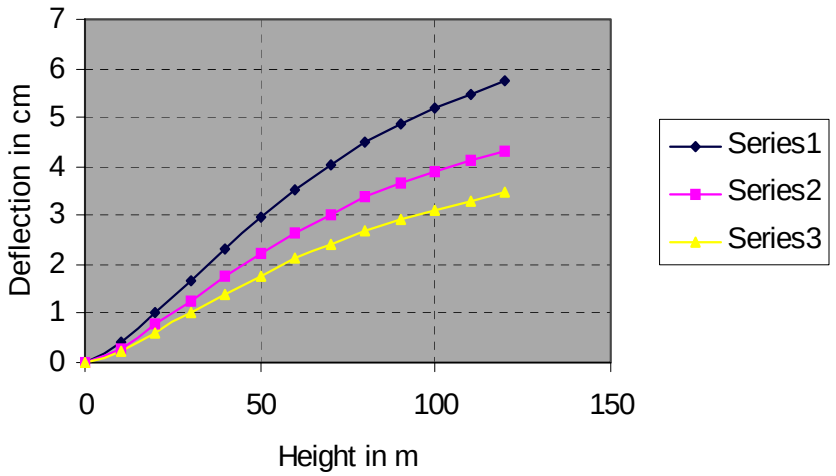

Fig 6.19: ***Variation in Radial Deflection due to modulus of elasticity***

6.2.2 Parametric study

The *USBR* dam geometry assumed is not varied for this parametric study. However, the reservoir water level is changed as per Table 6.12 to observe its influence on deflection. The trend of variation in deflection as shown in Fig 6.20 is different above a particular level. This study is very useful to have information in advance; regarding the dam deflection properties, once the reservoir is impounded after construction of the dam.

(i) Reservoir water level

Number of elements = 36
Number of nodes = 315
Modulus of elasticity, E = 2e+007 kN/m^2
Poisson's ratio = 0.2
Unit weight of solid = 25 kN/m^3
Unit weight of liquid = 10 kN/m^3

Table 6.12**: Variation of deflection due to reservoir water level**

Node	Height of dam	Deflection at crown in cm					
		Water level = 90 m		Water level = 100 m		Water level = 110 m	
		Radial	Vertical	Radial	Vertical	Radial	Vertical
1	0	0	0	0	0	0	0
4	10.0	-0.187	-0.171	-0.244	-0.215	-0.301	-0.259
6	20.0	-0.402	-0.256	-0.584	-0.310	-0.765	-0.364
9	30.0	-0.578	-0.296	-0.915	-0.349	-0.012	-0.402
11	40.0	-0.710	-0.312	-1.228	-0.358	-1.746	-0.404
14	50.0	-0.783	-0.307	-1.500	-0.344	-2.216	-0.381
16	60.0	-0.789	-0.292	-1.718	-0.327	-2.646	-0.363
19	70.0	-0.722	-0.267	-1.876	-0.309	-3.030	-0.350
21	80.0	-0.580	-0.230	-1.974	-0.287	-3.368	-0.343

24	90.0	-0.358	-0.184	-2.007	-0.263	-3.655	-0.343
26	100.0	-0.066	-0.128	-1.982	-0.238	-3.899	-0.349
29	110.0	0.277	-0.076	-1.916	-0.222	-4.110	-0.368
31	120.0	0.634	-0.024	-1.842	-0.212	-4.318	-0.400

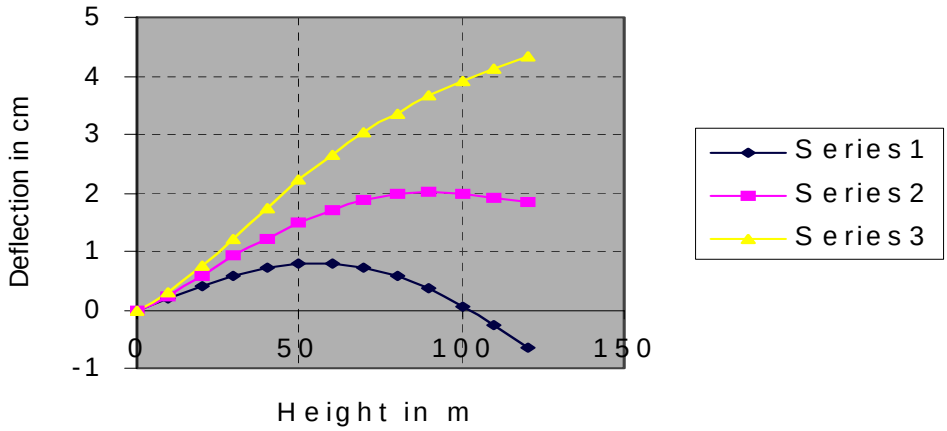

Fig 6.20: ***Variation in Radial deflection due to reservoir water***

6.3 CASE STUDY

A case study with the developed program is also included to see the effectiveness of the software developed. The Idukki arch dam in Kerala is taken for case study. The results of analysis are compared with the available. The Idukki hydroelectric project in Kerala State is commissioned by the *Kerala State Electricity Board,* in collaboration with the *Central Water & Power Commission of India* and the *Canadian International Development Agency* in the year 1976. The purpose of this project is to regulate the flow in *Periyar* and *Cheruthoni* rivers for irrigation and power generation. This reservoir necessitated the construction of three dams viz. *Kulamavu* masonry gravity dam, *Cheruthoni* concrete gravity dam and the *Idukki* concrete arch dam. A net head of 670 m produces 780 megawatts with a load factor of 0.3, in an underground powerhouse equipped with six Pelton turbines of 130 megawatts each.

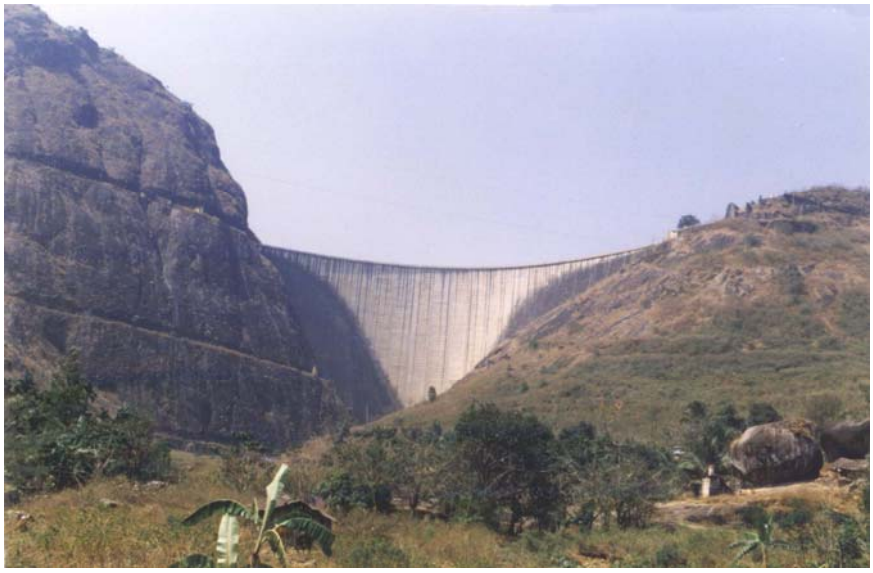

Fig 6.21: ***Idukki arch dam;*** *view from down stream.*

Site of Idukki

The Idukki site is located in a narrow gorge of the *Peryiar River valley*, has very steep banks extending 335.28 m above the river elevation. The width of gorge varies approximately from 9 m at low water level to 320 m at the top of elevation 160 m.[93]

Shape of Dam

To determine the shape of Idukki dam, preliminary studies involving radial adjustments were made of 17 alternative designs. Horizontal parabolas; *extrados and intrados,* define the selected alternative with foci following in vertical plane. Downstream, sectional and upstream views of the dam are shown in Fig 6.21, 6.22 and 6.23 respectively. The criteria for selection are:

- Best condition of support at foundations
- Favourable stress distribution in the dam proper
- Low concrete volume

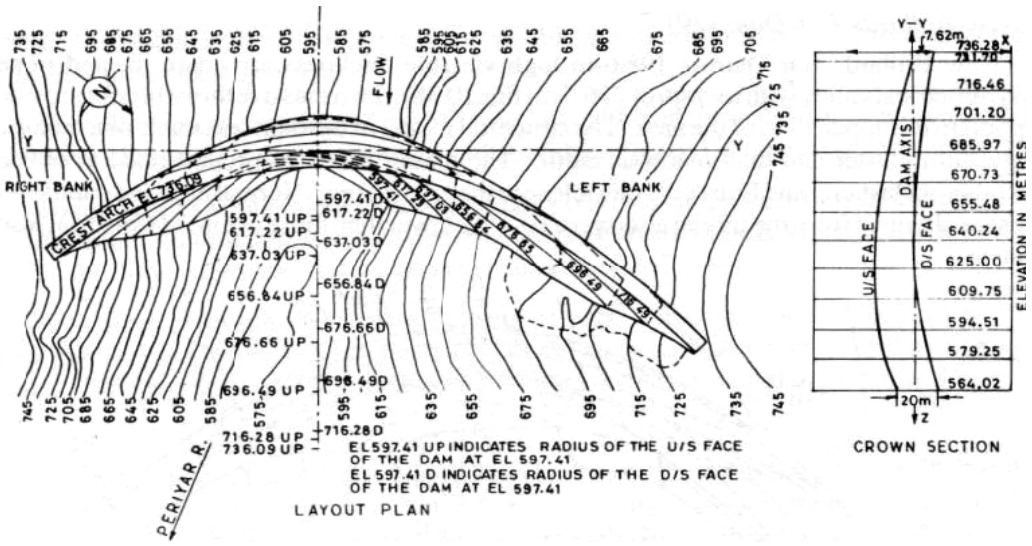

Fig 6.22: ***Idukki arch dam;*** *sectional plan and elevation*

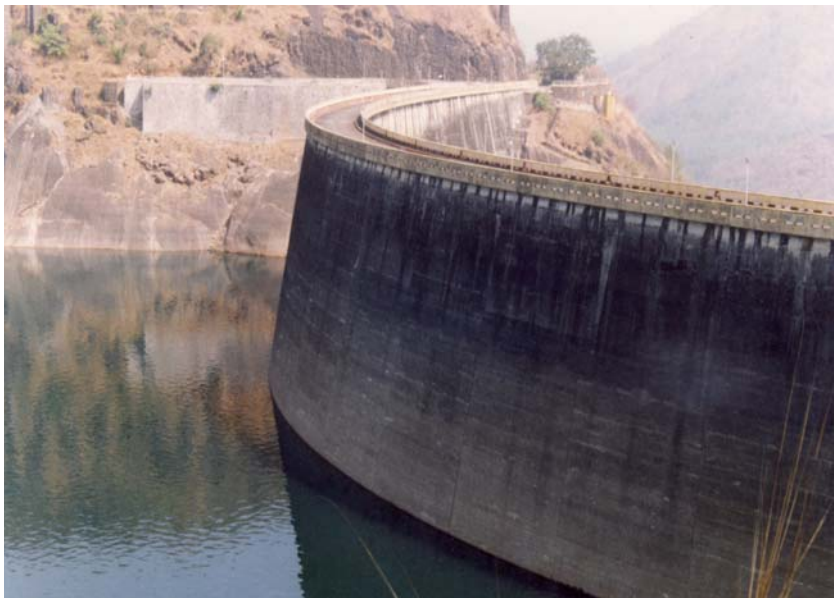

Fig 6.23: ***Idukki arch dam; view from upstream***

Water Levels

Maximum water level is at elevation 156.5 m above dam bottom.

Maximum silt level is at elevation 77.5 m above dam bottom.

6.3.1 Basic Assumptions and Design Criteria

Concrete

Concrete is considered homogeneous, isotropic and linearly elastic. Though, this assumption is not valid in the case of ordinary reinforced concrete structures, for a massive structure like a dam the error introduced is negligible under working loads. The material properties are taken as follows.

Modulus of elasticity	:	2.1×10^7 kN/m^2
Coefficient of thermal expansion	:	5.5×10^6/^{o}F
Poisson's ratio	:	0.20
Unit weight	:	24 kN/m^3
Compressive strength	:	28 N/mm^2

Rock

It is assumed that the foundations are homogeneous, isotropic and elastic with the following rock characteristics.

Modulus of elasticity	:	2.1×10^7 kN/m^2
Poisson's ratio	:	0.20

Stresses

The actual maximum allowable working stresses for the concrete in the case of normal loads are 7 N/mm^2 for compressive stresses and 0.7 N/mm^2 for tensile stresses. These stresses would be raised by 33% when the applied loads include earthquake acceleration of 0.1g.

Loads

Dead load (concrete)	:	24 kN/m^3
Dead load (water)	:	10 kN/m^3

Maximum water level	:	156.50m
Silt *(equivalent hydrostatic Pressure)*	:	12.5 kN/m^3
Maximum silt level	:	77.5m

Earthquake

Horizontal acceleration	:	0.02g and 0.10g

Temperature

Air (max. monthly av.)	:	80^oF
Water at surface	:	70^oF
Water at bottom	:	60^oF
Grouting	:	70^oF

Methods of Analysis

The arch dam is analyzed by the following methods.

1. Trial load method
2. Finite element method
3. Model studies

Trial load analysis

The *Trial load* method is adopted for the stress analysis. In this method, the dam is replaced by a system of vertical cantilevers and horizontal arches. This system is assumed to occupy the entire volume of the dam. Instead of investigating a great number of elements, only a few typical arches and cantilevers are analysed. The analysed structure then becomes a grid of intersecting arches and cantilevers which are called the design elements.[94]

1. For the trial load analysis of Idukki arch dam, the grid chosen consists of 8 arches at 19.5 m centres, the top one located along the crest at elevation 158.5 m and the bottom one at elevation 0.0 m. 14 cantilevers are located at the intersection of the upstream face of the arches with the foundation contour line.

2 Crown cantilever in the plane of arch centres. With this grid, stresses were obtained at 81 locations on each face of the dam.

Finite element method

Finite element analysis of Idukki arch dam was carried out at the Industrial Research Institute, University of Waterloo, Canada.[95] Curved boundary, isoparametric three-dimensional finite elements with 20 nodes were assumed for the analysis. A total of 26 elements were used, the elements along the rock face being placed normal to the boundary in order to model stresses as accurately as possible. The elements were distributed such that more detailed analysis of the left bank which is flatter could be obtained. Only 7 elements were used to model the right-bank, whereas, 19 elements were used for the left bank. Only one element grid arrangement was considered for which four analyses were performed. Two types of loading were considered viz.

(a) Dead load for the entire dam.

(b) Pressure loading due to the maximum water level and maximum silt level.

Model Test

M/s Surveyer in 1969 carried out tests on scale models of *Idukki* arch dam. A 2:1 mix by weight of molding plaster and celite; *white Kieselghur,* having a low modulus of elasticity was used for casting the models. The models were cast monolithically and they included a portion of the surrounding terrain. A model

prototype scale ratio of 1/240 was adopted. The hydrostatic loading is applied with mercury. Altogether, three models were tested. The tests on the first two models revealed a zone of tension that exceeded design values. Hence, by reshaping the lower upstream face of the first model, the third model was made. The test on these models indicated stresses both compressive and tensile, which remained within allowable limits. A study was also conducted by *Raveendran* to calculate the structural behaviour of the dam.[96]

6.3.2 Finite Element Analysis

Idukki full arch

The geometry of the Idukki arch dam, in the thesis, is modelled by adopting a degree of seven in length and four directions and one in thickness direction. The mesh is generated by inputting the global coordinates of 80 points of the dam as in Table 6.13. Any discretisation of the dam can be obtained by varying the values of nL, nT and nH. A plot of the mesh generated using 4 divisions in the tangential direction, 1 in the radial direction and 3 in the height direction is shown in Fig 6.24.

Input

L = 2, T = 2, H = 2, nL = 8, nT = 2, nH = 4

Degree L = 7, Degree T = 1, Degree H = 4

Table 6.13: **Global coordinates for mapping the Idukki arch dam geometry**

Nodes	X	Y	Z
1	18.8976	-10.9728	0
2	17.0688	5.4864	0
3	11.5824	-13.4112	0
4	10.9728	4.2672	0
5	5.4864	-14.6304	0
6	4.8768	4.2672	0

7	0	-14.6304	0
8	0	3.6576	0
9	-4.8768	-13.4112	0
10	-3.048	4.2672	0
11	-10.9728	-10.9728	0
12	-6.7056	5.4864	0
13	-17.0688	-8.5344	0
14	-10.3632	7.3152	0
15	-21.9456	-6.7056	0
16	-12.192	8.5344	0
17	56.0832	8.5344	39.624
18	42.672	28.0416	39.624
19	37.7952	-6.096	39.624
20	28.0416	12.192	39.624
21	22.5552	-14.6304	39.624
22	15.24	4.2672	39.624
23	0	-17.6784	39.624
24	0	0.6096	39.624
25	-18.8976	-14.6304	39.624
26	-12.192	2.4384	39.624
27	-34.7472	-9.144	39.624
28	-24.384	9.144	39.624
29	-51.2064	0	39.624
30	-35.9664	18.288	39.624
31	-60.96	10.9728	39.624
32	-43.8912	27.432	39.624
33	85.344	23.1648	79.248
34	71.9328	37.7952	79.248
35	62.1792	4.8768	79.248
36	51.2064	19.5072	79.248
37	32.9184	-9.7536	79.248
38	26.8224	4.8768	79.248
39	0	-15.8496	79.248
40	0	0	79.248
41	-26.8224	-12.192	79.248
42	-20.1168	3.048	79.248
43	-48.1584	-2.4384	79.248
44	-41.4528	12.192	79.248
45	-69.4944	9.7536	79.248
46	-57.912	24.384	79.248
47	-85.344	23.1648	79.248
48	-70.7136	36.576	79.248
49	106.07	33.528	118.872
50	97.536	45.72	118.872
51	75.5904	11.5824	118.872
52	67.056	23.1648	118.872
53	38.4048	-3.048	118.872
54	35.3568	8.5344	118.872
55	0	-9.144	118.872
56	0	3.048	118.872
57	-41.4528	-3.048	118.872
58	-37.7952	9.7536	118.872

59	-81.6864	15.24	118.872
60	-74.3712	26.2128	118.872
61	-115.824	39.0144	118.872
62	-106.07	51.2064	118.872
63	-146.304	73.152	118.872
64	-134.112	80.4672	118.872
65	130.454	51.2064	158.496
66	126.797	56.0832	158.496
67	90.2208	24.384	158.496
68	87.7824	30.48	158.496
69	47.5488	6.096	158.496
70	45.1104	13.4112	158.496
71	0	0	158.496
72	0	7.3152	158.496
73	-54.864	9.7536	158.496
74	-51.2064	14.6304	158.496
75	-103.632	31.6992	158.496
76	-98.7552	37.7952	158.496
77	-146.304	64.008	158.496
78	-141.427	70.7136	158.496
79	-184.099	102.413	158.496
80	-178.003	107.29	158.496

The dam is analysed with the developed program for the following loading conditions and the results are included as **Annexure.**

i. Self weight only

ii. Self weight, Maximum water level, Maximum silt level

iii. Self weight, Normal water level, Maximum silt level and Earthquake acceleration 0.02g

iv. Self weight, Normal water level, Maximum silt level and Earthquake acceleration 0.1g

v. Self weight, Normal water level, Maximum silt level, Earthquake acceleration 0.1g and Hydrodynamic effect

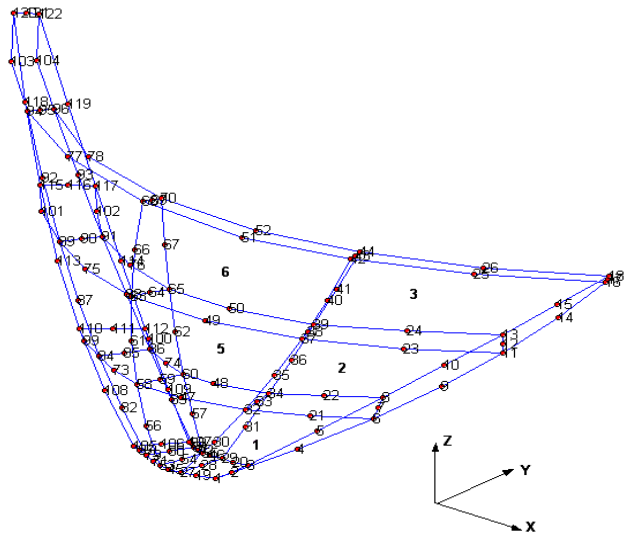

Fig 6.24: ***Idukki arch dam; Node numbering pattern***

The geometry of the dam is arrived with various degrees in length and height directions, by inputting corresponding basic element nodal points. It is found that higher degree polynomial defines the dam geometry accurately.[97,98] Here, the geometry arrived with 80 nodal inputs is analysed for various discretisations to see whether the values are comparable with the available results. Obtained radial deflections at the crown section of dam are compared with the value of maximum deflection of the original analysis; *by finite element method (4.06 cm), model test (4.83 cm) and trial load method (2.87 cm)*. It is found that the obtained results are conforming. Full set of earlier finite element analysis results are not available so also, assumptions on boundary conditions especially dam foundation load transfer, it being a crude analysis. However, the values at the crown cantilever are compared for various discretisations *with maximum water level and maximum silt level* and tabulated below in Table 6.14

Table 6.14: **Idukki arch dam maximum deflection for various discretisation**

No. of Elements	No. of Nodes	No. of Displ BC	No. of DOF	Maximum Deflection in cm
16	155	63	276	3.236
28	254	78	528	3.776
56	470	118	1056	3.793
112	741	189	1656	3.797

On finer discretisation, the maximum deflection of crown cantilever is found converging. The deflected shape of the dam with 28 elements is shown in Fig 6.25. The deflections under crown cantilever section are tabulated in Table 6.15. Radial deflection of arch at elevation 138.684 m are plotted in Fig 6.26. The values obtained for the element centroid stresses in the three directions arrived as the average of 27 Gauss point values are plotted below in Fig 6.27.

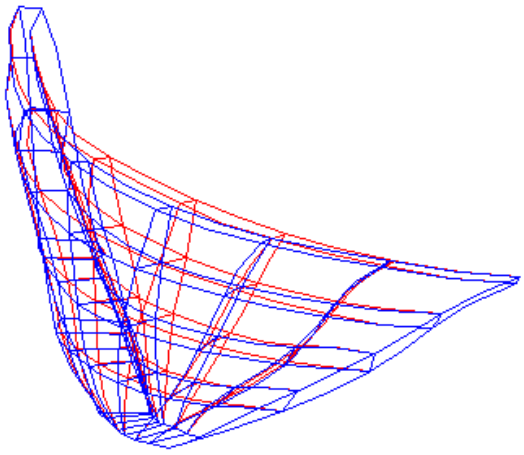

Fig 6.25*: **Deformed profile due to self weight and water pressure***
No. of elements = 28

Table 6.15: **Idukki arch dam Deflections under crown cantilever section**

Height	u in cm	v in cm	w in cm
0	0	0	0
19.812	0.05819	0.72205	-0.24186
39.624	0.06615	1.54211	-0.18641
59.436	0.03997	2.17384	-0.14036
79.248	0.02032	2.74785	-0.14886

99.06	0.04335	3.25346	-0.16200
118.872	0.07464	3.61830	-0.15322
138.684	0.11936	3.77658	-0.10680
158.496	0.13778	3.75169	-0.03664

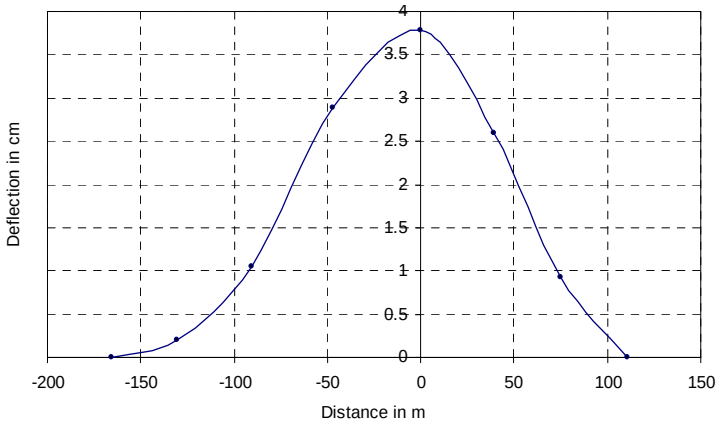

Fig 6.26: ***Radial deflection of Arch at elevation 138.684***

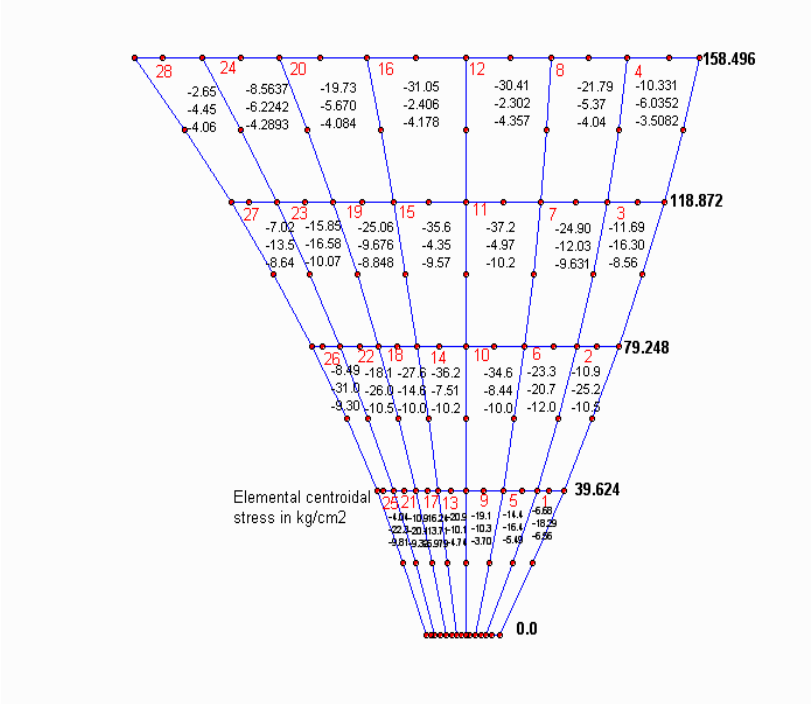

Fig 6.27: ***Idukki arch dam Elemental stresses***

Chapter 07

7.0 SUMMARY AND CONCLUSION

This chapter presents the conclusion and discussion regarding the effectiveness of the program developed together with domain of application and further scope.

7.1 DOMAIN OF APPLICATION

The finite element analysis program developed through the research, using linear and quadratic hexahedral elements is applicable for three dimensional continuums like beams; *straight and curved*, frames, thick plates, gravity dams, retaining walls, thin and thick gravity arch dams and the like structures. Since, *Lagrange shape functions* of higher order are used for defining the geometry accurately, structures with complex geometry like double and multiple curvature arch dams can also be effectively modeled and analysed with this software.[97] The software is developed using advanced programming technique in *Visual* C^{++} the results of which is verified by plotting. Further, it is versatile and capable of handling various load vectors and applicable to a variety of structural mechanics problems.

7.2 CONCLUSION

The *USBR* arch dam is analyzed for various loading combinations for *self weight, water pressure,* and *silt pressure, seismic* and *hydrodynamic effects*. The deflections under the crown cantilever are taken for different discretisations, values plotted and graphs checked and compared for convergence with established works for *USBR* type arch dams. It is found that the program is capable of accommodating the effect of curvature accurately with required degree of curve in each direction.[98] Various deflections and stresses obtained with the program are further, verified with the previous results of analysis by finite element method for *Idukki* arch dam.

The program developed is checked for its effectiveness and accuracy in handling the analysis of three-dimensional solid elastic continua of any geometry. It is further refined to accommodate body forces such as *self weight, gravity loads* and *earthquake acceleration*, surface forces due to hydrostatic, hydrodynamic, earth and silt pressures, concentrated nodal loads, age and uplift effects. The influence of curvature on dam-geometry; thereby, in load vectors resulting in stresses and deflection are arrived.[99] The computer simulation with specified reservoir level and loading conditions is adequate to predict the dam monitoring results.

The program developed is versatile enough and applicable to any type of three-dimensional solid structure, *i.e. not only to arch dams but to any type of solid continuum irrespective of geometry and loading*. Minor additions in the program will increase its versatility to handle a wide variety of structural mechanics applications too.

7.2.1 Scope for Future Work

The program is capable enough to facilitate researching the design and analysis of dams with different material properties, different geometry etc., to arrive an economic dam design. A complete finite element software for the analysis of three-dimensional solid continua including fluid retaining as well as hydraulic structures capable of accommodating temperature, earthquakes effects, body, hydrostatic surface and silt pressures both for static and dynamic analysis can be further developed by appropriately modifying this program. Structures situated to any climatic condition and seismic zone can then be easily analyzed, thereafter, to arrive at an optimal and economic design. Further, the computer simulation generated enhances effective prediction of the instrumented results during its entire life-span in effort to verify the reliability of the instrumentation, which is kernel to dam-performance.

Chapter 05

5.0 LOAD VECTORS

In finite element analysis, various loads acting on the structure are applied as *Global* and *Element load vectors*. Various loads considered in the analysis of an arch dam and how it can be effectively applied in finite element method is discussed in this Chapter. An arch dam will be acted upon by the following load vectors as.[2,5,85]

Body forces

(i) Gravity

(ii) Seismic inertia

(iii) Temperature

Surface forces

(i) Hydrostatic

(ii) Hydrodynamic

(iii) Silt and Earth

(iv) Uplift

(v) Wave

Nodal forces

(i) Concentrated

(ii) Distributed

These various loads are to be incorporated to the finite elements itself, or to the nodes as global equivalents in the finite element program by suitable means of distribution so as to ensure accuracy.

5.1 GLOBAL LOAD VECTOR

Concentrated loads acting at nodes along any degree of freedom direction are read directly in to the global load vector as:

```
// initialize global matrices

for (i=1; i<=neq; i++)
      {
            R[i]=0;
            For (j=1; i<=neq; i++)
            K[i][j]=0;
      }
//input nodal loads

int no_of_loaded_joints;
fin >> no_of_loaded_joints;
double load_X, load_Y, load_Z;
for (i=1; i<=no_of_loaded_joints; ++i)
      {
            fin >> k;  //node no
            fin >> load_X >> load_Y >> load_Z;
            global_load[id[1][k]] += load_X;
            global_load[id[2][k]] += load_Y;
            global_load[id[3][k]] += load_Z;
      }
```

Similarly, distributed line loads are applied at nodes as equivalent concentrated loads in the respective directions.[21]

5.2 ELEMENT BODY LOAD VECTOR

The body loads are applied as element load vectors in finite element method. The basic relationship between *load vector, displacement* and *stiffness matrices* for an element is given by:

$$[k^e]\ \{u^e\} = \{r^e\}$$

where, $[k^e]$, $\{u^e\}$, $\{r^e\}$ are the *element stiffness matrix*, *element nodal displacement vector* and *element load vector*, respectively.[20]

$$\left\{ u^e \right\} = \begin{bmatrix} u_1 & v_1 & w_1 & \cdots & u_n & v_n & w_n \end{bmatrix}^T$$

$$[k^e] = \int_{V_e} B^T DB\, dV_e$$

$$= \int_{-1}^{1}\int_{-1}^{1}\int_{-1}^{1} B^T DB\ dx\, dy\, dz$$

$$= \int_{-1}^{1}\int_{-1}^{1}\int_{-1}^{1} B^T DB\, J\ d\xi\, d\eta\, d\zeta \qquad (5.1)$$

where J is the determinant of the Jacobian matrix.

ξ, η, ζ are the natural coordinates

ξ_i, η_i, ζ_i are values of natural coordinates for node *i*.

The element load vector $\{r^e\}$ is given by:

$$\{ r^e\} = \int_{V_e} [N]^T \{b\}\ dV_e + \int_{S_e} [N^s]^T \{p\}\ dS_e \qquad (5.2)$$

where, $\int_{V_e} [N]^T \{b\}\ dV_e$ is the load vector due to ***body forces***

and $\int_{S_e} [N^s]^T \{p\}\, dS_e$ is the load vector due to ***surface traction***.

5.2.1 Gravity Loads

Magnitude of dead weight of the dam is considered as the weight of concrete in it along with the appurtenances such as gates and bridges. The self weight component of the dam is of considerable significance in the stability of a gravity dam. This self weight of the structure can be considered as a load vector due to body force and is given by: [20]

$$\{r^e\} = \int_{V_e} [N]^T \{b\} V_e \tag{5.3}$$

The nodal load vector at any node ***i*** is given by:

$$\{r^e\}_i = \int_{V_e} [N_i] \{b\} V_e$$

where, $[N_i] = \begin{bmatrix} N_i & 0 & 0 \\ 0 & N_i & 0 \\ 0 & 0 & N_i \end{bmatrix}$

{b} is the vector of body force component per unit volume and given by:

$$\{b\} = \begin{Bmatrix} 0 \\ 0 \\ -\rho \end{Bmatrix}$$

where, ρ is the weight density of the material of the structure.

The above equation is modified with functions expressed in natural coordinates for isoparametric element.

$$\{r^e\} = \int_{-1}^{+1}\int_{-1}^{+1}\int_{-1}^{+1} \begin{Bmatrix} 0 \\ 0 \\ -N_i\rho \end{Bmatrix} J \; d\xi \; d\eta \; d\zeta \tag{5.4}$$

Using Gauss quadrature the integral is evaluated as:

$$\{r^e\} = \sum_{i=1}^{n}\sum_{j=1}^{n}\sum_{k=1}^{n} w_i \;\; w_j \;\; w_k \; J \begin{Bmatrix} 0 \\ 0 \\ -N_i\rho \end{Bmatrix} \tag{5.5}$$

The integration order used for twenty noded element is 4×4×4, which is incorporated in the program as below.

```
//initialise element load vector and upper triangle of element
stiffness matrix
      for (k=1; k<=60; ++k)
      {
            elem_load[k] = 0.;
            for (l=k; l<=60; ++l)
                  elem_stiffness [k][l] = 0.00;
      }
// Start Gauss quadrature loop. Use ngauss by ngauss rule
      for (na=1; na<=ngauss; ++na)
      {
            pxi = place[na][ngauss];
            for (nb=1; nb<=ngauss; ++nb)
            {
```

```
                  pet = place[nb][ngauss];
                  for (nc=1; nc<=ngauss; ++nc)
                  {
                        pze = place[nc][ngauss];

 shape_fun(pxi, pet, pze); //function call

ds =  wgt[na][ngauss] * wgt[nb][ngauss] * wgt[nc][ngauss];
dv=  ds* det_Jac;

// Body weight
      int ii=0;
            for (nrow=1; nrow<=60; ++nrow)
            {
                  if (nrow%3 == 0)
                  {
                        ii ++;
                        elem_load[nrow] += - N[ii]* gama *dv;
                  }
```

5.2.2 Seismic Inertia

The earthquake; *seismic forces*, acting on the dam are computed by the pseudo static method. A concrete dam is treated as a rigid mass with a uniform distribution of acceleration, assumed to act along the height of the dam. Earthquake forces are treated as static inertial forces that are combined with water and gravity loads. The design earthquake intensity; *expressed as a ratio of design acceleration to the acceleration due to gravity,* is selected after consideration of horizontal and vertical accelerations which may reasonably be expected to occur at a particular site. These are determined from the geology of the site, proximity to faults, previous earthquake history of the region and other available records.[4,5,91]

Inertial force of the dam is the static lateral force generated as a result of horizontal acceleration applied to a concrete dam that is due to weight of the dam expressed as the product of the design earthquake intensity; *seismic coefficient,* and the weight of the portion of the dam being considered. The calculations are performed

incrementally along the height of the dam. The inertia forces are computed for each element as body force as arrived in 5.2.1 by numerical integration, where, the body force vector is given by:

$$\{b\} = \begin{Bmatrix} \pm \alpha_x \rho \\ \pm \alpha_y \rho \\ \pm \alpha_z \rho \end{Bmatrix} \tag{5.6}$$

where, $\alpha_x, \alpha_y, \alpha_z$ are the required earth quake intensities in the respective directions and can be assumed as per code provisions. Then inertia forces can be arrived by suitably giving `nrow%3 == 1,2,0` and `gamma` as `gamma_x, gamma_y, gamma_z` respectively.

```
// Inertia force
int ii=0;
      for (nrow=1; nrow<=60; ++nrow)
      {
            if (nrow%3 == 1)   // nrow%3 == 0,2
            {
                  ii ++;
                  elem_load[nrow]+=N[ii]*gamma*dv;// gamma_x,y,z
            }
```

The effect of vertical earthquake is equivalent to the momentary increments or decrements of the unit weight of concrete and water depending on the direction of the shock. Thus, any upward earthquake acceleration opposes the acceleration due to gravity. Consequently, the effective weight of the dam as well as reservoir water is momentarily reduced. The opposite is the case for downward earthquake acceleration.

5.2.3 Temperature

Temperature of the upstream and downstream faces of the dam may vary following the air and water temperature, similarly, from bottom to top of the dam. Effect of temperature changes in the interior of the dam also causes temperature

stresses and deflection. Since temperature changes are uniform in the vertical section, horizontal movements will not be appreciable. In horizontal sections, since the temperature changes are non uniform, it causes upstream deflection which works against or with the water load depending on the increase or decrease in temperature. However, the maximum decrease in temperature than the existing temperature at the time of grouting shall be taken in the analysis. This can be arrived at by modifying equation 2.6 as:

$$\{\sigma\}_{(6\text{ x }1)} = [D]_{(6\text{ x }6)}\ \{\varepsilon\}_{(6\text{ x }1)} - \frac{E\alpha \mathrm{T}}{(1-2\mu)}\begin{Bmatrix}1\\1\\1\\0\\0\\0\end{Bmatrix}$$

where, α is the coefficient of thermal expansion and T is the difference in temperature.

5.3 ELEMENT SURFACE LOAD VECTOR

The surface loads are applied as element load vectors in finite element method. Here, uniform pressure of intensity 'q' is considered as normal to the surface. Positive surface loads act in the direction of the outward normal of positive element face and along the inward normal of a negative element face.[20] The load vector due to surface pressure is given by:

$$\{r^e\} = \iint [N_i^s]^T \{p\}\, dA \qquad (5.7)$$

where, dA is the element face area where the pressure is acting.

For calculating the element load vector, element faces are defined and the orientation with respect to global axes worked out. The element faces correspond to $\pm\xi$, $\pm\eta$, $\pm\zeta$ directions. In addition, a set of local axes x', y', z' are considered for element faces. If x' is along the line joining the midpoint of opposite sides of a face, then z' is normal to x' and the line joining the midpoints of the other two sides and y' normal to x' and z' to form the right handed system as in Fig 5.1.

If, i, j, k are unit vectors along x, y, z directions

e_1, e_2, e_3 vectors along ξ, η, ζ directions

e'_1, e'_2, e'_3 vectors along ξ', η', ζ' directions

Then vectors along the global and natural coordinate directions are related by *Jacobian matrix* as:

$$\begin{Bmatrix} e_1 \\ e_2 \\ e_3 \end{Bmatrix} = \begin{bmatrix} J_{11} & J_{12} & J_{13} \\ J_{21} & J_{22} & J_{23} \\ J_{31} & J_{32} & J_{33} \end{bmatrix} \begin{Bmatrix} i \\ j \\ k \end{Bmatrix} \tag{5.8}$$

Depending on the face number, the vector e'_1 will be identical to one of the vectors along the natural coordinate axes. For example, if $+\xi$ is considered, e'_1 is identical to e_2 and e'_3 is perpendicular to the element face.

$$e'_3 = e_2 \times e_3 = (J_{22} J_{33} - J_{23} J_{32})\, i + (J_{23} J_{31} - J_{21} J_{33})\, j + (J_{21} J_{32} - J_{22} J_{31})\, k$$

$$e'_2 = e'_3 \times e'_1 = (J'_{21}\, i + J'_{22}\, j + J'_{23}\, k) \tag{5.9}$$

Thus,

$$\begin{Bmatrix} e'_1 \\ e'_2 \\ e'_3 \end{Bmatrix} = \begin{bmatrix} J'_{11} & J'_{12} & J'_{13} \\ J'_{21} & J'_{22} & J'_{23} \\ J'_{31} & J'_{32} & J'_{33} \end{bmatrix} \begin{Bmatrix} i \\ j \\ k \end{Bmatrix} \tag{5.10}$$

The direction cosines [l_1 m_1 n_1] for the x' is obtained by normalizing the vector

[J_{11} J_{12} J_{13}]

$$\begin{Bmatrix} l_1 \\ m_1 \\ n_1 \end{Bmatrix} = 1/\sqrt{J'_{11}{}^2 + J'_{21}{}^2 + J'_{31}{}^2} \begin{Bmatrix} J'_{11} \\ J'_{21} \\ J'_{31} \end{Bmatrix} \quad (5.11)$$

Similarly, direction cosines for other axes are worked out. *dA* are calculated as the cross product of vectors along the natural coordinates parallel to the loaded face of the element. Further, various pressures on an arch dam are discussed below.

5.3.1 Hydrostatic

Hydrostatic pressure is assumed as a distributed surface traction parallel to the water profile which is applied at nodes, giving a coefficient in most of the finite element soft wares. But, in the case of an arch dam of complex geometry; *curved in all the directions,* the water pressure at any point will be normal to the surface at that point. Therefore, on each element it acts in a direction normal to the surface; *surface being curved in the direction of water pressure,* also varies from element to element and depends on the height of water column. This is efficiently solved taking in to consideration, the direction cosines in the finite elements itself. If this is included in the software, then deflection, stress and strain corresponding to any height of water column is easily found out. This leads to an effective computer simulation even in the design stage for any reservoir water level, rather than load combinations, which makes dam monitoring results of instrumentation reliable as the theoretical values corresponding to all reservoir levels known in advance. The concept is detailed below.[20] Hydrostatically varying surface pressure on positive element faces can be specified by a

reference fluid surface and a fluid intensity ρ_L. The intensity of pressure q normal to any surface is calculated as:

$$q = \rho_L (z_{ref} - z) \tag{5.12}$$

where, z is the global z coordinate of the point at which q is calculated and z_{ref} specifies the fluid surface datum assuming gravity acts along the negative z-axis.

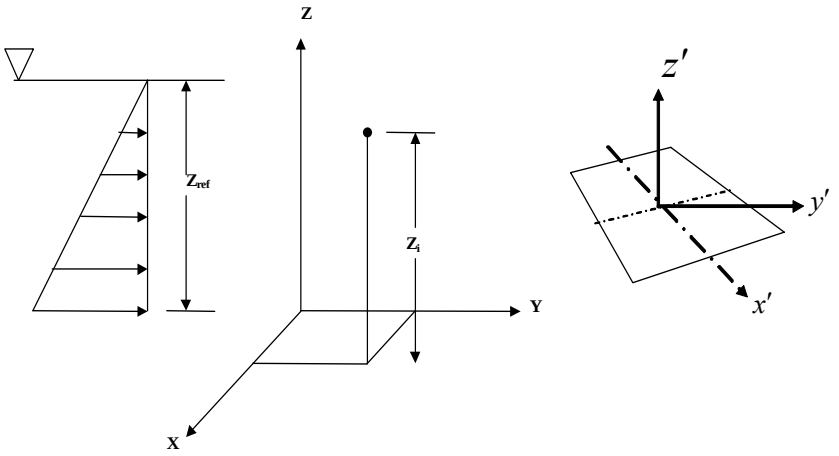

Fig 5.1: ***Hydrostatic pressure loading and local axes at element faces***

The value of 'q' from the above is substituted in the following equation.

$$\{r^e\} = \int_{-1}^{+1}\int_{-1}^{+1} \begin{Bmatrix} N_i^s & q & l_3 \\ N_i^s & q & m_3 \\ N_i^s & q & n_3 \end{Bmatrix} dA$$

where $\{r^e\}$ is the nodal load vector at node i

$$\{r^e\} = \iint [N_i^s]\{p\} dA \tag{5.13}$$

$$dA = |e_2 \times e_3| d\eta d\zeta$$

where, e_2, e_3 are vectors along η, ζ direction.

Value of $\left[N_i^s\right]$ in the above equation is given as:

$$\left[N_i^s\right] = \begin{bmatrix} N_i^s & 0 & 0 \\ 0 & N_i^s & 0 \\ 0 & 0 & N_i^s \end{bmatrix}$$

where, N_i^s is the shape function for the node *i*.

Depending on the face number, the value of N_i^s is obtained by substituting:

$$\xi = \pm 1,\ \eta = \pm 1, \text{ and } \zeta = \pm 1.$$

The surface pressure is expressed as:

$$\{p\} = \begin{Bmatrix} q & l_3 \\ q & m_3 \\ q & n_3 \end{Bmatrix}$$

where, l_3, m_3, n_3 are direction cosines of the new local axes defined for the particular element face. Using Gauss quadrature $\{r^e\}$ can be evaluated. In the program the elements on which water pressure is acting, `Lelem` may be arrived as:

```
// water pressure
      fin >> no_hydro_elems;
      for (j=1; j<=no_hydro_elems; ++j)
      {
        fin >> Lelem;
        hydroforce (Lelem);  //function call
            dof = 0;
            for (int i=1; i<=20; ++i)
            {
                  for (int j=1; j<=3; ++j)
                  {
                        dof ++;
                        node = nod[i][Lelem];
                        kk[dof] = id[j][node];
                  }
            }
            for (i=1; i<=60; ++i)
            {
                  if (kk[i] <= 0)
                        continue;
                        k = kk[i];
                        global_load[k] += elem_load[i];
            }
      }
//Calculation of element pressure
void hydroforce (int Lelem)
{
 ofstream fout("hydro20.out");
for (i=1; i<=20; ++i)
{
      node  = nod[i][Lelem];
             xl[i] = x[node];
            yl[i] = y[node];
            zl[i] = z[node];
}
```

```
for (k=1; k<=60; ++k)
            elem_load[k] = 0.;
      double  p[4], q, h;
      for (i=1; i<=3; ++i)
            p[i] =0.0;
      for (nb=1; nb<=ngauss; ++nb)
      {
            pet =place[nb][ngauss];
            for (nc=1; nc<=ngauss; ++nc)
            {
                  pze = place[nc][ngauss];
                  shape_fun (pxi, pet, pze); //function call
      dA =  wgt[nb][ngauss] * wgt[nc][ngauss] * det_Jac_Hydro;
      // get z-coordinate
            double zz = 0;
                  for (i=1; i<=20; i++)
                        zz += N[i]*zl[i];
                        h = zz - Zref;
                        q = h*ro_L ;
                              p[1] = q*l3*dA;
                              p[2] = q*m3*dA;
                              p[3] = q*n3*dA;
//   Hydro pressure
            int ii=0;
                  for(i=1; i<=20;i++)
                  {
                        for (j=1; j<=3; j++)
                        {
                              nrow = 3*i - 3 + j;
                              elem_load[nrow] += -N[i]*p[j];
                        }
                  }
              }
      }
}
// to find det_Jac_Hydro
      double J1, J2, J3;
      J1 = (Jac[2][2]* Jac[3][3])-(Jac[2][3]*Jac[3][2]);
      J2 = (Jac[2][3]* Jac[3][1])-(Jac[2][1]*Jac[3][3]);
      J3 = (Jac[2][1]* Jac[3][2])-(Jac[2][2]*Jac[3][1]);
         det_Jac_Hydro=sqrt(J1*J1 + J2*J2 + J3*J3);
            l3 = J1/det_Jac_Hydro;
            m3 = J2/det_Jac_Hydro;
            n3 = J3/det_Jac_Hydro;
```

5.3.2 Hydrodynamic

In addition to the hydrostatic reservoir pressure, hydrodynamic pressures are generated due to successive lateral movements of the upstream face of the dam against reservoir water by the horizontal acceleration under earthquake. This pressure is found to be the same as would occur if a body of water confined between a certain parabola

and the face of the dam were forced to move with the dam while the rest of the reservoir remained inactive. Following the added mass concept and Code provisions for the pseudo static analysis, this hydrodynamic effect is approximated as a distributed pressure on the upstream face is incorporated in this research by way of direction cosines and numerical integration.[91,92]

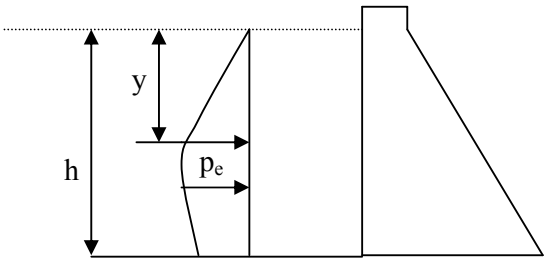

Fig 5.2: ***Hydrodynamic pressure distribution***

Assuming water to be incompressible the hydrodynamic pressure in Fig 5.2 at depth *y* below the reservoir surface is:

$$p_e = C_s \alpha_h w h \tag{5.14}$$

$$C_s = \frac{C_m}{2}\frac{y}{h}\left\{\left(2-\frac{y}{h}\right)+\sqrt{\frac{y}{h}}\sqrt{\left(2-\frac{y}{h}\right)}\right\} \tag{5.15}$$

p_e is the Hydrodynamic pressure in kg/m2

C_s is the Coefficient varies with shape and depth

α_h is the Design horizontal seismic coefficient

w is the Unit weight of water

h is the Depth of reservoir in m

C_m is the Maximum value of *Cs*

y is the Depth below surface

This is incorporated in the program as pressure just by substituting:

$q = C_s \alpha_h w \;\; ; \;\; p = qh$ as in 5.3.1

```
// Hydrodynamic pressure

      fin >> no_dyn_elems;
      for (j=1; j<=no_dyn_elems; ++j)
      {
        fin >> Delem;
        hydrodyn (Delem);     //function call
            dof = 0;
            for (int i=1; i<=20; ++i)
            {
                  for (int j=1; j<=3; ++j)
                  {
                        dof ++;
                        node = nod[i][Delem];
                        kk[dof] = id[j][node];
                  }
            }
            for (i=1; i<=60; ++i)
            {
                  if (kk[i] <= 0)
                        continue;
                        k = kk[i];
                        global_load[k] += elem_load[i];
            }
      }

//Calculation of element pressure

void hydrodyn (int Delem)
{
ofstream fout("hydrodyn.out");
fin >> Zrefd >> alf_h;
      for (i=1; i<=20; ++i)
      {
          node  = nod[i][Delem];
          xl[i] = x[node];
            yl[i] = y[node];
            zl[i] = z[node];
      }

      for (k=1; k<=60; ++k)
            elem_load[k] = 0.;

      double  p[4], q, h;
      for (i=1; i<=3; ++i)
            p[i] =0.0;

                  for (na=1; na<=ngauss; ++na)
            {
                  pxi =place[na][ngauss];
                  for (nc=1; nc<=ngauss; ++nc)
                  {
                        pze = place[nc][ngauss];
                        shape_fun (pxi, -1.0, pze);
      dA =  wgt[na][ngauss] * wgt[nc][ngauss] * det_Jac_Hydro;
```

```
// get z-coordinate
                        double zz = 0;
                        for (i=1; i<=20; i++)
                              zz += N[i]*zl[i];
                  h = zz - Zrefd;
double a,b,c,Cm,Cs,alf_h;
Cm=0.735;
c=-1*h/Zrefd;
a=(c*(2-c));
b=sqrt(a);
Cs=(0.5*Cm*(a+b));

q=h*ro_L*Cs*alf_h ;
      p[1] = q*l3*dA;
      p[2] = q*m3*dA;
      p[3] = q*n3*dA;

//   Hydrodynamic pressure

                  int ii=0;
                  for(i=1; i<=20;i++)
                  {
                        for (j=1; j<=3; j++)
                        {
                              nrow = 3*i - 3 + j;
                              elem_load[nrow] += N[i]*p[j];
                        }
                  }
            }
      }
}
// to find det_Jac_Hydro

      double J1, J2, J3;

      J1 = (Jac[2][2]* Jac[3][3])-(Jac[2][3]*Jac[3][2]);
      J2 = (Jac[2][3]* Jac[3][1])-(Jac[2][1]*Jac[3][3]);
      J3 = (Jac[2][1]* Jac[3][2])-(Jac[2][2]*Jac[3][1]);

         det_Jac_Hydro=sqrt(J1*J1 + J2*J2 + J3*J3);

            l3 = J1/det_Jac_Hydro;
            m3 = J2/det_Jac_Hydro;
            n3 = J3/det_Jac_Hydro;
```

However, this approach has limitations since seismic forces are evaluated as if the structure is rigid, whereas it is flexible. Moreover, accelerations resulting from dynamic response may be greater than that which acts on a rigid structure. Hence, dynamic response analysis which is beyond the scope of this work would be more reliable.

5.3.3 Silt and Earth

The silt and earth deposited at the upstream face of the dam after creation of reservoir exerts pressure on the surface. This acts only for a particular height of the dam as effective pressure due to submerged unit weight at the corresponding elements by numerical integration. Rankine's formula for silt pressure is given below.[85]

$$p_s = \frac{wh^2}{2}\left(\frac{1-\sin\theta}{1+\sin\theta}\right) \tag{5.16}$$

This is incorporated in the program as in 5.3.2 for the elements on which silt pressure acting by numerical integration by taking $p_s = qh$

where, $$q = \frac{wh}{2}\left(\frac{1-\sin\theta}{1+\sin\theta}\right) \tag{5.17}$$

```
// silt pressure
      fin >> no_silt_elems;
      for (j=1; j<=no_silt_elems; ++j)
      {
        fin >> silt_Lelem ;
        siltforce (silt_Lelem);
            dof = 0;
            for (int i=1; i<=20; ++i)
            {
                  for (int j=1; j<=3; ++j)
                  {
                        dof ++;
                        node = nod[i][silt_Lelem];
                        kk[dof] = id[j][node];
                  }
            }
            for (i=1; i<=60; ++i)
            {
                  if (kk[i] <= 0)
                        continue;
                        k = kk[i];
                        global_load[k] += elem_load[i];
            }
      }
void siltforce (int silt_Lelem)
{
 ofstream fout("silt20.out",ios::app);
      for (i=1; i<=20; ++i)
      {
```

```
            node  = nod[i][silt_Lelem];
            xl[i] = x[node];
              yl[i] = y[node];
              zl[i] = z[node];
        }

        for (k=1; k<=60; ++k)
              elem_load[k] = 0.;
        double  p[4], q, h;
        for (i=1; i<=3; ++i)
              p[i] =0.0;

              for (na=1; na<=ngauss; ++na)
              {
                    pxi =place[na][ngauss];
                    for (nc=1; nc<=ngauss; ++nc)
                    {
                          pze = place[nc][ngauss];
                          shape_fun (pxi, 1.0, pze);
        dA = wgt[na][ngauss] * wgt[nc][ngauss] * det_Jac_Hydro;

                    // get z-coordinate
                    double k,zz = 0;
                    for (i=1; i<=20; i++)
                          zz += N[i]*zl[i];
                    h = zz - Zsilt;

                    q =0.5*k* h*ro_Silt;    // k = (1 - sin θ)/(1 + sin θ)

                    p[1] = q*l3*dA;
                    p[2] = q*m3*dA;
                    p[3] = q*n3*dA;

//   Silt pressure
                    int ii=0;
                    for(i=1; i<=20;i++)
                    {
                          for (j=1; j<=3; j++)

                          {
                                nrow = 3*i - 3 + j;
                                elem_load[nrow] += N[i]*p[j];
                          }
                    }
              }
        }
```

5.3.4 Uplift

Uplift occurs due to internal pressure in the pores, cracks and seams in the dam and foundation. It is assumed on the basis of experimental studies that the uplift pressures act over 100% area of the concrete or the foundation rock.[5] Whenever this

occurs, part of the weight of the darn is taken by the water under pressure and the foundation reaction is reduced correspondingly, thus affecting the stability of the dam. Drainage holes are provided extending vertically, throughout the dam and into the foundation near the upstream face to intercept the percolating water. This reduces the magnitude of these uplift pressures which can be incorporated as surface force acting on the bottom face of the dam upwards. However, for Arch dams if cracking does not occur at the upstream face, the development of upstream pressure simply means a slight transfer of load to abutments and not many changes in stress magnitude or deformation; therefore, not generally included in the design.[5]

5.3.5 Wave

The upper portion of the dam may be subjected to wave action on the surface of reservoir by wind. The dimensions of the wave depend upon the extent of the water surface, fetch and the velocity of wind. The maximum pressure intensity 'p_w' due to wave action is given by:

$$P_w = 2.4\ w\ h_w$$

which acts at $h_w/2$ above the reservoir surface, where, 'w' is the unit weight of water and 'h_w' is the height of wave. This wave pressure can be expressed as a surface loading to the elements at the upper portion of the dam. Wave pressure distribution is shown in Fig 5.3.

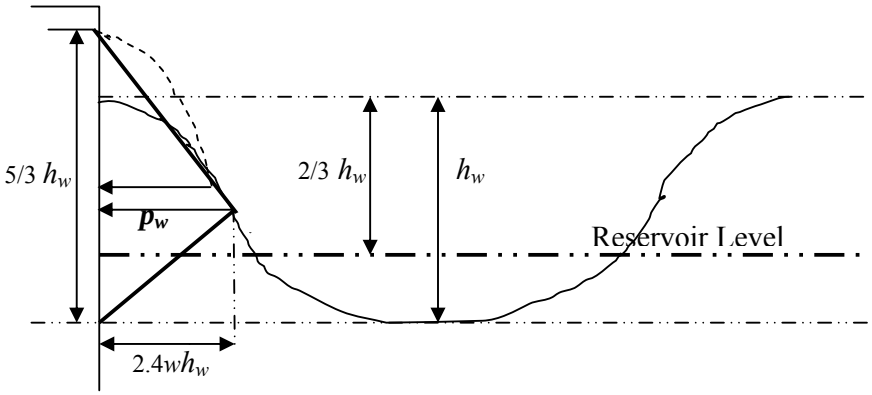

Fig 5.3: ***Wave pressure distribution***

5.4 VALIDATION OF LOAD VECTORS

The load vectors, arrived to incorporate as above in the developed finite element program for three-dimensional solid continuum, are validated with basic structural mechanics solutions on numerical examples.

5.4.1 Gravity

Gravity is validated by analyzing a cantilever beam (200x30x20) cm with its self-weight (25 kN/m^3) acting along the three directions. The deflected profiles are plotted in Fig 5.4, 5.5 and 5.6 and results are tabulated in Table 5.1.

(i) Self weight acting along X axis

Theoretical deflection at free end = $\frac{wL^2}{2AE}$

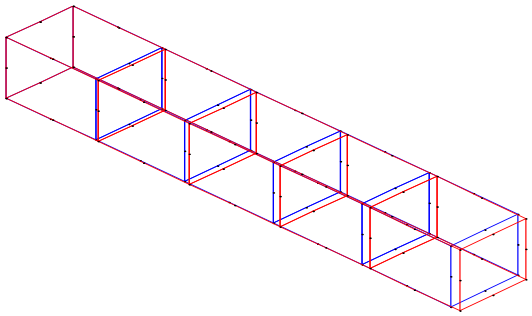

Fig 5.4: ***Deflected shape due to self weight in axial direction***

(ii) Self weight acting along Y axis

Theoretical deflection at free end = $\frac{wL^4}{8EI}$

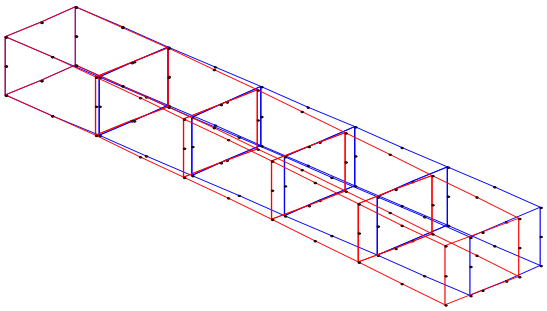

Fig 5.5: ***Deflected shape due to self weight in Y direction***

(iii) Self weight acting along Z axis

Theoretical deflection at free end = $\frac{wL^4}{8EI}$

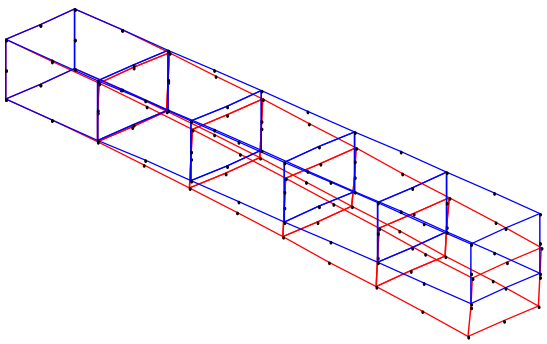

Fig 5.6: ***Deflected shape due to self weight in Z direction***

Table 5.1: **Deflection at free end of a cantilever beam due to gravity loading**

Sl. No.	Gravity loading (self weight)	No. of 20 noded elements	Maximum deflection at free end in cm	
			Program	Theory
1	*X direction*	5	0.0002500	0.00025
2	*Y direction*	5	0.033766	0.0333
3.	*Z direction*	5	0.075214	0.0750

5.4.2 Pressure

For validation of pressure, a vertical cantilever beam fixed at bottom shown in Fig 5.7 is proposed for analysis due to water pressure acting on the two vertical faces after arriving at a method to find out the same as explained above. The beam will be discretised assuming a fluid level. The unit weight of fluid will be taken in to account neglecting the unit weight of beam. The original and deflected profile will be plotted results verified and tabulated.

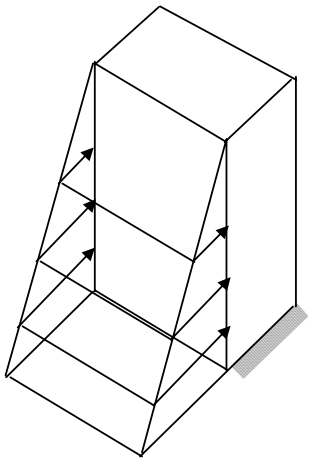

Fig 5.7: ***Hydrostatic pressure on vertical cantilever***

(1) Cantilever beam of (20x30x 200) cm

Fluid top level = 200.0cm

Number of elements	=	10
Number of nodes	=	128
Modulus of elasticity E	=	2000kN/cm^2
Unit weight of solid	=	0
Unit weight of liquid	=	1e-005 kN/cm^3

(a) Hydrostatic Pressure on 30cm wide face

Theoretical deflection $= wl^4/30EI = 0.0800$cm

Maximum deflection from the program = 0.08063670156cm

Deflected profile is plotted and shown in Fig 5.8

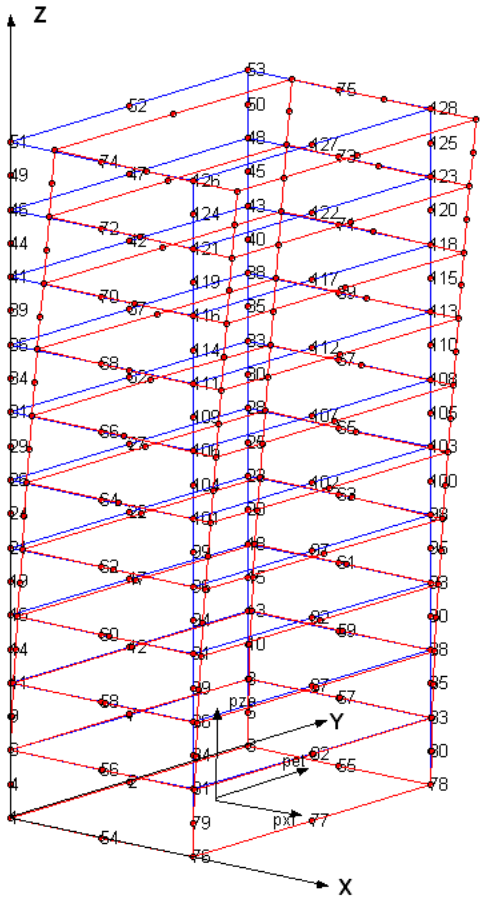

Fig 5.8: ***Deformed profile due to pressure on 30 cm face***

b. Hydrostatic Pressure on 20cm wide face

Theoretical deflection = $wl^4/30EI$ = 0.0237 cm

Maximum deflection from the program = 0.0241440588 cm

Deflected profile is plotted and shown in Fig 5.9

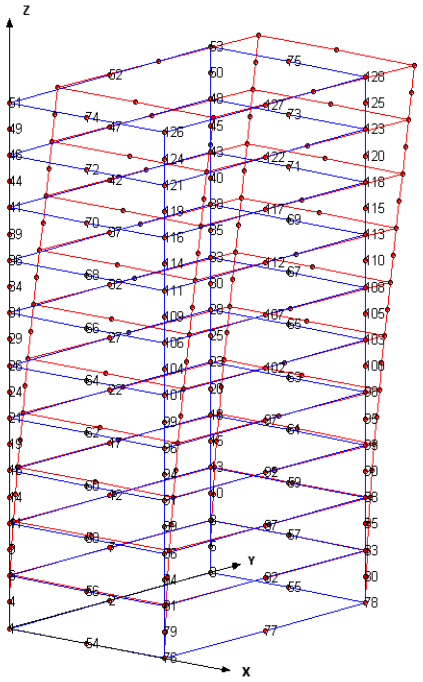

Fig 5.9: ***Deformed profile due to pressure on 20 cm face***

b. Hydrostatic and Hydrodynamic Pressure on 20cm wide face

Effect of hydrodynamic pressure is incorporated in the program developed, as above. A vertical cantilever is analysed with the program. Theoretical deflection due to Hydrostatic pressure is $wl^4/30EI$ = 0.0237 cm. Maximum deflection obtained with the program due to Hydrostatic pressure is 0.0241440588 cm. When hydrodynamic effect is combined, maximum deflection is observed to increase to 0.02901355 cm. The deflected profile is plotted in Fig 5.10 and tabulated in Table 5.2.

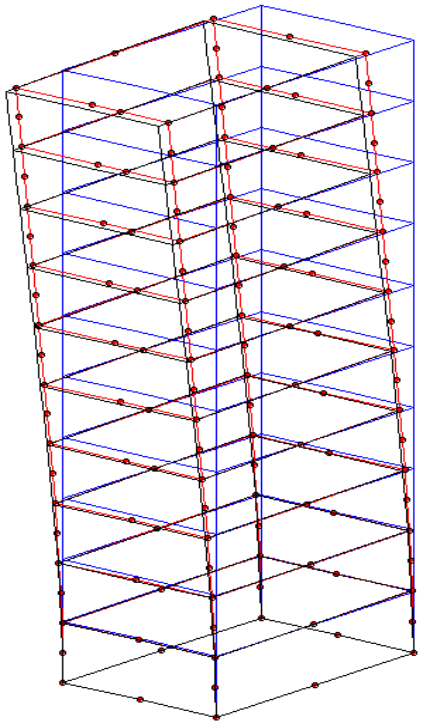

Fig 5.10: ***Deformed profile due to Hydrostatic and dynamic pressure on 20 cm face***

Table 5.2: **Deflection due to hydrostatic and dynamic pressure**

Node	Hydrostatic only Deflection in cm			Hydrodynamic combined Deflection in cm		
	x	y (-)	z (-)	x	y (-)	z (-)
78	0	0	0	0	0	0
83	0	0.000658	0.00076	0	0.00079	0.00092
88	0	0.002159	0.00131	0	0.00262	0.00158
93	0	0.004243	0.00168	0	0.00515	0.00203
98	0	0.006726	0.00193	0	0.00814	0.00232
103	0	0.009452	0.00208	0	0.01142	0.00250
108	0	0.012324	0.00216	0	0.01486	0.00259
113	0	0.015259	0.00220	0	0.01837	0.00263
118	0	0.018211	0.00221	0	0.02191	0.00265
123	0	0.021188	0.00222	0	0.02546	0.00265
128	0	0.024144	0.00222	0	0.02901	0.00265

(2) Cantilever wall of (20 x 100 x 200) cm

A cantilever wall having 100cm width is taken for analysis with hydrostatic pressure acting on the (100x200) cm face in two cases of discretisation.

a. Discretisation along length.

The discretisation is plotted in Fig 5.11 and deformed profile in Fig 5.12. Element connectivity, hydrostatic loading and global displacements, nodes where displacements restricted and element stresses are given Table 5.3, 5.4, 5.5 and 5.6 respectively.

Theoretical deflection = $wl^4/30EI$ = 0.0800cm

Maximum deflection from the program = 0.08063670156cm

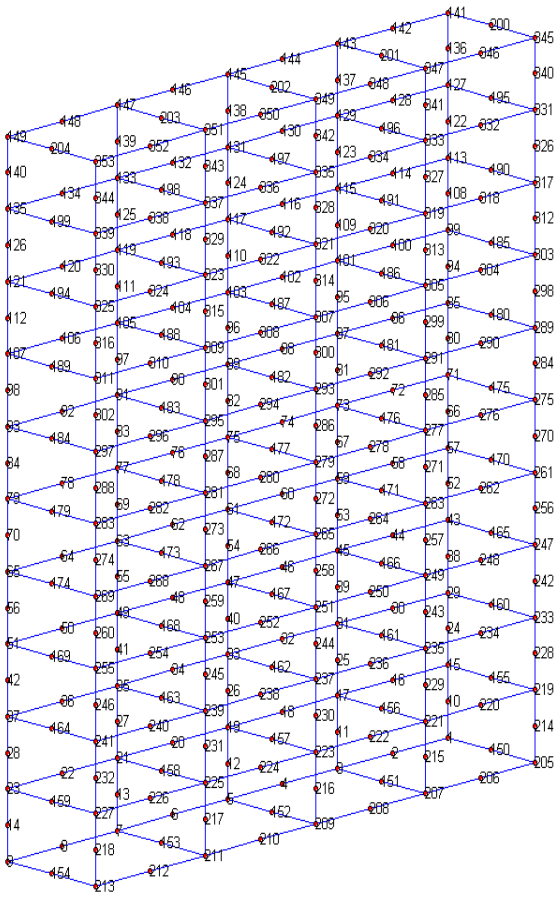

Fig 5.11: ***Descretisation along length of a cantilever wall***

Table 5.3: **Cantilever wall Element connectivity Descretisation along length**

Element	1	2	3	4	5	6	7	8	9	10	11	12	13	14	15	16	17	18	19	20
1	3	1	205	207	17	15	219	221	2	150	206	151	16	155	220	156	11	10	214	215
2	5	3	207	209	19	17	221	223	4	151	208	152	18	156	222	157	12	11	215	216
3	7	5	209	211	21	19	223	225	6	152	210	153	20	157	224	158	13	12	216	217
4	9	7	211	213	23	21	225	227	8	153	212	154	22	158	226	159	14	13	217	218
5	17	15	219	221	31	29	233	235	16	155	220	156	30	160	234	161	25	24	228	229
6	19	17	221	223	33	31	235	237	18	156	222	157	32	161	236	162	26	25	229	230
7	21	19	223	225	35	33	237	239	20	157	224	158	34	162	238	163	27	26	230	231
8	23	21	225	227	37	35	239	241	22	158	226	159	36	163	240	164	28	27	231	232
9	31	29	233	235	45	43	247	249	30	160	234	161	44	165	248	166	39	38	242	243
10	33	31	235	237	47	45	249	251	32	161	236	162	46	166	250	167	40	39	243	244
11	35	33	237	239	49	47	251	253	34	162	238	163	48	167	252	168	41	40	244	245
12	37	35	239	241	51	49	253	255	36	163	240	164	50	168	254	169	42	41	245	246
13	45	43	247	249	59	57	261	263	44	165	248	166	58	170	262	171	53	52	256	257
14	47	45	249	251	61	59	263	265	46	166	250	167	60	171	264	172	54	53	257	258
15	49	47	251	253	63	61	265	267	48	167	252	168	62	172	266	173	55	54	258	259
16	51	49	253	255	65	63	267	269	50	168	254	169	64	173	268	174	56	55	259	260
17	59	57	261	263	73	71	275	277	58	170	262	171	72	175	276	176	67	66	270	271
18	61	59	263	265	75	73	277	279	60	171	264	172	74	176	278	177	68	67	271	272
19	63	61	265	267	77	75	279	281	62	172	266	173	76	177	280	178	69	68	272	273
20	65	63	267	269	79	77	281	283	64	173	268	174	78	178	282	179	70	69	273	274
21	73	71	275	277	87	85	289	291	72	175	276	176	86	180	290	181	81	80	284	285
22	75	73	277	279	89	87	291	293	74	176	278	177	88	181	292	182	82	81	285	286
23	77	75	279	281	91	89	293	295	76	177	280	178	90	182	294	183	83	82	286	287
24	79	77	281	283	93	91	295	297	78	178	282	179	92	183	296	184	84	83	287	288
25	87	85	289	291	101	99	303	305	86	180	290	181	100	185	304	186	95	94	298	299
26	89	87	291	293	103	101	305	307	88	181	292	182	102	186	306	187	96	95	299	300
27	91	89	293	295	105	103	307	309	90	182	294	183	104	187	308	188	97	96	300	301
28	93	91	295	297	107	105	309	311	92	183	296	184	106	188	310	189	98	97	301	302
29	101	99	303	305	115	113	317	319	100	185	304	186	114	190	318	191	109	108	312	313
30	103	101	305	307	117	115	319	321	102	186	306	187	116	191	320	192	110	109	313	314
31	105	103	307	309	119	117	321	323	104	187	308	188	118	192	322	193	111	110	314	315
32	107	105	309	311	121	119	323	325	106	188	310	189	120	193	324	194	112	111	315	316
33	115	113	317	319	129	127	331	333	114	190	318	191	128	195	332	196	123	122	326	327
34	117	115	319	321	131	129	333	335	116	191	320	192	130	196	334	197	124	123	327	328
35	119	117	321	323	133	131	335	337	118	192	322	193	132	197	336	198	125	124	328	329
36	121	119	323	325	135	133	337	339	120	193	324	194	134	198	338	199	126	125	329	330
37	129	127	331	333	143	141	345	347	128	195	332	196	142	200	346	201	137	136	340	341
38	131	129	333	335	145	143	347	349	130	196	334	197	144	201	348	202	138	137	341	342
39	133	131	335	337	147	145	349	351	132	197	336	198	146	202	350	203	139	138	342	343
40	135	133	337	339	149	147	351	353	134	198	338	199	148	203	352	204	140	139	343	344

Table 5.4: **Hydrostatic input and Global displacements in X, Y, Z directions**

Node	Hydrostatic input in X, Y, Z directions			Global displacement in X, Y, Z directions			Node	Disp X	Disp Y	Disp Z
1	0	0	0	0	0	0	**205**	0	0	0
2	0	0	0	0	0	0	**206**	0	0	0
3	0	0	0	0	0	0	**207**	0	0	0
4	0	0	0	0	0	0	**208**	0	0	0
5	0	0	0	0	0	0	**209**	0	0	0
6	0	0	0	0	0	0	**210**	0	0	0
7	0	0	0	0	0	0	**211**	0	0	0
8	0	0	0	0	0	0	**212**	0	0	0
9	0	0	0	0	0	0	**213**	0	0	0
10	0.316667	0	0	0.000571	0	0.000921	**214**	0.0005626	0	-0.000921
11	0.633333	0	0	0.000571	0	0.000921	**215**	0.0005626	0	-0.000921
12	0.633333	0	0	0.000571	0	0.000921	**216**	0.0005626	0	-0.000921
13	0.633333	0	0	0.000571	0	0.000921	**217**	0.0005626	0	-0.000921
14	0.316667	0	0	0.000571	0	0.000921	**218**	0.0005626	0	-0.000921
15	-0.15	0	0	0.001988	0	0.001719	**219**	0.0019799	0	-0.001719
16	0.6	0	0	0.001988	0	0.001719	**220**	0.0019799	0	-0.001719
17	-0.3	0	0	0.001988	0	0.001719	**221**	0.0019799	0	-0.001719
18	0.6	0	0	0.001988	0	0.001719	**222**	0.0019799	0	-0.001719
19	-0.3	0	0	0.001988	0	0.001719	**223**	0.0019799	0	-0.001719
20	0.6	0	0	0.001988	0	0.001719	**224**	0.0019799	0	-0.001719
21	-0.3	0	0	0.001988	0	0.001719	**225**	0.0019799	0	-0.001719
22	0.6	0	0	0.001988	0	0.001719	**226**	0.0019799	0	-0.001719
23	-0.15	0	0	0.001988	0	0.001719	**227**	0.0019799	0	-0.001719
24	0.283333	0	0	0.004125	0	0.002385	**228**	0.0041166	0	-0.002385
25	0.566667	0	0	0.004125	0	0.002385	**229**	0.0041166	0	-0.002385
26	0.566667	0	0	0.004125	0	0.002385	**230**	0.0041166	0	-0.002385
27	0.566667	0	0	0.004125	0	0.002385	**231**	0.0041166	0	-0.002385
28	0.283333	0	0	0.004125	0	0.002385	**232**	0.0041166	0	-0.002385
29	-0.133333	0	0	0.006869	0	0.002951	**233**	0.0068614	0	-0.002952
30	0.533333	0	0	0.006869	0	0.002951	**234**	0.0068614	0	-0.002952
31	-0.266667	0	0	0.006869	0	0.002951	**235**	0.0068614	0	-0.002952
32	0.533333	0	0	0.006869	0	0.002951	**236**	0.0068614	0	-0.002952
33	-0.266667	0	0	0.006869	0	0.002951	**237**	0.0068614	0	-0.002952
34	0.533333	0	0	0.006869	0	0.002951	**238**	0.0068614	0	-0.002952
35	-0.266667	0	0	0.006869	0	0.002951	**239**	0.0068614	0	-0.002952
36	0.533333	0	0	0.006869	0	0.002951	**240**	0.0068614	0	-0.002952

37	-0.133333	0	0	0.006869	0	0.002951	**241**	0.0068614	0	-0.002952
38	0.25	0	0	0.010118	0	0.003414	**242**	0.0101113	0	-0.003414
39	0.5	0	0	0.010118	0	0.003414	**243**	0.0101113	0	-0.003414
40	0.5	0	0	0.010118	0	0.003414	**244**	0.0101113	0	-0.003414
41	0.5	0	0	0.010118	0	0.003414	**245**	0.0101113	0	-0.003414
42	0.25	0	0	0.010118	0	0.003414	**246**	0.0101113	0	-0.003414
43	-0.116667	0	0	0.013784	0	0.003799	**247**	0.0137773	0	-0.003799
44	0.466667	0	0	0.013784	0	0.003799	**248**	0.0137773	0	-0.003799
45	-0.233333	0	0	0.013784	0	0.003799	**249**	0.0137773	0	-0.003799
46	0.466667	0	0	0.013784	0	0.003799	**250**	0.0137773	0	-0.003799
47	-0.233333	0	0	0.013784	0	0.003799	**251**	0.0137773	0	-0.003799
48	0.466667	0	0	0.013784	0	0.003799	**252**	0.0137773	0	-0.003799
49	-0.233333	0	0	0.013784	0	0.003799	**253**	0.0137773	0	-0.003799
50	0.466667	0	0	0.013784	0	0.003799	**254**	0.0137773	0	-0.003799
51	-0.116667	0	0	0.013784	0	0.003799	**255**	0.0137773	0	-0.003799
52	0.216667	0	0	0.017786	0	0.004104	**256**	0.0177799	0	-0.004104
53	0.433333	0	0	0.017786	0	0.004104	**257**	0.0177799	0	-0.004104
54	0.433333	0	0	0.017786	0	0.004104	**258**	0.0177799	0	-0.004104
55	0.433333	0	0	0.017786	0	0.004104	**259**	0.0177799	0	-0.004104
56	0.216667	0	0	0.017786	0	0.004104	**260**	0.0177799	0	-0.004104
57	-0.1	0	0	0.022058	0	0.004351	**261**	0.0220522	0	-0.004352
58	0.4	0	0	0.022058	0	0.004351	**262**	0.0220522	0	-0.004352
59	-0.2	0	0	0.022058	0	0.004351	**263**	0.0220522	0	-0.004352
60	0.4	0	0	0.022058	0	0.004351	**264**	0.0220522	0	-0.004352
61	-0.2	0	0	0.022058	0	0.004351	**265**	0.0220522	0	-0.004352
62	0.4	0	0	0.022058	0	0.004351	**266**	0.0220522	0	-0.004352
63	-0.2	0	0	0.022058	0	0.004351	**267**	0.0220522	0	-0.004352
64	0.4	0	0	0.022058	0	0.004351	**268**	0.0220522	0	-0.004352
65	-0.1	0	0	0.022058	0	0.004351	**269**	0.0220522	0	-0.004352
66	0.183333	0	0	0.02654	0	0.00454	**270**	0.0265352	0	-0.004540
67	0.366667	0	0	0.02654	0	0.00454	**271**	0.0265352	0	-0.004540
68	0.366667	0	0	0.02654	0	0.00454	**272**	0.0265352	0	-0.004540
69	0.366667	0	0	0.02654	0	0.00454	**273**	0.0265352	0	-0.004540
70	0.183333	0	0	0.02654	0	0.00454	**274**	0.0265352	0	-0.004540
71	-0.083333	0	0	0.031185	0	0.004687	**275**	0.0311803	0	-0.004687
72	0.333333	0	0	0.031185	0	0.004687	**276**	0.0311803	0	-0.004687
73	-0.166667	0	0	0.031185	0	0.004687	**277**	0.0311803	0	-0.004687
74	0.333333	0	0	0.031185	0	0.004687	**278**	0.0311803	0	-0.004687
75	-0.166667	0	0	0.031185	0	0.004687	**279**	0.0311803	0	-0.004687
76	0.333333	0	0	0.031185	0	0.004687	**280**	0.0311803	0	-0.004687

77	-0.166667	0	0	0.031185	0	0.004687	**281**	0.0311803	0	-0.004687
78	0.333333	0	0	0.031185	0	0.004687	**282**	0.0311803	0	-0.004687
79	-0.083333	0	0	0.031185	0	0.004687	**283**	0.0311803	0	-0.004687
80	0.15	0	0	0.03595	0	0.004793	**284**	0.0359459	0	-0.004793
81	0.3	0	0	0.03595	0	0.004793	**285**	0.0359459	0	-0.004793
82	0.3	0	0	0.03595	0	0.004793	**286**	0.0359459	0	-0.004793
83	0.3	0	0	0.03595	0	0.004793	**287**	0.0359459	0	-0.004793
84	0.15	0	0	0.03595	0	0.004793	**288**	0.0359459	0	-0.004793
85	-0.066666	0	0	0.040803	0	0.004871	**289**	0.0407993	0	-0.004872
86	0.266667	0	0	0.040803	0	0.004871	**290**	0.0407993	0	-0.004872
87	-0.133333	0	0	0.040803	0	0.004871	**291**	0.0407993	0	-0.004872
88	0.266667	0	0	0.040803	0	0.004871	**292**	0.0407993	0	-0.004872
89	-0.133333	0	0	0.040803	0	0.004871	**293**	0.0407993	0	-0.004872
90	0.266667	0	0	0.040803	0	0.004871	**294**	0.0407993	0	-0.004872
91	-0.133333	0	0	0.040803	0	0.004871	**295**	0.0407993	0	-0.004872
92	0.266667	0	0	0.040803	0	0.004871	**296**	0.0407993	0	-0.004872
93	-0.066666	0	0	0.040803	0	0.004871	**297**	0.0407993	0	-0.004872
94	0.116667	0	0	0.045716	0	0.004924	**298**	0.045713	0	-0.004924
95	0.233333	0	0	0.045716	0	0.004924	**299**	0.045713	0	-0.004924
96	0.233333	0	0	0.045716	0	0.004924	**300**	0.045713	0	-0.004924
97	0.233333	0	0	0.045716	0	0.004924	**301**	0.045713	0	-0.004924
98	0.116667	0	0	0.045716	0	0.004924	**302**	0.045713	0	-0.004924
99	-0.05	0	0	0.05067	0	0.004959	**303**	0.050667	0	-0.004959
100	0.2	0	0	0.05067	0	0.004959	**304**	0.050667	0	-0.004959
101	-0.1	0	0	0.05067	0	0.004959	**305**	0.050667	0	-0.004959
102	0.2	0	0	0.05067	0	0.004959	**306**	0.050667	0	-0.004959
103	-0.1	0	0	0.05067	0	0.004959	**307**	0.050667	0	-0.004959
104	0.2	0	0	0.05067	0	0.004959	**308**	0.050667	0	-0.004959
105	-0.1	0	0	0.05067	0	0.004959	**309**	0.050667	0	-0.004959
106	0.2	0	0	0.05067	0	0.004959	**310**	0.050667	0	-0.004959
107	-0.05	0	0	0.05067	0	0.004959	**311**	0.050667	0	-0.004959
108	0.0833333	0	0	0.055647	0	0.004979	**312**	0.0556453	0	-0.004980
109	0.166667	0	0	0.055647	0	0.004979	**313**	0.0556453	0	-0.004980
110	0.166667	0	0	0.055647	0	0.004979	**314**	0.0556453	0	-0.004980
111	0.166667	0	0	0.055647	0	0.004979	**315**	0.0556453	0	-0.004980
112	0.0833333	0	0	0.055647	0	0.004979	**316**	0.0556453	0	-0.004980
113	-0.033333	0	0	0.060639	0	0.004991	**317**	0.0606373	0	-0.004992
114	0.133333	0	0	0.060639	0	0.004991	**318**	0.0606373	0	-0.004992
115	-0.066666	0	0	0.060639	0	0.004991	**319**	0.0606373	0	-0.004992
116	0.133333	0	0	0.060639	0	0.004991	**320**	0.0606373	0	-0.004992

117	-0.066666	0	0	0.060639	0	0.004991	**321**	0.0606373	0	-0.004992
118	0.133333	0	0	0.060639	0	0.004991	**322**	0.0606373	0	-0.004992
119	-0.066666	0	0	0.060639	0	0.004991	**323**	0.0606373	0	-0.004992
120	0.133333	0	0	0.060639	0	0.004991	**324**	0.0606373	0	-0.004992
121	-0.033333	0	0	0.060639	0	0.004991	**325**	0.0606373	0	-0.004992
122	0.05	0	0	0.065636	0	0.004997	**326**	0.0656355	0	-0.004997
123	0.1	0	0	0.065636	0	0.004997	**327**	0.0656355	0	-0.004997
124	0.1	0	0	0.065636	0	0.004997	**328**	0.0656355	0	-0.004997
125	0.1	0	0	0.065636	0	0.004997	**329**	0.0656355	0	-0.004997
126	0.05	0	0	0.065636	0	0.004997	**330**	0.0656355	0	-0.004997
127	-0.016666	0	0	0.070636	0	0.004999	**331**	0.0706359	0	-0.004999
128	0.0666667	0	0	0.070636	0	0.004999	**332**	0.0706359	0	-0.004999
129	-0.033333	0	0	0.070636	0	0.004999	**333**	0.0706359	0	-0.004999
130	0.0666667	0	0	0.070636	0	0.004999	**334**	0.0706359	0	-0.004999
131	-0.033333	0	0	0.070636	0	0.004999	**335**	0.0706359	0	-0.004999
132	0.0666667	0	0	0.070636	0	0.004999	**336**	0.0706359	0	-0.004999
133	-0.033333	0	0	0.070636	0	0.004999	**337**	0.0706359	0	-0.004999
134	0.0666667	0	0	0.070636	0	0.004999	**338**	0.0706359	0	-0.004999
135	-0.016666	0	0	0.070636	0	0.004999	**339**	0.0706359	0	-0.004999
136	0.0166667	0	0	0.075636	0	0.004999	**340**	0.0756364	0	-0.005000
137	0.0333333	0	0	0.075636	0	0.004999	**341**	0.0756364	0	-0.005000
138	0.0333333	0	0	0.075636	0	0.004999	**342**	0.0756364	0	-0.005000
139	0.0333333	0	0	0.075636	0	0.004999	**343**	0.0756364	0	-0.005000
140	0.0166667	0	0	0.075636	0	0.004999	**344**	0.0756364	0	-0.005000
141	-0.005555	0	0	0.080636	0	0.004999	**345**	0.0806367	0	-0.005000
142	0.0111111	0	0	0.080636	0	0.004999	**346**	0.0806367	0	-0.005000
143	-0.011111	0	0	0.080636	0	0.004999	**347**	0.0806367	0	-0.005000
144	0.0111111	0	0	0.080636	0	0.004999	**348**	0.0806367	0	-0.005000
145	-0.011111	0	0	0.080636	0	0.004999	**349**	0.0806367	0	-0.005000
146	0.0111111	0	0	0.080636	0	0.004999	**350**	0.0806367	0	-0.005000
147	-0.011111	0	0	0.080636	0	0.004999	**351**	0.0806367	0	-0.005000
148	0.0111111	0	0	0.080636	0	0.004999	**352**	0.0806367	0	-0.005000
149	-0.005555	0	0	0.080636	0	0.004999	**353**	0.0806367	0	-0.005000

Table 5.5: **Cantilever wall - Displacement prescribed nodes and hydrostatically loaded elements**

Nodes at which displacement prescribed				**Hydrostatically loaded elements**	
1	1	1	1	1	21
2	1	1	1	2	22
3	1	1	1	3	23
4	1	1	1	4	24
5	1	1	1	5	25
6	1	1	1	6	26
7	1	1	1	7	27
8	1	1	1	8	28
9	1	1	1	9	29
150	1	1	1	10	30
151	1	1	1	11	31
152	1	1	1	12	32
153	1	1	1	13	33
154	1	1	1	14	34
213	1	1	1	15	35
212	1	1	1	16	36
211	1	1	1	17	37
210	1	1	1	18	38
209	1	1	1	19	39
208	1	1	1	20	40
207	1	1	1		
206	1	1	1		
205	1	1			

Table 5.6: **Stresses at Centroid of Element Average of Gauss Points**

Element	**sig_x**	**sig_y**	**sig_z**	**sig_xz**
1	-0.0007	3.82e-16	1.60e-06	0.009453
2	-0.00073	2.35e-16	1.66e-06	0.009803
3	-0.00073	-1.95e-16	1.66e-06	0.009816
4	-0.00073	-3.51e-16	1.66e-06	0.009817
5	-0.00087	4.85e-16	-2.84e-06	0.007922
6	-0.00088	3.04e-17	-3.01e-06	0.007852

7	-0.00088	-1.03e-17	-3.02e-06	0.007849
8	-0.00088	-3.86e-16	-3.02e-06	0.007849
9	-0.00078	-4.29e-16	4.71e-07	0.006179
10	-0.00078	7.70e-17	6.00e-07	0.006118
11	-0.00078	4.42e-16	6.05e-07	0.006115
12	-0.00078	-8.34e-17	6.05e-07	0.006115
13	-0.00068	-9.08e-16	-1.10e-07	0.004651
14	-0.00068	-1.15e-16	-1.36e-07	0.004597
15	-0.00068	1.21e-15	-1.37e-07	0.004595
16	-0.00068	1.74e-16	-1.37e-07	0.004595
17	-0.00057	-1.52e-15	2.44e-08	0.00334
18	-0.00057	-2.40e-16	3.04e-08	0.003294
19	-0.00057	9.01e-16	3.06e-08	0.003292
20	-0.00057	-3.41e-17	3.06e-08	0.003292
21	-0.00047	-2.15e-15	-5.45e-09	0.002246
22	-0.00047	-9.30e-16	-6.79e-09	0.002208
23	-0.00047	1.50e-15	-6.84e-09	0.002206
24	-0.00047	-2.60e-16	-6.84e-09	0.002206
25	-0.00037	-4.50e-16	1.22e-09	0.00137
26	-0.00036	-2.55e-15	1.52e-09	0.001339
27	-0.00036	1.04e-15	1.53e-09	0.001338
28	-0.00036	-8.79e-16	1.53e-09	0.001338
29	-0.00026	3.24e-15	-2.73e-10	0.00071
30	-0.00026	-1.98e-15	-3.40e-10	0.000687
31	-0.00026	4.97e-16	-3.42e-10	0.000686
32	-0.00026	-7.55e-16	-3.42e-10	0.000686
33	-0.00016	3.59e-15	6.20e-11	0.000268
34	-0.00016	1.55e-15	7.70e-11	0.000253
35	-0.00016	1.07e-15	7.75e-11	0.000252
36	-0.00016	1.50e-15	7.75e-11	0.000252
37	-5.57e-05	3.65e-15	-1.90e-11	4.33e-05
38	-5.20e-05	5.65e-15	-2.26e-11	3.56e-05
39	-5.19e-05	5.04e-15	-2.27e-11	3.53e-05
40	-5.19e-05	2.89e-15	-2.27e-11	3.53e-05

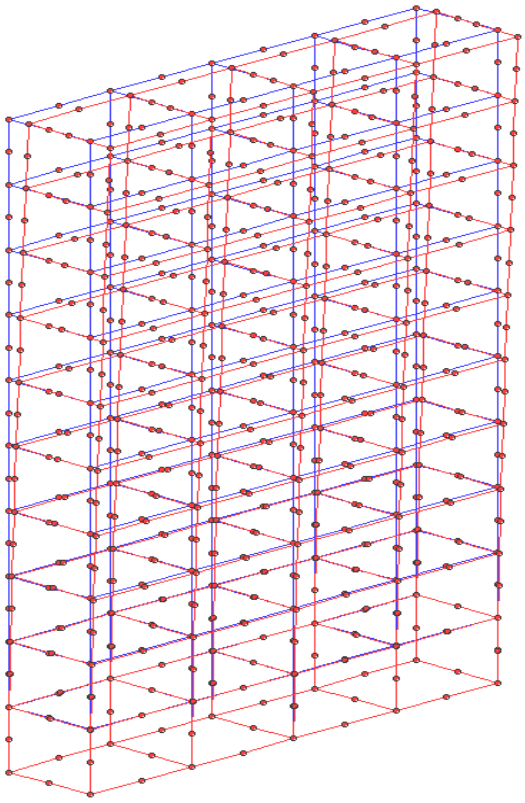

Fig 5.12: ***Deflected profile of a cantilever wall***; *Pressure on longitudinal face*

b. Discretisation along thickness

The discretisation is potted in Fig 5.13 and deformed profile in Fig 5.14. Element connectivity, Nodes where displacements prescribed, global displacement and element stresses as arrived are given in Table 5.7, 5.8, 5.9 and 5.10 respectively.

Theoretical deflection	=	$wl^4/30EI$ = 0.0800 cm
Maximum deflection from the program	=	0.0807500502 cm

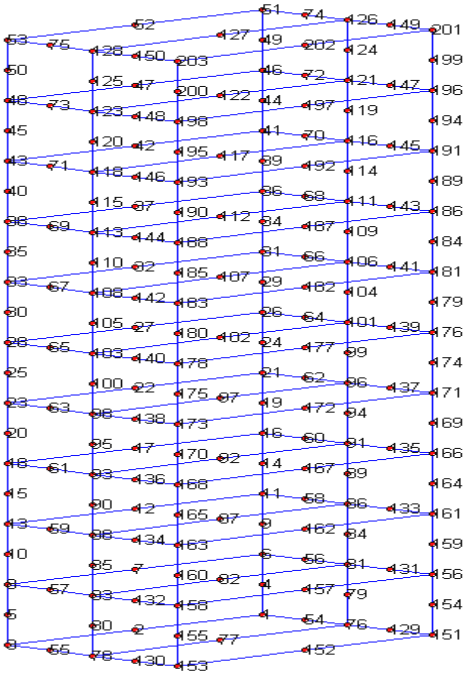

Fig 5.13: ***Descretisation along thickness of a cantilever wall***

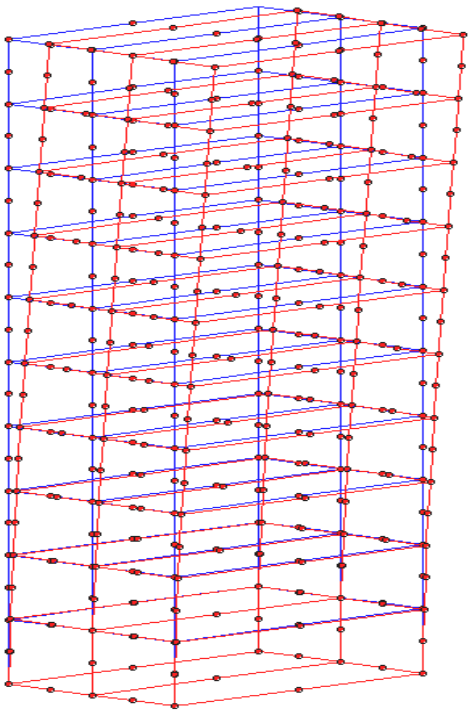

Fig 5.14: ***Deflected profile of a cantilever wall***; *Pressure on lateral face*

Table 5.7: **Cantilever wall Element connectivity Descretisation along thickness**

1	3	1	76	78	8	6	81	83	2	54	77	55	7	56	82	57	5	4	79	80
2	8	6	81	83	13	11	86	88	7	56	82	57	12	58	87	59	10	9	84	85
3	13	11	86	88	18	16	91	93	12	58	87	59	17	60	92	61	15	14	89	90
4	18	16	91	93	23	21	96	98	17	60	92	61	22	62	97	63	20	19	94	95
5	23	21	96	98	28	26	101	103	22	62	97	63	27	64	102	65	25	24	99	100
6	28	26	101	103	33	31	106	108	27	64	102	65	32	66	107	67	30	29	104	105
7	33	31	106	108	38	36	111	113	32	66	107	67	37	68	112	69	35	34	109	110
8	38	36	111	113	43	41	116	118	37	68	112	69	42	70	117	71	40	39	114	115
9	43	41	116	118	48	46	121	123	42	70	117	71	47	72	122	73	45	44	119	120
10	48	46	121	123	53	51	126	128	47	72	122	73	52	74	127	75	50	49	124	125
11	78	76	151	153	83	81	156	158	77	129	152	130	82	131	157	132	80	79	154	155
12	83	81	156	158	88	86	161	163	82	131	157	132	87	133	162	134	85	84	159	160
13	88	86	161	163	93	91	166	168	87	133	162	134	92	135	167	136	90	89	164	165
14	93	91	166	168	98	96	171	173	92	135	167	136	97	137	172	138	95	94	169	170
15	98	96	171	173	103	101	176	178	97	137	172	138	102	139	177	140	100	99	174	175
16	103	101	176	178	108	106	181	183	102	139	177	140	107	141	182	142	105	104	179	180
17	108	106	181	183	113	111	186	188	107	141	182	142	112	143	187	144	110	109	184	185
18	113	111	186	188	118	116	191	193	112	143	187	144	117	145	192	146	115	114	189	190
19	118	116	191	193	123	121	196	198	117	145	192	146	122	147	197	148	120	119	194	195
20	123	121	196	198	128	126	201	203	122	147	197	148	127	149	202	150	125	124	199	200

Table 5.8: **Cantilever wall - Prescribed displacement and Hydrostatic loading**

Nodes where displacement restricted				Hydrostatically loaded Elements
54	1	1	1	1
55	1	1	1	2
129	1	1	1	3
130	1	1	1	4
76	1	1	1	5
77	1	1	1	6
78	1	1	1	7
151	1	1	1	8
152	1	1	1	9
153	1	1	1	10
1	1	1	1	
2	1	1	1	
3	1	1	1	

Output

```
Number of elements                  = 20
Number of nodes                     = 203
Number of Gaussian points           = 4
E= 2000kN/cm2     Poisson's ratio   = 0
Unit weight of solid                = 0
Unit weight of liquid               = 1e-005 kN/cm3
Z refer datum = 200cm Ebar          = 2000
Number of degrees of freedom        = 570
Semi band width                     = 570
```

Table 5.9: **Cantilever wall - Global Displacement Array**

Node	Displ X	Displ Y	Displ Z	Node	Displ X	Displ Y	Displ Z
1	0	0	0	151	0	0	0
2	0	0	0	152	0	0	0
3	0	0	0	153	0	0	0
4	0.000575	0	0.000932	154	0.000566	0	-0.00093
5	0.000575	0	0.000932	155	0.000566	0	-0.00093
6	0.002008	0	0.001739	156	0.001999	0	-0.00174
7	0.002008	0	0.001739	157	0.001999	0	-0.00174
8	0.002008	0	0.001739	158	0.001999	0	-0.00174
9	0.004163	0	0.0024	159	0.004155	0	-0.0024
10	0.004163	0	0.0024	160	0.004155	0	-0.0024
11	0.00692	0	0.002963	161	0.006912	0	-0.00296
12	0.00692	0	0.002963	162	0.006912	0	-0.00296
13	0.00692	0	0.002963	163	0.006912	0	-0.00296

14	0.01018	0	0.003424	164	0.010172	0	-0.00342
15	0.01018	0	0.003424	165	0.010172	0	-0.00342
16	0.013855	0	0.003809	166	0.013848	0	-0.00381
17	0.013855	0	0.003809	167	0.013848	0	-0.00381
18	0.013855	0	0.003809	168	0.013848	0	-0.00381
19	0.017866	0	0.004113	169	0.017859	0	-0.00411
20	0.017866	0	0.004113	170	0.017859	0	-0.00411
21	0.022145	0	0.004359	171	0.022139	0	-0.00436
22	0.022145	0	0.004359	172	0.022139	0	-0.00436
23	0.022145	0	0.004359	173	0.022139	0	-0.00436
24	0.026634	0	0.004546	174	0.026628	0	-0.00455
25	0.026634	0	0.004546	175	0.026628	0	-0.00455
26	0.031283	0	0.004692	176	0.031278	0	-0.00469
27	0.031283	0	0.004692	177	0.031278	0	-0.00469
28	0.031283	0	0.004692	178	0.031278	0	-0.00469
29	0.036053	0	0.004797	179	0.036048	0	-0.0048
30	0.036053	0	0.004797	180	0.036048	0	-0.0048
31	0.040909	0	0.004875	181	0.040905	0	-0.00488
32	0.040909	0	0.004875	182	0.040905	0	-0.00488
33	0.040909	0	0.004875	183	0.040905	0	-0.00488
34	0.045825	0	0.004926	184	0.045821	0	-0.00493
35	0.045825	0	0.004926	185	0.045821	0	-0.00493
36	0.05078	0	0.004961	186	0.050777	0	-0.00496
37	0.05078	0	0.004961	187	0.050777	0	-0.00496
38	0.05078	0	0.004961	188	0.050777	0	-0.00496
39	0.055759	0	0.004981	189	0.055757	0	-0.00498
40	0.055759	0	0.004981	190	0.055757	0	-0.00498
41	0.060752	0	0.004993	191	0.06075	0	-0.00499
42	0.060752	0	0.004993	192	0.06075	0	-0.00499
43	0.060752	0	0.004993	193	0.06075	0	-0.00499
44	0.06575	0	0.004998	194	0.065748	0	-0.005
45	0.06575	0	0.004998	195	0.065748	0	-0.005
46	0.07075	0	0.005	196	0.070749	0	-0.005
47	0.07075	0	0.005	197	0.070749	0	-0.005
48	0.07075	0	0.005	198	0.070749	0	-0.005
49	0.07575	0	0.005	199	0.07575	0	-0.005
50	0.07575	0	0.005	200	0.07575	0	-0.005
51	0.08075	0	0.005	201	0.08075	0	-0.005
52	0.08075	0	0.005	202	0.08075	0	-0.005
53	0.08075	0	0.005	203	0.08075	0	-0.005

Table5.10: **Stresses at Centroid of Element Average of Gauss Points**

Element	sig_x	sig_y	sig_z	sig_xz
1	-0.00064	4.28e-16	0.085779	0.009507
2	-0.00148	6.56e-16	0.064889	0.00792
3	-0.00125	4.89e-15	0.044793	0.006183
4	-0.00111	1.12e-14	0.029311	0.004655
5	-0.00093	1.02e-14	0.017881	0.003343
6	-0.00077	4.40e-15	0.009904	0.002249
7	-0.0006	9.73e-16	0.004755	0.001373
8	-0.00043	-4.18e-15	0.001811	0.000713
9	-0.00026	-7.72e-15	0.000448	0.00027
10	-9.11e-05	-1.75e-14	4.34e-05	4.46e-05
11	-0.0008	-9.37e-16	-0.08578	0.009387
12	-0.00026	-7.40e-16	-0.06489	0.007902
13	-0.00032	-5.00e-15	-0.04479	0.006182
14	-0.00025	-1.06e-14	-0.02931	0.004655
15	-0.00022	-1.05e-14	-0.01788	0.003343
16	-0.00018	-7.38e-15	-0.0099	0.002249
17	-0.00014	-1.22e-15	-0.00475	0.001373
18	-9.88e-05	4.04e-15	-0.00181	0.000713
19	-5.99e-05	1.11e-14	-0.00045	0.00027
20	-2.07e-05	1.93e-14	-4.34e-05	4.46e-05

Sector of an arch dam

A sector of an arch dam near the crown is analyzed with the program to see the deflection pattern due to surface pressure and is plotted below in Fig 5.15.

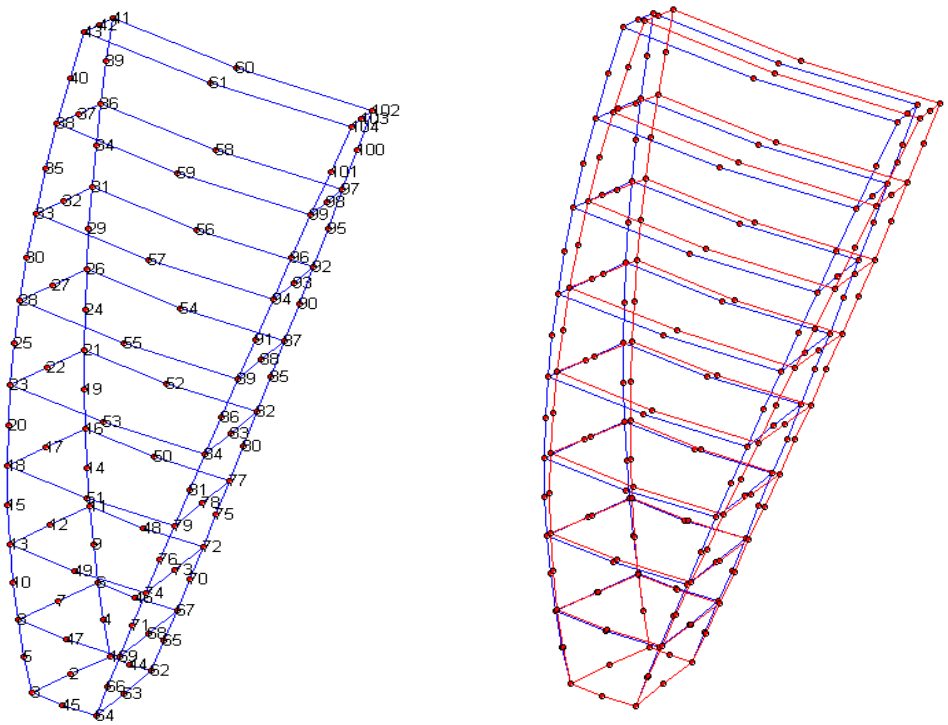

Fig 5.15: ***Sector of arch dam- Deflected profile due to hydrostatic loading***

References

1. Thomas H. H., "The Engineering of Large Dams" Part 1, John Wiley & Sons, 1976

2. Varshney R.S., "Concrete Dams", Oxford and IBH publishing company, 1988

3. Hubert Chanson and Patrick James., "Historical Development of Arch Dams", University of Queensland, Brisbane, Australia, www.uq.edu.au/~e2hchans/arch_dam.html, 2000

4. Inter national workshop on Arch dams/Coimbra/April 1987., "Arch Dams" Edited by Laginha Serafim J, Clough R.W, Balkema A.A Publishers, USA 1990

5. Sharma H.D ., "Concrete dams", publication No 266, Central Board of Irrigation and Power, January 1998

6. ICOLD., "4th Benchmark Committee on Numerical Analysis of Dams", Paris, France, International committee on Large Dam and French Committee 1994

7. International Committee on Large Dams., Bulletin 30, "Finite Element Analysis and Design of Dams ", pp 293-317, January 1978

8. ICOLD., "5th Benchmark Committee on Numerical Analysis of Dams", Denver Co, International committee on Large Dam and Bureau of Reclamation and US Committee on Large Dam 1999

9. ICOLD., Bulletin. 122. "Computational procedures for dam engineering"' 2001

10. Zienkiewicz O.C and Philips D.V., "An automatic mesh generator scheme for plane and curved surface by isoparametric coordinates", International Journal for Numerical methods in Engineering vol 3 1971

11. Rao S.S, Singh and Praveen T.V., "Two Dimensional Stress Analysis of Selected Concrete Gravity Dams by Finite Element Method", Journal of Irrigation and Power Vol. 49, Central Board of Irrigation and Power 1992

12. ICOLD., "Evaluation of ultimate strength of gravity dams with curved shape against sliding-Synthesis of results"; 7th Benchmark Workshop on Numerical Analysis of Dams, Bucharest, Romania, September 2003

13. ICOLD., “Proceedings of the twenty first International Congress on Large Dams” Monreal , Canada 2003

14. Ghanaat Y. 1993a (Aug)., "GDAP - Graphics-based Dam Analysis Program," Instruction Report ITL-93-3, U.S. Army Engineer Waterways Experiment Station, Vicksburg. 1993

15. Ghanaat Y. 1993b (Jul)., "Theoretical Manual For Analysis of Arch Dams," Instruction Report ITL-93-3, U.S. Army Engineer Waterways Experiment Station, Vicksburg, MS 1993

16. Berkeley C.A., “SAP 2000, Integrated Finite Element Analysis and Design of Structures”, Computers and Structures, Inc. 2000 http://www.csiberkeley.com

17. Lotfi V., “MAP 76: A program for analysis of concrete dams”, Amirkabir University of Technology, Tehran, Iran. 2001

18. NISA 2001., Structural Analysis and Design Software

19. STADPRO 2005., Structural Analysis and Design Software for Civil Engineers

20. Krishnamoorthy C.S., "Finite Element Analysis (Theory and Programming)", Tata McGraw-Hill Publishing Co. Ltd, 1997

21. Robert. D. Cook., David S Malkus et. al., "Concepts and applications of Finite Element Analysis", John Wiley & Sons, 2002

22. U.S. Bureau of Reclamation. "Design of Arch Dams," Design Manual for Concrete Arch Dams, U.S. Department of the Interior, Denver, CO 1977

23. William H, Lee K, Hiroo Kanamori and Paul.C. Jenning., International Handbook of Earthquake Engineering Seismology Part B, pp 26; 1-44,2003

24. Zienkiewicz O.C., "The Finite Element Method", Tata McGraw-Hill Publishing Company. Ltd., 1990

25. Zienkiewicz O.C and Morgan K., "Finite elements and approximation", John Wiley & Sons, 1983

26. Zienkiewicz O.C and Taylor R.L., “ Finite Element Method: Volume 2, Solid Mechanics”, 2000

27. Zienkiewicz O.C and Taylor R.L., “The Finite Element Method for Solid and Structural Mechanics’, Sixth Edition 2005

28. Ikegawa Y and Hudson J.A., ‘‘A novel automatic identification system for three-dimensional multi-block system.’’ Engineering Computers 1992

29. Chen S.H., ‘‘A new development in the elastic viscoplastic block theory of rock masses.’’ Journal of Computer methods and advances in Geomechanics 1994

30. Chen S.H, Shen B.K and Huang M.H., ‘‘Stochastic elastic viscoplastic analysis for discontinuous rock masses.’’ International. Journal. Numerical Methods Engineering., 2429–2444, 1994

31. Wang W.M, and Chen S.H., ‘‘A new implementation of elastic visco plastic block theory for rock masses.’’ 10th Int. Conf. on Computer Methods and Advances in Geomechanics, Arizona 2001

32. Wang W.M and Chen S.H., ‘‘A new implementation of elastic visco plastic block theory for rock masses.’’ 10th Int. Conf. on Computer Methods and Advances in Geomechanics, Arizona, 2001

33. Chen S.H, Xu M.Y, Shahrour I and Effer P., “Analysis of arch dams using coupled trial load and block element methods”. Journal of Geo technical and Geo environmental Engineering;129(11):977–86, 2004

34. Yua X, Zhoub Y.F and Pengb S.Z., “Stability Analysis of dam abutments by 3D elasto plastic finite element method” a case study of Houhe gravity arch dam in China International Journal of Rock Mechanics & Mining Sciences 42 415– 430, 2005

35. Fanelli M, Mazza G, Ruggeri G and Palumbo P., “Gravity Dams: Safety Evaluation against Sliding with 3D Rigid Body Formulation”. Proceedings on Research and Development in the field of Dams, Crans Montana (Switzerland), Sept 1995

36. Duncan J.M., State of the art: limit equilibrium and finite element analysis of slopes. Journal of Geotechnical Engineering; pp 577–596, 1996

37. Griffiths D.W and Lane P.A., Slope stability analysis by finite elements, Journal Geotechnical Engineering;49(3):387–403, 1999

38. Li Z and Long Y.X., Discussion on sliding stability analysis of dam foundation. Journal of Hydraulic Engineering; pp 8 :1–10 2000

39. Chen S.H, Wang W.M, She, C.X and Xu M.Y., ‘‘Unconfined seepage analysis of discontinuous rock slope.’’ Journal of Hydrodynamics.,75–86, 2000

40. Linsbauer, Ingraffea H.N, Rossmanith H.P and Wawrzynek P., ‘‘Simulation of cracking in large arch dam: part I’’ Journal of Structural Engineering., 1599–1615, 1989

41. Ingraffea A.R., ‘‘Case studies of simulation of fracture in concrete dams.’’ Journal of Engineering and Fracture Mechanics., 553–564, 1990

42. Zhang C and Karihaloo B.L., ‘‘Stability of a crack in a large concrete dam.’’ Australian Civil Engineering Trans. IEAust., 369–375, 1992

43. Dewey R.R., Ronald, W.R., and Saouma., ‘‘Uplift modeling for fracture mechanics analysis of concrete dams.’’ Journal of Structural Engineering., 3025–3044, 1994

44. Zihai Shi, Masaki Suzuki and Masaaki Nakano., “ Numerical Analysis of Multiple Discrete Cracks in Concrete Dams Using Extended Fictitious Crack Model” pp 336-342 Journal of Structural Engineering March 2000

45. Ohtsu M and Chahrour A.H., ‘‘Fracture analysis of concrete based on the discrete crack model by the boundary element method’’1993

46. Malla S and Wieland M., “Analysis of an arch gravity dam with a horizontal crack”. Computer Structure Division; 72:267–78, 1999

47. Karan S Surana and Robert M.,“P-version hierarchical three dimensional curved shell element for elastostatics” International Journal for Numerical Methods in Engineering Volume 31, Issue 4, pp. 649 – 676 Published Online: Sorem University of Kansas, U.S.A. 24 Jun 2005

48. Humar J.L and Jablonski A.M., “ Boundary element reservoir model for seismic analysis of gravity dams” Earthquake Engineering and Structural Dynamics 16, 1129-1156,1988

49. Wep D.H, Wolf J.P and Bachmann H., “Hydrodynamic-stiffness matrix based on boundary elements for time-domain dam-reservoir-soil analysis”, Earthquake Engineering and Structural Dynamics,417-432 1988

50. Medina F and Dominguez J., “Boundary elements for the analysis of the seismic response of dams including dam-water-foundation interaction effects” Journal of Engineering. Analysis., 6, 152-157,1989

51. Hanchen T and Chopra A.K., “Dam-foundation rock interaction effects in earthquake response of arch dams”, Journal of structural Engineering, ASCE, 122(5), 528-538, 1996

52. Hall J.F, Chopra A.K., “Dynamic Analysis of Arch Dams Including Hydrodynamic Effects”, Journal of Engineering Mechanics Vol. 109 pp.149-167, Feb 1983

53. Chopra A.K.," Hydrodynamic effects in earthquake response of arch dams"; Proceedings of China-US Workshop on Earthquake Behavior of Arch Dams. Beijing, China, 110-12, 1987

54. Tsai C.S and Lee G.C., "Arch dam-fluid interactions FEM-BEM and substructure concept"; International Journal for Numerical Methods in Engineering Vol. 24pp. 2367-2388 1987

55. Von O, Estorff and Antes H., "FEM-BEM coupling for Fluid Structure interaction Analyses in the Time Domain", International Journal Numerical Methods in Engineering., 31, 1151-1168,1991

56. Taskov L and Jurukovski D., ''Shaking table tests of an arch dam fragment.'' Proc., China-US Workshop on Earthquake Behaviour of Arch Dams, 1987

57. Donlon N.W.P and Hall J.F., ''Shaking table study of concrete gravity dam monoliths.'' Earthquake Engineering. and Structural Dynamics 20 , 1991

58. Fok K and Chopra A.K., ''Earthquake analysis of arch dams including dam-water interaction, reservoir boundary absorption and foundation flexibility.'' Earthquake Engineering. Structural Dynamics ,1986

59. Connor P.F and Boot J.C., "A solution procedure for the earthquake analysis of arch dam-reservoir systems with compressible water", Earthquake Engineering. Structural Dynamics., 16, 757-773,1988

60. Bruhwiler E and Wittmann F.H., ''Failure of dam concrete subjected to seismic loading conditions.'' Engineering. Fracture Mechanics., (35), 565–571, 1990

61. Nowak P.S and Hall J.F., ''Arch dam response to non uniform seismic input.'' Journal of. Engineering. Mechanics., 125–139, 1990

62. Maeso O and Domınguez., ''Earthquake analysis of arch dams. I: Dam-foundation interaction'' Journal of Engineering Mechanics., 496–512, 1993

63. Hanchen T and Chopra A.K., "Dam-foundation rock interaction effects in earthquake response of arch dams". Journal of structural Engineering., ASCE, 122(5), 528-538, 1996

64. Ventura C.E, Finn W.D.L and Schuster N.D., ''Seismic response of instrumented structures during the 1994, Northridge, California earthquake.'' Can. J. Civ. Engrg., Ottawa, (22), 316–337, 1995

65. Mitchell D, Devall R.H, Kobaysshi K, Tinawi R and Tso W.K. ''Damage to concrete structure due to the January 17, 1995, Hyogo-Ken Nanbu (Kobe) earthquake.'' Can. Journal of Civil Engineering, Ottawa, (23), 757–770, 1996

66. Tan H and Chopra A.K. 1995b, ‘‘Dam-foundation rock interaction effects in frequency-response functions of arch dams’’, Earthquake Engineering. Structural Dynamics 24, 1475–1489, 1995

67. Zhang L and Chopra A.K., ‘‘Three-dimensional analysis of spatially varying ground motions around a uniform canyon in a homogeneous half-space’’, Earthquake Engineering. Structural Dynamics., 911–926, 1991a

68. Orlando Maeso and Jose Domınguez., “Effects of space distribution of excitation on seismic response of arch dams”, 768 Journal of Engineering Mechanics July 2002

69. Lotfi V., “Seismic analysis of concrete dams using the pseudo symmetric technique”, Journal of Dam Engineering, XIII (2) 2002

70. Vahid Lotfi ., “Frequency domain analysis of concrete arch dams by decoupled modal approach”, Journal of Structural Engineering and Mechanics, Vol.21, No.4, 423-435, 2005

71. Lotfi V., “Direct frequency domain analysis of concrete arch dams based on FE-(FE-HE)-BE technique”, Journal of Computers & Concrete, 1(3), 285-302, 2004

72. Tan H and Chopra A.K., “Earthquake analysis of arch dam including dam water foundation rock interaction”, Earthquake Engineering and Structural Dynamics 24, 1453-1474, 1995a

73. Lotfi V., “Significance of rigorous fluid-foundation interaction in dynamic analysis of concrete gravity dams”, Journal of Structural Engineering and Mechanics, Vol. 21 No 2 137-150, 2005

74. Tan H and Chopra A.K., “Dam-foundation rock interaction effects in frequency response functions of arch dams”, Earthquake Engineering and Structures, 1475-1489 1995b

75. Zhang L and Chopra A.K., ‘‘Impedance functions for three dimensional foundation supported on an infinitely long canyon of uniform cross-section in a homogeneous half-space.’’ Earthquake Engineering. Structural Dynamics, 1011–1027, 1991

76. Vahid Lotfi ., “An efficient three dimensional fluid hyper element for dynamic analysis of concrete arch dams”, Journal of Structural Engineering and Mechanics, Vol. 24, No.6, 683-698, 2006

77. Ahmad Aftabi Sani and Vahid Lotfi., “Linear dynamic analysis of arch dams utilizing modified efficient fluid hyper element”. Engineering Structures, Science Direct www.elsevier.com/locate/finel 2007

78. Valliappan S, Yazdchi M and Khalili N., “Seismic analysis of arch dams - A continuum damage mechanics approach”, International Journal of Numerical Methods in Engineering, 45, 1695-1724, 1999

79. Karaton M, Calayir Y and Bayraktar A., “Seismic analysis of arch dams including dam reservoir interaction via a continuum damage model”, Structural Engineering and Mechanics, Vol. 22, No. 3 351-370, 2006

80. Karaton M and Calayir Y., “A continuum damage concrete model for earthquake analysis of arch dams”, 6th International Congress on Advances in Civil Engineering, Turkey,October 2004

81. Calayir Y and Karaton M., “A continuum damage concrete model for earthquake analysis of concrete gravity dam reservoir systems”, International Journal for Soil Dynamics and Earthquake Engineering, 25, 857-869, 2005

82. Yaoru Liu, Weiyuan Zhou and QiangYang., “A distributed memory parallel element by element scheme based on Jacobi conditioned conjugate gradient for 3D finite element analysis”, Finite Elements in Analysis and Design 43, 494–503, Science Direct www.elsevier.com/locate/finel 2007

83. Susan Abraham and Narayanan K.V., “Automatic Mesh Generator for Arch Dams using Three Dimensional Mapping Technique”; Proceedings of International Conference on Numerical Analysis and Applied Mathematics, Wiley VCH, pp 787-792 ICNAAM 2005

84. Rao S S., " Finite Element Method in Engineering", Elsevier, 2005

85. Sathya Narayana Murthy Chella., “Water resources Engineering principles and Practice” 2002

86. Harsh K Gupta., “Dams and Earthquakes”, Elsevier Newyork1976

87. Mohammed Ameen., “Computational Elasticity”, Narosa publishers New Delhi 2005

88. Robert. D. Cook.," Finite Element Modelling for Stress Analysis", John Wiley & Sons, 2002

89. Sharma J N., “Numerical Methods for Engineers and Scientists”, Narosa publishers New Delhi 2007

90. Kattan P.I., “Matlab Guide to Finite Elements” Springer Germany 2003

91. Proceedings of Conference held at the Institution of Civil Engineers, London 1980., “Dams and Earthquake” Thomas Telford Ltd London 1981

92. Bureau of Indian Standards. "Criteria for Earthquake Resistant Design of Structures", Indian Standard Specification 1893, 1994 Re affirmed 2003

93. Itty Darwin C., “Idukki Dam, Design and construction of selected dams in India” pp 293-317 ICOLD, CBIP publication no 138, October 1979

94. Surveyer, Nenniger and Chenevert Inc., "Idukki Dam Trial load Analysis", Report of Canadian International Development Agency, 1969

95. Industrial Research Institute University of Waterloo., "Report on Idukki Arch Dam – Finite Element Analysis", 1969

96. Raveendran B., "Structural Behavior of Arch Dams with Special Reference to Idukki Arch Dam", Dissertation of M.E, Water Resources Development Training Centre, Roorkee, 1985

97. Susan Abraham and Narayanan K.V., “Automatic Mesh Generator for Arch Dams using Three Dimensional Mapping Technique”; ESCMSE, International Journal of Numerical Analysis Industrial and Applied Mathematics JNAIAM, 2006

98. Susan Abraham and Narayanan K.V., “Definition of Geometry of Variable Radius Arch Dam with Degree of Polynomial in the 3D Finite Element analysis”. C*ommunicated 2008*

99. Susan Abraham and Narayanan K.V., “Comparison of Deflection and Stresses in Arch Dams with Definition of Geometry in the 3D Finite Element analysis”. ”. C*ommunicated 2008*

Annexure

A.0 IDUKKI ARCH DAM - ANALYSIS FOR VARIOUS LOAD CASES AND DISCRETISATIONS

In this *Annexure,* Idukki arch dam chosen for case study is analyzed with the developed program for various load conditions and discretisations as required for arch dams and a comparison made with the available results. The out put of the program gives nodal data, connectivity, boundary conditions, band width, element stiffness matrices, element load vectors, global load vectors, deflection at all the nodes in the three directions, stresses and strains in the six directions at the 27 gauss points of each element, nodal points, average elemental stresses, upstream and downstream elements' face centre stresses, original profile, deflected profile, plans at various levels and elevation. Since presenting all the results is rather extensive, only the major values of deflection and stresses at crown section are tabulated and plotted.

A.1 GEOMETRY AND DISCRETISATION-1 SELECTED

The Idukki arch dam geometry derived by 80 nodal points with degree of polynomial 7 in length, 1 in thickness and 4 in height directions is discretised to 28 elements as arrived in section 6.3.2 and taken for analysis. The mesh of the dam with node numbering is shown in Fig. A.1. Displacement is restricted at the 78 boundary

nodes assuming the sides and bottom faces fixed as given in Table A.1. The nodal connectivity as arrived by the program is tabulated below in Table A.2.

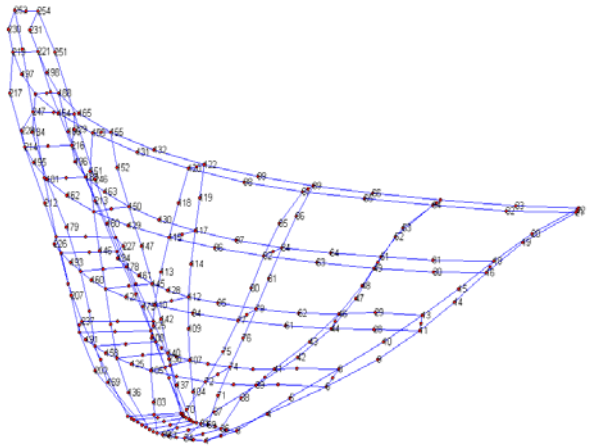

Fig A.1: ***Idukki arch dam Node numbering pattern 28 elements***

Table A.1: **Idukki arch dam Nodes at which displacements prescribed 28 elements**

Node	u	v	w	Node	u	v	w	Node	u	v	w
1	1	1	1	251	1	1	1	123	1	1	1
2	1	1	1	250	1	1	1	124	1	1	1
3	1	1	1	249	1	1	1	156	1	1	1
4	1	1	1	248	1	1	1	157	1	1	1
5	1	1	1	247	1	1	1	189	1	1	1
6	1	1	1	246	1	1	1	190	1	1	1
7	1	1	1	245	1	1	1	222	1	1	1
8	1	1	1	244	1	1	1	223	1	1	1
9	1	1	1	243	1	1	1	34	1	1	1
10	1	1	1	242	1	1	1	35	1	1	1
11	1	1	1	241	1	1	1	36	1	1	1
12	1	1	1	240	1	1	1	67	1	1	1
13	1	1	1	239	1	1	1	68	1	1	1
14	1	1	1	238	1	1	1	69	1	1	1
15	1	1	1	237	1	1	1	100	1	1	1
16	1	1	1	236	1	1	1	101	1	1	1
17	1	1	1	235	1	1	1	102	1	1	1
18	1	1	1	234	1	1	1	133	1	1	1
19	1	1	1	233	1	1	1	134	1	1	1
20	1	1	1	232	1	1	1	135	1	1	1
21	1	1	1	24	1	1	1	166	1	1	1
22	1	1	1	25	1	1	1	167	1	1	1
23	1	1	1	57	1	1	1	168	1	1	1
254	1	1	1	58	1	1	1	199	1	1	1
253	1	1	1	90	1	1	1	200	1	1	1
252	1	1	1	91	1	1	1	201	1	1	1

Table A.2: **Idukki arch dam Nodal connectivity 28 elements**

Element	**1**	**2**	**3**	**4**	**5**	**6**	**7**	**8**	**9**	**10**	**11**	**12**	**13**	**14**	**15**	**16**	**17**	**18**	**19**	**20**
1	3	1	34	36	8	6	39	41	2	24	35	25	7	26	40	27	5	4	37	38
2	8	6	39	41	13	11	44	46	7	26	40	27	12	28	45	29	10	9	42	43
3	13	11	44	46	18	16	49	51	12	28	45	29	17	30	50	31	15	14	47	48
4	18	16	49	51	23	21	54	56	17	30	50	31	22	32	55	33	20	19	52	53
5	36	34	67	69	41	39	72	74	35	57	68	58	40	59	73	60	38	37	70	71
6	41	39	72	74	46	44	77	79	40	59	73	60	45	61	78	62	43	42	75	76
7	46	44	77	79	51	49	82	84	45	61	78	62	50	63	83	64	48	47	80	81
8	51	49	82	84	56	54	87	89	50	63	83	64	55	65	88	66	53	52	85	86
9	69	67	100	102	74	72	105	107	68	90	101	91	73	92	106	93	71	70	103	104
10	74	72	105	107	79	77	110	112	73	92	106	93	78	94	111	95	76	75	108	109
11	79	77	110	112	84	82	115	117	78	94	111	95	83	96	116	97	81	80	113	114
12	84	82	115	117	89	87	120	122	83	96	116	97	88	98	121	99	86	85	118	119
13	102	100	133	135	107	105	138	140	101	123	134	124	106	125	139	126	104	103	136	137
14	107	105	138	140	112	110	143	145	106	125	139	126	111	127	144	128	109	108	141	142
15	112	110	143	145	117	115	148	150	111	127	144	128	116	129	149	130	114	113	146	147
16	117	115	148	150	122	120	153	155	116	129	149	130	121	131	154	132	119	118	151	152
17	135	133	166	168	140	138	171	173	134	156	167	157	139	158	172	159	137	136	169	170
18	140	138	171	173	145	143	176	178	139	158	172	159	144	160	177	161	142	141	174	175
19	145	143	176	178	150	148	181	183	144	160	177	161	149	162	182	163	147	146	179	180
20	150	148	181	183	155	153	186	188	149	162	182	163	154	164	187	165	152	151	184	185
21	168	166	199	201	173	171	204	206	167	189	200	190	172	191	205	192	170	169	202	203
22	173	171	204	206	178	176	209	211	172	191	205	192	177	193	210	194	175	174	207	208
23	178	176	209	211	183	181	214	216	177	193	210	194	182	195	215	196	180	179	212	213
24	183	181	214	216	188	186	219	221	182	195	215	196	187	197	220	198	185	184	217	218
25	201	199	232	234	206	204	237	239	200	222	233	223	205	224	238	225	203	202	235	236
26	206	204	237	239	211	209	242	244	205	224	238	225	210	226	243	227	208	207	240	241
27	211	209	242	244	216	214	247	249	210	226	243	227	215	228	248	229	213	212	245	246
28	216	214	247	249	221	219	252	254	215	228	248	229	220	230	253	231	218	217	250	251

A.1.1 Dead Load Only

Modulus of elasticity = 20670000 kN/m^2

Poisson's ratio = 0.2

Unit weight of dam material = 23.5615 kN/m^3

Global displacement obtained for the crown portion is shown in Table A.3 and elemental stresses in Table A.4. Radial deflection and hoop stress at crown cantilever section are plotted in Fig A.2 and Fig A.3 respectively.

Table A.3: **Global displacement array** -Load Case I.

Node	Displ X cm	Displ Y cm	Displ Z cm
101	0	0	0
102	0	0	0
103	-0.00377	- 0.08294	-0.22574
104	-0.0124	-0.05052	-0.12176
105	-0.00344	-0.19263	-0.38512
106	-0.00899	-0.18538	-0.32689
107	-0.015	-0.17484	-0.26447
108	-0.00157	-0.30415	-0.49049
109	-0.00324	-0.28815	-0.4029
110	0.002483	-0.38255	-0.56613
111	0.002168	-0.37941	-0.54514
112	0.002068	-0.37271	-0.52178
113	0.00465	-0.41964	-0.62237
114	0.001045	-0.41217	-0.62353
115	0.002615	-0.40649	-0.67669
116	-0.00242	-0.40287	-0.69155
117	-0.00746	-0.3998	-0.70484
118	-0.00876	-0.37003	-0.72783
119	-0.01583	-0.36467	-0.75189
120	-0.01994	-0.32798	-0.74716
121	-0.02121	-0.32506	-0.75491
122	-0.02245	-0.3225	-0.76213
123	0	0	0
124	0	0	0
125	-0.03332	-0.1885	-0.38242
126	-0.01455	-0.17523	-0.26578
127	-0.02946	-0.37515	-0.56273
128	-0.00592	-0.36834	-0.51454
129	-0.00292	-0.42959	-0.65354
130	-0.01727	-0.42075	-0.67398
131	0.058062	-0.37254	-0.69921
132	0.044328	-0.36525	-0.7186

Table A.4: **Element stresses as average of Gauss points in kg/cm^2 -** Load case 1

Element	Sig x	Sig y	Sig z	Sig xy	Sig yz	Sig xz
1	-1.6676	-1.176	-14.56	0.4125	2.386	2.939
2	0.33161	1.489	-12.26	1.7912	3.617	3.3923
3	1.6441	2.1172	-9.387	2.2259	3.652	4.0404
4	4.9833	2.4098	-4.489	3.4014	1.569	1.9399
5	-1.9659	-0.334	-15.47	0.262	1.553	1.2577
6	0.96725	1.0937	-12.02	1.0346	2.514	2.8142
7	1.9034	0.4961	-8.784	1.1477	1.889	3.5969
8	1.266	0.3264	-3.808	0.7289	1.031	2.4347
9	-2.0339	-0.961	-16.71	0.1167	0.301	0.5901
10	1.1748	-0.222	-12.07	0.2949	0.346	1.6445
11	1.2139	-0.062	-8.232	0.2035	-0.03	1.6454
12	-2.4175	-0.153	-3.644	-0.33	-0.16	0.9938
13	-1.9541	-1.197	-16.91	0.1128	0.3	-0.185
14	1.1046	-0.178	-11.82	-0.248	0.215	-0.094
15	0.63692	-0.134	-7.951	-0.0077	-0.2	-1.194
16	-2.0254	-0.145	-3.671	0.23074	-0.03	-1.399
17	-1.7559	-1.032	-15.65	0.10342	1.056	-1.043
18	0.72919	0.1937	-12.07	-0.7096	1.288	-1.696
19	0.97407	0.2349	-9.773	-0.6138	1.309	-3.162
20	2.2395	0.5353	-4.269	-1.1317	0.85	-1.649
21	-1.4578	-0.619	-13.31	0.06684	2.42	-1.845
22	0.63782	1.6651	-11.54	-1.2753	3.249	-3.315
23	1.2722	1.5845	-12.85	-1.63	2.276	-2.451
24	2.6053	1.6677	-4.946	-2.0402	0.413	-0.08
25	-1.8505	-1.595	-10.26	0.09442	3.608	-2.754
26	0.29445	2.7444	-11.73	-1.9629	5.457	-4.678
27	0.2054	1.907	-12.62	-1.7789	1.091	-0.292
28	0.75871	2.2402	-4.227	-1.5656	0.122	0.3047

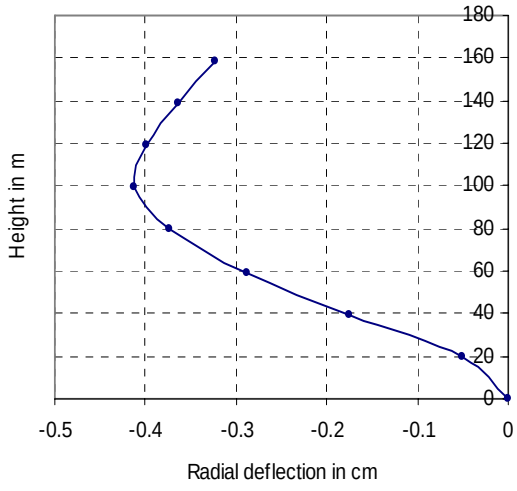

Fig A.2: ***Radial deflection at crown cantilever section - Load case 1***

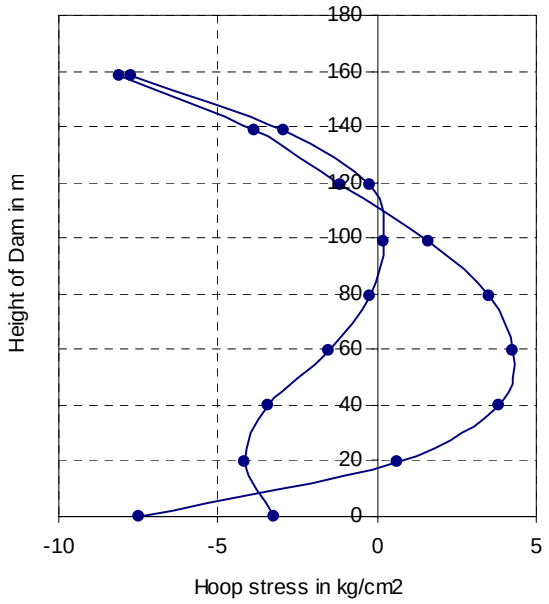

Downstream	
-3.22495	0
-4.12983	19.812
-3.41119	39.624
-1.4904	59.436
-0.23196	79.248
0.199313	99.06
-0.2509	118.872
-2.92207	138.684
-7.70976	158.496
Upstream	
-7.50359	0
0.657038	19.812
3.847251	39.624
4.252418	59.436
3.548518	79.248
1.6334	99.06
-1.1257	118.872
-3.8526	138.684
-8.07606	158.496

Fig A.3: ***Hoop stress at crown cantilever section- Load case 1***

A.1.2 Dead Load, Maximum Water and Maximum Silt

Unit weight of reservoir water =10 kN/m^3

Unit weight of silt material = 11.780775 kN/m^3

Reference datum of reservoir = 156.516 m

Reference datum of reservoir = 77.504 m

Global displacement obtained for the crown portion is shown in Table A.5 and elemental stresses in Table A.6. Radial deflection and hoop stress at crown cantilever section are plotted in Fig A.4 and Fig A.5 respectively.

TableA.5: **Global Displacement at Crown Cantilever** -Load Case 2

Node	Displ X cm	Displ Y cm	Displ Z cm
100	0	0	0
101	0	0	0
102	0	0	0

103	-0.01586	0.784074	0.354834
104	0.058191	0.722058	-0.24187
105	-0.03652	1.530954	0.415447
106	0.021097	1.527623	0.116252
107	0.066154	1.542116	-0.18641
108	-0.01364	2.146569	0.376576
109	0.039974	2.173848	-0.14036
110	0.01866	2.696991	0.292424
111	0.016153	2.729326	0.069827
112	0.020324	2.747855	-0.14887
113	0.017232	3.20768	0.162771
114	0.043355	3.25346	-0.16201
115	0.021781	3.578005	0.026566
116	0.04492	3.602849	-0.0691
117	0.074644	3.618308	-0.15322
118	0.014843	3.743738	-0.06618
119	0.119366	3.776583	-0.1068
120	0.014318	3.738834	-0.06391
121	0.077349	3.74749	-0.05128
122	0.137786	3.751699	-0.03664
123	0	0	0
124	0	0	0
125	0.203354	1.506036	0.401416
126	0.100997	1.54125	-0.16751
127	0.360954	2.54087	0.310231
128	0.08645	2.652331	-0.1355
129	0.460675	3.380419	0.085407
130	0.227057	3.449925	-0.16938
131	0.469753	3.726678	-0.04349
132	0.378521	3.775685	-0.08799

Table A.6: **Element stresses as average of Gauss points in kg/cm^2 -**Load case 2

Element	**sig x**	**sig y**	**sig z**	**sig xy**	**sig yz**	**sig xz**
1	-6.6873	-18.291	-6.5659	-11.675	13.399	2.0341
2	-10.967	-25.266	-10.535	-12.989	11.195	2.9363
3	-11.691	-16.304	-8.5638	-10.57	7.0189	3.5763
4	-10.331	-6.0352	-3.5082	-6.5615	2.2692	2.3658
5	-14.411	-16.436	-5.4992	-7.711	10.729	2.9397
6	-23.355	-20.75	-12.002	-13.891	6.7727	5.7196

7	-24.901	-12.035	-9.6314	-12.939	4.6001	4.8552
8	-21.792	-5.3772	-4.0489	-9.184	0.7064	2.2994
9	-19.151	-10.371	-3.7085	-3.9587	10.601	1.0515
10	-34.633	-8.4473	-10.068	-7.398	2.1298	2.7726
11	-37.256	-4.9765	-10.209	-6.4948	0.3285	2.6762
12	-30.411	-2.3022	-4.3572	-4.6283	-1.101	1.1073
13	-20.906	-10.107	-4.7473	2.074	11.399	-1.1501
14	-36.266	-7.511	-10.236	5.574	0.7689	-3.0879
15	-35.676	-4.3566	-9.5711	5.3563	0.2821	-2.0815
16	-31.052	-2.4069	-4.1788	4.8119	-0.773	-1.02
17	-16.245	-13.71	-6.9795	6.2961	12.213	-1.5681
18	-27.675	-14.664	-10.079	13.171	3.983	-5.9437
19	-25.066	-9.6766	-8.8489	12.254	4.4013	-5.3084
20	-19.738	-5.6708	-4.084	9.0234	1.0987	-2.2171
21	-10.951	-20.165	-9.3256	6.7036	11.798	-0.9308
22	-18.192	-26.027	-10.591	15.274	7.2558	-6.1097
23	-15.85	-16.582	-10.075	10.734	9.3699	-5.0932
24	-8.5637	-6.2242	-4.2893	5.933	2.511	-1.9056
25	-4.0464	-22.32	-9.8192	6.6981	11.05	-0.0025
26	-8.4923	-31.027	-9.3019	11.681	9.1558	-2.6519
27	-7.0292	-13.512	-8.6414	6.1029	9.7314	-2.3133
28	-2.6546	-4.4587	-4.0638	1.7751	2.7664	-0.7596

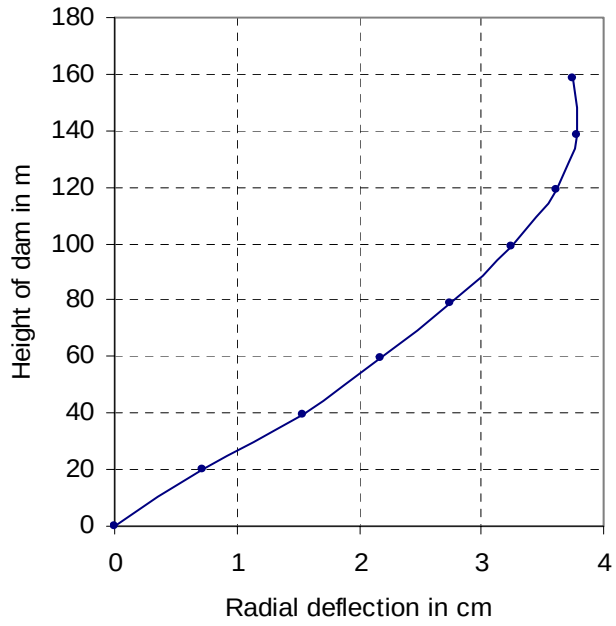

Fig A.4: ***Radial deflection at crown cantilever section -Load case 2***

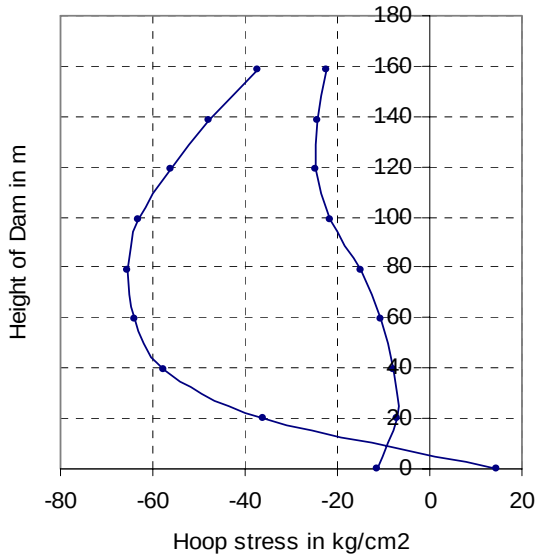

Downstream		
102	-11.317	0
104	-6.918	19.812
107	-7.7907	39.624
109	-10.6	59.436
112	-14.9	79.248
114	-21.667	99.06
117	-24.781	118.872
119	-24.409	138.684
122	-22.383	158.496
Upstream		
100	14.5467	0
103	-35.906	19.812
105	-57.6	39.624
108	-64	59.436
110	-65.5	79.248
113	-63.058	99.06
115	-56.137	118.872
118	-47.935	138.684
120	-37.386	158.496

Fig A.5: ***Hoop stress at crown cantilever section- Load case 2***

A.1.3 Dead Load, Normal Water, Maximum Silt and Earthquake C=0.02g

Unit weight of reservoir water = 10 kN/m^3

Unit weight of silt material = 11.780775 kN/m^3

Reference datum of reservoir = 154.838 m

Reference datum of reservoir = 77.504 m

Table A.7: **Global Displacement at crown cantilever**- Load case 3

Node	Displ X cm	Displ Y cm	Displ Z cm
100	0	0	0
101	0	0	0
102	0	0	0
103	-0.01582	0.778424	0.348303
104	0.057653	0.717593	-0.2418
105	-0.0363	1.515703	0.403518
106	0.020727	1.513046	0.109475
107	0.065304	1.527831	-0.18814
108	-0.01386	2.117737	0.359278
109	0.038794	2.145529	-0.14256
110	0.017638	2.646338	0.270895
111	0.014374	2.678909	0.058236
112	0.017757	2.697389	-0.15003
113	0.01514	3.125296	0.138614
114	0.037605	3.170677	-0.15947
115	0.017606	3.450964	0.004356
116	0.038201	3.475463	-0.07635
117	0.06511	3.490378	-0.14495
118	0.008947	3.56298	-0.08152
119	0.001052	3.594049	-0.09387
120	0.007372	3.498197	-0.0711
121	0.066042	3.506164	-0.0473
122	0.122316	3.509518	-0.02138
123	0	0	0
124	0	0	0
125	0.201134	1.491274	0.389583
126	0.099877	1.526988	-0.16944
127	0.353883	2.491662	0.287311
128	0.082892	2.602652	-0.13693
129	0.440669	3.25166	0.060112
130	0.208449	3.319911	-0.15932
131	0.421394	3.467692	-0.05042
132	0.328995	3.51535	-0.07117

Table A.8: **Element stresses as average of Gauss points in kg/cm^2 -**Load case 3

Element	sig x	sigy	sigz	sigxy	sigyz	sigxz
1	-6.668	-18.199	-6.7203	-11.612	13.369	2.0558
2	-10.807	-24.964	-10.525	-12.814	11.107	2.9023
3	-11.34	-15.851	-8.4503	-10.252	6.8686	3.4793
4	-9.8678	-5.6118	-3.4918	-6.1757	2.1238	2.3388
5	-14.326	-16.302	-5.6941	-7.6554	10.703	2.9337
6	-23.051	-20.472	-12.056	-13.724	6.7307	5.641
7	-24.221	-11.721	-9.5972	-12.617	4.4619	4.667
8	-20.616	-5.0777	-3.9801	-8.7257	0.55387	2.1343
9	-19.009	-10.284	-3.9624	-3.9235	10.566	1.0487
10	-34.237	-8.3254	-10.234	-7.3207	2.1045	2.7416
11	-36.352	-4.8506	-10.269	-6.3484	0.26147	2.538
12	-28.64	-2.1788	-4.3541	-4.4151	-1.1539	0.96768
13	-20.729	-10.032	-5.0104	2.0711	11.364	-1.1479
14	-35.871	-7.3944	-10.449	5.5184	0.76238	-3.0521
15	-34.845	-4.2461	-9.6564	5.242	0.22891	-2.0493
16	-29.119	-2.2656	-4.1445	4.5488	-0.832	-0.9753
17	-16.09	-13.61	-7.1882	6.2581	12.184	-1.5712
18	-27.371	-14.473	-10.242	13.025	3.9584	-5.8787
19	-24.452	-9.4013	-8.8806	11.971	4.2619	-5.1451
20	-18.518	-5.321	-4.0382	8.4966	0.96256	-2.1068
21	-10.857	-20.029	-9.4539	6.6602	11.784	-0.9426
22	-17.969	-25.671	-10.668	15.094	7.2138	-6.0519
23	-15.454	-16.068	-10.065	10.441	9.1084	-4.9308
24	-8.0691	-5.7706	-4.2721	5.6032	2.3259	-1.8698
25	-4.0344	-22.209	-9.882	6.6687	11.049	-0.0306
26	-8.3909	-30.643	-9.368	11.514	9.1168	-2.656
27	-6.8917	-13.045	-8.6842	5.914	9.4287	-2.2757
28	-2.5672	-4.0833	-4.0642	1.687	2.6138	-0.8263

Global displacement obtained for the crown portion is shown in Table A.7 and elemental stresses in Table A.8. Radial deflection and hoop stress at crown cantilever section are plotted in Fig A.6 and Fig A.7 respectively.

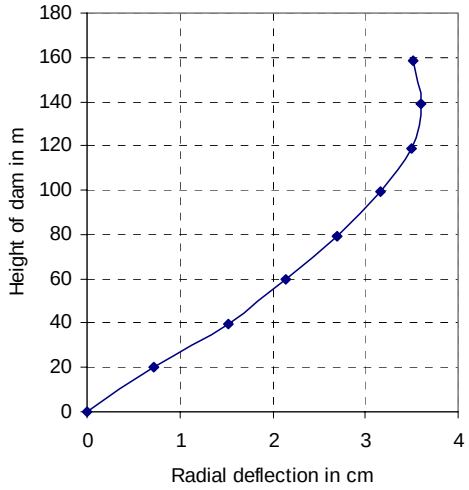

Fig A.6: ***Radial deflection Vs Height of dam - Load case 3***

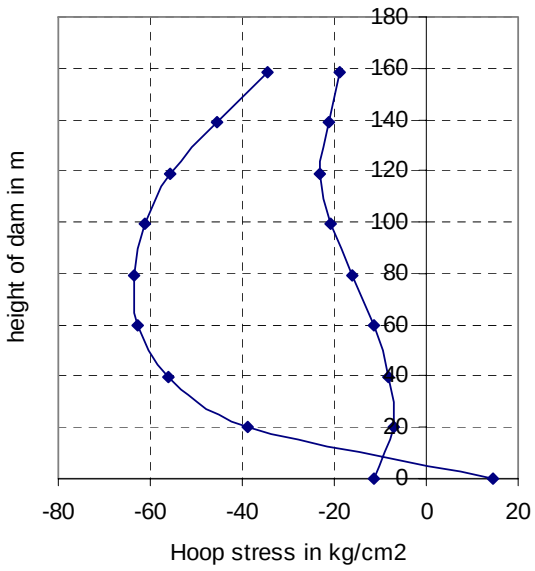

Downstream		
102	-11.289	0
104	-6.8833	19.812
107	-8.3	39.624
109	-11.420	59.436
112	-16.2	79.248
114	-20.919	99.06
117	-23.332	118.872
119	-21.188	138.684
122	-18.7	158.496
Upstream		
100	14.341	0
103	-38.793	19.812
105	-56.163	39.624
108	-62.853	59.436
110	-63.559	79.248
113	-61	99.06
115	-55.6	118.872
118	-45.418	138.684
120	-34.666	158.496

Fig A.7: ***Hoop stress Vs Height of dam- Load case 3***

A.1.4 Dead Load, Normal Water, Maximum Silt and Earthquake C=0.1g

Global displacement obtained for the crown portion is shown in Table A.9 and elemental stresses in Table A.10. Radial deflection and hoop stress at crown cantilever section are plotted in Fig A.8 and Fig A.9 respectively.

Table A.9: **Global Displacement at crown cantilever -** Load case 4

Node	Displ X cm	Displ Y cm	Displ Z cm
100	0	0	0
101	0	0	0
102	0	0	0
103	-0.01631	0.794316	0.364929
104	0.058651	0.732678	-0.24196
105	-0.03745	1.554259	0.432731
106	0.020849	1.552051	0.126268
107	0.066542	1.567364	-0.18371
108	-0.01461	2.188563	0.398675
109	0.039231	2.217054	-0.13418
110	0.017472	2.7578	0.317178
111	0.014316	2.79162	0.086543
112	0.018081	2.810845	-0.14013
113	0.014646	3.290234	0.187688
114	0.040267	3.337329	-0.15125
115	0.018174	3.680067	0.050177
116	0.040936	3.706039	-0.0518
117	0.070341	3.722234	-0.14225
118	0.010288	3.87239	-0.04415
119	0.114095	3.906091	-0.0987
120	0.00887	3.898889	-0.04652
121	0.071909	3.907894	-0.0399
122	0.132301	3.912053	-0.03132
123	0	0	0
124	0	0	0
125	0.205778	1.528674	0.41804
126	0.100688	1.565959	-0.16455
127	0.365769	2.597061	0.334957
128	0.083287	2.712132	-0.12669
129	0.465017	3.474254	0.109406
130	0.221335	3.546195	-0.15904
131	0.472716	3.865751	-0.02706
132	0.374421	3.917862	-0.0809

Table A.10: **Element stresses as average of Gauss points in kg/cm^2 -** Load case 4

Element	sigx	sigy	sigz	sigxy	sigyz	sigxz
1	-6.7276	-18.415	-6.2835	-11.885	13.515	2.0237
2	-11.2	-25.647	-10.402	-13.355	11.33	2.9661

3	-12.105	-16.644	-8.497	-10.989	7.1034	3.6308
4	-10.89	-6.2429	-3.4455	-6.9616	2.3205	2.4409
5	-14.43	-16.433	-5.1169	-7.8444	10.805	2.9673
6	-23.589	-20.88	-11.759	-14.167	6.841	5.769
7	-25.318	-12.126	-9.4734	-13.25	4.6641	4.8997
8	-22.303	-5.4258	-3.9885	-9.4804	0.75388	2.3412
9	-19.165	-10.27	-3.2451	-4.0193	10.704	1.0531
10	-34.894	-8.3489	-9.7066	-7.5259	2.1839	2.7658
11	-37.676	-4.8938	-9.9666	-6.6248	0.34694	2.6703
12	-30.879	-2.2297	-4.2674	-4.7362	-1.074	1.1164
13	-20.938	-9.9892	-4.2917	2.1098	11.514	-1.1708
14	-36.543	-7.3854	-9.8647	5.677	0.80642	-3.159
15	-36.048	-4.2498	-9.3254	5.4503	0.32468	-2.1632
16	-31.481	-2.329	-4.0837	4.921	-0.7382	-1.0789
17	-16.283	-13.651	-6.6188	6.4074	12.322	-1.5942
18	-27.94	-14.691	-9.7612	13.43	4.0563	-6.0419
19	-25.405	-9.6966	-8.6319	12.526	4.5132	-5.4596
20	-20.105	-5.6877	-3.9946	9.2592	1.1703	-2.3121
21	-11.008	-20.222	-9.1041	6.8579	11.885	-0.9513
22	-18.486	-26.253	-10.364	15.644	7.33	-6.208
23	-16.217	-16.787	-9.8818	11.105	9.5515	-5.3393
24	-8.841	-6.3508	-4.214	6.2286	2.6581	-2.0703
25	-4.1497	-22.512	-9.7522	6.8795	11.136	-0.0158
26	-8.8307	-31.464	-9.16	12.078	9.2103	-2.7014
27	-7.3064	-13.823	-8.488	6.4716	9.9796	-2.6244
28	-2.8485	-4.7626	-4.0789	2.0797	2.9434	-0.9548

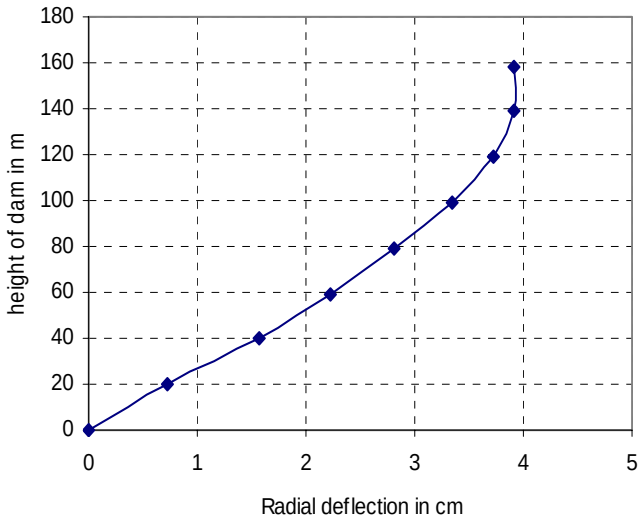

Fig A.8: ***Radial deflection Vs Height of dam - Load case 4***

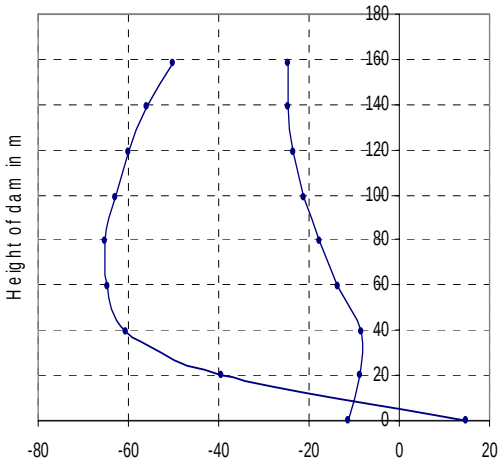

Fig A.9: ***Hoop stress Vs Height of dam - Load case 4***

Downstream		
102	-11.3623	0
104	-8.61493	19.812
107	-8.48179	39.624
109	-13.6967	59.436
112	-17.7	79.248
114	-21.0952	99.06
117	-23.5998	118.872
119	-24.6	138.684
122	-24.7199	158.496
Upstream		
100	14.88138	0
103	-39.339	19.812
105	-60.5021	39.624
108	-64.7	59.436
110	-65.338	79.248
113	-62.942	99.06
115	-60.1064	118.872
118	-56	138.684
120	-50.067	158.496

A.1.5 Dead Load, Normal Water, Maximum Silt, Earthquake C=0.1g and Hydrodynamic Effect

Global displacement obtained for the crown portion is shown in Table A.11 and elemental stresses in Table A.12. Radial deflection and hoop stress at crown cantilever section are plotted in Fig A.10 and Fig A.11 respectively.

Table A.11: **Global Displacement at crown cantilever** - Load case 5

Node	Displ X cm	Displ Y cm	Displ Z cm
100	0	0	0
101	0	0	0
102	0	0	0
103	-0.01825	0.931431	0.458736
104	0.069716	0.8554	-0.26314
105	-0.04296	1.835703	0.564309
106	0.025394	1.831862	0.196242
107	0.079166	1.847967	-0.17641
108	-0.01696	2.596957	0.538291
109	0.045604	2.627579	-0.09556

110	0.019427	3.266411	0.448866
111	0.014982	3.305264	0.182955
112	0.018531	3.326114	-0.07795
113	0.015223	3.863218	0.301516
114	0.042736	3.91659	-0.06633
115	0.018206	4.267497	0.152548
116	0.043761	4.296745	0.051851
117	0.076933	4.314639	-0.03548
118	0.009652	4.436585	0.061192
119	0.126474	4.473689	0.023491
120	0.009284	4.422069	0.069218
121	0.080149	4.431392	0.08442
122	0.148058	4.435303	0.101626
123	0	0	0
124	0	0	0
125	0.244003	1.805161	0.54663
126	0.118903	1.846213	-0.15389
127	0.430071	3.077555	0.468012
128	0.097398	3.21009	-0.06354
129	0.529597	4.02969	0.215493
130	0.248973	4.111181	-0.05944
131	0.507862	4.381235	0.083365
132	0.395462	4.43937	0.036922

Table A.12: **Element stresses as average of Gauss points in kg/cm^2 -** Load case 5

Elements	sig_x	sig_y	sig_z	sig_xy	sig_yz	sig_xz
1	-7.5517	-21.144	-5.0696	-13.822	15.284	1.9232
2	-13.016	-30.165	-10.129	-15.794	12.661	2.852
3	-14.13	-19.538	-8.2666	-12.942	7.5406	3.4685
4	-13.152	-7.3687	-3.2671	-8.3676	2.3438	2.4745
5	-16.41	-18.963	-3.5703	-9.1219	12.259	3.278
6	-27.646	-24.555	-11.842	-16.642	7.6473	6.2312
7	-29.507	-14.133	-9.6295	-15.468	4.9721	4.995
8	-25.38	-6.1857	-3.9977	-10.831	0.5918	2.1633
9	-21.853	-11.728	-1.2147	-4.6583	12.317	1.137
10	-40.924	-9.7415	-9.508	-8.8064	2.5862	2.9525
11	-43.834	-5.7129	-10.388	-7.6882	0.28106	2.7642
12	-34.352	-2.5161	-4.4216	-5.3129	-1.2585	1.0198
13	-23.904	-11.373	-2.4115	2.433	13.259	-1.3407

14	-42.847	-8.6319	-9.7752	6.6541	1.0078	-3.6515
15	-41.886	-4.9639	-9.7078	6.3128	0.28673	-2.2935
16	-35.021	-2.6205	-4.1814	5.5109	-0.8958	-0.9566
17	-18.555	-15.638	-5.3148	7.4028	14.091	-1.7092
18	-32.728	-17.197	-9.5577	15.741	4.6218	-6.735
19	-29.546	-11.273	-8.5192	14.566	4.8695	-5.7188
20	-22.987	-6.5056	-3.9453	10.615	1.119	-2.2921
21	-12.52	-23.311	-8.5519	7.9267	13.381	-0.8447
22	-21.621	-30.884	-10.283	18.388	8.0934	-6.6527
23	-18.907	-19.606	-9.4144	13.017	10.534	-5.668
24	-10.395	-7.3654	-4.0919	7.3438	2.8791	-2.3288
25	-4.5296	-25.794	-9.7671	7.9535	12.319	0.36862
26	-10.259	-37.128	-8.8208	14.305	9.9031	-2.3471
27	-8.4482	-16.152	-7.8485	7.6662	11.213	-2.9236
28	-3.3465	-5.6173	-4.0599	2.5588	3.2695	-1.1624

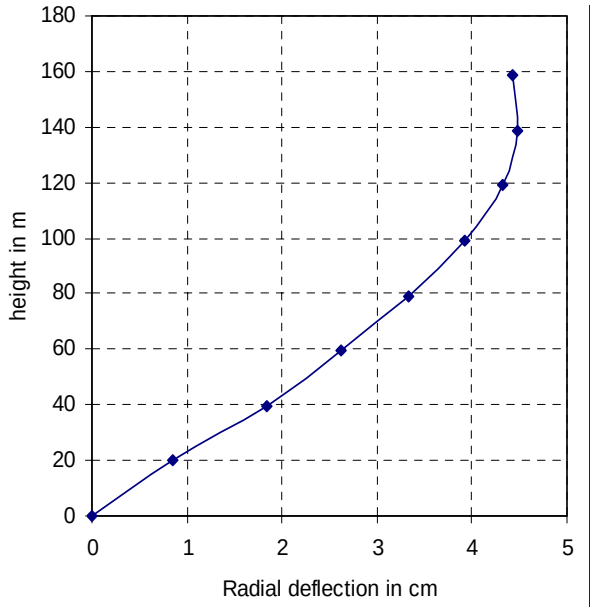

Fig A.10: ***Radial deflection Vs Height of dam - Load case 5***

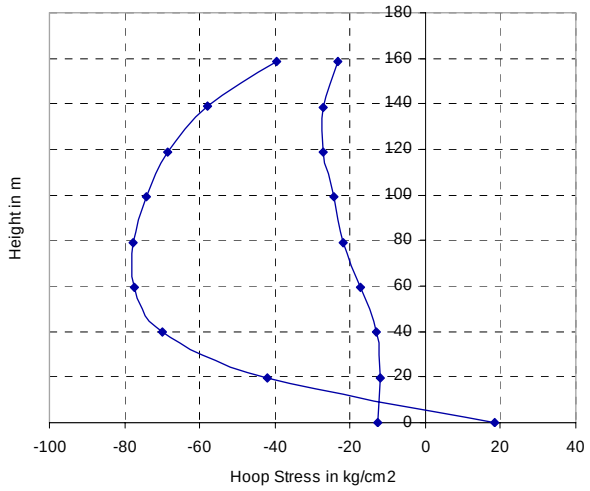

Fig A.11: ***Hoop stress Vs Height of dam - Load case 5***

Downstream		
102	-12.6959	0
104	-12.0426	19.812
107	-13.2	39.624
109	-17.1	59.436
112	-21.7602	79.248
114	-24.4	99.06
117	-27.2	118.872
119	-27.3	138.684
122	-23.3	158.496
Upstream		
100	18.41196	0
103	-41.8525	19.812
105	-69.9	39.624
108	-77.2	59.436
110	-77.8	79.248
113	-74.1	99.06
115	-68.5014	118.872
118	-57.8	138.684
120	-39.4325	158.496

A comparison of global displacements at crown cantilever section due to hydrostatic, seismic and hydrodynamic effects is tabulated in Table A.13. It is found that radial deflection due to combined hydrodynamic and seismic effects exceeds 30% approximately than the hydrostatic effect.

Table A.13: **Comparison of Global displacements due to Seismic and Hydrodynamic effect**

	Dead load, Normal water and Maximum silt			Dead load, Normal water, Maximum silt and Earthquake C=0.1g			Dead load, Normal water, Maximum silt, Earthquake C=0.1g and Hydrodynamic effect		
Node	**Displ X cm**	**Displ Y cm**	**Displ Z cm**	**Displ X cm**	**Displ Y cm**	**Displ Z cm**	**Displ X cm**	**Displ Y cm**	**Displ Z cm**
100	0	0	0	0	0	0	0	0	0
101	0	0	0	0	0	0	0	0	0
102	0	0	0	0	0	0	0	0	0
103	-0. 0156	0.77445	0. 344147	-0.0163	0.7943	0.36492	-0.01824	0.93143	0.4587
104	0.0574	0.71382	-0. 24176	0.05865	0.7326	-0.2419	0.069715	0.85539	-0.263
105	-0.0360	1.50606	0. 396215	-0.0374	1.5542	0.43273	-0.04295	1.83570	0.5643
106	0.0206	1.50329	0. 105276	0.02084	1.5520	0.12626	0.025394	1.83186	0.1962
107	0.06499	1.51794	-0. 18924	0.06654	1.5673	-0.1837	0.079166	1.84796	-0.176
108	-0.0136	2.10003	0. 349428	-0.0146	2.1885	0.39867	-0.01695	2.59695	0.5382
109	0.03868	2.12764	-0. 14466	0.03923	2.2170	-0.1341	0.045604	2.62757	-0.095
110	0.01768	2.61847	0. 259325	0.01747	2.7578	0.31717	0.019426	3.26641	0.4488
111	0.01438	2.65073	0. 051159	0.01431	2.7916	0.08654	0.014982	3.30526	0.1829
112	0.01767	2.66902	-0. 15250	0.01808	2.8108	-0.1401	0.018530	3.32611	-0.077
113	0.01526	3.08406	0. 126345	0.01464	3.2902	0.18768	0.015223	3.86321	0.3015
114	0.03694	3.12901	-0. 16152	0.04026	3.3373	-0.1512	0.042736	3.91658	-0.066
115	0.01746	3.39368	-0.07098	0.01817	3.6800	0.05017	0.018205	4.26749	0.1525
116	0.03751	3.41781	-0.08249	0.04093	3.7060	-0.0517	0.043761	4.29674	0.0518
117	0.06380	3.43241	-0.14562	0.07034	3.7222	-0.1422	0.076933	4.31463	-0.035
118	0.08615	3.48562	-0.09086	0.01028	3.8723	-0.0441	0.096525	4.43658	0.0611
119	0.10302	**3.51603**	-0.09266	**0.11409**	**3.9060**	-0.0987	0.126473	**4.47368**	0.0234
120	0.06996	3.39802	-0.07724	0.08875	3.8988	-0.0465	0.092835	4.42206	0.0692
121	0.06457	3.40573	-0.04915	0.07190	3.9078	-0.0399	0.080149	4.43139	0.0844
122	0.11981	3.40888	-0.01889	0.13230	3.9120	-0.0313	0.148057	4.43530	0.1016

A.2 GEOMETRY AND DISCRETISATION-2 SELECTED

The dam geometry generated as shown above; with 80 nodal points, is tried for a finer discretisation, *(112 elements)* with number of divisions 8 in height and 14 in length. The generated mesh is plotted in Fig A.12.

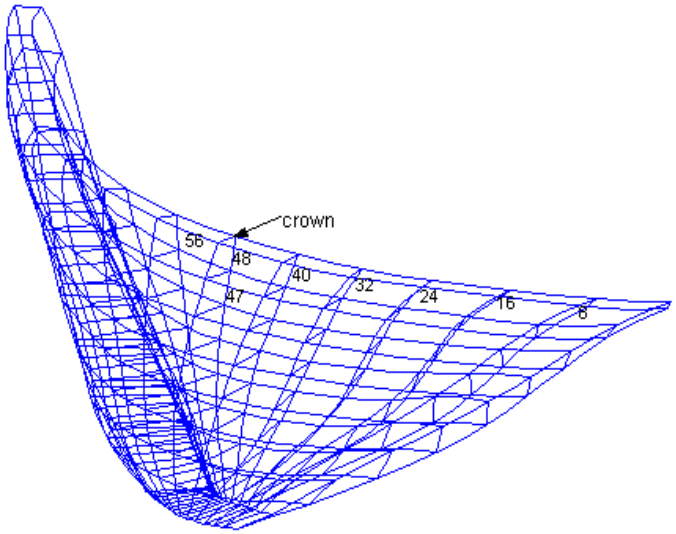

Fig A.12: ***Descretisation with 112 elements***

The dam is analyzed for the following load cases:

1. *Dead load, Normal water, Maximum silt*
2. *Dead load, Normal water, Maximum silt and Earthquake C=0.1g*
3. *Dead load, Normal water, Maximum silt, Earthquake C=0.1g and Hydrodynamic effect.*

The deflected profile in the Load cases 2 & 3are shown in Fig A.13

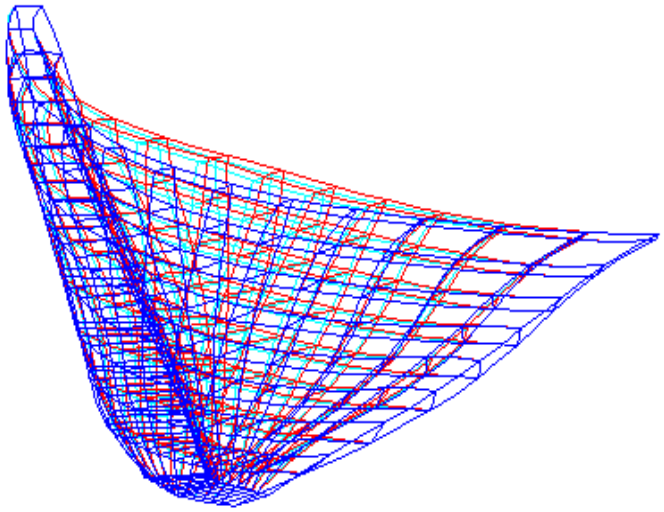

Fig A.13: ***Deflected profile in Load cases 2 & 3***

A.2.1 Dead Load, Normal Water, Maximum Silt

Global displacement obtained for the crown portion is shown in Table A.14 and elemental stresses in Table A.15. Element stresses are plotted in Fig A.14.

Table A.14: **Global Displacement at crown cantilever -** Load case 1

Node	Displ X	Displ Y	Displ Z	Coord X	Coord Y	Coord Z
367	0	0	0	0	-14.6304	0
368	0	0	0	0	-5.4864	0
369	0	0	0	0	3.6576	0
370	-0.00894	0.004349	0.26313	0	-15.7579	9.906
371	0.041289	0.003481	-0.21537	0	2.87119	9.906
372	-0.02285	0.008488	0.384963	0	-16.6687	19.812
373	0.02703	0.008018	0.059633	0	-7.31044	19.812
374	0.065796	0.008018	-0.25118	0	2.04787	19.812
375	-0.02907	0.01223	0.417249	0	-17.32	29.718
376	0.073016	0.012007	-0.22265	0	1.27099	29.718
377	-0.02771	0.015578	0.409088	0	-17.6784	39.624
378	0.024449	0.015589	0.120788	0	-8.5344	39.624
379	0.067593	0.015602	-0.17952	0	0.6096	39.624
380	-0.01972	0.018618	0.387305	0	-17.7201	49.53
381	0.055701	0.01884	-0.14112	0	0.118467	49.53
382	-0.00791	0.021388	0.356245	0	-17.4307	59.436
383	0.016776	0.021571	0.119078	0	-8.79634	59.436
384	0.041513	0.021742	-0.12142	0	-0.16192	59.436

385	0.003691	0.434886	0.31992	0	-16.8057	69.342
386	0.029188	0.348087	-0.12163	0	-0.20538	69.342
387	0.013409	0.848826	0.27616	0	-15.8496	79.248
388	0.015477	0.80179	0.070147	0	-7.9248	79.248
389	0.023065	0.801835	-0.13444	0	0	79.248
390	0.019568	1.223042	0.221955	0	-14.5768	89.154
391	0.023807	1.200739	-0.15003	0	0.451842	89.154
392	0.021879	1.557791	0.157508	0	-13.0112	99.06
393	0.023162	1.55889	-0.00523	0	-5.93884	99.06
394	0.031907	1.560199	-0.16139	0	1.13348	99.06
395	0.020446	1.861759	0.083747	0	-11.1859	108.966
396	0.045767	1.884045	-0.15894	0	2.01394	108.966
397	0.016168	2.138813	0.013205	0	-9.144	118.872
398	0.036407	2.157071	-0.0713	0	-3.048	118.872
399	0.062997	2.174228	-0.14291	0	3.048	118.872
400	0.009616	2.398735	-0.04629	0	-6.93777	128.778
401	0.081388	2.44184	-0.11465	0	4.17612	128.778
402	0.004018	2.650182	-0.08006	0	-4.62915	138.684
403	0.04877	2.678044	-0.08317	0	0.347662	138.684
404	0.095795	2.698993	-0.07919	0	5.32447	138.684
405	-0.00136	2.898496	-0.07923	0	-2.28957	148.59
406	0.107019	2.946547	-0.05223	0	6.40497	148.59
407	**0.003661**	**3.129821**	**-0.05582**	**0**	**0**	**158.496**
408	**0.056539**	**3.158114**	**-0.04279**	**0**	**3.6576**	**158.496**
409	**0.107034**	**3.177006**	**-0.03029**	**0**	**7.3152**	**158.496**
410	0	0	0	-1.1995	-14.452	0
411	0	0	0	-0.8465	3.692	0
412	0.038648	0.858526	0.385474	-3.7025	-16.2914	19.812
413	0.072995	0.811121	-0.2458	-2.4313	2.02874	19.812
414	0.098806	1.56727	0.403787	-5.2630	-17.3473	39.624
415	0.086339	1.57121	-0.16881	-3.3023	0.529354	39.624
416	0.157644	2.123975	0.352696	-6.3891	-17.2352	59.436
417	0.065851	2.170157	-0.10949	-4.1617	-0.21547	59.436
418	0.200904	2.610431	0.282286	-7.4489	-15.7601	79.248
419	0.056868	2.675825	-0.12737	-5.421	0.094387	79.248
420	0.228662	3.080916	0.173891	-8.6705	-12.9168	99.06
421	0.085171	3.141323	-0.16342	-7.2014	1.46852	99.06
422	0.238776	3.44606	0.032734	-10.142	-8.88962	118.872
423	0.13926	3.490272	-0.15621	-9.3338	3.62594	118.872
424	0.228605	3.600014	-0.06905	-11.813	-4.05236	138.684
425	0.18486	3.628009	-0.10232	-11.358	5.99513	138.684
426	**0.213374**	**3.600735**	**-0.05981**	**-13.490**	**1.03155**	**158.496**
427	**0.197906**	**3.618538**	**-0.05935**	**-12.524**	**7.714**	**158.496**
428	0	0	0	-2.3845	-14.192	0
429	0	0	0	-1.9931	-5.18785	0
430	0	0	0	-1.6016	3.81625	0
431	0.042768	0.438837	0.264184	-5.1944	-14.9685	9.906
432	0.040863	0.350109	-0.21234	-3.5535	3.12951	9.906
433	0.098069	0.854034	0.381522	-7.2985	-15.6988	19.812
434	0.088893	0.810071	0.06105	-6.0628	-6.69336	19.812
435	0.079863	0.810481	-0.24108	-4.8272	2.31204	19.812
436	0.158735	1.220322	0.406712	-8.8942	-16.2927	29.718

437	0.099642	1.208839	-0.20803	-5.6948	1.50201	29.718
438	0.21395	1.533259	0.39327	-10.153	-16.6747	39.624
439	0.152723	1.548203	0.123301	-8.2696	-7.93105	39.624
440	0.103283	1.560288	-0.16161	-6.3853	0.812602	39.624
441	0.260358	1.80668	0.371523	-11.224	-16.7836	49.53
442	0.096641	1.869043	-0.12138	-7.0844	0.331989	49.53
443	0.299622	2.04912	0.345417	-12.228	-16.5728	59.436
444	0.182728	2.094867	0.124137	-10.081	-8.22472	59.436
445	0.08774	2.138628	-0.10272	-7.9349	0.123358	59.436
446	0.331116	2.273912	0.318817	-13.261	-16.01	69.342
447	0.081148	2.381417	-0.10671	-9.0366	0.224893	69.342
448	0.359368	2.494671	0.287399	-14.395	-15.0775	79.248
449	0.212462	2.555971	0.08095	-12.420	-7.21385	79.248
450	0.084889	2.61144	-0.12505	-10.445	0.649784	79.248
451	0.385024	2.716638	0.246792	-15.676	-13.7719	89.154
452	0.099811	2.830229	-0.1479	-12.176	1.38622	89.154
453	0.408751	2.93038	0.194548	-17.124	-12.1045	99.06
454	0.26177	2.986398	0.010184	-15.661	-4.85355	99.06
455	0.126214	3.034416	-0.16707	-14.198	2.3974	99.06
456	0.428438	3.120243	0.130176	-18.736	-10.1008	108.966
457	0.160205	3.208674	-0.17269	-16.439	3.62151	108.966
458	0.441802	3.273214	0.063625	-20.481	-7.80097	118.872
459	0.317902	3.314167	-0.0563	-19.632	-1.41461	118.872
460	0.196174	3.344444	-0.16482	-18.783	4.97175	118.872
461	0.446411	3.375262	0.001788	-22.30	-5.25949	128.778
462	0.229588	3.430665	-0.14359	-21.072	6.33633	128.778
463	0.439327	3.425143	-0.04134	-24.126	-2.54538	138.684
464	0.347826	3.45113	-0.08097	-23.615	2.51654	138.684
465	0.254007	3.469625	-0.11436	-23.103	7.57846	138.684
466	0.422968	3.435005	-0.05552	-25.841	0.257913	148.59
467	0.272481	3.478777	-0.08909	-24.63	8.53633	148.59
468	**0.405454**	**3.435284**	**-0.04659**	**-27.318**	**3.05246**	**158.496**
469	**0.344141**	**3.462562**	**-0.05695**	**-26.344**	**6.03781**	**158.496**
470	**0.284917**	**3.48689**	**-0.06666**	**-25.369**	**9.02315**	**158.496**

Table A.15: **Element stresses as average of Gauss points in kg/cm^2 -** Load case 1

Element	Sig x	Sig y	Sig z	Sig xy	Sig yz	Sig xz
1	-4.6811	-14.243	-5.3616	-11.048	13.205	1.8499
2	-8.4314	-26.545	-9.9842	-15.308	15.774	2.495
3	-8.3843	-26.28	-10.151	-13.384	13.32	1.9672
4	-8.312	-22.781	-9.7636	-11.485	10.455	2.2888
5	-9.063	-18.71	-9.1246	-10.211	8.3918	3.0354
6	-9.6898	-13.707	-7.453	-8.7991	6.2396	3.4093
7	-9.1431	-7.9955	-5.0509	-6.5516	3.8922	3.2312
8	-6.7618	-3.1525	-2.1758	-3.6507	1.1807	2.2247
9	-9.8851	-14.786	-4.3803	-7.1109	11.808	2.8505
10	-16.352	-28.618	-10.878	-13.832	11.019	5.3759
11	-15.616	-29.004	-11.754	-13.248	10.01	4.3761
12	-14.167	-23.486	-10.636	-12.008	8.2772	3.8214
13	-13.976	-17.803	-9.4862	-11.207	7.046	3.9003
14	-14.248	-12.451	-7.7884	-10.003	5.3062	4.1317
15	-13.427	-7.5164	-5.1689	-7.9251	3.0802	3.5347

16	-11.813	-4.0539	-1.9428	-6.2947	0.90319	1.6849
17	-10.476	-12.899	-3.966	-4.552	12.048	2.2292
18	-19.282	-25.59	-9.8062	-12.395	7.89	5.6332
19	-21.303	-27.462	-12.777	-14.233	7.9276	5.8253
20	-21.275	-22.757	-12.221	-14.113	7.1282	5.5095
21	-21.309	-16.679	-10.481	-13.415	6.3	5.0075
22	-20.727	-10.885	-8.2802	-11.671	4.601	4.4084
23	-18.649	-6.1703	-5.5526	-9.0473	2.1155	3.182
24	-16.376	-3.9781	-2.1945	-7.5095	0.21862	1.3114
25	-11.227	-11.373	-3.5882	-3.125	13.269	1.586
26	-22.274	-19.507	-7.9049	-10.967	6.0179	4.8472
27	-26.106	-19.267	-11.235	-13.946	5.4982	5.8491
28	-27.47	-15.294	-11.741	-14.313	4.8714	5.8987
29	-28.484	-11.288	-10.555	-13.546	4.0913	5.282
30	-28.076	-7.9028	-8.4567	-11.695	2.4967	4.2593
31	-24.905	-5.055	-5.6724	-9.0575	0.52971	2.8086
32	-20.312	-2.968	-2.1878	-6.96	-0.4298	1.2335
33	-12.281	-10.381	-2.837	-2.0612	14.62	1.0712
34	-26.239	-13.995	-6.4616	-8.2014	4.8146	3.0867
35	-31.768	-11.804	-9.7275	-10.497	2.9572	4.0747
36	-33.666	-8.6499	-11.173	-10.421	2.0541	4.3
37	-34.75	-6.3741	-10.798	-9.6958	1.3957	3.9335
38	-34.371	-4.8461	-8.9046	-8.6082	0.21592	3.1022
39	-30.564	-3.3853	-5.9291	-7.0055	-0.9177	1.9347
40	-23.718	-1.7053	-2.2315	-5.1165	-0.889	0.75749
41	-13.266	-9.8881	-2.2283	-1.0279	15.526	0.49081
42	-29.668	-10.85	-6.2728	-3.7482	4.0496	0.61697
43	-36.499	-7.96	-9.5681	-4.2723	1.0459	1.0359
44	-37.916	-5.2948	-11.218	-3.8437	0.01876	1.2932
45	-38.023	-3.6896	-11.086	-3.5071	-0.2826	1.4338
46	-37.16	-2.816	-9.2838	-3.2071	-0.9546	1.2533
47	-33.328	-2.0098	-6.2049	-2.7439	-1.597	0.72983
48	-26.16	-0.8134	-2.3206	-2.0555	-1.1432	0.19625
49	-13.768	-10.095	-2.5759	0.15906	16.025	-0.2658
50	-30.755	-10.524	-7.2352	1.4398	3.9885	-1.9462
51	-37.743	-7.6471	-10.161	2.6684	0.50566	-2.0812
52	-38.238	-5.0873	-11.344	3.078	-0.3691	-1.8493
53	-37.201	-3.4773	-10.952	2.9006	-0.3511	-1.2789
54	-35.697	-2.59	-9.0351	2.6608	-0.7869	-0.7689
55	-32.35	-1.8725	-5.9624	2.3809	-1.359	-0.5228
56	-27.146	-0.861	-2.236	2.0241	-1.126	-0.3634
57	-13.491	-11.122	-4.0542	1.3969	16.396	-0.7461
58	-29.003	-12.669	-8.6142	5.8928	4.8231	-3.7521
59	-35.231	-9.965	-10.553	8.2611	1.2787	-4.2914
60	-35.058	-7.1918	-11.061	8.5359	0.62978	-4.2
61	-33.245	-5.2369	-10.355	7.9832	0.88649	-3.5061
62	-31.28	-4.0766	-8.4039	7.3592	0.42682	-2.6139
63	-28.476	-3.204	-5.5909	6.6689	-0.4582	-1.8125
64	-25.207	-2.1214	-2.1783	5.9432	-0.7514	-0.9712
65	-12.52	-12.62	-5.7773	2.4009	16.584	-0.6063
66	-25.281	-15.991	-9.7865	8.7139	6.0858	-4.438
67	-30.54	-13.551	-10.533	11.912	2.6752	-5.4331
68	-30.434	-10.701	-10.511	12.299	2.4168	-5.7124
69	-28.319	-8.4005	-9.7763	11.453	3.0106	-5.2007
70	-25.792	-6.6975	-8.1156	10.255	2.3934	-4.165
71	-22.719	-5.2102	-5.607	8.9827	0.85556	-2.8487
72	-19.781	-3.7807	-2.1889	7.8461	-0.3063	-1.1762
73	-11.066	-14.251	-7.0741	3.0783	16.396	-0.1299

74	-20.887	-19.542	-10.842	9.9989	7.0531	-4.3811
75	-25.274	-18.01	-10.577	14.238	4.1446	-5.8566
76	-25.919	-15.628	-10.281	15.079	4.9167	-6.6464
77	-23.871	-12.689	-9.9039	13.63	6.1169	-6.3831
78	-20.535	-9.5593	-8.5422	11.186	4.9541	-5.0384
79	-16.503	-6.7065	-5.7946	8.8377	2.2564	-3.1181
80	-13.361	-4.6379	-2.1674	7.3522	0.15725	-1.1196
81	-9.4113	-16.141	-8.1561	3.485	15.947	0.31411
82	-16.872	-23.531	-12.135	10.092	7.3373	-4.1265
83	-20.337	-24.134	-11.021	15.448	5.2083	-5.8213
84	-21.758	-22.506	-10.799	16.638	7.8717	-6.9299
85	-19.982	-17.563	-10.945	13.857	9.6814	-6.6141
86	-15.872	-11.851	-9.2704	10.015	7.1988	-4.8754
87	-11.105	-7.1196	-5.9141	7.0268	3.2483	-2.7661
88	-8.2444	-4.5343	-2.1996	5.6218	0.61209	-1.0888
89	-7.748	-18.335	-9.4151	3.8212	15.595	0.66928
90	-13.533	-28.039	-13.373	9.3149	7.2345	-3.7899
91	-15.78	-31.231	-11.385	14.69	5.7061	-5.2808
92	-17.398	-29.001	-11.237	14.952	9.8185	-5.9667
93	-15.78	-20.724	-11.282	11.022	11.142	-5.4138
94	-11.181	-12.672	-9.2529	7.1894	7.789	-3.7612
95	-6.8168	-6.7542	-6.0265	4.6381	3.6473	-2.0979
96	-4.7142	-3.7366	-2.2709	3.6905	0.9043	-0.9641
97	-5.494	-19.75	-10.253	4.5617	15.605	1.2295
98	-9.5713	-30.944	-13.01	8.5701	7.6933	-2.8774
99	-10.387	-33.84	-10.218	12.57	6.4482	-3.8226
100	-11.938	-27.279	-9.6269	11.852	9.9159	-3.8163
101	-10.41	-17.54	-9.4064	7.9828	10.09	-3.6072
102	-6.7063	-10.865	-8.2959	4.4129	7.0937	-2.2693
103	-3.8868	-5.7484	-5.9581	2.5542	3.6163	-1.2368
104	-2.3833	-2.5539	-2.2885	2.0031	0.97333	-0.7116
105	-1.3818	-18.471	-8.8077	5.435	15.091	2.5835
106	-2.8775	-30.988	-10.287	8.7101	8.609	-1.005
107	-4.3027	-36.031	-9.214	11.919	8.2615	-1.3217
108	-8.2114	-26.379	-8.3439	11.274	11.638	-1.6255
109	-6.9045	-14.917	-8.5523	6.6644	11.009	-2.3879
110	-3.9589	-9.091	-8.208	2.739	7.4212	-0.9845
111	-2.3047	-4.8733	-5.8725	1.0402	3.6445	-0.3822
112	-0.9635	-1.224	-1.8136	0.56855	1.1777	-0.4739

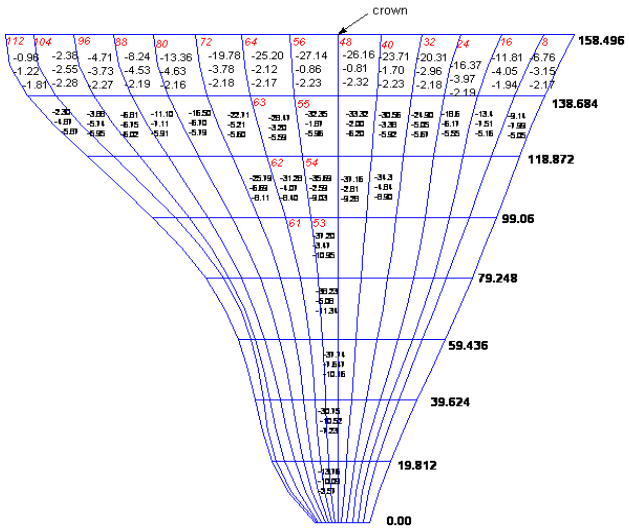

Fig A.14: ***Element stresses*** **-** *Load case 1*

A.2.2 Dead Load, Normal Water, Maximum Silt and Earthquake C=0.1g

Global displacement obtained for the crown portion is shown in Table A.16 and elemental stresses in Table A.17. Element stresses are plotted in Fig A.15.

Table A.16: **Global displacement at crown cantilever -** Load case 2

Node	Displ X	Displ Y	Displ Z	Coord X	Coord Y	Coord Z
367	0	0	0	0	-14.6304	0
368	0	0	0	0	-5.4864	0
369	0	0	0	0	3.6576	0
370	-0.00904	0.4396	0.269425	0	-15.7579	9.906
371	0.041814	0.351231	-0.21627	0	2.87119	9.906
372	-0.02309	0.859272	0.396348	0	-16.6687	19.812
373	0.027427	0.8113	0.065099	0	-7.31044	19.812
374	0.066738	0.811033	-0.25118	0	2.04787	19.812
375	-0.02939	1.240344	0.432875	0	-17.32	29.718
376	0.074155	1.21699	-0.22124	0	1.27099	29.718
377	-0.02802	1.583259	0.428672	0	-17.6784	39.624
378	0.02493	1.583867	0.132078	0	-8.5344	39.624
379	0.068761	1.584891	-0.17663	0	0.6096	39.624
380	-0.0199	1.897017	0.410823	0	-17.7201	49.53
381	0.056881	1.918816	-0.137	0	0.118467	49.53
382	-0.00784	2.185943	0.383521	0	-17.4307	59.436
383	0.017472	2.203943	0.135252	0	-8.79634	59.436
384	0.042839	2.221105	-0.1166	0	-0.16192	59.436

385	0.00413	2.460197	0.350669	0	-16.8057	69.342
386	0.030959	2.503306	-0.11686	0	-0.20538	69.342
387	0.014336	2.728935	0.309755	0	-15.8496	79.248
388	0.017191	2.756815	0.089207	0	-7.9248	79.248
389	0.025705	2.778027	-0.13047	0	0	79.248
390	0.021147	2.997854	0.257594	0	-14.5768	89.154
391	0.027817	3.046485	-0.14767	0	0.451842	89.154
392	0.024239	3.253388	0.193998	0	-13.0112	99.06
393	0.027131	3.282025	0.01273	0	-5.93884	99.06
394	0.037766	3.301486	-0.16144	0	1.13348	99.06
395	0.023749	3.480221	0.119771	0	-11.1859	108.966
396	0.053885	3.525018	-0.16208	0	2.01394	108.966
397	0.020447	3.660323	0.047216	0	-9.144	118.872
398	0.043638	3.685911	-0.05733	0	-3.048	118.872
399	0.073551	3.70092	-0.14967	0	3.048	118.872
400	0.014855	3.780731	-0.01585	0	-6.93777	128.778
401	0.094396	3.816199	-0.12509	0	4.17612	128.778
402	0.010014	3.838956	-0.05455	0	-4.62915	138.684
403	0.059126	3.85671	-0.07717	0	0.347662	138.684
404	0.11078	3.867647	-0.09303	0	5.32447	138.684
405	0.006256	3.853329	-0.05979	0	-2.28957	148.59
406	0.12344	3.878128	-0.06833	0	6.40497	148.59
407	**0.010644**	**3.859584**	**-0.04233**	**0**	**0**	**158.496**
408	**0.068495**	**3.869756**	**-0.04444**	**0**	**3.6576**	**158.496**
409	**0.123737**	**3.877286**	**-0.04722**	**0**	**7.3152**	**158.496**
410	0	0	0	-1.1995	-14.452	0
411	0	0	0	-0.8465	3.692	0
412	0.039258	0.869066	0.396882	-3.7025	-16.2914	19.812
413	0.073935	0.82045	-0.24573	-2.4313	2.02874	19.812
414	0.100573	1.592785	0.423382	-5.2630	-17.3473	39.624
415	0.087605	1.596024	-0.16563	-3.3023	0.529354	39.624
416	0.161089	2.170827	0.380273	-6.3891	-17.2352	59.436
417	0.067356	2.216965	-0.10427	-4.1617	-0.21547	59.436
418	0.206729	2.688844	0.316806	-7.4489	-15.7601	79.248
419	0.060101	2.754751	-0.12317	-5.421	0.094387	79.248
420	0.238089	3.204971	0.211899	-8.6705	-12.9168	99.06
421	0.09318	3.266357	-0.16397	-7.2014	1.46852	99.06
422	0.253677	3.632292	0.06823	-10.142	-8.88962	118.872
423	0.155728	3.67798	-0.16468	-9.3338	3.62594	118.872
424	0.251175	3.864743	-0.04324	-11.813	-4.05236	138.684
425	0.212389	3.894673	-0.11886	-11.358	5.99513	138.684
426	**0.246414**	**3.954718**	**-0.0483**	**-13.490**	**1.03155**	**158.496**
427	**0.236032**	**3.973991**	**-0.07835**	**-12.524**	**7.714**	**158.496**
428	0	0	0	-2.3845	-14.192	0
429	0	0	0	-1.9931	-5.18785	0
430	0	0	0	-1.6016	3.81625	0
431	0.043349	0.443571	0.270517	-5.1944	-14.9685	9.906
432	0.041298	0.353314	-0.21326	-3.5535	3.12951	9.906
433	0.099501	0.864477	0.392845	-7.2985	-15.6988	19.812
434	0.090059	0.819679	0.066482	-6.0628	-6.69336	19.812
435	0.080802	0.819819	-0.24099	-4.8272	2.31204	19.812
436	0.161216	1.237438	0.422128	-8.8942	-16.2927	29.718
437	0.100885	1.225173	-0.2064	-5.6948	1.50201	29.718
438	0.217594	1.558101	0.412573	-10.153	-16.6747	39.624
439	0.155084	1.572853	0.134612	-8.2696	-7.93105	39.624
440	0.104641	1.58488	-0.15833	-6.3853	0.812602	39.624
441	0.265263	1.840715	0.394859	-11.224	-16.7836	49.53
442	0.098059	1.903435	-0.11678	-7.0844	0.331989	49.53

443	0.305971	2.094362	0.372817	-12.228	-16.5728	59.436
444	0.186449	2.140448	0.140592	-10.081	-8.22472	59.436
445	0.089393	2.184778	-0.0974	-7.9349	0.123358	59.436
446	0.339123	2.332869	0.3502	-13.261	-16.01	69.342
447	0.08343	2.441794	-0.10158	-9.0366	0.224893	69.342
448	0.369433	2.570541	0.322296	-14.395	-15.0775	79.248
449	0.219007	2.632603	0.100657	-12.420	-7.21385	79.248
450	0.088549	2.689091	-0.12103	-10.445	0.649784	79.248
451	0.397647	2.81302	0.284488	-15.676	-13.7719	89.154
452	0.105823	2.928636	-0.14609	-12.176	1.38622	89.154
453	0.424672	3.05146	0.233778	-17.124	-12.1045	99.06
454	0.274304	3.108419	0.029498	-15.661	-4.85355	99.06
455	0.135905	3.157619	-0.16848	-14.198	2.3974	99.06
456	0.448557	3.270402	0.169485	-18.736	-10.1008	108.966
457	0.175066	3.360974	-0.17814	-16.439	3.62151	108.966
458	0.467249	3.45718	0.101067	-20.481	-7.80097	118.872
459	0.34128	3.499145	-0.04217	-19.632	-1.41461	118.872
460	0.217843	3.530571	-0.17488	-18.783	4.97175	118.872
461	0.478459	3.59759	0.035421	-22.30	-5.25949	128.778
462	0.259713	3.655179	-0.15804	-21.072	6.33633	128.778
463	0.479376	3.690179	-0.0135	-24.126	-2.54538	138.684
464	0.387669	3.717296	-0.07583	-23.615	2.51654	138.684
465	0.293819	3.736903	-0.1324	-23.103	7.57846	138.684
466	0.47232	3.746103	-0.03523	-25.841	0.257913	148.59
467	0.322884	3.792029	-0.10865	-24.63	8.53633	148.59
468	**0.466259**	**3.794551**	**-0.03423**	**-27.318**	**3.05246**	**158.496**
469	**0.404852**	**3.822724**	**-0.05996**	**-26.344**	**6.03781**	**158.496**
470	**0.345527**	**3.847945**	**-0.08506**	**-25.369**	**9.02315**	**158.496**

Table A.17: **Element stresses as average of Gauss points** -Load case 2

Element	**Sig x**	**Sig y**	**Sig z**	**Sig xy**	**Sig yz**	**sigxz**
1	-4.6629	-14.292	-5.0445	-11.135	13.248	1.7905
2	-8.53	-26.792	-9.7734	-15.51	15.866	2.4751
3	-8.5662	-26.674	-10.07	-13.657	13.457	1.9802
4	-8.5832	-23.317	-9.8016	-11.836	10.626	2.3328
5	-9.4716	-19.384	-9.2696	-10.67	8.5977	3.1305
6	-10.245	-14.48	-7.6132	-9.3739	6.4604	3.5328
7	-9.7578	-8.7699	-5.0998	-7.1765	4.1098	3.3151
8	-7.3803	-3.7465	-2.1272	-4.1708	1.3392	2.2569
9	-9.9118	-14.882	-3.9966	-7.1885	11.845	2.8434
10	-16.513	-28.919	-10.642	-14.012	11.04	5.4014
11	-15.879	-29.454	-11.657	-13.507	10.073	4.44
12	-14.536	-24.028	-10.633	-12.35	8.3893	3.9186
13	-14.512	-18.418	-9.5858	-11.657	7.2225	4.0518
14	-15.014	-13.104	-7.9622	-10.561	5.5524	4.3468
15	-14.393	-8.1261	-5.3201	-8.5416	3.3624	3.7243
16	-12.844	-4.6002	-2.0131	-6.9428	1.0773	1.7299
17	-10.516	-12.989	-3.5672	-4.6116	12.102	2.239
18	-19.465	-25.882	-9.5499	-12.546	7.8907	5.6715
19	-21.641	-27.904	-12.653	-14.484	7.9689	5.9133
20	-21.786	-23.28	-12.172	-14.466	7.2301	5.6528
21	-22.05	-17.221	-10.487	-13.882	6.4821	5.2152
22	-21.749	-11.383	-8.3519	-12.235	4.8677	4.681
23	-19.942	-6.5761	-5.6662	-9.6634	2.4074	3.4595
24	-17.833	-4.3814	-2.2611	-8.1918	0.39537	1.4401
25	-11.289	-11.448	-3.1625	-3.1728	13.346	1.6004

26	-22.482	-19.727	-7.5863	-11.092	6.0237	4.8762
27	-26.49	-19.563	-11.021	-14.168	5.5368	5.9265
28	-28.065	-15.623	-11.597	-14.633	4.9647	6.0467
29	-29.374	-11.621	-10.453	-13.964	4.2449	5.5113
30	-29.338	-8.2111	-8.4039	-12.192	2.7033	4.5608
31	-26.563	-5.3329	-5.6827	-9.6114	0.74572	3.1314
32	-22.307	-3.2694	-2.2169	-7.6016	-0.3035	1.4357
33	-12.37	-10.441	-2.3724	-2.0998	14.718	1.0849
34	-26.485	-14.14	-6.0719	-8.2919	4.8298	3.0949
35	-32.205	-11.967	-9.4203	-10.655	2.9889	4.1138
36	-34.326	-8.8199	-10.947	-10.638	2.1224	4.4042
37	-35.737	-6.5473	-10.636	-9.9727	1.4954	4.1219
38	-35.809	-5.0174	-8.7971	-8.9443	0.3346	3.3622
39	-32.541	-3.5544	-5.8786	-7.4049	-0.8002	2.2141
40	-26.243	-1.8856	-2.232	-5.6008	-0.8216	0.9297
41	-13.382	-9.9344	-1.7334	-1.0549	15.635	0.4989
42	-29.951	-10.951	-5.8379	-3.7893	4.0649	0.6014
43	-36.983	-8.0578	-9.2016	-4.3329	1.0625	1.0266
44	-38.613	-5.39	-10.934	-3.9233	0.0598	1.3242
45	-39.036	-3.7837	-10.888	-3.6086	-0.2238	1.5315
46	-38.655	-2.9101	-9.1653	-3.3302	-0.891	1.4102
47	-35.48	-2.1044	-6.1561	-2.891	-1.5389	0.89034
48	-29.11	-0.9101	-2.3242	-2.2396	-1.1093	0.27041
49	-13.905	-10.137	-2.0796	0.14902	16.136	-0.2665
50	-31.055	-10.617	-6.7973	1.456	3.9985	-1.9813
51	-38.239	-7.7399	-9.7744	2.7119	0.5106	-2.1299
52	-38.92	-5.177	-11.026	3.1364	-0.3375	-1.8905
53	-38.162	-3.5625	-10.73	2.9698	-0.2971	-1.2904
54	-37.12	-2.6722	-8.9197	2.7577	-0.7248	-0.7531
55	-34.485	-1.9573	-5.9413	2.5334	-1.2982	-0.5199
56	-30.295	-0.9613	-2.2586	2.2533	-1.0874	-0.3978
57	-13.637	-11.172	-3.5895	1.4084	16.504	-0.7515
58	-29.292	-12.786	-8.211	5.9583	4.8313	-3.794
59	-35.698	-10.097	-10.182	8.3889	1.2825	-4.3593
60	-35.681	-7.3299	-10.743	8.7061	0.6713	-4.2929
61	-34.1	-5.3743	-10.139	8.1938	0.96873	-3.616
62	-32.547	-4.2178	-8.3176	7.6431	0.53445	-2.7381
63	-30.42	-3.3693	-5.6108	7.0902	-0.3425	-1.9533
64	-28.146	-2.3463	-2.2227	6.5797	-0.6732	-1.0753
65	-12.656	-12.688	-5.3624	2.4328	16.689	-0.6082
66	-25.539	-16.147	-9.4399	8.8107	6.0964	-4.4735
67	-30.956	-13.742	-10.204	12.098	2.685	-5.5033
68	-30.988	-10.92	-10.226	12.554	2.4791	-5.8373
69	-29.063	-8.6429	-9.6011	11.775	3.1398	-5.3877
70	-26.873	-6.9672	-8.0785	10.681	2.5745	-4.3963
71	-24.334	-5.5283	-5.6573	9.5823	1.0487	-3.0703
72	-22.077	-4.1959	-2.2343	8.697	-0.1951	-1.2832
73	-11.174	-14.341	-6.7136	3.1217	16.493	-.12293
74	-21.106	-19.742	-10.567	10.111	7.0625	-4.4058
75	-25.636	-18.274	-10.308	14.468	4.1604	-5.9225
76	-26.42	-15.962	-10.048	15.411	5.0119	-6.7922
77	-24.533	-13.086	-9.7771	14.051	6.3187	-6.6272
78	-21.434	-10.006	-8.5332	11.704	5.2368	-5.3316
79	-17.715	-7.1913	-5.8344	9.4833	2.5349	-3.3513
80	-14.873	-5.1899	-2.1965	8.1631	0.2914	-1.2064
81	-9.4835	-16.252	-7.8518	3.5305	16.032	0.3297
82	-17.054	-23.782	-11.945	10.208	7.3336	-4.1438
83	-20.653	-24.504	-10.829	15.709	5.2167	-5.8807

84	-22.226	-23.014	-10.628	17.034	8.0043	-7.0831
85	-20.588	-18.163	-10.859	14.34	9.9817	-6.884
86	-16.601	-12.484	-9.2607	10.539	7.6007	-5.177
87	-11.938	-7.7187	-5.9323	7.5817	3.609	-2.9608
88	-9.1432	-5.1121	-2.2245	6.2428	0.7729	-1.1546
89	-7.788	-18.459	-9.1683	3.8658	15.668	0.69188
90	-13.684	-28.339	-13.272	9.4255	7.2092	-3.8009
91	-16.051	-31.726	-11.277	14.954	5.6866	-5.3267
92	-17.819	-29.701	-11.125	15.347	9.9586	-6.0991
93	-16.308	-21.514	-11.215	11.458	11.494	-5.66
94	-11.733	-13.45	-9.2437	7.5981	8.2574	-4.0117
95	-7.3648	-7.4092	-6.0603	5.0184	4.0535	-2.2196
96	-5.2342	-4.2591	-2.3092	4.1018	1.0787	-0.9991
97	-5.5017	-19.864	-10.051	4.6097	15.669	1.2633
98	-9.6794	-31.252	-12.966	8.6774	7.6597	-2.869
99	-10.59	-34.369	-10.16	12.815	6.4074	-3.8297
100	-12.256	-27.96	-9.5086	12.209	10.033	-3.897
101	-10.76	-18.26	-9.295	8.3474	10.414	-3.8034
102	-7.0306	-11.639	-8.2918	4.6929	7.5407	-2.4408
103	-4.2408	-6.4492	-6.0342	2.7602	4.0119	-1.277
104	-2.7015	-3.0655	-2.3394	2.2496	1.1259	-0.7010
105	-1.349	-18.557	-8.6222	5.4834	15.15	2.639
106	-2.9108	-31.264	-10.256	8.8138	8.5907	-0.9524
107	-4.436	-36.581	-9.1633	12.167	8.2268	-1.2371
108	-8.4803	-27.052	-8.1392	11.661	11.805	-1.6353
109	-7.1191	-15.519	-8.3457	7.0362	11.415	-2.5319
110	-4.039	-9.6772	-8.1009	3.0042	7.9278	-1.0524
111	-2.4002	-5.4218	-5.8513	1.1776	4.0338	-0.3254
112	-1.0699	-1.7444	-1.8724	0.69191	1.2455	-0.4223

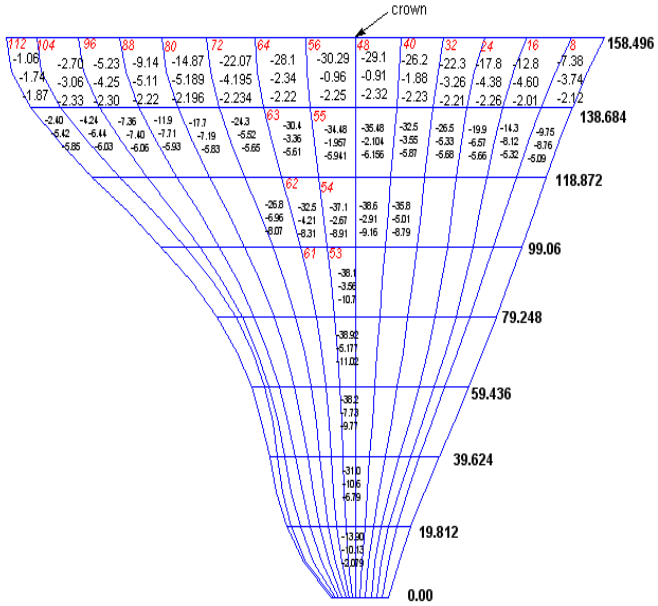

Fig A.15: ***Element stresses*** - *Load case 2*

A.2.3 Dead Load, Normal Water, Maximum Silt, Earthquake C=0.1g and Hydrodynamic Effect

Global displacement obtained for the crown portion is shown in Table A.18. Elemental face centre stresses of upstream and downstream are shown in Table A.19 and A.20. Element stresses are plotted in Fig A.16 and hoop stresses at crown cantilever section in Fig A.17.

Table A.18: **Global Displacement at crown cantilever** - Load case 3

Node	Displ X	Displ Y	Displ Z
367	0	0	0
368	0	0	0
369	0	0	0
370	-0.01058	0.516085	0.337181
371	0.049514	0.409614	-0.24236
372	-0.02685	1.013379	0.505902
373	0.032794	0.956287	0.107386
374	0.079529	0.954617	-0.2728
375	-0.03421	1.472077	0.565878
376	0.088519	1.441956	-0.22734
377	-0.03279	1.888626	0.575552
378	0.02966	1.888937	0.213086
379	0.08163	1.888822	-0.16424
380	-0.02368	2.273972	0.566366
381	0.066432	2.297785	-0.10589
382	-0.01018	2.629272	0.542983
383	0.018926	2.650694	0.23911
384	0.04834	2.669685	-0.06952
385	0.002988	2.965691	0.509698
386	0.03267	3.015091	-0.05603
387	0.013898	3.288875	0.46472
388	0.015926	3.322107	0.202941
389	0.024842	3.345869	-0.05761
390	0.020671	3.604912	0.40555
391	0.025775	3.661142	-0.06339
392	0.02301	3.896186	0.333861
393	0.024907	3.930253	0.129339
394	0.03599	3.952273	-0.0662
395	0.021143	4.148105	0.251661
396	0.05339	4.199726	-0.05609
397	0.016242	4.340507	0.173403
398	0.041695	4.37037	0.062998
399	0.074844	4.387387	-0.03321
400	0.008992	4.463436	0.108088
401	0.097542	4.503818	0.001422
402	0.003153	4.516215	0.07061
403	0.05785	4.536531	0.051217
404	0.115225	4.548801	0.039172

405	-0.00983	4.52385	0.069974
406	0.128961	4.551313	0.067233
407	0.004242	4.525452	0.09163
408	0.068172	4.536529	0.091004
409	0.129185	4.544278	0.089657
410	0	0	0
411	0	0	0
412	0.046862	1.025008	0.506578
413	0.087321	0.965834	-0.26639
414	0.120141	1.899594	0.569193
415	0.103151	1.901796	-0.15081
416	0.191607	2.610498	0.53896
417	0.077106	2.664174	-0.05455
418	0.243576	3.24011	0.472624
419	0.06575	3.317246	-0.04905
420	0.275738	3.837444	0.353851
421	0.100747	3.909212	-0.06967
422	0.286951	4.304872	0.196083
423	0.167401	4.357624	-0.05134
424	0.276234	4.53982	0.081338
425	0.223983	4.573768	0.003934
426	0.261017	4.621701	0.082795
427	0.24188	4.6438	0.053722
428	0	0	0
429	0	0	0
430	0	0	0
431	0.051218	0.52069	0.338638
432	0.048172	0.412328	-0.23925
433	0.118102	1.019351	0.501644
434	0.106411	0.966261	0.108706
435	0.094748	0.965253	-0.26114
436	0.191784	1.468065	0.552605
437	0.118525	1.451602	-0.20983
438	0.259255	1.8576	0.555609
439	0.18376	1.87506	0.215613
440	0.122619	1.888347	-0.14238
441	0.316192	2.205287	0.546385
442	0.114106	2.27862	-0.08176
443	0.364552	2.518005	0.529124
444	0.220408	2.573362	0.244728
445	0.102903	2.625249	-0.04685
446	0.403297	2.811509	0.507804
447	0.094791	2.940316	-0.03847
448	0.43769	3.097503	0.477839
449	0.256805	3.171934	0.21497
450	0.099425	3.238185	-0.04764
451	0.468257	3.382233	0.434905
452	0.117883	3.51886	-0.06344
453	0.496045	3.653356	0.377311
454	0.316235	3.721431	0.145987
455	0.150305	3.779013	-0.07718
456	0.518813	3.895979	0.305229
457	0.192055	4.002264	-0.07836
458	0.534368	4.095281	0.230063
459	0.38402	4.144803	0.075468
460	0.236279	4.181406	-0.06678
461	0.540215	4.23939	0.159825

462	0.277838	4.30633	-0.04277
463	0.533218	4.32755	0.109084
464	0.422568	4.359149	0.045738
465	0.309016	4.381974	-0.01129
466	0.516111	4.37701	0.088874
467	0.333695	4.430409	0.015442
468	0.497588	4.420319	0.091686
469	0.423019	4.453597	0.065784
470	0.350983	4.483313	0.04059

Table A.19: **Upstream Element face centre stresses in kg/cm^2** - Load case 3

Element	sigx	sig y	sig z	sig xy	sig yz	sig xz
1	22.10723	-10.629	44.09748	-11.5612	13.07159	-22.2376
2	7.871942	-24.237	18.46917	-7.08638	6.354392	-13.1064
3	4.189793	-16.093	10.55192	-4.87011	3.631607	-8.87335
4	2.781013	-10.323	6.058822	-3.16569	1.175552	-6.01111
5	0.879673	-6.9168	2.047477	-2.25467	0.943519	-3.47015
6	-2.23904	-6.7593	-1.1182	-2.85882	2.213542	-0.70494
7	-4.53717	-7.8089	-2.33641	-4.71962	3.52573	1.313946
8	-6.84528	-6.8155	-2.17614	-5.48052	2.766105	2.043328
9	-9.70691	-23.009	32.76183	-2.78873	5.860344	-8.57051
10	-24.6748	-40.645	-3.44579	-4.46373	-0.74813	0.233092
11	-20.4479	-27.982	-6.25174	-4.35092	0.569768	1.338487
12	-17.0471	-19.606	-5.31005	-3.9178	0.233648	1.049937
13	-14.6172	-15.024	-4.86751	-4.30276	0.445711	-0.01626
14	-13.0131	-11.295	-5.58999	-4.50986	0.577389	0.19864
15	-11.411	-6.7997	-4.8828	-4.18815	0.689061	0.941819
16	-9.71116	-2.7482	-1.58104	-4.73421	0.297514	-0.16463
17	-16.2435	-20.911	30.55453	-2.49426	9.055346	-4.34559
18	-30.7955	-38.948	-7.94777	-7.25104	-1.1719	1.621944
19	-27.4159	-29.635	-11.0913	-7.85737	0.462658	2.398142
20	-24.1274	-21.725	-8.099	-7.57875	0.902257	1.924004
21	-22.9633	-16.111	-6.7784	-8.78491	2.02035	1.026716
22	-23.7246	-11.918	-9.30559	-10.0945	2.486542	1.608518
23	-23.8972	-7.7140	-10.4819	-9.92988	1.54388	2.622296
24	-22.5152	-4.8486	-4.71125	-9.1125	-0.41911	1.480794
25	-18.7176	-18.323	32.64093	-1.98328	12.52323	-4.12454
26	-38.6167	-34.298	-7.94394	-9.73878	0.356105	0.52794
27	-38.7819	-27.491	-12.2953	-13.4282	2.275946	1.909522
28	-38.5387	-21.594	-11.8167	-14.7561	2.696268	2.818175
29	-40.536	-15.952	-12.8473	-15.3994	2.985567	3.990663
30	-42.2527	-11.549	-15.8052	-14.513	1.853159	5.343718
31	-38.8869	-7.5464	-14.6297	-11.9756	0.364336	5.385461
32	-30.8461	-4.2742	-5.92785	-9.97374	-0.09991	3.073713
33	-20.4077	-16.988	35.13645	-1.22358	15.52192	-4.54357
34	-50.426	-28.739	-8.63148	-9.46322	1.736982	-0.53578
35	-58.2778	-21.193	-15.4646	-14.5117	2.793915	2.527333
36	-62.1579	-16.369	-17.5263	-16.0872	2.01645	4.533294
37	-63.7041	-12.048	-19.4875	-15.6662	0.813248	5.307881

38	-61.1676	-8.9855	-20.7556	-13.5152	-1.20495	5.049422
39	-51.2621	-5.9032	-16.283	-10.2353	-2.02614	3.843894
40	-35.9331	-2.3834	-5.09207	-7.26001	-0.86728	1.919257
41	-21.4153	-16.798	36.15429	-0.46601	17.41804	-4.28311
42	-60.8599	-25.481	-11.5467	-4.22577	2.168625	-1.33742
43	-73.823	-16.637	-19.2742	-6.54801	1.418029	1.948513
44	-76.9428	-11.981	-20.52	-7.37696	-0.17368	2.960087
45	-75.1585	-8.3304	-21.4903	-7.32035	-1.46199	2.353127
46	-70.119	-6.2568	-21.977	-6.25402	-3.22177	0.930992
47	-59.3865	-4.2267	-17.1239	-4.34426	-3.52784	-0.44544
48	-43.1045	-1.0578	-5.33689	-2.2225	-1.5801	-0.87794
49	-21.8791	-17.324	34.96324	0.139613	18.02292	-3.39819
50	-64.9066	-25.603	-15.1874	3.324908	2.104808	-1.82159
51	-76.6425	-16.258	-20.9607	5.084969	0.513554	-0.14132
52	-76.0449	-11.345	-19.6132	4.786124	-0.78953	-0.86708
53	-72.0122	-7.5399	-19.4561	4.001352	-1.34125	-2.15636
54	-67.5599	-5.5730	-20.2339	3.665739	-2.63957	-3.25153
55	-60.1436	-4.0247	-16.8871	3.749911	-3.06324	-3.62286
56	-48.1823	-1.6392	-6.2845	4.008853	-1.40006	-2.61267
57	-21.6986	-18.516	31.72184	0.7665	17.62498	-1.66414
58	-62.5964	-28.487	-17.8613	9.629247	1.961232	-1.567
59	-70.652	-19.843	-20.3912	14.30691	0.784344	-1.99543
60	-67.1019	-14.821	-16.6427	14.34988	0.399313	-4.21362
61	-61.5336	-10.368	-15.9056	13.0637	0.824393	-5.68338
62	-56.919	-7.7481	-17.4326	11.63158	-0.38668	-5.78271
63	-50.9483	-5.7300	-15.3391	10.20303	-1.68549	-4.55831
64	-42.6788	-2.8998	-6.10273	9.157006	-1.12918	-2.31144
65	-20.3391	-19.873	28.10662	1.301048	16.71328	1.081924
66	-54.9778	-31.849	-18.4085	12.52526	1.71243	-0.21377
67	-60.5441	-24.552	-17.9788	19.12758	1.500878	-2.48628
68	-56.2941	-20.237	-12.6224	19.94966	2.456541	-6.26831
69	-48.6221	-15.208	-12.0703	17.87102	3.946445	-8.09098
70	-41.3214	-11.082	-14.8092	14.55801	2.324711	-7.01735
71	-33.9746	-7.5622	-13.4561	11.6566	-0.30846	-4.21683
72	-28.1236	-4.6257	-5.49802	9.931957	-1.06943	-1.29276
73	-17.4632	-21.067	25.45176	1.340737	15.36386	4.398294
74	-43.6073	-33.937	-17.3009	11.48313	0.786495	1.749909
75	-46.3904	-28.201	-13.9265	19.08126	1.701915	-1.27218
76	-42.9326	-25.289	-7.00341	20.23477	4.494877	-6.29347
77	-33.3719	-19.261	-7.12659	16.60195	6.89944	-8.25356
78	-24.7912	-12.982	-11.5645	11.65088	4.5602	-5.81849
79	-18.5983	-8.1165	-10.923	8.473789	1.107617	-2.63165
80	-15.481	-5.1090	-4.22132	7.68981	-0.46957	-0.74501
81	-13.4774	-22.090	24.0087	0.531073	13.46723	7.546208
82	-32.1258	-34.774	-16.4346	7.04847	-1.43237	2.708699
83	-29.6999	-30.187	-9.26112	13.57053	0.311774	0.510496
84	-25.4803	-26.828	0.489127	13.03426	4.537814	-3.78527
85	-18.0929	-18.936	0.820087	8.701712	6.937975	-4.37624
86	-14.5617	-12.522	-5.90283	5.845582	4.467011	-2.58898
87	-11.0338	-7.5893	-7.52706	5.275721	1.827415	-1.12644
88	-9.22106	-5.1177	-3.02675	5.975634	0.240316	-0.54353

89	-8.63128	-22.270	24.11612	-1.05644	11.37902	10.20015
90	-22.8874	-34.030	-16.1771	0.416555	-4.51714	1.845202
91	-14.7679	-28.68	-5.01483	4.326764	-2.16148	0.85957
92	-11.119	-21.513	6.361138	1.776665	2.018796	-1.01877
93	-11.5674	-13.017	7.231059	0.726357	3.302148	-1.30656
94	-11.5202	-9.9677	-1.73405	2.604522	2.89479	-2.03445
95	-7.9747	-7.0289	-5.60449	3.556134	1.967256	-1.10847
96	-6.04998	-4.5854	-2.55879	4.374284	0.467158	-0.33126
97	0.451646	-19.694	29.77813	-2.46299	10.35645	14.73054
98	-11.5544	-29.474	-11.7952	-7.76549	-6.87901	1.834652
99	-1.20209	-23.123	0.030537	-5.97545	-3.93143	2.002799
100	-3.93965	-13.873	10.01809	-4.76397	-0.48289	2.146667
101	-9.6209	-8.8161	7.86495	-0.13325	1.767420	-1.64865
102	-8.9751	-8.9872	-2.2444	1.861038	2.752753	-2.85064
103	-5.71796	-6.4898	-5.47301	2.092431	2.079961	-1.20508
104	-3.29715	-3.1245	-2.41595	2.529617	0.446137	-0.19403
105	27.89476	-9.7769	53.96844	-0.06297	14.54998	30.1239
106	23.55612	-17.116	7.66526	-10.5838	-5.70021	11.81519
107	25.6993	-14.739	9.79301	-9.85843	-4.10181	10.63206
108	8.006063	-7.6222	19.513	-1.02246	0.640087	9.646828
109	-3.60324	-7.3252	11.33612	3.759302	5.974569	-0.13987
110	-4.30458	-8.5970	-1.65353	2.370189	6.099339	-1.31602
111	-3.4726	-6.3787	-6.07111	1.100983	3.402708	-0.80427
112	-1.59032	-2.6183	-2.27997	0.944759	0.991116	-0.60529

Table A.20: **Downstream Element face centre stresses in kg/cm^2 -** Load case 3

Element	**sigx**	**sig y**	**sig z**	**sig xy**	**sig yz**	**sig xz**	**element**
1	-30.0404	-27.2213	-41.5655	-19.083	-19.083	18.93649	23.76332
2	-23.8581	-38.1872	-29.2925	-27.5569	-27.5569	26.46812	14.32754
3	-18.967	-39.3242	-22.2218	-24.8435	-24.8435	22.56892	9.164443
4	-18.961	-36.2716	-19.5437	-22.9511	-22.9511	18.94998	8.257677
5	-21.4034	-32.1635	-16.8632	-22.0569	-22.0569	15.75578	8.513524
6	-22.5885	-25.6466	-12.3381	-20.4101	-20.4101	11.37508	7.30881
7	-19.1777	-16.6092	-7.01436	-16.0734	-16.0734	7.132497	4.926387
8	-10.8707	-7.53591	-1.48397	8.944949	-8.94495	3.195792	2.271672
9	-23.3205	-20.5341	-31.9378	-14.7544	-14.7544	15.26376	18.36929
10	-26.1978	-37.1923	-24.0698	-29.4913	-29.4913	23.76991	15.77078
11	-20.6177	-44.7599	-18.6783	-26.9935	-26.9935	20.67383	8.855367
12	-17.9018	-38.5277	-15.9031	-24.7501	-24.7501	17.32603	6.781215
13	-20.7725	-30.053	-14.76	-23.6775	-23.6775	14.8841	8.23046
14	-24.8797	-20.3653	-11.1646	-21.2854	-21.2854	10.93201	9.264047
15	-25.8282	-11.7035	-6.05629	-16.2557	-16.2557	5.781989	7.427494
16	-23.8822	-6.75632	-1.7143	-12.3906	-12.3906	2.128626	2.970333
17	-13.445	-15.3977	-28.4942	-6.83322	-6.83322	12.30619	11.42361
18	-24.4956	-31.3503	-16.1749	-24.892	-24.892	17.8596	14.41625
19	-32.1241	-43.9747	-19.7413	-29.3107	-29.3107	18.59734	12.93461
20	-34.5357	-39.1636	-19.9719	-29.3036	-29.3036	16.1311	11.82384
21	-34.5717	-27.7218	-16.2304	-26.0378	-26.0378	12.55312	10.81806
22	-31.1186	-14.9684	-8.40215	-19.6658	-19.6658	7.597432	8.429311
23	-25.1363	-5.96775	-1.45777	-12.598	-12.598	2.804728	4.345831
24	-22.0626	-3.73429	0.108873	-9.34029	-9.34029	0.100742	1.178395
25	-9.87126	-14.2569	-29.4025	-2.91346	-2.91346	12.9358	8.289381
26	-21.0274	-17.5904	-8.19331	-18.0813	-18.0813	11.44415	11.88143

27	-29.6744	-20.4322	-10.965	-21.485	-21.485	10.41271	12.10161
28	-33.6316	-15.1346	-12.3956	-20.7566	-20.7566	8.287574	10.95977
29	-34.723	-10.5426	-8.96789	-18.1128	-18.1128	5.610576	8.323206
30	-31.8721	-6.93168	-2.26704	-14.4319	-14.4319	2.83984	4.601899
31	-26.4156	-4.50305	1.654021	-10.5515	-10.5515	0.5975	1.16762
32	-22.005	-2.93496	0.818591	-7.80327	-7.80327	-0.30187	-0.22452
33	-9.60031	-14.7436	-30.4393	-1.51682	-1.51682	14.35715	6.870158
34	-18.0895	-7.7754	-2.52448	-11.4392	-11.4392	7.317671	7.925897
35	-22.9734	-6.72237	-2.90052	-11.6461	-11.6461	4.164771	6.79208
36	-24.5819	-3.68081	-5.12131	-9.80684	-9.80684	2.64394	5.383207
37	-26.6948	-2.70914	-3.26714	-8.48162	-8.48162	1.532079	3.928875
38	-28.4944	-2.31691	1.25201	-7.7615	-7.7615	0.46544	2.174565
39	-28.1185	-2.09422	2.624422	-6.86233	-6.86233	-0.3245	0.504071
40	-24.6984	-1.62	0.011291	-5.4056	-5.4056	-0.38281	-0.25442
41	-10.5779	-15.1274	-30.2867	-0.89086	-0.89086	14.87892	4.721593
42	-16.8075	-2.74244	0.979219	-5.69136	-5.69136	4.847	2.742744
43	-20.1446	-2.24878	0.808092	-4.77362	-4.77362	1.106418	0.547281
44	-20.8511	-0.62071	-2.8166	-3.29044	-3.29044	0.22615	0.206967
45	-23.0446	-0.32533	-2.29575	-2.46729	-2.46729	0.061879	1.115423
46	-25.6086	-0.19427	1.4739	-1.99087	-1.99087	-0.09353	1.830656
47	-26.0975	-0.40082	2.75208	-1.66084	-1.66084	-0.34335	1.664951
48	-23.3342	-0.38076	0.110486	-1.2715	-1.2715	-0.25133	0.818091
49	-11.5374	-15.8803	-30.566	0.106755	0.106755	15.10746	0.862061
50	-16.2842	-1.66028	1.773881	0.235763	0.235763	4.40939	-3.22543
51	-20.938	-1.54798	0.913309	1.240571	1.240571	0.605456	-4.71209
52	-22.3336	-0.25895	-3.81531	2.033568	2.033568	-0.07315	-3.48281
53	-23.5956	-0.18881	-3.71102	2.385037	2.385037	-0.11929	-0.83591
54	-23.8678	-0.10596	0.555402	2.689222	2.689222	-0.1178	1.383841
55	-22.2559	-0.15723	3.254946	2.630522	2.630522	-0.21616	2.252226
56	-20.362	-0.40659	1.180703	2.093139	2.093139	-0.16857	1.566239
57	-11.8715	-17.7339	-32.6737	1.417324	1.417324	16.23782	-3.19912
58	-14.9374	-4.80318	0.182525	5.908127	5.908127	6.712142	-8.18696
59	-20.8377	-4.10766	-0.56521	7.012367	7.012367	2.276965	-8.21858
60	-22.9113	-2.28119	-5.69274	7.148285	7.148285	1.247704	-5.89321
61	-23.6128	-1.80763	-5.30244	6.83813	6.83813	0.74946	-2.67587
62	-23.3654	-1.56527	-0.32362	6.539081	6.539081	0.30516	-0.28687
63	-22.4826	-1.49513	2.985382	5.97376	5.97376	-0.17116	0.675635
64	-22.713	-1.26242	1.439497	5.210014	5.210014	-0.28668	0.587859
65	-11.8684	-20.1789	-35.2564	2.56528	2.56528	18.1172	-5.99082
66	-13.1483	-10.4142	-2.72515	10.29707	10.29707	10.38515	-10.9639
67	-19.1684	-8.94736	-2.72822	11.87787	11.87787	4.898568	-10.2598
68	-22.1613	-6.30708	-7.89464	11.59469	11.59469	3.522719	-7.51124
69	-24.0702	-5.19151	-7.21393	11.07566	11.07566	2.643169	-4.55721
70	-25.4683	-4.63516	-1.96208	10.82442	10.82442	1.675033	-3.14643
71	-25.9423	-4.3414	1.223894	10.35361	10.35361	0.620773	-2.56941
72	-25.632	-4.08897	0.737098	9.889701	9.889701	-0.03361	-1.0744
73	-12.055	-22.8289	-37.4019	3.939749	3.939749	20.43163	-7.92915
74	-12.4784	-17.007	-6.68975	13.92812	13.92812	13.80839	-12.2428
75	-19.7565	-16.2464	-6.57274	17.54234	17.54234	7.974937	-12.0501
76	-25.1002	-13.7801	-12.4462	18.14191	18.14191	7.444717	-9.74702
77	-28.8357	-11.944	-12.0244	17.52919	17.52919	6.996643	-7.7356
78	-28.9571	-10.1585	-6.23063	16.20065	16.20065	5.449372	-7.14977
79	-25.1803	-8.70555	-1.71425	14.15245	14.15245	3.060609	-5.27802
80	-21.0622	-7.55054	-0.29607	12.13939	12.13939	0.727984	-1.79851
81	-13.0469	-26.8923	-40.466	6.117065	6.117065	23.76938	-9.52456
82	-13.6114	-25.9446	-11.7844	17.79098	17.79098	16.66555	-12.5738
83	-24.4242	-29.9415	-12.6508	25.94665	25.94665	11.48859	-13.4818
84	-33.6664	-30.3016	-21.295	29.34185	29.34185	14.91175	-13.1024

85	-35.4268	-25.3937	-22.3862	26.04878	26.04878	16.31278	-12.6172
86	-27.2558	-18.0636	-13.5687	19.47247	19.47247	12.01288	-10.2753
87	-17.6617	-11.4041	-4.59108	13.27	13.27	5.791914	-5.74214
88	-12.6832	-7.36526	-1.05377	9.606843	9.606843	1.532084	-2.00515
89	-15.3115	-32.9081	-45.5446	9.137942	9.137942	28.20525	-10.5724
90	-16.1497	-38.954	-17.718	22.16585	22.16585	19.33322	-11.6809
91	-28.8867	-52.5614	-19.1154	34.27932	34.27932	14.88978	-12.6349
92	-37.6803	-56.5607	-29.5916	37.66467	37.66467	24.03845	-13.382
93	-31.0638	-42.2447	-30.1058	27.53863	27.53863	25.49168	-12.6626
94	-17.3382	-23.6308	-17.5738	15.91341	15.91341	16.32296	-8.16648
95	-9.26517	-10.8054	-6.51637	8.868238	8.868238	7.013878	-4.34524
96	-6.81301	-5.49581	-1.70316	6.105213	6.105213	2.153806	-1.9771
97	-17.2161	-36.8052	-49.9829	12.402	12.402	31.43289	-10.9108
98	-17.5967	-49.4898	-22.1898	26.93035	26.93035	21.75508	-9.49816
99	-24.7127	-62.2542	-19.6962	36.73261	36.73261	17.05064	-9.05959
100	-24.678	-53.5825	-24.5355	32.7572	32.7572	23.6536	-8.28556
101	-15.0584	-33.383	-21.8393	18.93218	18.93218	21.36065	-6.54779
102	-7.32473	-18.9522	-14.0781	9.026203	9.026203	13.93354	-3.55404
103	-4.29658	-9.17432	-7.15727	4.92973	4.92973	6.873126	-2.45175
104	-3.6434	-3.93251	-1.94401	3.798506	3.798506	2.185165	-1.63907
105	-15.8011	-36.367	-48.8017	12.74985	12.74985	30.43109	-8.71667
106	-16.8024	-56.0359	-23.6188	26.40251	26.40251	20.56168	-6.81159
107	-23.9561	-73.3084	-22.571	35.23034	35.23034	19.51967	-6.62171
108	-22.805	-51.7601	-23.5013	28.12601	28.12601	24.96953	-7.2927
109	-11.1698	-24.645	-19.9151	13.07216	13.07216	19.29619	-5.18731
110	-4.18199	-13.4624	-12.9118	4.934327	4.934327	11.65064	-1.69987
111	-2.03061	-7.29611	-5.98304	2.299997	2.299997	5.892395	-0.57505
112	-1.2955	-3.20402	-1.65832	1.634202	1.634202	1.419238	-0.40627

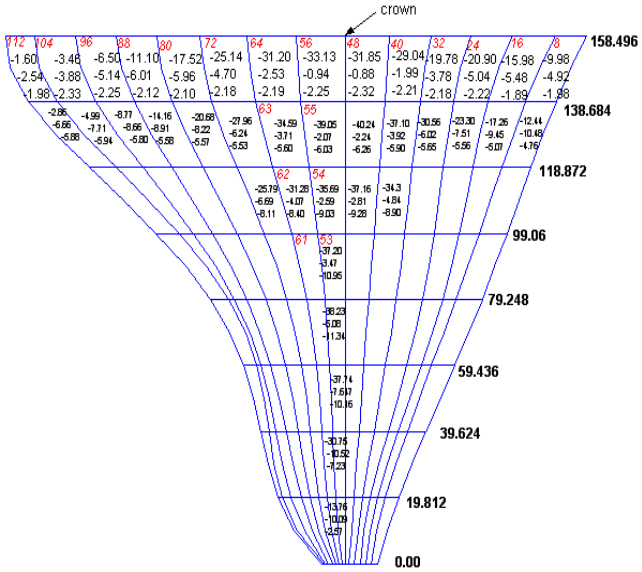

Fig A.16: ***Element stresses*** - *Load case 3*

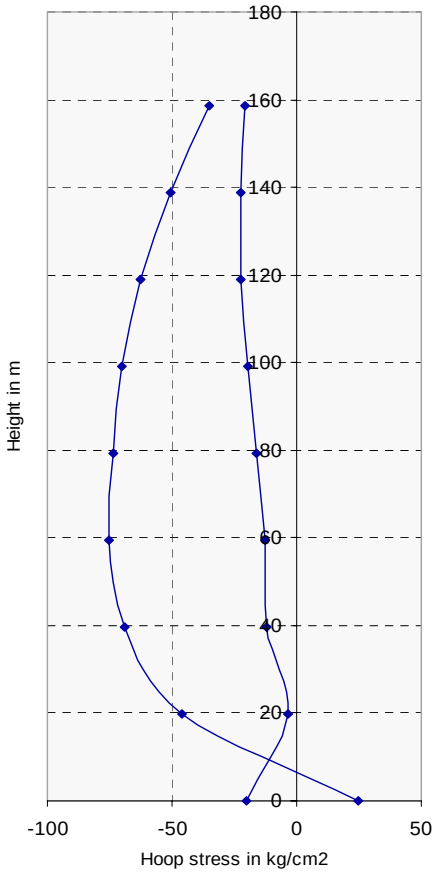

Upstream Crown	
24.4255	0
-46.1665	19.812
-68.9826	39.624
-75.319	59.436
-73.7515	79.248
-69.9247	99.06
-62.8401	118.872
-50.3569	138.684
-35.2521	158.496
Downstream crown	
-20.1894	0
-3.62843	19.812
-11.7873	39.624
-12.7806	59.436
-15.8212	79.248
-19.807	99.06
-22.563	118.872
-22.5991	138.684
-20.7018	158.496

Fig A.17: ***Hoop stress at crown cantilever****- Load case 3*

A.3 GEOMETRY AND DISCRETISATION-3 SELECTED

The same dam geometry arrived as above with 80 nodal points is tried for a finer discretisation with number of divisions 8 in height and 7 in length and 2 in thickness; 112 elements. Since this is a thick arch dam, it is checked for better results with multilayer in thickness.

A.3.1 Dead Load, Maximum Water, Maximum Silt

The dam is analysed for this load case. The deflected profile is shown in Fig A.18. Global displacement obtained for the crown portion is shown in Table A.21.

Elemental face centre stresses of upstream and downstream are shown in Table A.22 and A.23. Hoop stress at crown cantilever section is shown in Fig A.19.

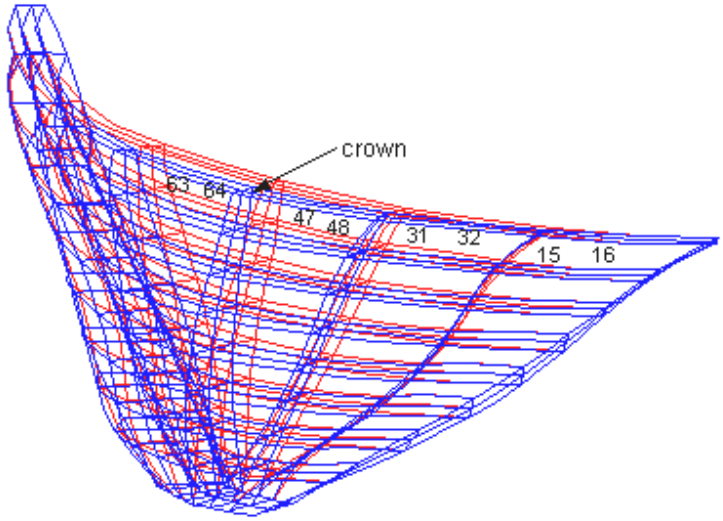

Fig A.18: ***Deformed profile due to self weight and water pressure***
No. of elements = 112

Table A.21: **Global displacement at crown cantilever -** Load case

Node	Displ X m	Displ Y m	Displ Z m
289	0	0	0
290	0	0	0
291	0	0	0
292	0	0	0
293	0	0	0
294	-9.5e-03	0.004515	0.00288
295	0.000213	0.003734	0.000134
296	0.00047	0.003643	-0.00212
297	-0.00024	0.00869	0.004087
298	8.12e-03	0.00845	0.002237
299	0.00031	0.008297	0.00073
300	0.00053	0.008114	-0.00081
301	0.000761	0.008096	-0.00269
302	-0.00029	0.012553	0.004344
303	0.000329	0.012318	0.00112
304	0.000845	0.012326	-0.00221
305	-0.00028	0.015956	0.004247
306	6.34e-03	0.015931	0.002807
307	0.000309	0.015928	0.001347

308	0.00055	0.015974	-0.00013
309	0.000811	0.015977	-0.00165
310	-0.00018	0.019029	0.004067
311	0.000267	0.019115	0.001428
312	0.000668	0.019225	-0.00128
313	-4.2e-03	0.021867	0.003786
314	9.85e-03	0.021943	0.002576
315	0.000235	0.022034	0.001365
316	0.000381	0.022134	0.000134
317	0.000501	0.022188	-0.00109
318	7.57e-03	0.024557	0.003454
319	0.000213	0.024774	0.00118
320	0.000374	0.024947	-0.00111
321	0.000201	0.027184	0.003031
322	0.000197	0.02732	0.001952
323	0.000231	0.027449	0.00088
324	0.000279	0.027573	-0.00019
325	0.000308	0.027648	-0.00125
326	0.000245	0.029813	0.002505
327	0.00026	0.030082	0.000515
328	0.000343	0.030275	-0.00143
329	0.000295	0.032285	0.00186
330	0.000294	0.032432	0.000968
331	0.000331	0.032565	0.000107
332	0.000384	0.032682	-0.00074
333	0.000443	0.03276	-0.00157
334	0.000263	0.03446	0.001106
335	0.000411	0.034734	-0.00028
336	0.000635	0.034919	-0.00156
337	0.000231	0.036145	0.000391
338	0.000358	0.036286	-0.00011
339	0.000503	0.036405	-0.00058
340	0.000665	0.036507	-0.00102
341	0.000845	0.036577	-0.00143
342	0.000183	0.037219	-0.00023
343	0.000606	0.037451	-0.00074
344	0.001074	0.037607	-0.00115
345	0.000127	0.037653	-0.00059
346	0.000402	0.037755	-0.00066
347	0.000676	0.03784	-0.00073
348	0.00096	0.037913	-0.00078
349	0.001252	0.037971	-0.0008
350	0.000119	0.03766	-0.00059
351	0.000758	0.037809	-0.00058
352	0.001388	0.037922	-0.00053
353	0.000167	0.037571	-0.00037
354	0.000485	0.037619	-0.00035
355	0.000788	0.037659	-0.00033
356	0.001082	0.037695	-0.00031
357	0.001384	0.037724	-0.00028
358	0	0	0
359	0	0	0

360	0	0	0
361	0.001013	0.008745	0.004076
362	0.000955	0.00839	0.000777
363	0.000893	0.008194	-0.00259
364	0.002202	0.01578	0.004121
365	0.001637	0.015869	0.001387
366	0.001179	0.016022	-0.00145
367	0.003062	0.020994	0.003704
368	0.001936	0.021418	0.00144
369	0.000994	0.021825	-0.00088
370	0.003677	0.025638	0.003195
371	0.002243	0.026219	0.001031
372	0.000979	0.026749	-0.00113
373	0.004226	0.030333	0.002311
374	0.002795	0.03087	0.000325
375	0.001462	0.031333	-0.0016
376	0.004665	0.034244	0.000983
377	0.003478	0.034634	-0.00037
378	0.002312	0.034927	-0.00163
379	0.004789	0.036377	-0.00013
380	0.003956	0.036628	-0.00068
381	0.003113	0.036808	-0.00118
382	0.004659	0.037387	-0.00028
383	0.004143	0.037645	-0.00055
384	0.003655	0.037868	-0.00082

Table A.22: **Upstream Element face centre stresses in kg/cm^2 -** Load case

Element	**Sig x**	**Sig y**	**Sig z**	**Sig xy**	**Sig yz**	**Sig xz**
1	10.61384	-15.7566	39.81613	-5.06321	6.632685	-17.344
3	-5.08403	-23.5763	7.354046	-0.48597	-1.88444	-6.71021
5	-4.80931	-16.3974	2.351694	-0.6927	-0.59214	-4.61034
7	-4.44786	-11.4661	-0.51892	-0.75643	-0.39749	-2.57739
9	-5.04596	-8.87337	-2.88579	-1.41061	0.488866	-1.07767
11	-7.04157	-8.11501	-4.60958	-2.51386	1.354186	1.04974
13	-8.54686	-7.2893	-4.04783	-4.42746	2.553305	2.404354
15	-8.34049	-5.34143	-3.16783	-6.13637	2.840975	1.436884
17	-23.4651	-25.381	24.91908	2.489818	2.845288	-1.75778
19	-39.8807	-32.16	-14.6742	-4.58858	-4.58094	4.816526
21	-33.814	-24.064	-14.0243	-7.14991	0.031502	3.377748
23	-31.1192	-18.5953	-11.0919	-7.99486	0.555142	3.251857
25	-30.7761	-13.9291	-10.4452	-9.13756	1.465435	3.050729
27	-31.3828	-10.2739	-13.6917	-9.60356	1.389853	3.73053
29	-29.2487	-6.66271	-13.8434	-8.71471	0.454798	4.39648
31	-24.5184	-3.93169	-5.62815	-7.89869	-0.25629	2.915899
33	**-22.7134**	**-22.0154**	**31.35257**	**0.814266**	**10.30225**	**-4.46925**
35	**-54.0704**	**-24.0563**	**-14.1563**	**-4.58532**	**-0.46468**	**-0.78847**
37	**-61.8407**	**-17.2685**	**-18.8838**	**-8.19925**	**1.503811**	**2.368808**
39	**-63.9544**	**-12.7838**	**-19.4407**	**-9.97287**	**0.388506**	**3.790006**
41	**-63.7596**	**-9.33328**	**-20.4946**	**-10.042**	**-0.89877**	**3.900497**

43	**-61.1136**	**-6.99258**	**-22.0376**	**-8.40353**	**-2.86599**	**3.087566**
45	**-52.5789**	**-4.42595**	**-18.1005**	**-5.91984**	**-3.14006**	**1.749311**
47	**-38.179**	**-1.36949**	**-6.29337**	**-3.92746**	**-1.10458**	**0.523855**
49	-23.6861	-23.2703	28.32805	-0.02507	10.77568	-4.28381
51	**-61.9463**	-25.281	-21.5574	5.958685	-0.5562	-1.83073
53	**-69.8289**	-17.3863	-22.811	7.917084	0.09379	-0.62492
55	**-66.595**	-12.1277	-18.3489	7.518256	-0.69938	-2.03514
57	-62.1027	-8.4052	-17.2332	6.684077	-0.77033	-3.56699
59	-58.386	-6.50087	-19.0065	6.245884	-1.90904	-4.49263
61	-52.3122	-4.5627	-16.8126	6.104664	-2.53027	-4.39639
63	-42.9509	-2.04748	-6.0655	6.023649	-0.87758	-2.85345
65	-22.4325	-24.0652	20.51293	-0.32468	9.060074	-0.00831
67	-49.1502	-28.3773	-22.1231	10.60358	-0.31277	0.558747
69	-53.562	-23.0595	-18.2723	15.51567	1.555588	-1.82922
71	-49.0137	-18.8221	-10.8799	16.35691	2.620058	-6.31151
73	-39.2032	-13.7669	-9.36965	13.80173	3.467939	-8.81869
75	-31.3345	-9.68121	-13.0938	10.57336	1.697269	-7.57434
77	-25.8012	-6.96211	-13.071	8.724604	-0.19719	-4.42091
79	-21.7877	-5.18412	-6.19809	8.358584	-0.61665	-1.40067
81	-18.8463	-23.8715	14.14375	-3.13772	4.506859	3.258556
83	-32.3353	-27.7356	-22.1608	1.228214	-4.7986	0.306828
85	-24.9298	-22.3882	-8.51725	4.72332	-0.68951	0.515977
87	-18.3419	-18.1578	2.964511	3.93647	1.751213	-3.55291
89	-13.5134	-13.7528	3.056591	2.70301	3.438108	-4.18289
91	-11.4893	-10.9744	-4.97295	3.298172	2.836795	-2.44474
93	-8.12126	-7.04661	-7.16103	3.618244	1.5932	-0.40535
95	-5.95851	-4.2039	-3.07623	4.106804	0.086196	0.159247
97	**14.98067**	-10.4531	46.03921	-2.83209	8.044887	22.70578
99	**4.922791**	-16.8305	-2.9991	-9.25873	-6.12573	5.576375
101	**12.51415**	-14.4919	4.90131	-9.68441	-2.65469	5.512247
103	**5.18019**	-9.1568	13.10725	-5.32841	0.671341	6.456164
105	-4.05439	-7.74822	8.342904	0.418537	3.362222	0.496616
107	-5.66183	-8.63561	-3.95627	1.175464	3.678095	-1.21417
109	-4.12037	-6.11027	-6.98167	0.853702	2.380235	-0.52147
111	-2.15634	-2.68027	-2.72291	1.142757	0.612341	-0.24603

Table A.23: **Downstream Element face centre stresses in kg/cm^2 -** Load case

Element	Sig x	Sig y	Sig z	Sig xy	Sig yz	Sig xz
2	-33.1746	-22.3268	-46.6154	-22.5769	20.63252	28.66227
4	-29.5948	-38.3711	-32.7051	-32.5578	27.7486	20.22987
6	-20.1449	-40.8068	-24.7579	-29.375	24.32725	11.50909
8	-19.6549	-34.9674	-21.8703	-26.9102	20.80781	10.20509
10	-23.055	-29.1846	-19.3804	-25.4439	17.54417	10.99802
12	-26.9503	-24.4154	-15.4887	-23.6829	13.0447	10.43085
14	-26.8552	-18.6891	-10.9978	-19.9465	8.939525	8.259872
16	-19.4862	-10.5249	-3.54653	-14.1458	5.428139	4.337139
18	-15.1581	-5.8696	-37.0394	-6.7085	13.37133	13.34032
20	-29.8883	-23.5565	-16.755	-25.2495	15.78897	18.72741
22	-39.5604	-34.7561	-21.8334	-30.1343	17.86945	16.38322
24	-42.7357	-28.7038	-22.4261	-29.4344	14.63823	15.32497

26	-42.3443	-18.8881	-17.5062	-25.2161	10.4059	13.20646
28	-37.1798	-9.27616	-7.11909	-18.6168	5.677857	9.098531
30	-30.1851	-4.20821	0.209095	-12.7072	1.804946	3.778155
32	**-26.7993**	**-3.66296**	**-0.24356**	**-9.99734**	**-0.36211**	**0.564514**
34	**-9.19653**	**-7.9148**	**-39.9317**	**-1.06638**	**15.0166**	**8.137428**
36	**-17.3381**	**-0.35796**	**-0.50343**	**-7.81422**	**3.386959**	**8.255015**
38	**-20.7816**	**0.392892**	**-1.82467**	**-6.45607**	**1.691698**	**4.644648**
40	**-21.0278**	**1.397902**	**-5.49738**	**-5.11361**	**0.621707**	**3.376671**
42	**-23.1774**	**0.684984**	**-4.00882**	**-4.24188**	**0.090228**	**2.879641**
44	**-26.2858**	**-0.18757**	**1.927044**	**-3.67066**	**-0.23311**	**2.054869**
46	**-27.7586**	**-0.82627**	**4.167141**	**-3.2399**	**-0.12121**	**0.970133**
48	**-26.0947**	**-0.55725**	**0.769691**	**-2.70112**	**0.032338**	**0.239018**
50	-10.3338	-10.3768	-41.0859	1.800684	16.84654	-1.47249
52	-14.191	0.568999	2.02233	2.979372	2.578536	-7.29999
54	-19.2454	-1.71057	-1.07128	2.734035	1.322842	-7.51522
56	-21.1989	-1.19679	-7.42017	2.513221	0.535212	-5.21342
58	-21.9904	-0.72145	-6.69235	2.74323	0.062148	-1.56931
60	-21.8608	-0.21236	0.273952	3.500741	-0.19796	1.395019
62	-21.0678	-0.11129	4.620208	3.833578	-0.12827	2.764202
64	-21.6366	-0.51397	1.50192	3.319598	-0.17011	2.132581
66	-12.1775	-15.8218	-47.3172	5.659889	22.79105	-9.01671
68	-12.3673	-8.30509	-4.08581	12.8873	11.66351	-15.9364
70	-20.3831	-8.45686	-6.44277	13.89162	8.042047	-13.3245
72	-25.2938	-5.87016	-13.584	13.98753	5.707122	-10.3559
74	-29.9583	-5.13368	-13.2182	14.15138	3.217337	-7.82622
76	-31.9723	-5.22028	-5.90451	13.8586	1.687891	-6.74459
78	-30.2085	-5.81704	-0.61079	13.0168	1.176831	-5.193
80	-26.9922	-6.30511	0.562683	12.33014	0.448811	-1.87434
82	-16.6669	-27.0231	-55.7282	12.42617	32.79723	-13.4746
84	-19.1193	-29.8142	-17.1172	24.34981	21.84619	-17.4902
86	-34.8253	-39.3032	-20.4171	34.38659	17.12552	-16.5577
88	-45.1759	-46.3514	-33.841	39.02088	23.73649	-17.1737
90	-40.6198	-40.8575	-37.6405	32.26062	26.48728	-16.707
92	-25.9225	-26.4194	-24.4769	21.51112	18.83534	-12.1666
94	-14.954	-13.8854	-9.34702	13.38414	8.907522	-6.78106
96	-10.7664	-7.51552	-2.11686	9.152787	2.894033	-2.77304
98	-15.9377	-38.4731	-34.6869	16.70809	37.01044	-9.60793
100	-21.5461	**-58.4115**	-27.6505	32.8501	26.1156	-11.7397
102	-26.83	**-62.2808**	-23.4514	36.29565	21.84062	-9.08865
104	-23.6175	**-52.5636**	-27.8925	34.36892	26.70156	-8.2865
106	-10.3004	-28.9442	-24.2016	18.14206	22.17178	-5.0214
108	-4.42024	-17.3935	-16.3991	8.039819	14.99109	-2.00656
110	-2.81149	-9.26438	-8.54451	4.012411	7.730396	-1.19088
112	-2.45828	-4.28428	-2.61616	2.817541	2.228406	-1.03678

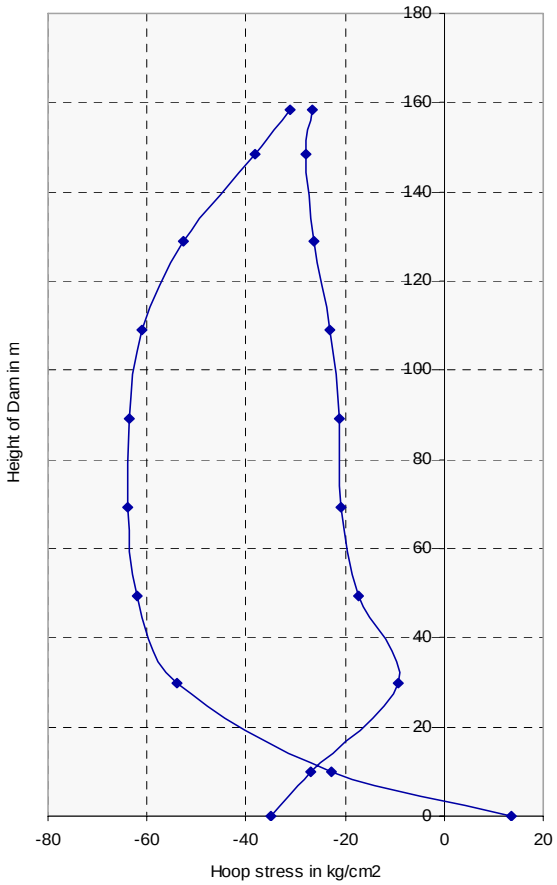

Fig A.19: ***Hoop stress at crown cantilever***

Comparing with the earlier results, the maximum compressive stress on the upstream face computed is 75.5 kg/cm^2 near crown bottom whereas obtained is 69.8 kg/cm^2. The maximum tensile stress on the upstream face computed is 11.8 kg/cm^2 at elevation 148m of left abutment whereas obtained is 14.98 kg/cm^2. The maximum compressive stress on the downstream face computed is 68.5 kg/cm^2 whereas obtained is 62.28 kg/cm^2 at left abutment bottom. The maximum tensile stress on the downstream face computed is 4.8 kg/cm^2 whereas obtained is 1.39 kg/cm^2 at middle portion of crown.[95,96] The results are found comparable.